

*TNO-report*

## Results of Sexbierum Wind Farm; single wake measurements

Reference number 93-082  
File number 112324-22420  
Date March 1993  
NP

St-code  
C19.3

Author  
J.W. Cleijne

Keywords  
– wind energy  
– full-scale measurements  
– wake effects

Intended for  
Participants JOUR-0064  
Participants JOUR-0087

All rights reserved.

No part of this publication may be reproduced and/or published by print, photoprint, microfilm or any other means without the previous written consent of TNO.

In case this report was drafted on instructions, the rights and obligations of contracting parties are subject to either the 'Standard Conditions for Research Instructions given to TNO', or the relevant agreement concluded between the contracting parties.

Submitting the report for inspection to parties who have a direct interest is permitted.

© TNO

## Summary

In the framework of the JOULE-0064 'Full-scale Measurements in Wind Turbine Arrays' in the period between June-November 1992 measurements have been performed in the Sexbierum Wind Farm. The aim of the measurements is to provide data for the validation of wake and wind farm models, which are being developed simultaneously, and to provide input data for wind turbine load calculation programmes.

The campaign concerned measurement of the wind speed, turbulence and shear stress behind a single wind turbine at distances of 2.5, 5.5 and 8 rotor diameters, respectively. Besides detailed measurements of the wind field, the power of the turbine was measured.

A database has been compiled containing 1-minute averaged values of the measured quantities. The database was analysed using a two-dimensional bin analysis with respect to the undisturbed wind direction and wind speed.

The analysis contains horizontal and vertical profiles of the:

- U-, V-, and W-component of the wind in the wake;
- turbulence intensities in three directions and turbulent kinetic energy in the wake;
- shear stresses  $u'v'$ ,  $u'w'$  and  $v'w'$  in the wake.

These quantities are presented both in dimensional as in non-dimensionalized form.

With the data base a useful set of data is created for the validation of wake and wind farm models.

## Table of contents

	<b>Summary</b> .....	2
	<b>List of symbols</b> .....	4
<b>1</b>	<b>Introduction</b> .....	5
<b>2</b>	<b>Experimental set-up</b> .....	6
2.1	Sexbierum wind farm .....	6
2.1.1	Lay-out .....	6
2.1.2	Turbines .....	7
2.1.3	Data acquisition .....	9
2.1.4	Instrumentation .....	10
2.2	Measuring campaign .....	11
2.2.1	Description .....	11
2.2.2	Observations .....	12
<b>3</b>	<b>Analysis</b> .....	13
3.1	Pre-processing and resulting database .....	13
3.2	Time averaging .....	13
3.3	Frame of reference .....	14
3.4	Bin-sorting .....	14
3.5	Dimensionless quantities .....	15
<b>4</b>	<b>Results</b> .....	16
4.1	Undisturbed wind conditions .....	16
4.1.1	Wind speed distribution .....	16
4.1.2	Undisturbed wind profile .....	17
4.1.3	Turbulence intensity .....	18
4.2	Wind turbine power .....	19
4.2.1	Free-stream power curve .....	19
4.2.2	Pitch control .....	19
4.3	Wake deficit .....	20
4.3.1	Wake deficit per bin .....	20
4.3.2	Aggregated results .....	22
4.4	Turbulence intensity .....	24
4.4.1	Turbulence intensity data per bin .....	24
4.4.2	Aggregated results .....	27
4.5	Shear stress .....	30
4.5.1	Shear stress per bin .....	30
4.5.2	Aggregated results .....	32
4.6	Wake decay .....	35
<b>5</b>	<b>Conclusions</b> .....	36
<b>6</b>	<b>References</b> .....	37
<b>7</b>	<b>Authentication</b> .....	38

Annex 1-4

## List of symbols

$a_{\text{hub}}$	Weibull scale factor at hub height
$c_p$	Power coefficient
$D$	Rotor diameter
$H$	Hub height
$I$	Turbulence intensity (e.g. $u'/U$ )
$k$	turbulent kinetic energy per unit mass $\frac{1}{2}(u'^2+v'^2+w'^2)$
$k_{\text{hub}}$	Weibull shape factor
$M_{42}$	Meteo mast 4, height 2 (= hub height)
$P$	Turbine Power
$T_{36}$	Turbine 36
$T_{18}$	Turbine 18
$T_{27}$	Turbine 27
$U$	wind speed component along the undisturbed wind
$u'$	rms value of turbulent velocity fluctuations in U-directions
$u'v'$	U-V component of turbulent shear stress
$u'w'$	U-W component of turbulent shear stress
$U_0$	undisturbed wind speed
$u'_0$	undisturbed U-component of turbulent velocity fluctuations
$V$	wind speed component perpendicular to the undisturbed wind direction
$v'$	rms value of turbulent velocity fluctuations in V-directions
$v'w'$	V-W component of turbulent shear stress
$W$	vertical wind speed component
$w'$	rms value of turbulent velocity fluctuations in W-directions
$z$	height
$z_0$	roughness height
$\delta$	wind direction
$\kappa$	Von Kármán constant
$\lambda$	tip speed ratio
$\rho$	air density
<b>suffix</b>	
max	maximum value
min	minimum value
0	undisturbed conditions

## 1 Introduction

During 1992, a detailed measuring campaign was carried out in the Sexbierum Wind Farm in order to collect experimental data on the wind speed, turbulence intensity and shear stresses in the wake of a single wind turbine at distances of 2.5, 5.5 and 8 rotor diameters, respectively. This report gives the results of the measurements and of the bin analysis of the data. Further, it describes the measuring conditions and the geometry of the wind farm and the turbines. A campaign concerning the wake conditions in a double wake situation was described in a previous report. In a later stage the reports will be combined in a final report. This final report will also contain the results of long term power measurements and turbulence spectra in the wake. The purpose of this report is to document the results of the analysis and to pass the information to the participants in the project Wake and Wind Farm Modelling (JOUR-0087), who will use it for the development and validation of wake models.

The measuring campaign is part of the CEC JOULE project 'Full-Scale measurements in Wind Turbine Arrays' (JOUR-0064). The project aims at collecting full-scale data for the purpose of:

- validation of wake and wind farm models;
- providing input data for load calculations.

To this end long term measurements and short term campaigns are carried out in various wind farms within the CEC.

In the Sexbierum wind farm the following quantities are monitored:

- fast rate wind speed data in wakes: spectra and wake data;
- wind turbine power;
- fatigue loads: rain flow counts of load cycles in various components, such as blades, hub and shaft.

Spectral wake data, wind turbine power data and results of rain flow counts will be reported, separately.

In The Netherlands KEMA and TNO jointly carry out the measurements and the analysis of the wake data. KEMA is responsible for the measurements and pre-processing of the data; TNO is responsible for the experimental set-up and the analysis of the data.

Chapter 2 describes the experimental set-up of the measurements. It gives details on wind farm lay-out, properties of the wind turbines and measuring sensors and procedures. Chapter 3 describes the data analysis procedure, which has been applied and chapter 4 describes the results of the analysis.

## **2 Experimental set-up**

### **2.1 Sexbierum wind farm**

#### **2.1.1 Lay-out**

The Dutch Experimental Wind Farm at Sexbierum is located in the Northern part of The Netherlands at approximately 4 km distance of the seashore. The wind farm is located in flat homogeneous terrain, mainly grassland used by farmers for the grazing of cows. In the direct vicinity of the wind farm only a few scattered farms are found.

The wind farm has a total of 5.4 MW installed capacity consisting of 18 turbines of 300 kW rated power each. The wind turbines are placed in a semi-rectangular grid of 3×6 rows at inter-distances of 5 rotor diameters along one major grid line and at an inter-distance of 8 diameters perpendicular to this grid line (see figure 2.1). The direction of the rows is at 7° with the North.

Around the wind farm there are 7 meteorological masts, which enables the measurement of the undisturbed wind conditions for every wind direction. Further, the pressure and temperature are measured. Masts 4 and 6 are parallel to the prevailing wind direction and have wind sensors at 3 heights. The other 5 masts have sensors at hub height. Turbine T36 has been instrumented to study the wake effects on the wind turbine loads.

The prevailing wind direction in the wind farm is along the line T18 to T36. The wind climate at hub height is given by Weibull frequency distribution with scale factor  $a_{hub}=8.6$  m/s and shape factor  $k_{hub}=2.1$ . The average wind speed is 7.6 m/s.

---

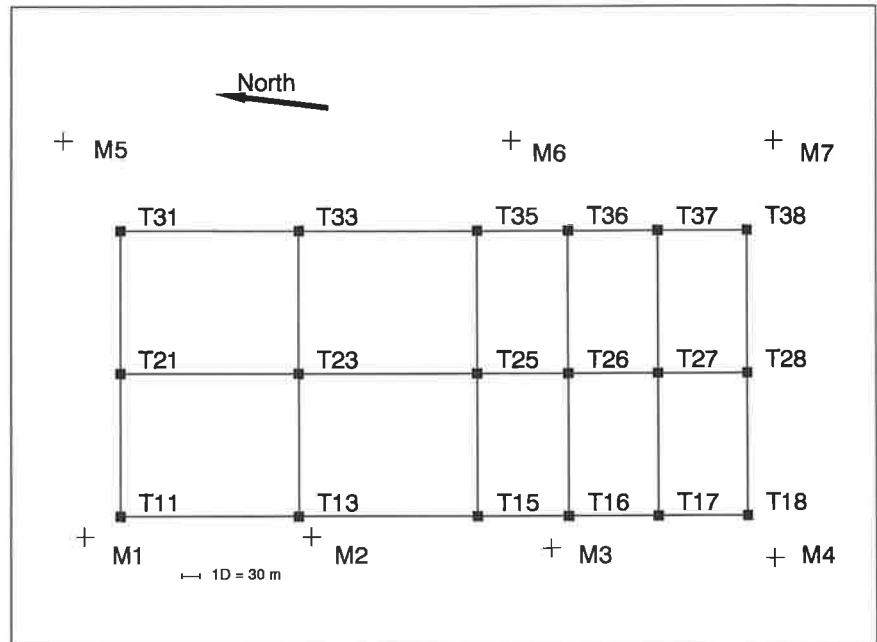
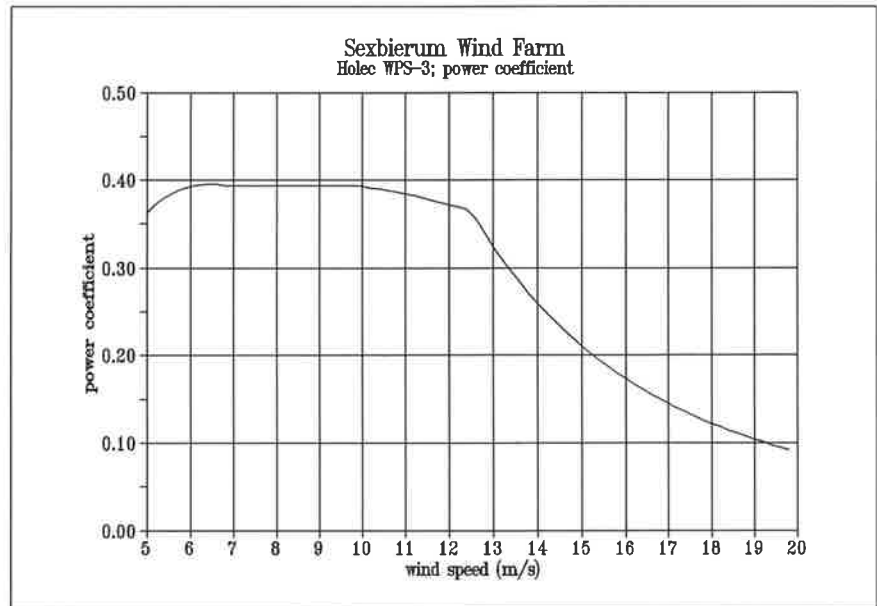
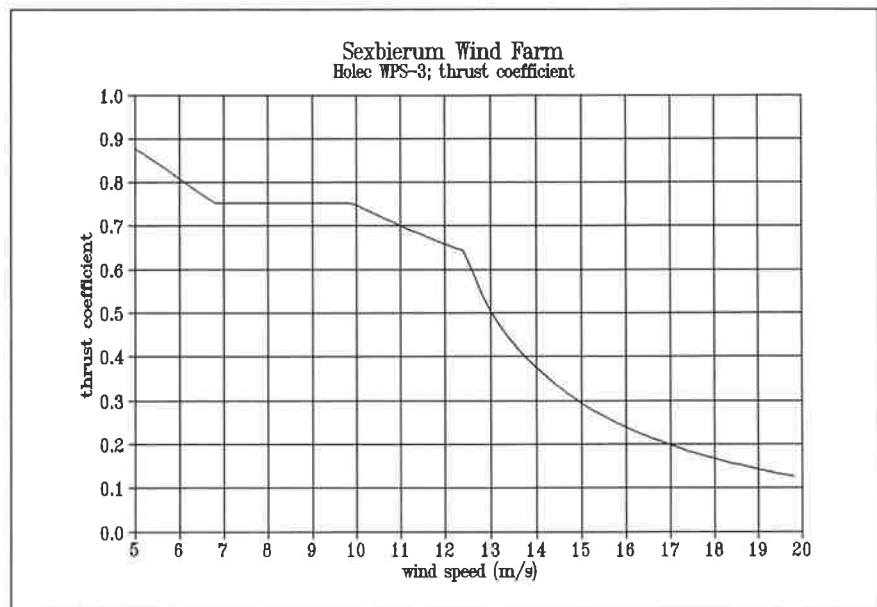
*Results of Sexbierum Wind Farm; single wake measurements*


Figure 2.1 Lay-out of Sexbierum Wind Farm

### 2.1.2 Turbines

The wind turbines in the wind farm are HOLEC machines with three WPS 30/3 blades and with a rated power of 310 kW. The rotor diameter is 30.1 m, the hub height is 35 m. The turbines contain synchronous generators and operate at variable speed. In order to obtain maximum efficiency the tip speed ratio is kept constant up to a wind speed of 10 m/s. Above this wind speed the power is limited by means of pitch control. The machines have a cut-in wind speed of 5 m/s; a rated wind speed of 14 m/s and a cut out wind speed of 20 m/s.

The control computer of the turbine takes care of these action and also takes care of yawing. The input data for the yawing actions comes from the wind farm control computer.

*Results of Sexbierum Wind Farm; single wake measurements**Figure 2.2 Calculated power coefficient of HOLEC WPS-30 wind turbine**Figure 2.3 Calculated thrust coefficient of HOLEC WPS-30 wind turbine*



## Results of Sexbierum Wind Farm; single wake measurements

Figure 2.2 gives the calculated power coefficient; figure 2.3 gives the calculated thrust coefficient of the wind turbine. In Annex A1 more detailed data can be found on the HOLEC wind turbine.

### 2.1.3 Data acquisition

The data-acquisition system and instrumentation of the wind farm serves the following purposes:

- monitoring and control of the wind farm;
- detailed measurements of the wake structure inside the farm;
- wake effects on the mechanical loads on the turbines;
- wake effects on the aggregate wind farm power;
- electrical behaviour of the wind farm.

For this purpose the wind farm has a central computer, which takes care of monitoring and control of the wind farm and a data-acquisition system consisting of measuring computers and data elaboration computers (see figure 2.4).

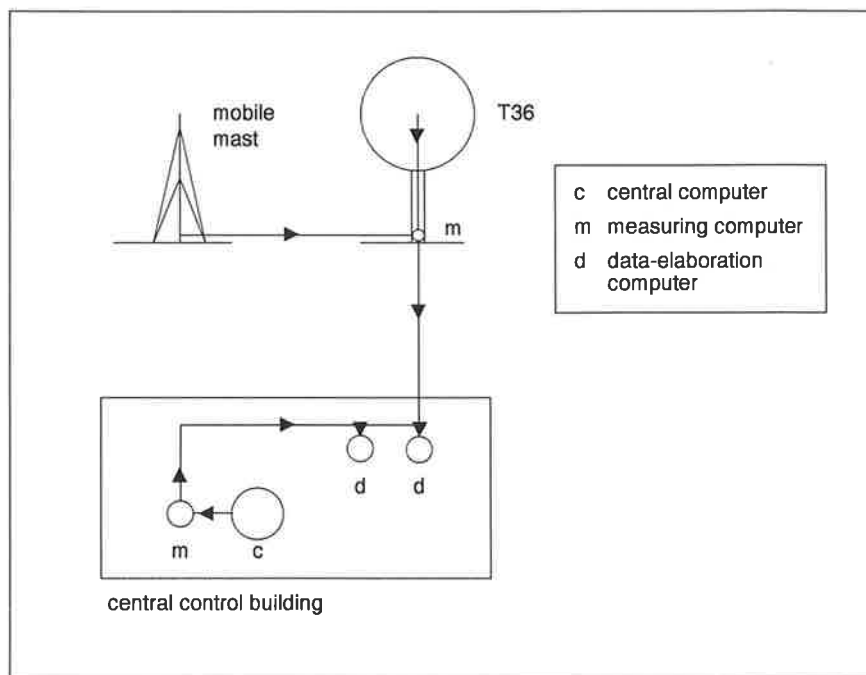


Figure 2.4 The data-acquisition system of the Sexbierum wind farm

The signals from the extra-instrumented turbine T36 are sampled at 32 Hz by a measuring computer inside the tower. The signals from the mobile measuring masts are also connected to this computer and sampled at 4 Hz.

---

*Results of Sexbierum Wind Farm; single wake measurements*

Signals with respect to the electrical behaviour of the wind farm are sampled at 32 Hz by a measuring computer in the central control building. This computer is connected to the central computer which supplies at 1 Hz the following data:

- undisturbed wind speed and wind direction from the stationary wind masts;
- air pressure and temperature;
- status of each wind turbine.

All acquired data are passed to the two central data elaboration computers in the central control building. The data can be processed on-line using statistical software or can be stored on tape or optical data for further processing off-line.

#### **2.1.4 Instrumentation**

##### **Meteorological masts**

The wind farm is surrounded by 7 fixed wind measurement towers. The locations of the towers are given in figure 2.1. Each tower has a wind anemometer and a wind vane at 35 m (hub height). The towers 4 and 6 have also wind sensors at 20 m and 50 m height. At mast 3 the temperature and the air pressure are measured. The signals from the meteorological tower are sampled at a rate of 1 Hz.

##### **Instrumentation of turbines**

Turbine T36 (see figure 2.1) has been extra instrumented. It contains sensors for the measurements of mechanical loads in the blades, the hub, the tower and the drive train. Sensors have been mounted for measurement of the pitch angle, blade position and nacelle direction. Further, various electrical signals are measured. The signals are sampled at a 32 Hz sampling rate. A complete list of the measured signals is given in annex A2.

##### **Mobile wind measuring masts**

There are three mobile masts in the wind farm for detailed wake measurements. It is possible to install the masts at any place inside the wind farm enabling detailed wind measurements of the wake structure.

One mast is equipped with 3-component propeller anemometers at 47 m, 35 m and 23 m, respectively. At heights of 41 m and 29 m two extra cup anemometers have been mounted. The other two masts contain 3-component propeller anemometers at 35 m. The signals from the mobile masts are sampled at a 4 Hz sampling rate.

The 3-component propeller anemometer consists of three light-weight carbon fibre propellers mounted on a pyramid-shaped rig at angles of 30° relative to each other. Combination of the three anemometer signals gives the X, Y and Z components of the wind. The sensor was calibrated in a wind tunnel and yields reliable results within a cone of approximately 30° relative to the sensor centre-line.

## 2.2 Measuring campaign

### 2.2.1 Description

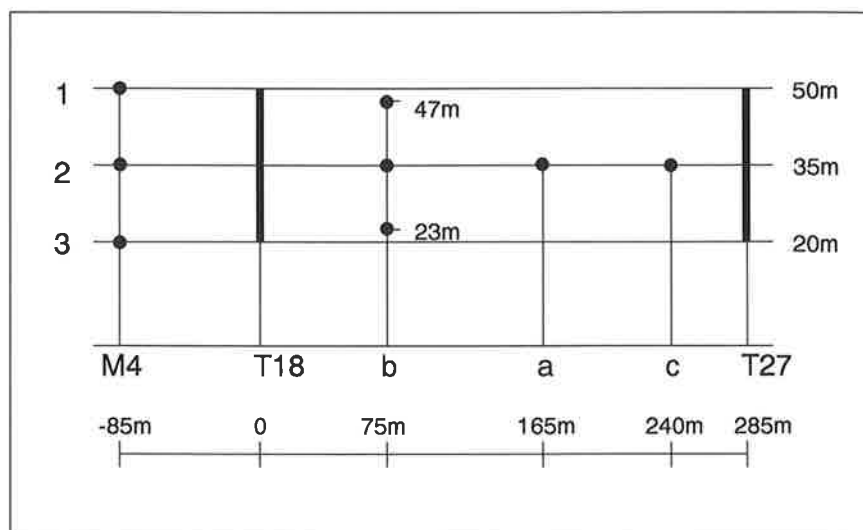


Figure 2.5 Experimental set-up during the measuring campaign

Between 1992 measurements have been made in the wake of T18, ahead of T27 (see figure 2.5). In the indicated direction the distance between the turbines is 285 m, i.e. 9.4.

Mast b, installed 75 m (2.5D) behind T18, contained the 3-component propeller anemometers at 47 m, 35 m and 23 m, denoted b1, b2 and b3. The middle anemometer was thus mounted at hub height, the top and bottom anemometers at 0.4 rotor diameters above and below hub height. Mast a was erected 165 m (5.5D) behind T18 and contained a 3-component propeller anemometer at hub height, denoted a2. Mast c was installed at 240 m (8D) behind T18 and contained a 3-component propeller anemometer at hub height, denoted c2. The undisturbed wind conditions were measured with cup anemometers at wind vanes at mast 4 at 3 levels (20 m, 35 m and 50 m). Simultaneously with the wind measurements the power of T18 was measured. Table 2.1 gives an overview of the stored data.

---

*Results of Sexbierum Wind Farm; single wake measurements*

Table 2.1 Overview of the measured and stored data

Sensor	Signal
a2..c2	$U, V, W, U_{\max}, U_{\min}, V_{\max}, V_{\min}, W_{\max}, W_{\min}, u'^2, v'^2, w'^2, u'v', u'w', v'w'$
b2l, b2h	$U, u', U_{\max}, U_{\min}$
P18	$P, \sigma_P, P_{\max}, P_{\min}$
wvel41, 42, 43	$U_0, u'_0, U_{0\max}, U_{0\min}$
wdir41, 42, 43	$\delta_0, \sigma_{\delta_0}, \delta_{0\max}, \delta_{0\min}$
sblh18	pitch angle T18, $\sigma_{\text{pitch}}, \text{pitch}_{\max}, \text{pitch}_{\min}$

The measured data were stored on hard disk and every day a back-up was made on magnetic tape. Later, the tapes were pre-processed off-line into 1-minute averaged samples.

### 2.2.2 Observations

During the measuring campaign no serious problems arose and a body of approximately 2700 1-minute samples were recorded successfully.

The following problems were observed:

- sensor wv1c2 ( $X/D=8$ ) had no signal for about one third of the samples;
- the wind direction sensors at the undisturbed wind measuring mast had a misalignment of  $+5^\circ$ ,  $+5^\circ$  and  $-10^\circ$  for height 1, 2 and 3, respectively. The measurements have been corrected for this;
- the topmost sensor wvel41 shows a dip in the wind speed measurements due to shading of a lightning conductor for wind directions between  $170^\circ$  and  $210^\circ$ .
- sensor wvel42 showed malfunctioning at the end of the measuring period, indicating too low wind speeds. During a first analysis this resulted in 'skew' profiles of (for instance)  $U/U_0$  combined with considerable scatter. In the final analysis use was made of sensor wvel43, which resulted in 'flat' profiles with reduced scatter.

### 3 Analysis

#### 3.1 Pre-processing and resulting database

A first data-reduction and quality control of the measured data was done during pre-processing of the data. The 1 Hz and 4 Hz time series of the measured quantities were manipulated in order to obtain time series of 1-minute averages of various quantities such as the wind speed, the turbulent velocities and the shear stress. Table 2.1 gives an overview of the time series contained in the data base. The 1-minute data have served as the working data base. The chosen format makes it possible to combine the 1-minute averages into samples with multiple-minute averages. Annex A3 gives the statistical operations used for the data manipulation.

#### 3.2 Time averaging

Before the data base was further analysed, the samples were combined to obtain 3-minutes averaged quantities. Considerations for selecting a period of 3 minutes were the following:

- **stationarity of the data**

It is common practice to assume a spectral gap for wind velocity data between 10 minutes and 1 hour. Shorter averaging periods will result in non-stationary data;

- **coherence between undisturbed wind signal and wake signal**

Meteorological mast 4 and mobile mast c are 330 m apart, assuming a wind speed of 8 m/s, this corresponds to a delay of 45 seconds, approximately. In order to obtain a reasonable coherence between the wake wind data and the undisturbed wind data it is necessary to use an averaging period greater than this period.

- **effect of slow wind direction variations**

If the averaging period is chosen too long, slow variations in the wind direction will blur the details of the wake.

- **number of available records**

Longer averaging periods result in less samples. A 3-minutes averaging period resulted in a database with 857 samples.

- **effect on wind turbines**

Power curves for wind turbines are most often determined using averaging periods of 10 minutes; Wind fluctuations shorter than 1 minute are most important for the determination of wind turbine loads. Slower fluctuations are absorbed by the control system.

The wake deficit profiles are hardly affected by the averaging period. However, non-linear signals, such as turbulent velocities and shear stresses are indeed affected by the changing averaging period. Longer averaging periods result in higher turbulent velocities, for instance. Nevertheless, it is not easy to select an optimum averaging period. Taking into account the arguments listed above, it was decided to analyse the data on the basis of 3-minutes averaged samples.

### 3.3 Frame of reference

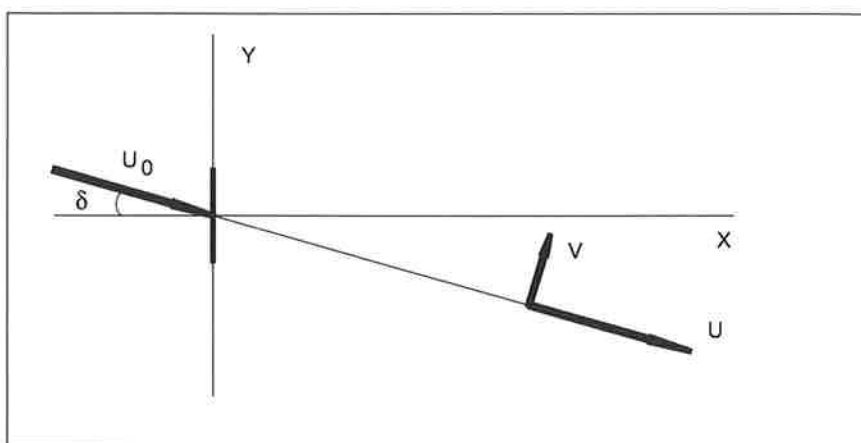


Figure 3.1 Definition of the frame of reference

Besides scalar quantities, such as the wind turbine power and the total turbulent kinetic energy  $k$ , also vector quantities (wind vector) and tensor quantities (turbulent co-variance matrix) had to be analysed. Therefore it was necessary to define a proper frame of reference for the presentation of the data. It was decided to couple the frame of reference of the wake data to the co-ordinate system of the undisturbed wind. The definition of the frame of reference is given in figure 3.1. The undisturbed wind direction is given with respect to the line connecting the turbines T18 and T27, defined as 0 degrees. The  $u$ -component is parallel to the undisturbed wind, the  $v$ -component is perpendicular to the undisturbed wind in the horizontal plane. The  $w$ -component is in the vertical direction.  $u, v$  and  $w$  define a right-handed co-ordinate system. This conforms to the normal meteorological definitions. Before the 3-minutes samples were bin-sorted, they were converted first to the above given coordinate system, using the co-ordinate transformation formulas given in Annex A3.

### 3.4 Bin-sorting

The 3-minutes samples were sorted into different bands of undisturbed wind speed and wind direction. Between 5 m/s and 12 m/s a bin width of 1 m/s was used; above 12 m/s the bin width was taken equal to 2 m/s. The selected wind direction bin width was 2.5°.

---

*Results of Sexbierum Wind Farm; single wake measurements*

For each bin the mean value, variance, minimum and maximum values of the measured quantities were determined and saved in separate files. Together with these quantities the number of samples in the bin, the average undisturbed wind speed and the average wind direction were saved.

Since the wind turbines operate at constant tip speed ratio in the interval 6-10 m/s, it was expected that the wake effects would not vary much over this speed range. A selected number of bin analyses has been made using a single wind speed bin of 5-10 m/s.

### 3.5 Dimensionless quantities

Except in dimensional form the results are also presented in a non-dimensionalized form.

First, the measured quantities have been non-dimensionalized with the undisturbed wind speed:

- $U/U_0, V/U_0, W/U_0;$
- $u'/U_0, v'/U_0, w'/U_0, k/U_0^2, u'/u'_0;$
- $u'v'/U_0^2, u'w'/U_0^2, v'w'/U_0^2.$

Second the quantities have been non-dimensionalized using local parameters:

- $V/U, W/U;$
- $u'/U, v'/U, w'/U, k/U^2;$
- $u'v'/k, u'w'/k, v'w'/k.$

In the next chapter the results of the analysis are presented.

## 4 Results

This chapter contains the results of the analysis performed on the single wake data described in the previous chapters. First, the undisturbed wind conditions during the measuring period are described. Secondly, the power output of the turbine in the free-stream (T18) investigated. The next sections describe the results of the wind measurements on the mobile measuring masts. Successively, the wind speed, the turbulence levels and the shear stresses in the wake are treated for a selected number of cases. A comprehensive overview of the analysis results can be found in annex A4.

### 4.1 Undisturbed wind conditions

This section describes the undisturbed wind conditions at the Sexbierum wind farm during the single wake measuring period. Further a description of the undisturbed turbulence intensity is given and the roughness length of the upwind terrain is estimated.

#### 4.1.1 Wind speed distribution

Figure 4.1 gives the wind speed distribution during the measuring period. It shows that the majority of the data has been found between 7 and 9 m/s. The average wind speed in the measuring period was 8.4 m/s. Negative wind directions clearly prevail. Figure 4.2 show the frequency distribution during the measuring campaign.

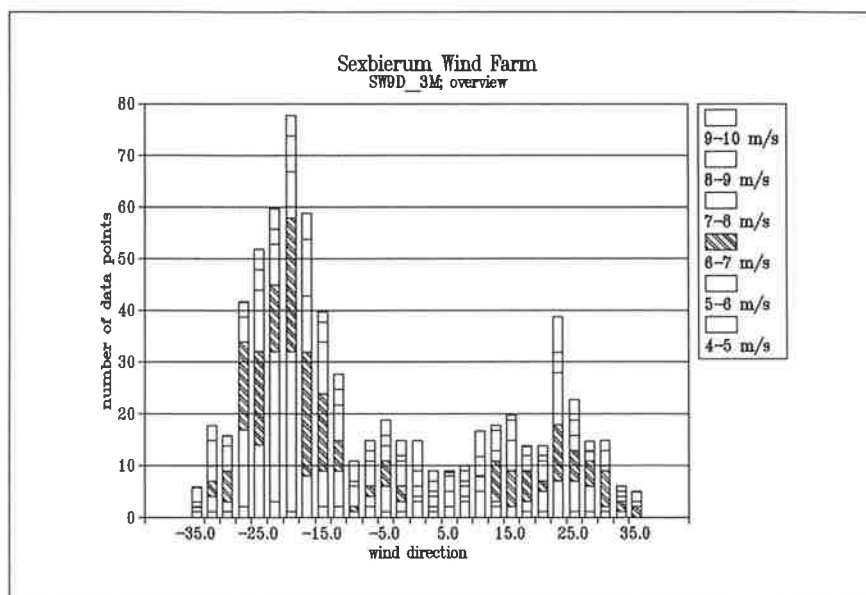


Figure 4.1 Overview of available data



Results of Sexbierum Wind Farm; single wake measurements

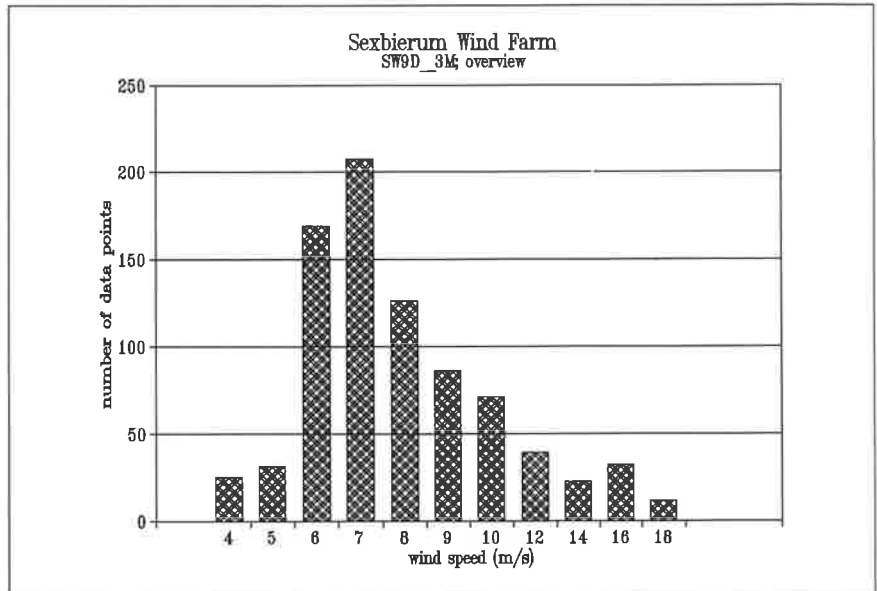


Figure 4.2 Frequency distribution of the wind speed during the measuring campaign

The average wind speed during the measuring campaign was 8.4 m/s

4.1.2 Undisturbed wind profile

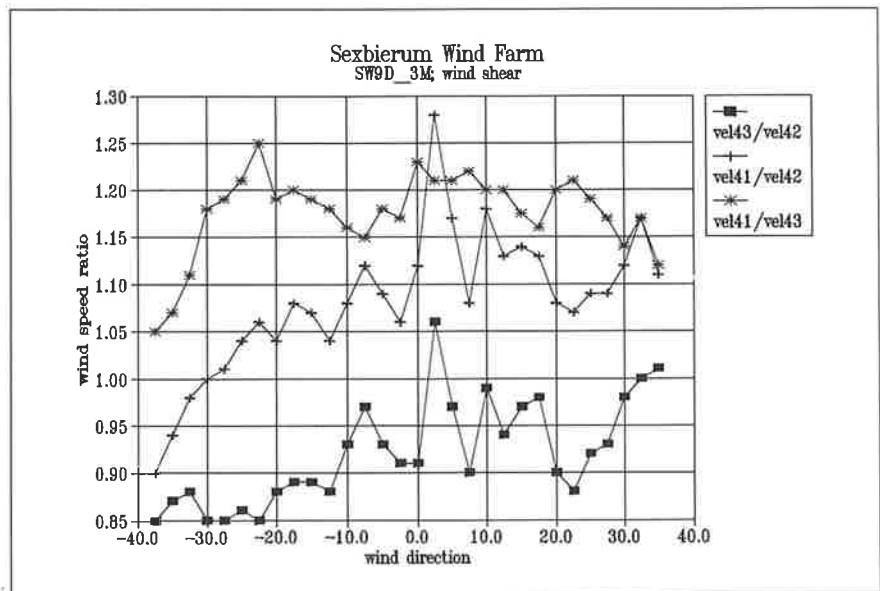


Figure 4.3 Ratio of the undisturbed wind speeds at three heights

---

*Results of Sexbierum Wind Farm; single wake measurements*

Figure 4.3 gives the ratio of the wind speed for the combinations wvel41/wvel42, wvel43/wvel41 and wvel41/wvel43 in the wind sector under consideration. The following remarks can be made:

- for wind directions from -40 to -20 degrees wvel41/wvel43 and wvel41/wvel42 show a dip. This is caused by the wake of a lightning conductor which is mounted on top of meteorological mast 4. The other anemometers are not affected by this effect because they are connected to the mast by means of a boom;
- Except for the velocity dip due to the lightning conductor the ratio wvel41/wvel43 is constant. The ratio wvel42/wvel43 and wvel41/wvel42 shows a steady increase with increasing values of the wind direction. During initial analysis of the single wake data, making use of wvel42 for binning the data, this resulted in skew wind profiles. Reviewing of the wvel42 records showed that this anemometer showed irregular malfunctioning during the last period of the measuring campaign. Therefore it was decided to use the undisturbed anemometer wvel43 for the analysis of the wake data.

Due to the abovementioned effects it is hard to determine a reliable estimate of the roughness length  $z_0$ . Yet, using the data resulted in a roughness length of  $z_0=0.13$  m. In the next section the roughness length is also estimated from the measured turbulence intensity.

#### 4.1.3 Turbulence intensity

Table 4.1 Turbulence intensity at 3 measuring heights

Measuring height	Turbulence intensity	Corrected intensity	$z_0$
20 m	0.100	0.145	0.046
35 m	0.095	0.138	0.058
50 m	0.086	0.125	0.044

The turbulence intensity has been determined by applying linear regression on pairs of undisturbed wind speed  $U_0$  and turbulent velocity  $u'_0$  for an averaging time of 3 minutes. In order to estimate the turbulence intensity for a 1-hour average the correction was applied as described in [Cleijne, 1992]. The result is shown in table 4.1 for the three measuring heights.

Using the expressions given in [Panofsky and Dutton, 1984] the roughness length has been estimated. This results in a roughness length of  $z_0 = 0.047$  m, which seems to agree well with the results from the double wake campaign. It should be noted that this estimate is insensitive to calibration errors in the sensors.

Finally, it is possible to estimate  $z_0$  from the turbulence intensity **profile**  $I(z)$  using regression. This method resulted in the estimate  $z_0 = 0.049$  m.

## Results of Sexbierum Wind Farm; single wake measurements

Taking into account the uncertainties in the measurement of the wind profile, the roughness length estimate from the turbulence intensity is preferred to the one from the wind profile.

### 4.2 Wind turbine power

#### 4.2.1 Free-stream power curve

Figure 4.4 gives the power curve of turbine T18 using data from all available undisturbed wind directions with respect to the wind speed at 20 m height.

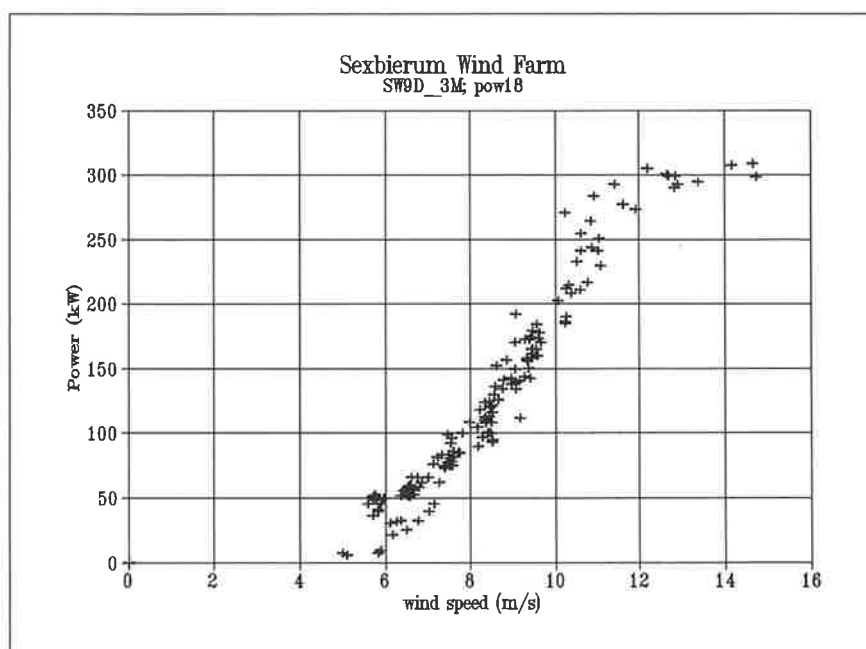


Figure 4.4 Power curve and power coefficient of wind turbine T18, based on 3-minutes averages

#### 4.2.2 Pitch control

The HOLEC WPS turbines have a constant pitch angle below 10 m/s and are kept at constant tip speed ratio by load variation. Above 10 m/s the pitch angle is varied in such a way that the power is limited to 310 kW maximum. Figure 4.5 shows the pitch angle of turbine T18 as a function of the undisturbed wind speed wvel43.

Results of Sexbierum Wind Farm; single wake measurements

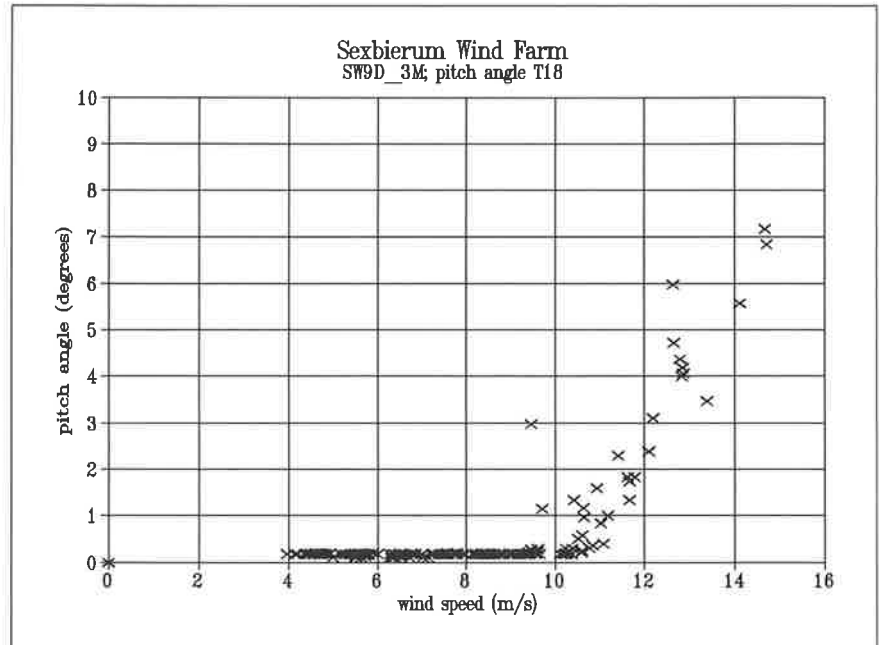


Figure 4.5 Pitch angle as a function of undisturbed wind speed

### 4.3 Wake deficit

#### 4.3.1 Wake deficit per bin

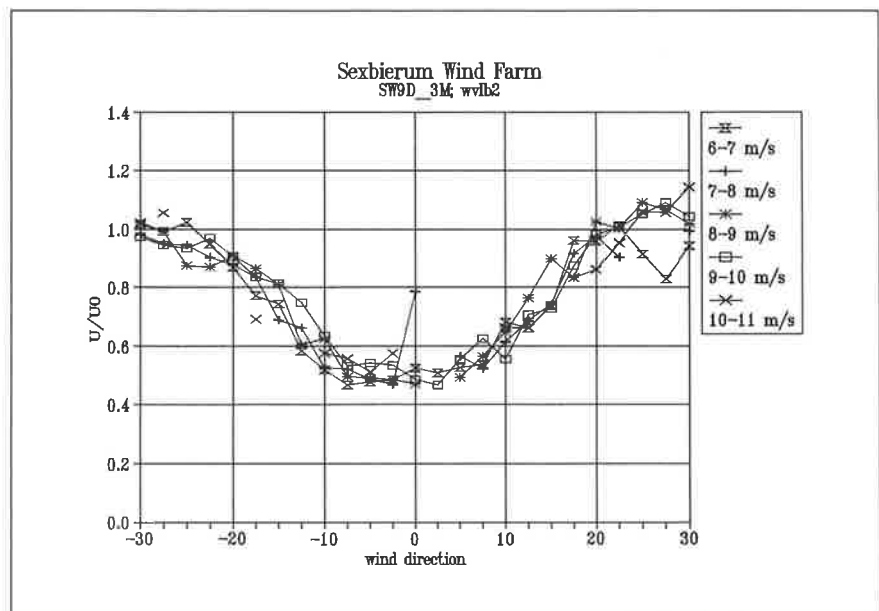


Figure 4.6 Wind speed ratio  $U/U_0$  at sensor b2 as a function of the undisturbed wind direction

### Results of Sexbierum Wind Farm; single wake measurements

Figure 4.6 shows the wind speed ratio  $U/U_0$  at sensor b2 as a function of the undisturbed wind direction for the wind speed classes between 6 m/s and 11 m/s. Sensor b2 was located at hub height  $2.5D$  behind T18. The graphs of  $U/U_0$  of the other sensors have been gathered in annex A4.

The figure shows that the wind speed ratio  $U/U_0$  is almost equal for the depicted wind speed classes, which can be explained by the fact that the wind turbines operate at constant tip speed ratio between 6 and 10 m/s. In this range the thrust or axial force is therefore almost constant.

At the wake centre-line  $U/U_0$  reaches a minimum of 0.50, approximately. At an undisturbed wind direction of 20 degrees the edge of the wake is observed and  $U/U_0$  is equal to unity. The shape of the wake profile is not completely Gaussian, but more flattened. This is probably due to the fact that mast b is at a distance of  $2.5 D$  only.

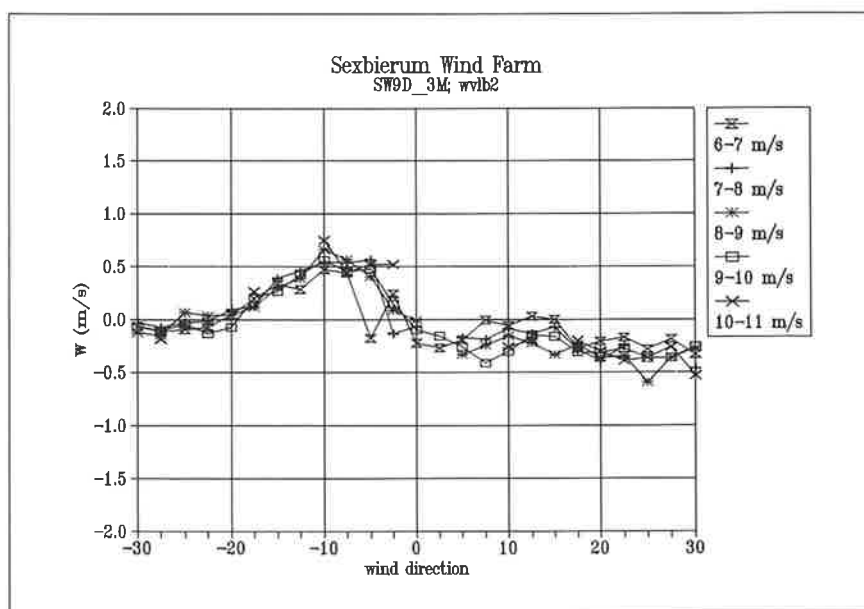


Figure 4.7 Vertical wind speed  $W$  as a function of wind direction at sensor b2

The values of the lateral wind speed  $V$  are small compared to those of the longitudinal component and have not been depicted.

Figure 4.7 shows the vertical velocity  $W$ . The figure shows that  $W/U_0$  is positive for negative wind directions and  $W$  is negative for positive wind directions. This agrees with the fact that the rotor rotates clock-wise, when looking down-wind. The velocities are small, however.

## 4.3.2 Aggregated results

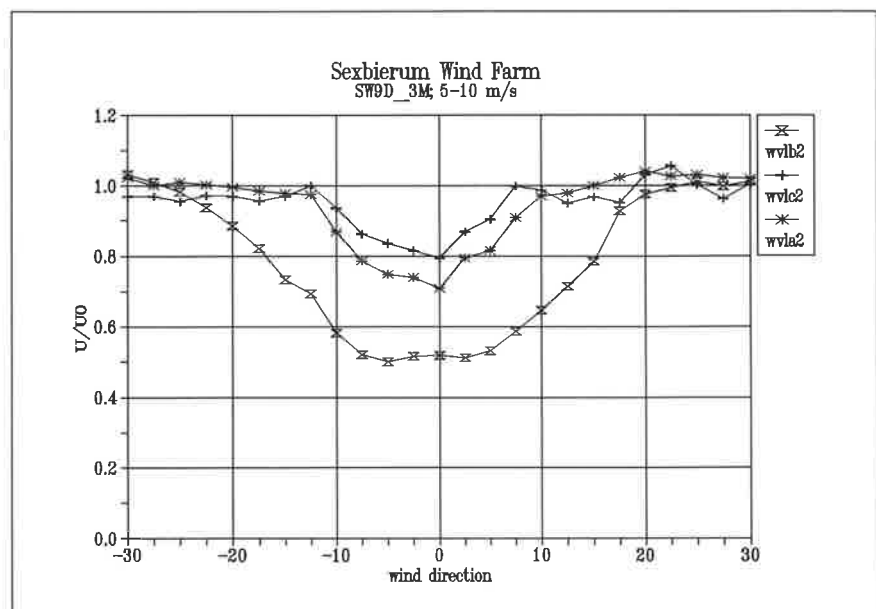


Figure 4.8 Wind speed ratio  $U/U_0$  as a function of wind direction for sensors b2, a2 and c2

Figure 4.8 shows the aggregated results in the wind speed range of 5-10 m/s for the three sensors b2, a2, c2 at hub height. Sensor b2 is at 2.5D behind the rotor; a2 at 5.5D and c2 at 8D.

At  $x = 2.5D$  the wind speed ratio is 0.5; at  $x=5.5D$  a value of  $U/U_0=0.7$  is found and at  $x=8D$  the wind speed ratio is 0.8.

Clearly, the flattened profile at  $x=2.5D$  develops in a more pronounced profile.

Results of Sexbierum Wind Farm; single wake measurements

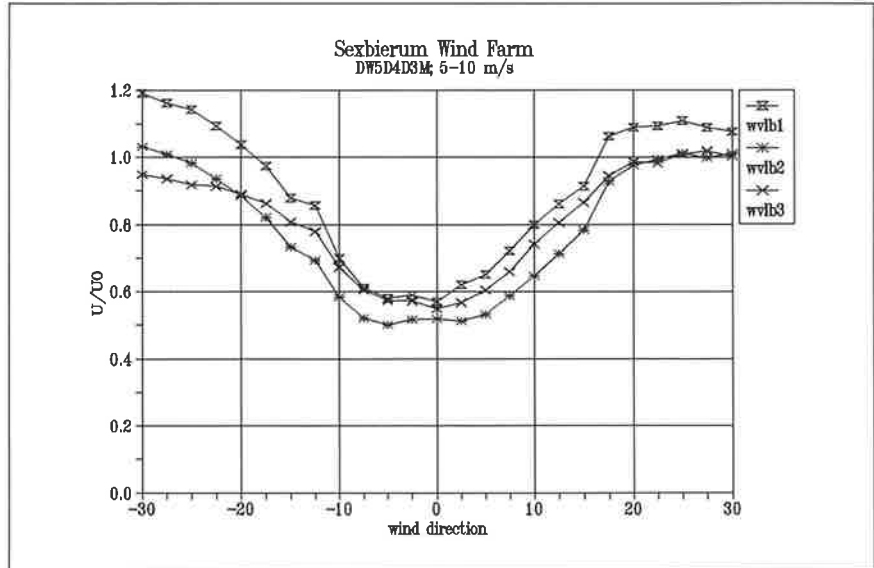


Figure 4.9 Wind speed ratio  $U/U_0$  as a function of wind direction for sensors b1, b2 and b3

Figure 4.9 gives the ratio  $U/U_0$  at the 3 sensors mounted at different heights on mast b, which is at 2.5D behind turbine T18. The figure clearly reveals that the wake profiles are almost identical in shape at the given heights, with the lowest values of  $U/U_0$  at hub height. Outside the wake (see negative wind direction), the wind speeds increase from the lowest sensor b3 to the highest sensor b1, which agrees with a normal boundary layer flow.

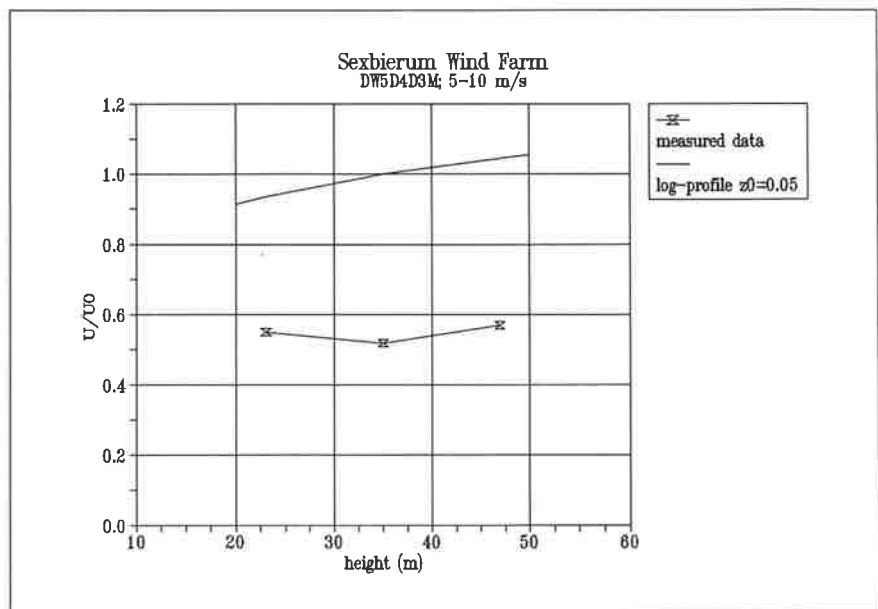


Figure 4.10 Vertical wake profile at the wake centre-line

## Results of Sexbierum Wind Farm; single wake measurements

In figure 4.10 the vertical profile of  $U/U_0$  is given, together with the calculated undisturbed wind profile using  $z_0=0.045$  m.

### 4.4 Turbulence intensity

#### 4.4.1 Turbulence intensity data per bin

In this section we show the results of the analysis on the measured turbulence in non-dimensional form.

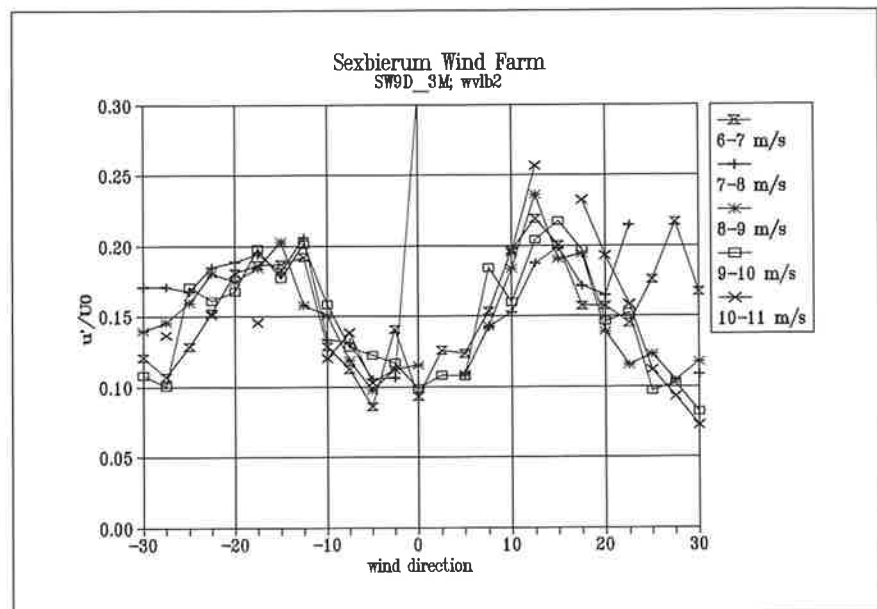


Figure 4.11 Turbulence intensity  $u'/U_0$  as a function of wind direction at sensor b2

Figure 4.11 shows the turbulence intensity (non-dimensionalized with  $U_0$ ) of the horizontal wind component for sensor b2 as a function of the wind direction. Figures 4.12 and 4.13 show the lateral and vertical turbulence intensity. The figures show that the turbulence intensity increases towards the centre of the wake.  $u'/U_0$  is strongly peaked for wind directions of -15 and +15 degrees, which corresponds to the locus of the maximum wind speed gradient (see figure 4.6). There the turbulence production is at a maximum:  $u'/U_0 \approx 0.2$ , compared with an undisturbed value of  $u'/U_0 \approx 0.1$ .

The peaks in the lateral and vertical turbulence intensity are less pronounced (see figure 4.12 and 4.13).



## Results of Sexbierum Wind Farm; single wake measurements

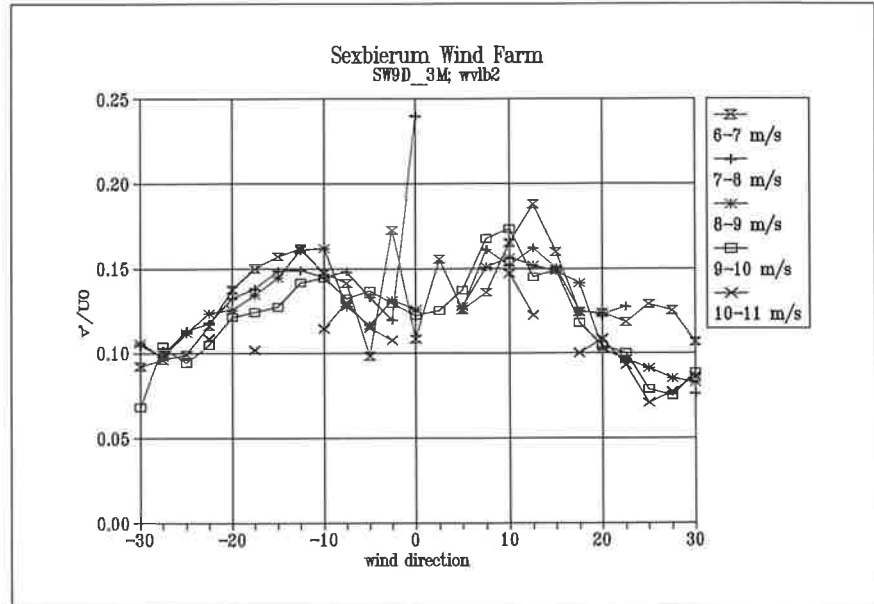
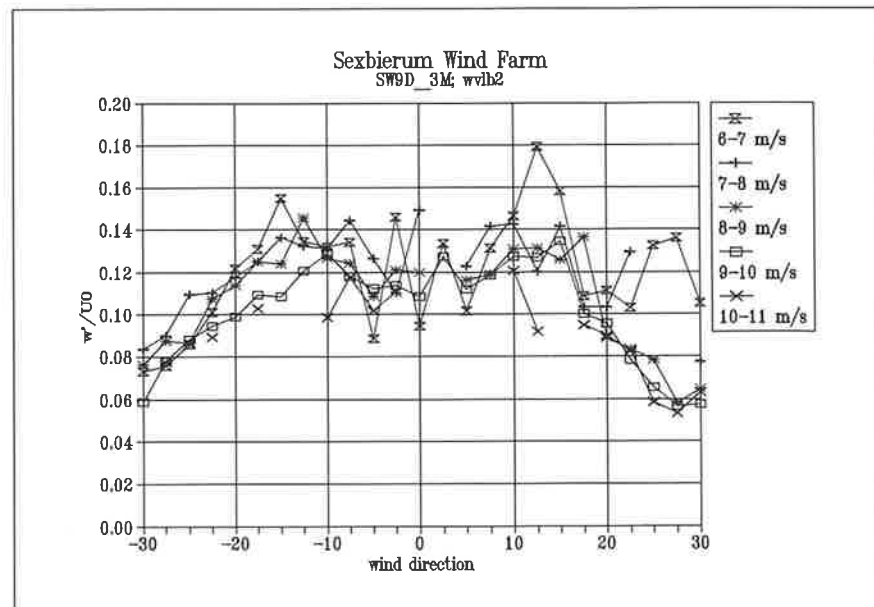
Figure 4.12 Lateral turbulence intensity  $v'/U_0$  as a function of wind direction at sensor b2Figure 4.13 Vertical turbulence intensity  $w'/U_0$  as a function of wind direction at sensor b2

Figure 4.14 shows the turbulent kinetic energy  $k$  (non-dimensionalized with  $U_0$ ) as a function of the wind direction. The behaviour of  $k$  is roughly the same as that of the components of the turbulence.

## Results of Sexbierum Wind Farm; single wake measurements

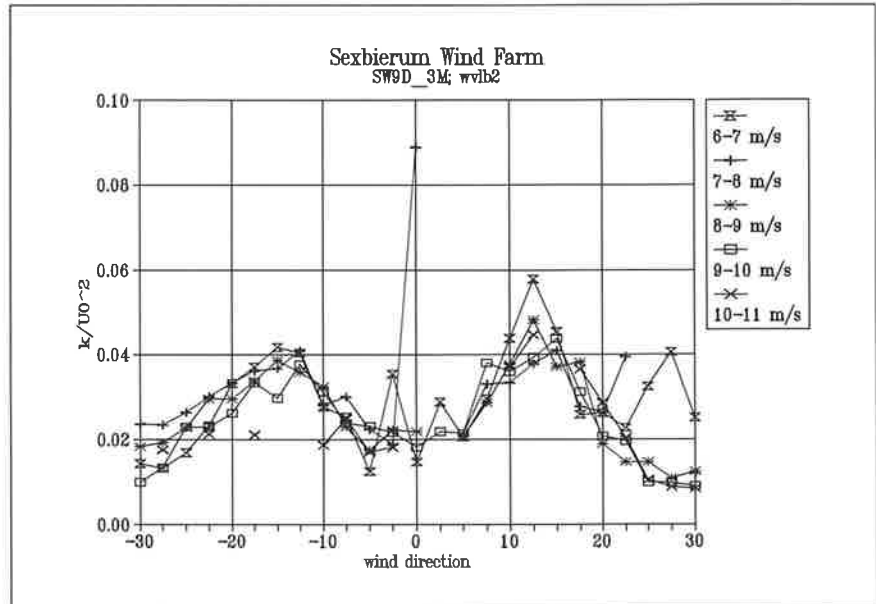


Figure 4.14 Turbulent kinetic energy  $k/U_0^2$  as a function of wind direction at sensor b2

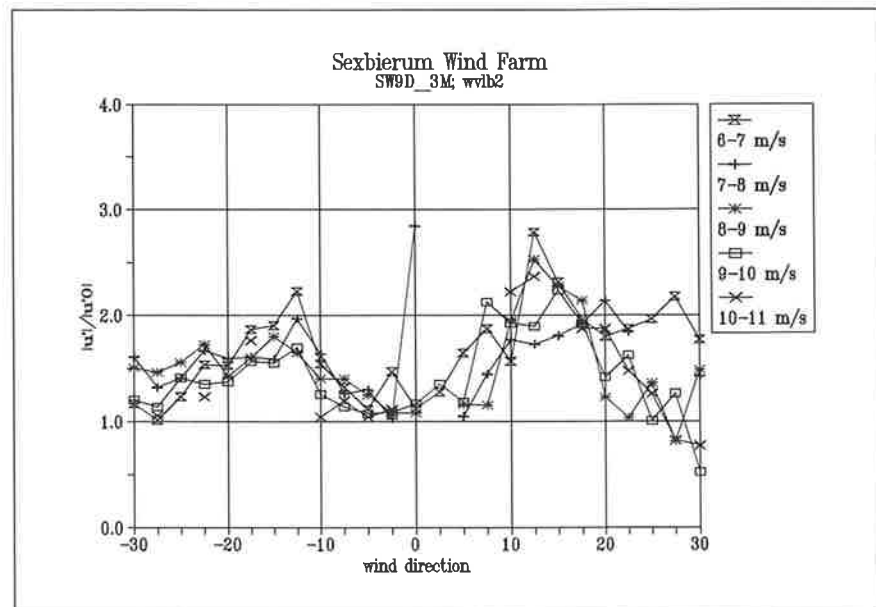


Figure 4.15 Ratio of wake turbulence and undisturbed turbulence  $u'/u'_0$  as a function of wind direction at sensor b2

In figure 4.15 the ratio  $u'/u'_0$  is given as a function of the wind direction. The figure shows again that the turbulence level is increased in distinct peaks at this distance ( $x=2.5 D$ ). The turbulence are increased by a factor of 2 in the peaks, approximately.

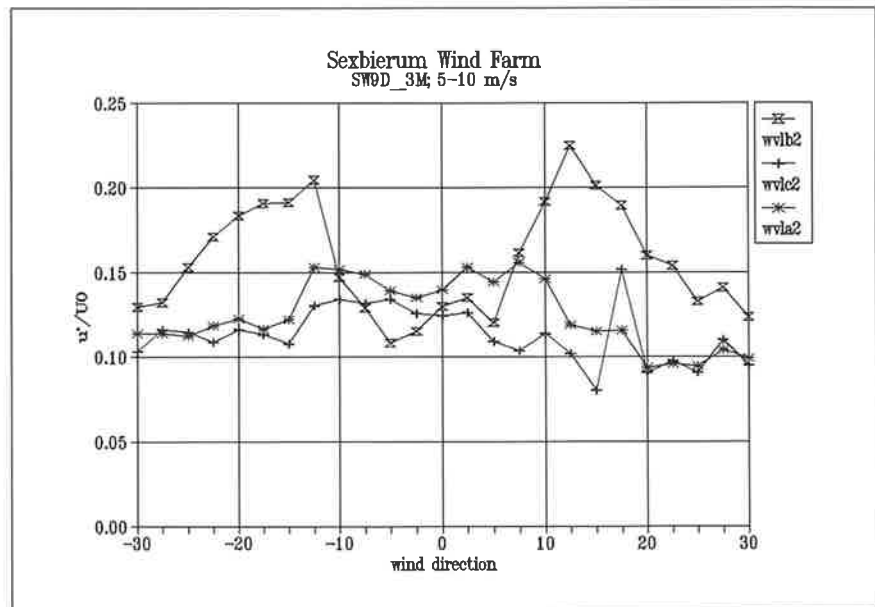
*Results of Sexbierum Wind Farm; single wake measurements***4.4.2 Aggregated results**

Figure 4.16 Aggregated turbulence intensity  $u'/U_0$  at different distances behind the rotor (wvlb2:  $x=2.5D$ ), wvla2  $x=5.5D$ ; wvlc2:  $x=8D$ )

Figure 4.16 shows the development of the turbulence intensity profile as a function of the distance behind the wind turbine. Clearly, at a distance of  $x=5.5D$  the peaks have diffused into a plateau, with a level about 1.5 times higher than the undisturbed turbulence intensity.

## Results of Sexbierum Wind Farm; single wake measurements

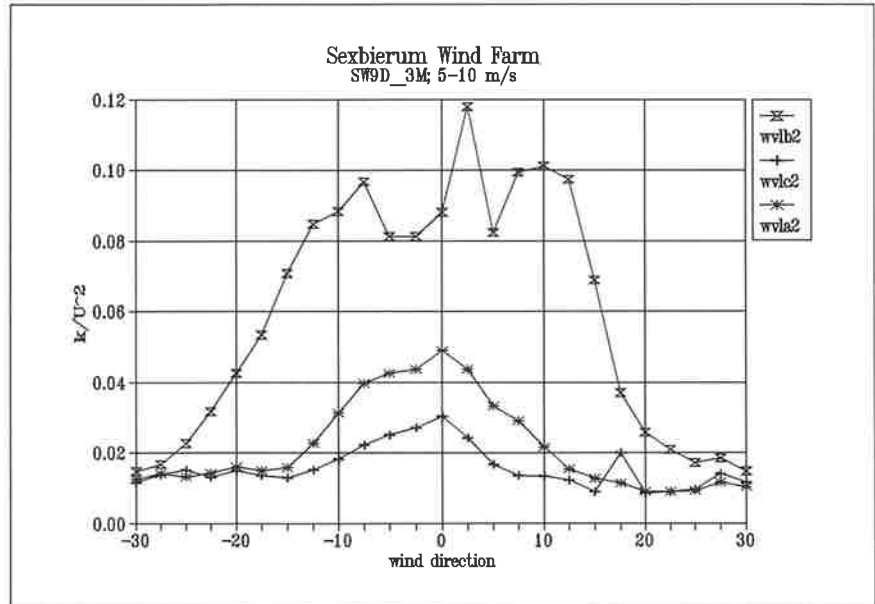


Figure 4.17 Aggregated turbulent kinetic energy  $k$  non-dimensionalized with the local wind speed  $U$  at  $x=2.5D$  (wvlb2);  $k=5.5D$ (wvla2)  $x=8D$  (wvlc2)

Figure 4.17 shows the development of the turbulent kinetic energy non-dimensionalized with the local wind speed  $U$  at the three measuring positions  $x=2.5D$ ,  $x=5.5D$  and  $x=8D$ .

At  $x=2.5D$   $k/U^2 \approx 0.10$ ; at  $x=5.5D$   $k/U^2 \approx 0.05$  and at  $x=8D$   $k/U^2 \approx 0.03$ .

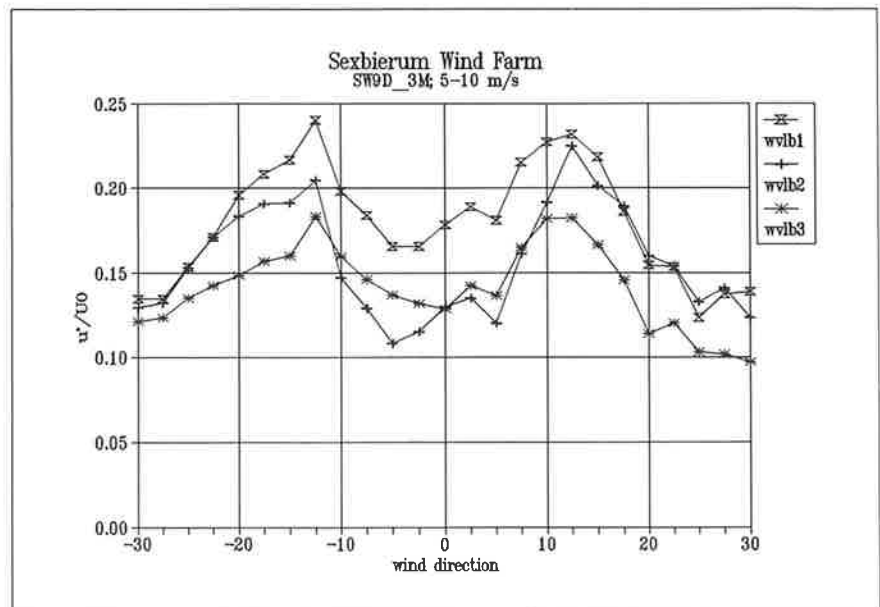


Figure 4.18 Aggregated turbulence intensity  $u'/U_0$  as a function of wind direction at mast b

*Results of Sexbierum Wind Farm; single wake measurements*

Figure 4.18 depicts the turbulence intensity  $u'/U_0$  at mast b for the positions 1, 2 and 3. Peaks are found at wind directions of  $-12.5$  and  $+12.5$  degrees. Clearly, the turbulence intensity is the highest at the top-most sensor ( $k/U_0^2=0.24$ ) and lowest at the bottom-most sensor ( $k/U_0^2=0.18$ ). This corresponds well to what is expected. As production of turbulence is related to the wind velocity gradient, the highest turbulence is expected where the gradients are at maximum. At the highest sensor position the boundary layer wind velocity gradient is increased by the presence of the wake, while the wake decreases the gradient at the lowest sensor position (see figure 4.26).

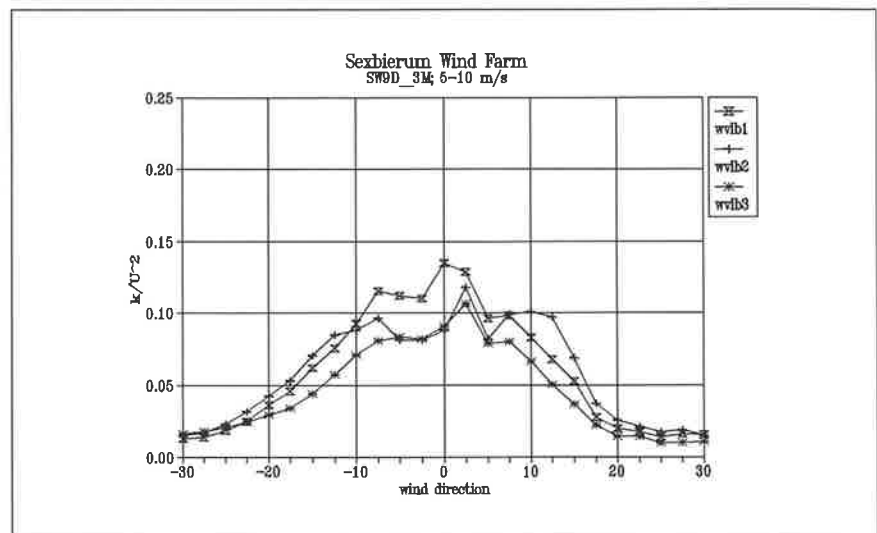


Figure 4.19 Turbulent kinetic energy non-dimensionalized with local velocity as a function of wind direction

Figure 4.19 depicts the turbulent kinetic energy non-dimensionalized with the local wind speed.

## 4.5 Shear stress

### 4.5.1 Shear stress per bin

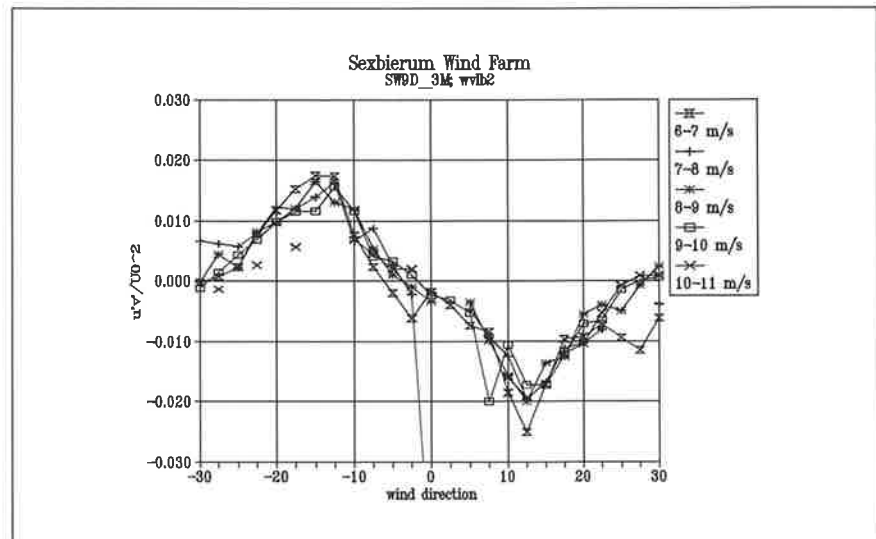


Figure 4.20 Shear stress  $u'v'/U_0^2$  as a function of wind direction at sensor b2

The Reynolds-stress  $u'v'$  is the turbulent shear stress which is the driving force for the recovery of the wake deficit in horizontal direction. Figure 4.20 shows the shear stress  $u'v'$  non-dimensionalized with the undisturbed wind speed  $U_0$  against the undisturbed wind. Starting from the right side of the figure (positive wind directions) and going to the negative wind directions it shows that at the edge of the wake  $u'v'/U_0^2$  is equal to zero and then shows a minimum of -0.020. At  $0^\circ$  wind direction it goes through zero, it then shows a maximum of 0.015 before it relaxes again to 0 at the left edge of the wake. Generally speaking this is expected, since it is generally assumed that the shear stress is proportional to the local wind shear, i.e. the horizontal wind gradient. The fact that the curves return to zero at the edge of the wake, and that they cross the x-axis at  $0^\circ$  wind directions gives confidence in the quality of the data. Scaling of the data with  $U_0$  seems to be successful.

## Results of Sexbierum Wind Farm; single wake measurements

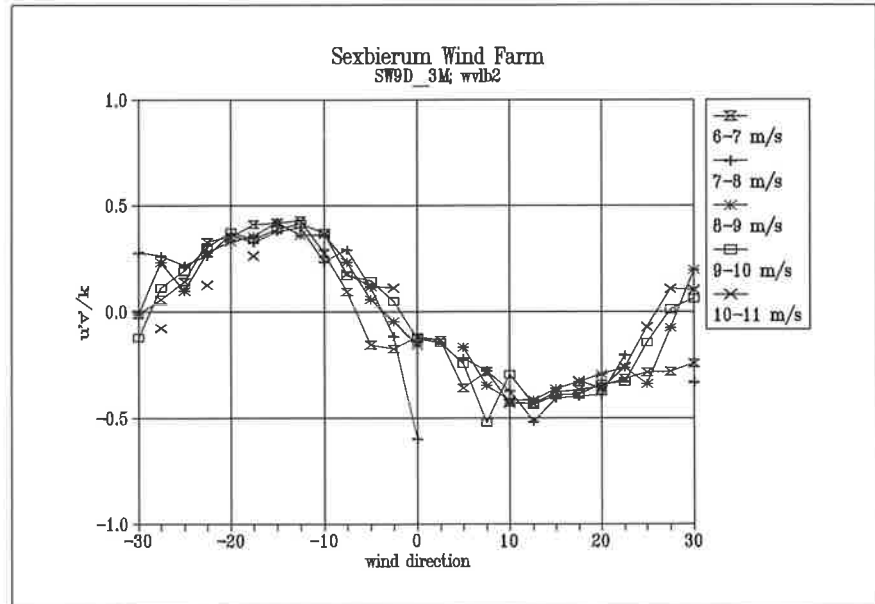


Figure 4.21 Shear stress  $u'v'$  non-dimensionalized with the local turbulent kinetic energy as a function of wind direction at sensor b2

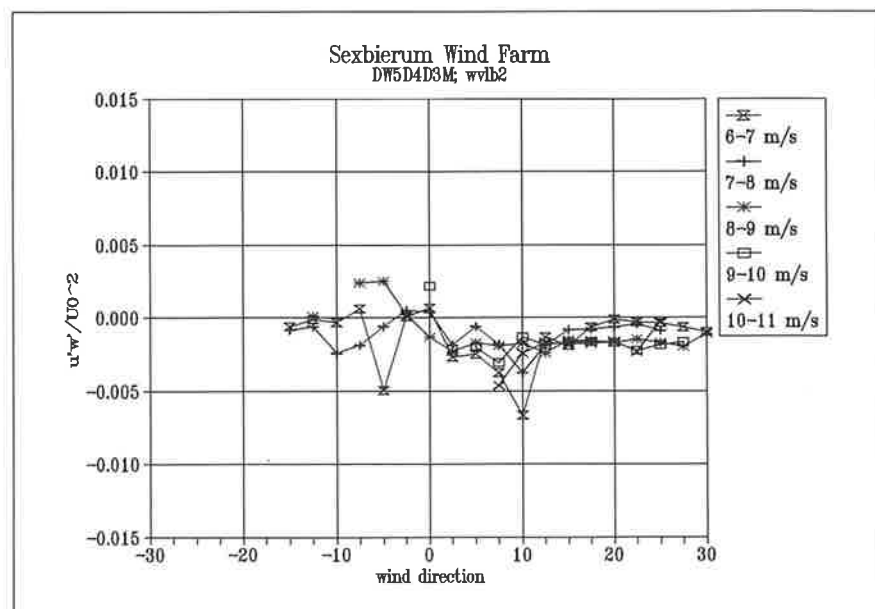


Figure 4.22 Shear stress  $u'w'/U_0^2$  as a function of wind direction at sensor b2

The  $u'w'$ -component is given in figure 4.22. Apparently there is hardly a  $u'w'$ -component at sensor b2. This can be explained by the fact that sensor is at the symmetry plane of the wake. Indeed the sensors at different positions show a significant  $u'w'$ -component variation over the wind directions. This will be discussed in the next section.

## Results of Sexbierum Wind Farm; single wake measurements

The  $v'w'$ -component of the shear stress also turns out to be very small at sensor position b2. This shear stress component is proportional to the spatial derivatives of  $V$  and  $W$ , which are both very small. Hence the shear stresses are also small.

### 4.5.2 Aggregated results

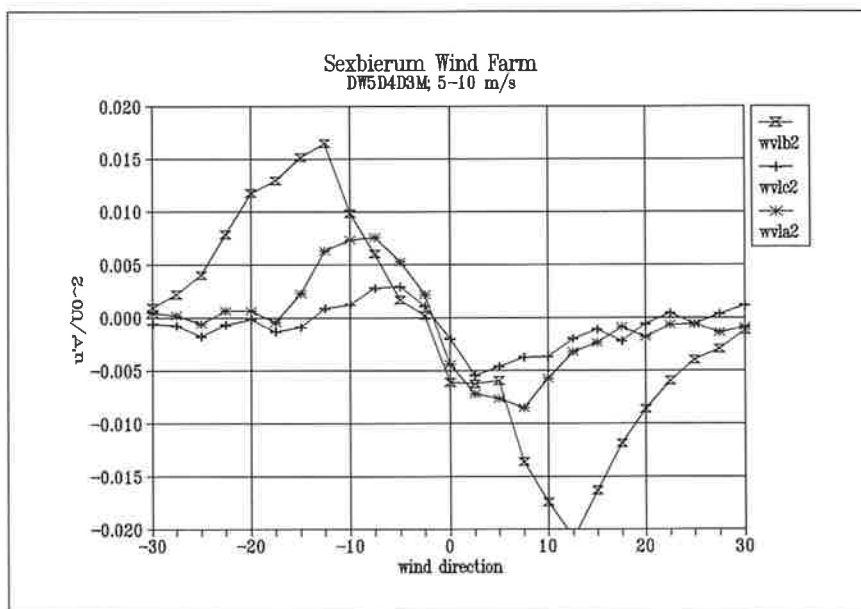


Figure 4.23 Non-dimensionalized shear stresses  $u'v'/U_0^2$  as a function of wind direction in wind speed bin 5-10 m/s.

Distance  $x = 2.5D$  : wvlb2

$x = 5.5D$  : wvla2

$x = 8D$  : wvlc2

Figure 4.23 shows the horizontal shear stress  $u'v'/U_0^2$  as a function of wind direction at 3 different axial position  $x=2.5D$ ,  $x=5.5D$  and  $x=8D$ . With the relaxation of the wake the maximum values of  $u'v'/U_0^2$  decrease with increasing distance.



## Results of Sexbierum Wind Farm; single wake measurements

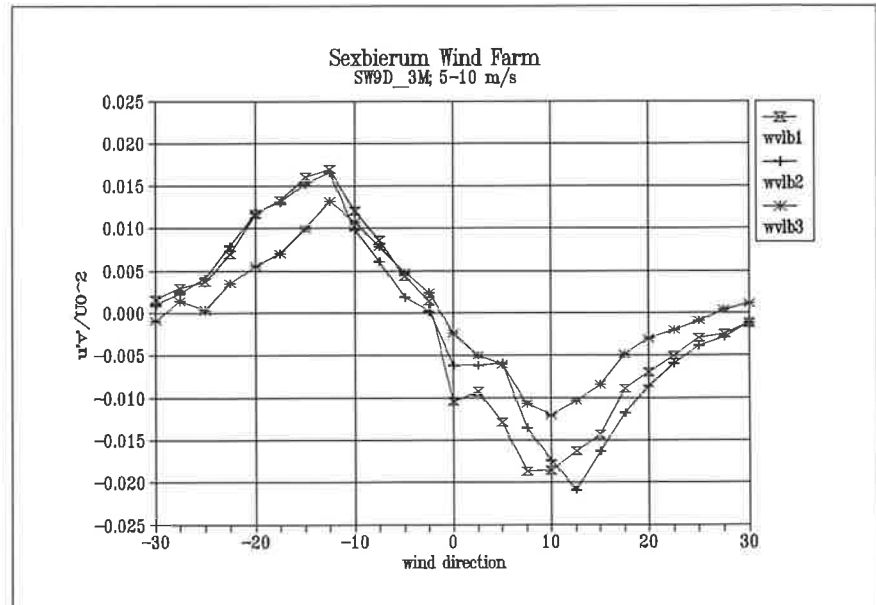


Figure 4.24 Shear stress  $u'v'/U_0^2$  as a function of wind direction for sensors b1, b2 and b3

Figure 4.24 shows the non-dimensional shear-stress  $u'v'/U_0^2$  for the three sensors at mast b as a function of the undisturbed wind direction. The shape of the three curves is again very similar. Eddy-viscosity theory for turbulence assumes that the turbulent shear stress is proportional to the local shear. This is clearly reflected in the curves of figure 4.24. Outside the wake no horizontal wake effect is present and hence the horizontal wind gradient is zero. At the maximum gradient  $dU/dy$  shear stress reaches a maximum, after which it decreases zero, where the wind speed shows a minimum. For larger wind directions the shear shows a similar behaviour but of an opposite sign.

The shape and the magnitude of the shear stress curves compare well with results of wind tunnel tests [Smith].

## Results of Sexbierum Wind Farm; single wake measurements

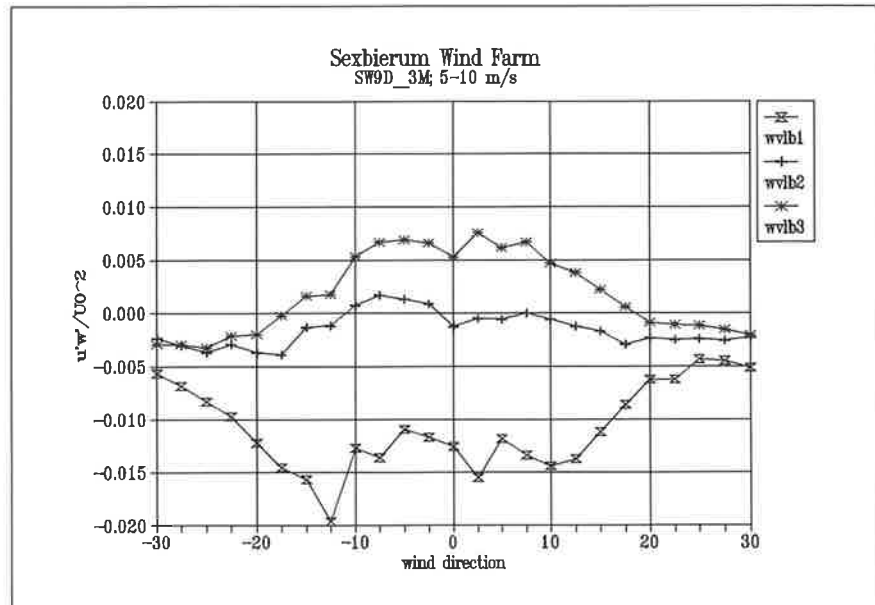


Figure 4.25 Shear stress  $u'w'/U_0^2$  as a function of wind direction for sensors b1, b2 and b3

Figure 4.25 shows the non-dimensional turbulent shear stress  $u'w'/U_0^2$  as a function of the wind direction at the three sensor positions b1, b2, b3. The graphs show quite a distinct behaviour from the horizontal shear.

The shear stress  $u'w'$  is proportional to the vertical wind speed gradient  $dU/dz$ . Outside the wake the  $u'w'$  is negative corresponding to the shear stress in the atmospheric boundary layer. Traversing through the wake at the top position b1, the vertical gradient increases with the increasing wake effect and so  $u'w'$  becomes more negative (figure 4.26). At the bottom sensor b3 the situation is different. When the wind direction changes the wake effect becomes stronger; the wind gradient and hence  $u'w'$  changes sign.

Results of Sexbierum Wind Farm; single wake measurements

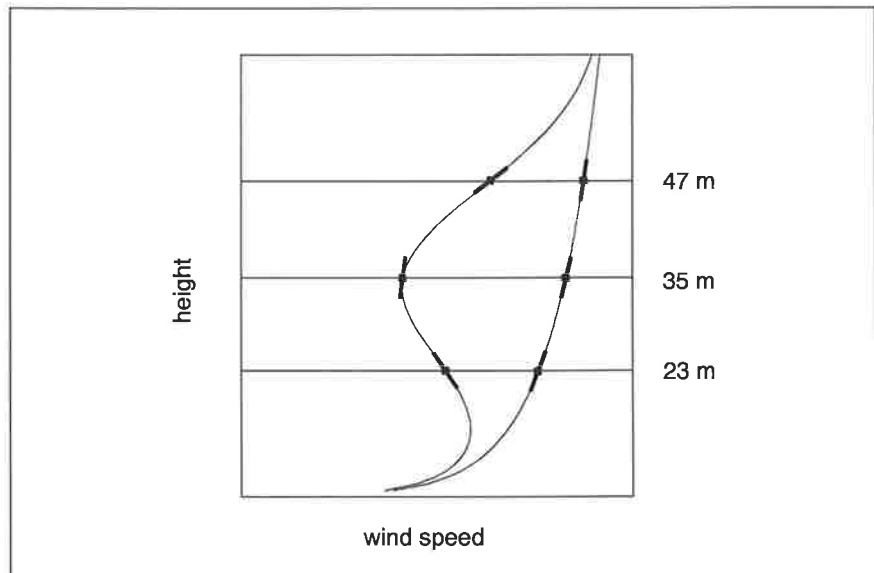


Figure 4.26 Change of the vertical wind gradient under influence of the wake deficit

#### 4.6 Wake decay

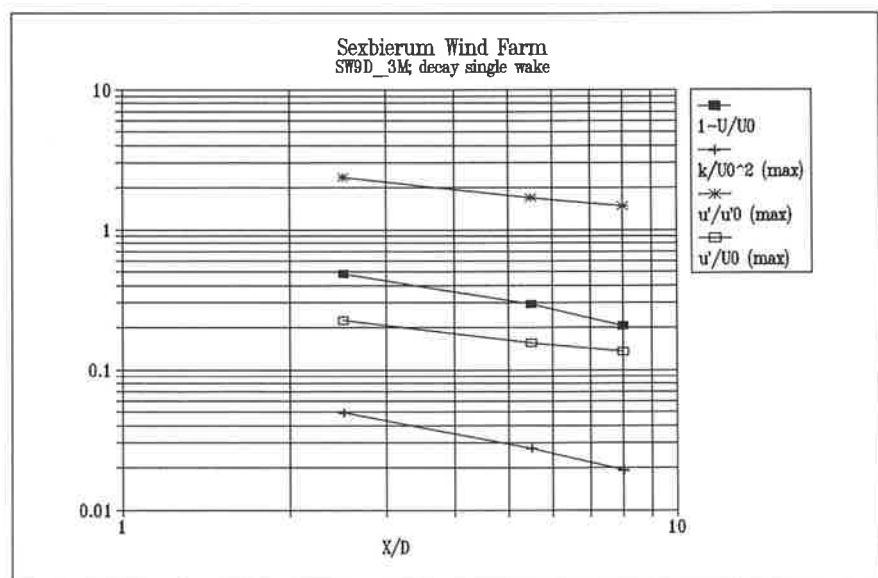


Figure 4.27 Wake decay for quantities  $1-U/U_0$ ,  $u'/U_0$ ,  $u'/u_0'$  and  $k/U_0^2$  as a function of the longitudinal distance  $X/D$

Figure 4.27 shows the decay of various quantities as a function of the non-dimensional distance behind turbine T18.  $U/U_0$  gives the centreline deficit as a function of the distance.  $k/U_0^2$ ,  $u'/u_0$ ,  $u'/u_0'$  give the maximum value (taken across the wake) of these quantities at the given position  $X/D$ .

## 5 Conclusions

The measurement campaign in the wake a single wind turbine at distances of  $x=2.5 D$ ,  $5,5 D$  and  $8 D$  has resulted in a useful data base for the validation of wake and wind farm models and for input to wind turbine load calculation programs.

The data base is built up of 873 3-minute samples containing data on undisturbed wind conditions, wind turbine power, wind speed components, turbulence and shear stress data. The data base has been analysed with respect to the undisturbed wind conditions, i.e. with respect to wind speed and wind direction outside the wind farm.

During the measurements no serious problems arose. However, a number of systematic errors in the measurement of the undisturbed wind measurement was detected, for which the data had to be corrected. Because the undisturbed wind speed sensor at hub height was malfunctioning for part of the measuring campaign, the wind sensor at 20 m height has been used for the analysis.

The abovementioned problems in the undisturbed wind measurements have seriously hampered a good determination of the upstream roughness length. Estimates of the upstream roughness length vary between  $z_0=0.05\text{m}$  and  $z_0=0.15\text{m}$ .

The wake deficit at the various measuring positions has been determined. At  $X=2.5D$  the wake profile deviates markedly from a Gaussian shape, at larger distances this deviation disappears.

At  $X=2.5D$  turbulence intensity shows peaks at the maximum wind speed gradient. These peaks disappear for positions further downstream the turbine ( $X=5.5D$  and  $X=8D$ ).

The shear stresses have been measured successfully. The course of the individual shear stresses can be explained qualitatively by making some simple assumptions about the wind speed gradient in the wake. Further the shape is very similar to the one measured previously in the wind tunnel.

## 6 References

- [1] Beljaars, A.C.M.;  
The measurement of gustiness at routine wind stations - A review;  
WMO-instruments and observing methods, report no. 31, Geneva 1987.
- [2] Bendat, J.S., A.G. Piersol;  
Random data; Analysis and Measurement procedures; 2nd edition;  
Wiley, 1986.
- [3] Bulder, B.H., J.G. Schepers;  
Calculation data base of the WPS-30 wind turbine;  
ECN report ECN-CX--91-053, September 1991.
- [4] Cleijne, J.W.;  
Local wind speed distribution around the SEP experimental wind farm (in Dutch);  
TNO-report 91-421; January 1992.
- [5] Cleijne, J.W.;  
Results of Sexbierum Wind Farm double wake measurements;  
TNO-report 92-388; November 1992.
- [6] Crespo, A.;  
2nd progress report JOUR-0087 'Wake and wind farm modelling';  
May, 1992.
- [7] Panofsky, H.A., J.A. Dutton;  
Atmospheric Turbulence, models and methods for engineering applications;  
Wiley, 1984.
- [8] Smith, D.;  
An experimental and theoretical investigation of wind turbine wakes in arrays and complex terrain;  
Ph.D. Thesis, NP-TEC, 1991.
- [9] Strong winds in the atmospheric boundary layer: part 2 discrete gust speeds;  
Engineering Sciences Data Item 83045;  
ESDU, November 1983.
- [10] Taylor, G.J.;  
Full-Scale Measurements in Wind Turbine Arrays JOUR-0064;  
Kick-off document, 1990.
- [11] Toussaint, P., H.K. Hutting, J.W. Cleijne, M. Mortier;  
Results from operation and research of the experimental wind farm of the Dutch Electricity Generating Board;  
Proceedings EWEA special topic conference '92, Herning, 1992.

*Results of Sexbierum Wind Farm; single wake measurements*

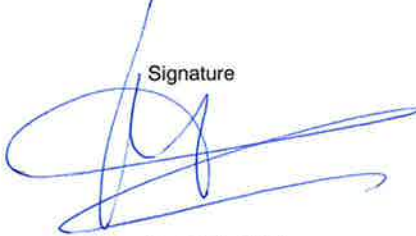
## 7 Authentication

Name and address of the principal  
Commission of the European Community  
contract JOUR-0064

Names and functions of the cooperators  
Ir. J.W. Cleijne - research engineer

Names of establishments to which part of the research was put out to contract  
-

Date upon which, or period in which, the research took place  
June 1992 - March 1993

Signature  


Ir. J.W. Cleijne  
project manager

Approved by



Ir. N.J. Duijm  
section manager  
wind engineering

## **Annex A1      Specification of the hoolec WPS-30/3 wind turbine**

Type	:	HAWT
Rotor	:	upwind
Number of blades	:	3
Blade material	:	steel
Rotor diameter	:	30.1 m
Blade root radius	:	1.14 m <sup>1)</sup>
Blade profiles	:	NACA 230xxx series
Mass of one blade	:	1800 kg
Mass of blade foot	:	1360 kg
Mass of rotor (incl. hub)	:	15400 kg
First flap-wise Own-frequency	:	3.35 Hz
Rotor rotation direction	:	clockwise (looking downwind)
Tilt angle	:	5.5°
Cone angle	:	0.0°
Tower material	:	steel
Tower diameter -base	:	3.2 m
-top	:	1.32 m
Tower height	:	35 m
Distance rotor-tower	:	1.67 m (at hub height)
Rated Power	:	310 kW
Rated wind speed	:	14 m/s
Cut-in wind speed	:	5 m/s
Cut-out wind speed	:	20 m/s
Generator	:	synchronous with DC link
Control	:	variable speed/ variable pitch

---

<sup>1)</sup> The blade root is defined to be the position of the outer bearing of the blade, see figure 5 the blade lay-out

## **Annex A2      Specification of the extra instrumentation on turbine T36**

### **Channels**

#### **blades and hub**

8 strain gauges on each blade

4 strain gauges on the hub

strain gauges on the joint between hub and blades

#### **rest of turbine**

torque on the main shaft

torque on the fast shaft

bending moments in N-S and E-W directions 6 m below the tower top

bending moments in N-S and E-W directions 4 m above the tower base

pitch angle

blade position

nacelle direction

#### **Electrical and control signals**

field voltage of the generator

field current of the generator

voltage of all 3 phases of the generator

current of all 3 phases of the generator

frequency of the generator

set point field current

set point DC current

set point pitch angle

DC voltage

DC current turbine

DC current converter

voltage of all phase of the 10 kV grid connection

All above signals are sampled at a 32 Hz rate



## Annex A3 Data transformation and averaging

### A3.1 Co-ordinate transformation

The various quantities are measured in a frame of reference fixed to the wind farm, having co-ordinates X, Y and Z. X is horizontal, Y is horizontal and perpendicular to X, and Z points vertically upwards. X, Y, Z form a right handed co-ordinate system.

Scalar quantities, vectors, as well as tensor quantities (Reynolds-stresses) are measured in the fixed frame of reference. For analysis purposes these quantities need to be transformed to the wind frame of reference U, V, W. U is in the direction of the average undisturbed wind speed, V is perpendicular to the wind and W is vertical. Again a right handed frame of reference is used. For a definition of the two coordinate systems see figure 3.2. The directions of X and U are at an angle  $\delta$ . The transformation from the fixed co-ordinate system to the wind co-ordinate system is hence a simple rotation about the Z-axis over an angle  $\delta$ . The transformation matrix is given by:

$$\Delta_{ij} = \begin{bmatrix} \cos \delta & -\sin \delta & 0 \\ \sin \delta & \cos \delta & 0 \\ 0 & 0 & 1 \end{bmatrix}$$

Scalars are insensitive to a rotation of the frame of reference and thus need not to be transformed. However the components of a vector are affected by a rotation of the frame of reference. The components in the wind frame of reference are found by applying the following expression:

$$U_{\text{wind},i} = \sum_{j=1}^3 \Delta_{ij} \cdot U_{x,j}$$

The components of a tensor are changed according to the following transformation formula

$$T_{ij}' = \sum_{k=1}^3 \sum_{l=1}^3 \Delta_{ik} T_{kl} \Delta_{lj}'$$

### A3.2 Merging of 1-minute records to obtain multiple-minute averages

The data-base consists of records with one-minute averages of the measured quantities. However, for further analysis it is necessary to use multiple-minute records (for instance 3-minutes averages as was done in this report). It is possible to obtain averages over several minutes, combining subsequent records without losing accuracy using the formulas given below.

A distinction is made between linear averaged quantities (wind speed, power, wind direction, etc.) and non-linear quantities, such as the variance of the given quantities.

#### Linear averaged quantities

Subsequent records are simply averaged arithmetically to obtain the multiple-minute averaged value:

$$\mu_M = \frac{1}{M} \sum_{m=1}^M \mu_m$$

$\mu_M$  denotes the overall mean,  $\mu_m$  denotes the means of the separate records.

#### Quadratic averaged quantities

Co-variance and variance mean values cannot be found by simply averaging their record values, but should be corrected for the variance and covariance of the record means.

The overall covariance is found in the following way:

$$(u'_i u'_j)_M = \frac{1}{M} \sum_{m=1}^M (u'_i u'_j)_m = \frac{1}{M} \sum_{m=1}^M (\mu_{i,m} - \mu_{i,M}) (\mu_{j,m} - \mu_{j,M})$$

$\mu_m$  and  $\mu_M$  are as defined before.  $(u'_i u'_j)_M$  denotes the overall average of the co-variance.  $(u'_i u'_j)_m$  denotes the average of the co-variance in record m.

Calculating the average variance is a special case of this expression and is found by taking equal i and j.

$$\sigma_{i,M}^2 = \frac{1}{M} \sum_{m=1}^M \sigma_{i,m}^2 + \frac{1}{M} \sum_{m=1}^M (\mu_{i,m} - \mu_{i,M})^2$$

$\sigma_{i,M}$  denotes the overall variance of the i-component,  $\sigma_{i,m}$  denotes the variance of record m.

**Results of Sexbierum Wind Farm; single wake  
measurements  
Annex 4 - Figures**

Reference number 93-082  
File number 112324-22420  
Date March 1993  
NP

Author  
J.W. Cleijne

Intended for  
Participants JOUR-0064  
Participants JOUR-0087

*Results of Sexbierum Wind Farm; single wake measurements*

## **Annex A4      Figures**

In this annex a comprehensive overview is given of the analysis results. The results are given in the following order:

1. Results of sensor a2
2. Results of sensor b1
3. Results of sensor b2
4. Results of sensor b3
5. Results of sensor c2
6. Vertical profiles
7. Horizontal profiles

*Results of Sexbierum Wind Farm; single wake measurements*

**A4.1 Sensor a2**

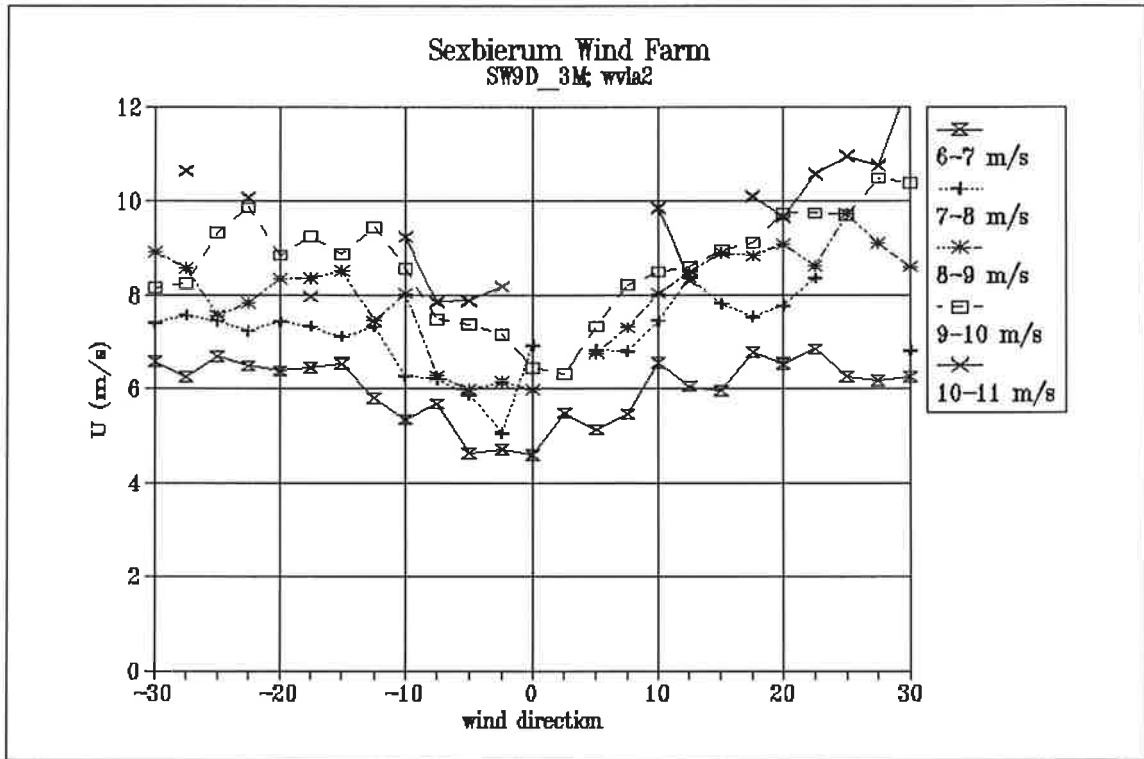


Figure 1 Horizontal wind speed  $U$  as a function of wind direction and wind speed bin

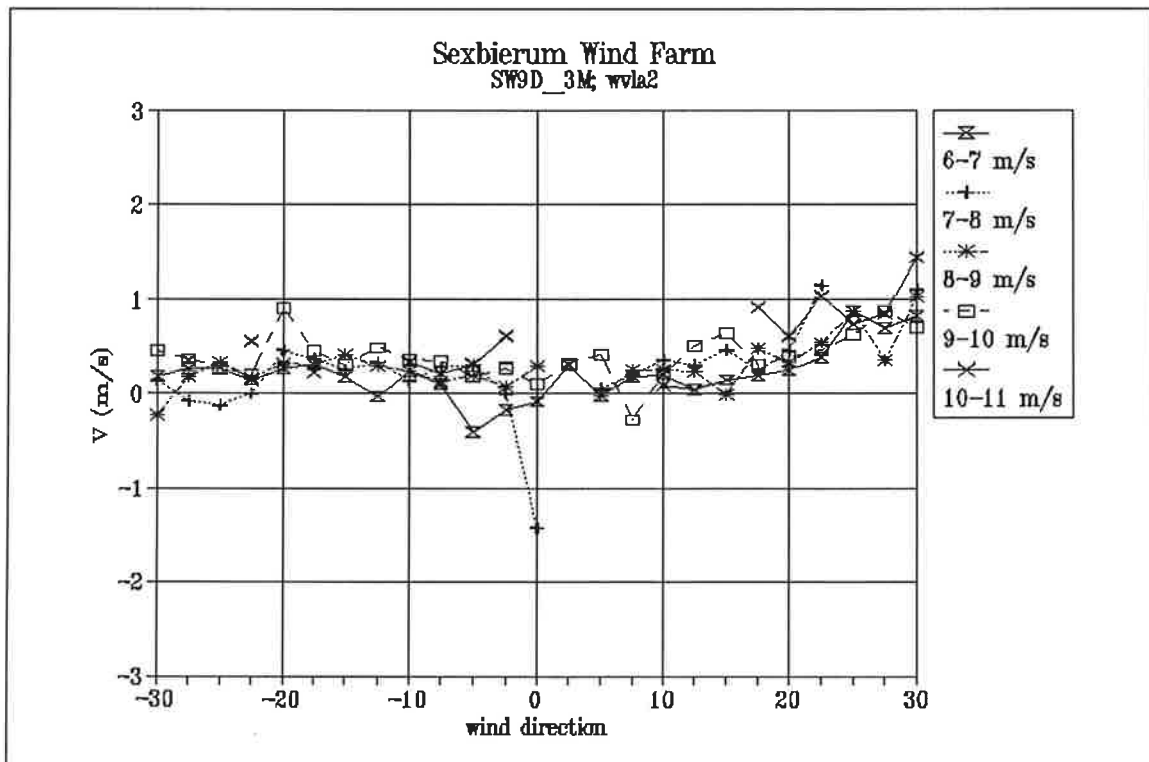


Figure 2 Lateral wind speed  $V$  as a function of wind direction and wind speed bin

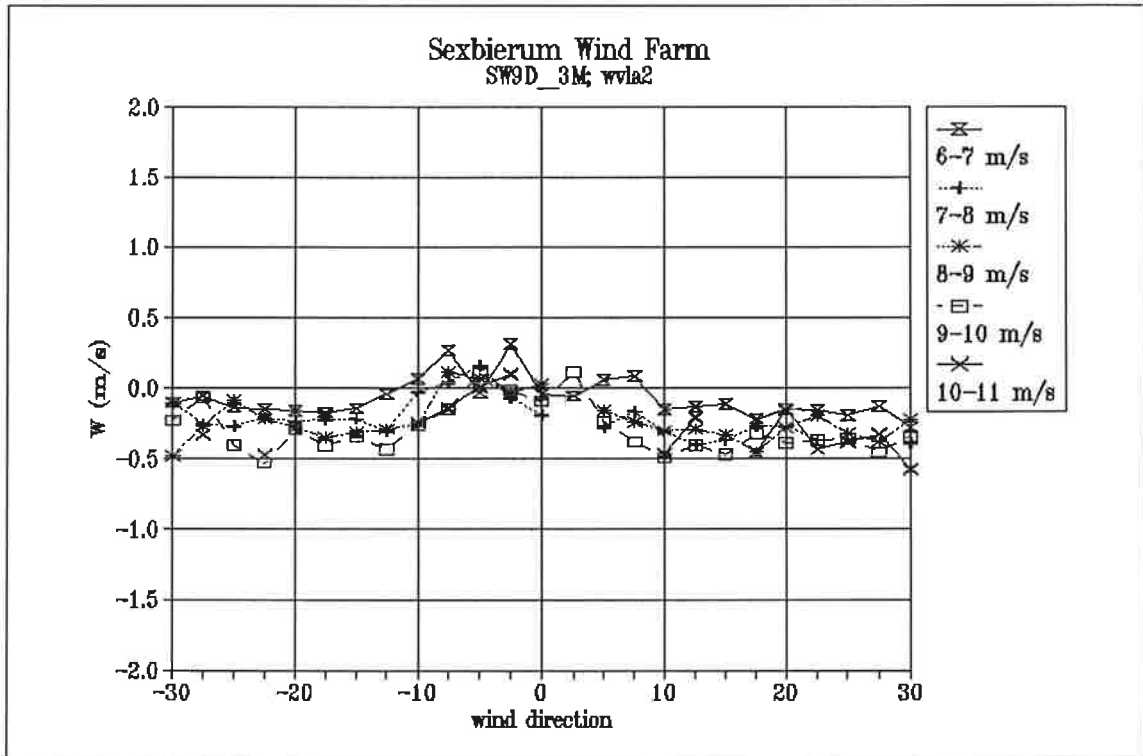


Figure 3 Vertical wind speed  $W$  as a function of wind direction and wind speed bin

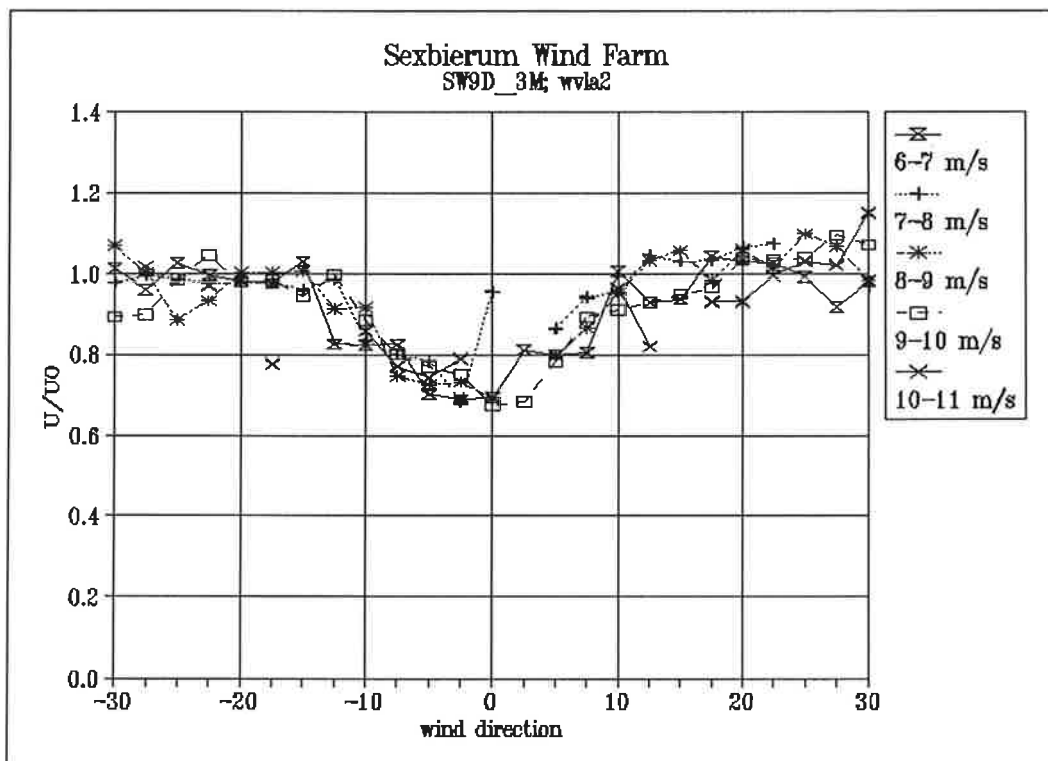


Figure 4 Wake deficit  $U/U_0$  as a function of wind direction and wind speed bin

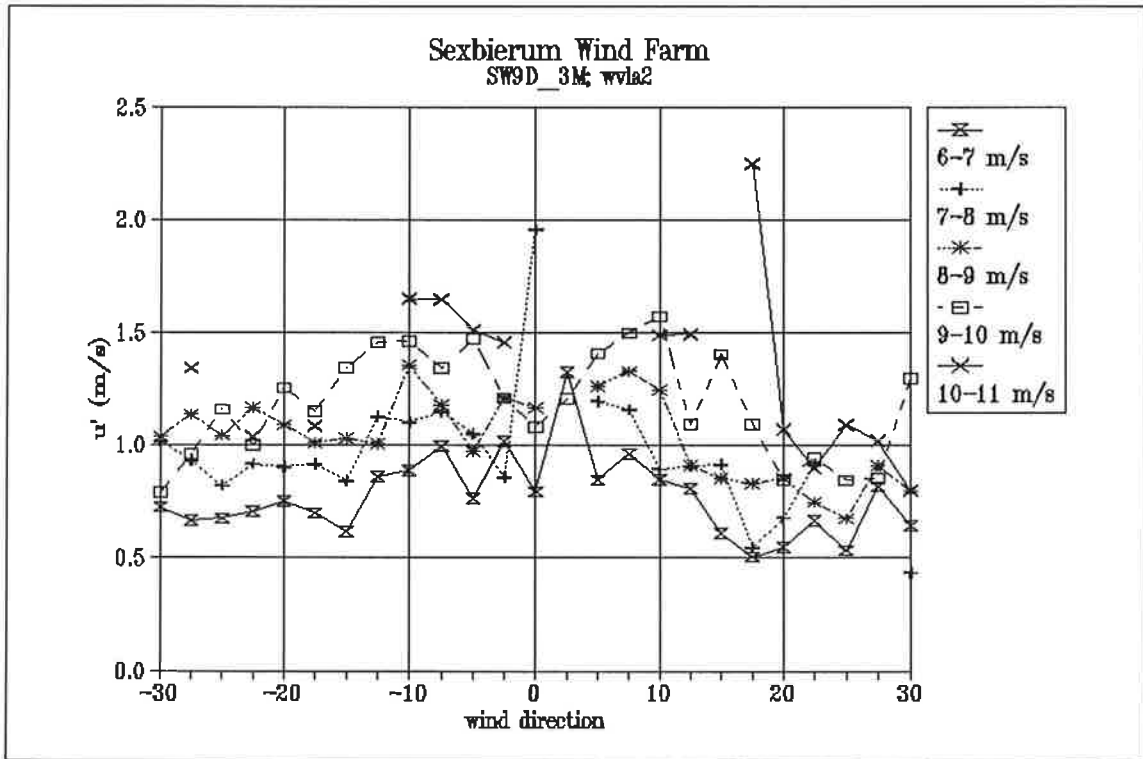


Figure 5 Longitudinal turbulent fluctuations  $u'$  as a function of wind direction and wind speed bin

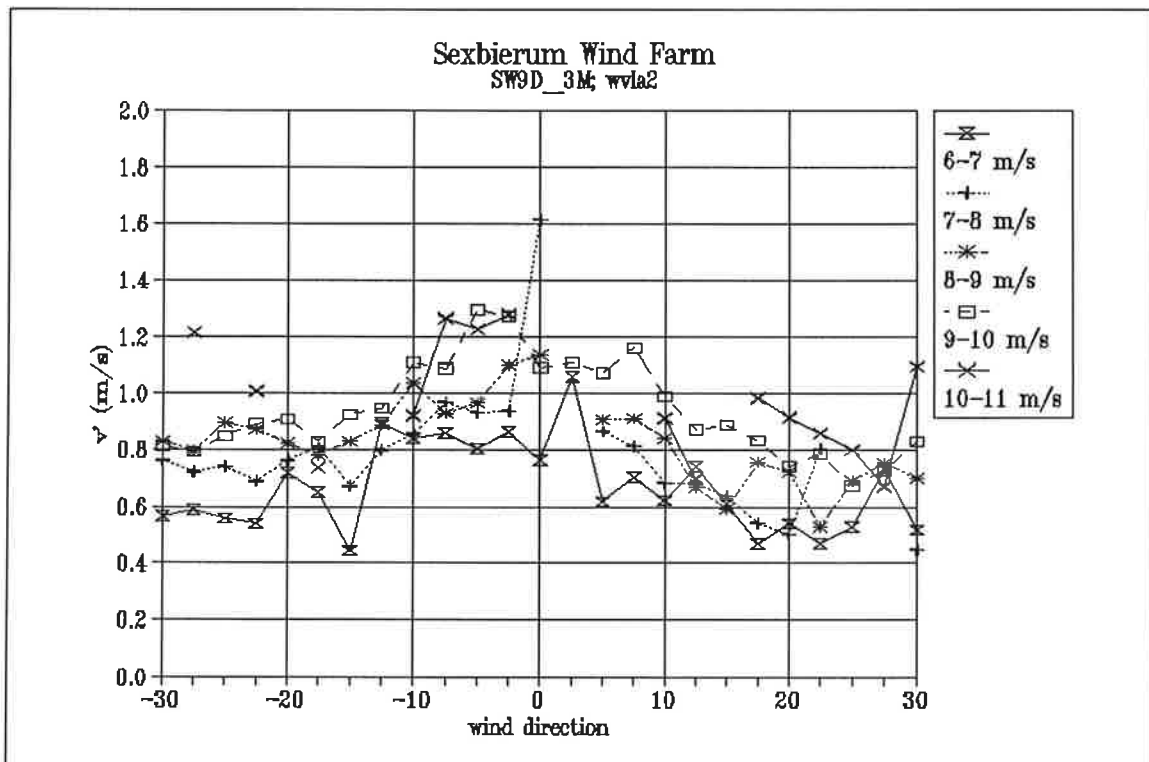


Figure 6 Lateral turbulent fluctuations  $v'$  as a function of wind direction and wind speed bin



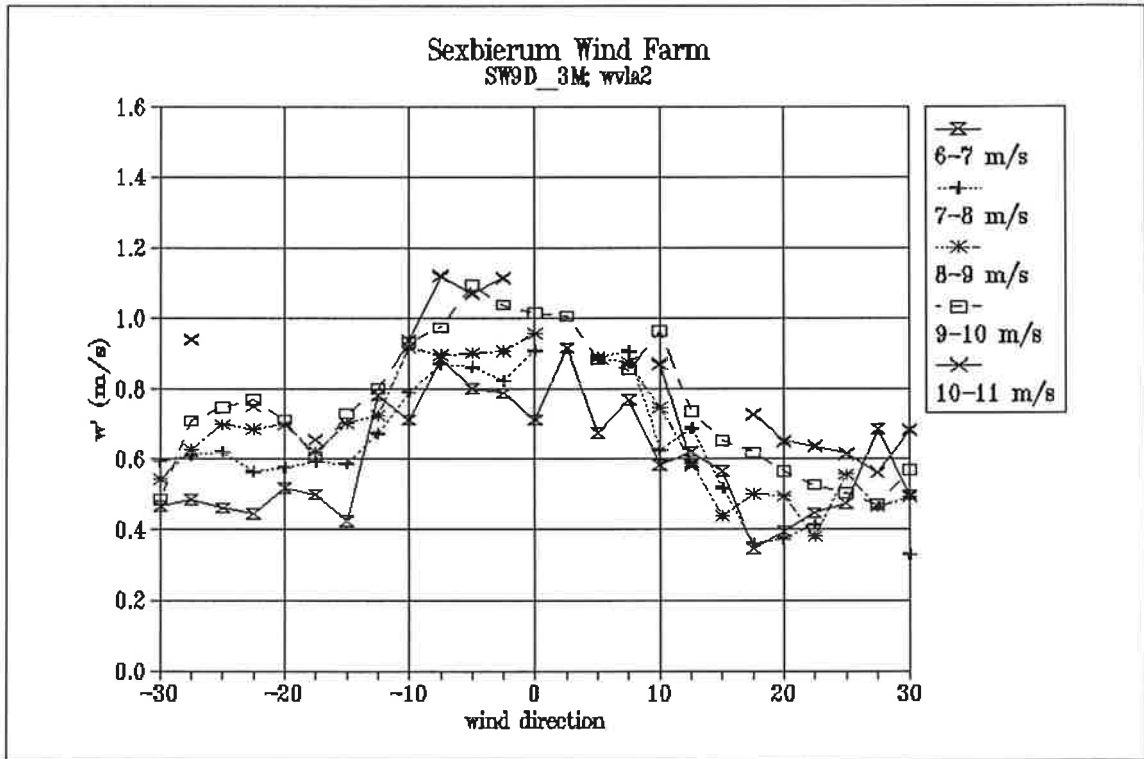


Figure 7 Vertical turbulent fluctuations  $w'$  as a function of wind direction and wind speed bin

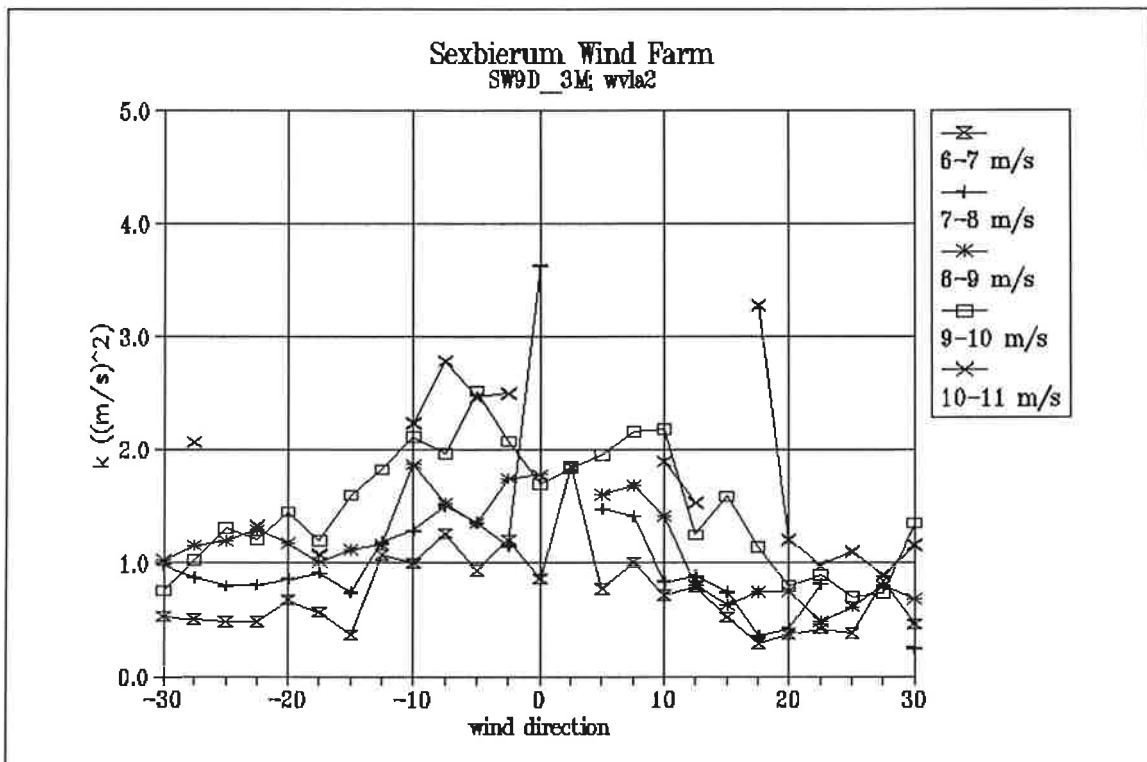


Figure 8 Turbulent kinetic energy per unit mass as a function of wind direction and wind speed bin

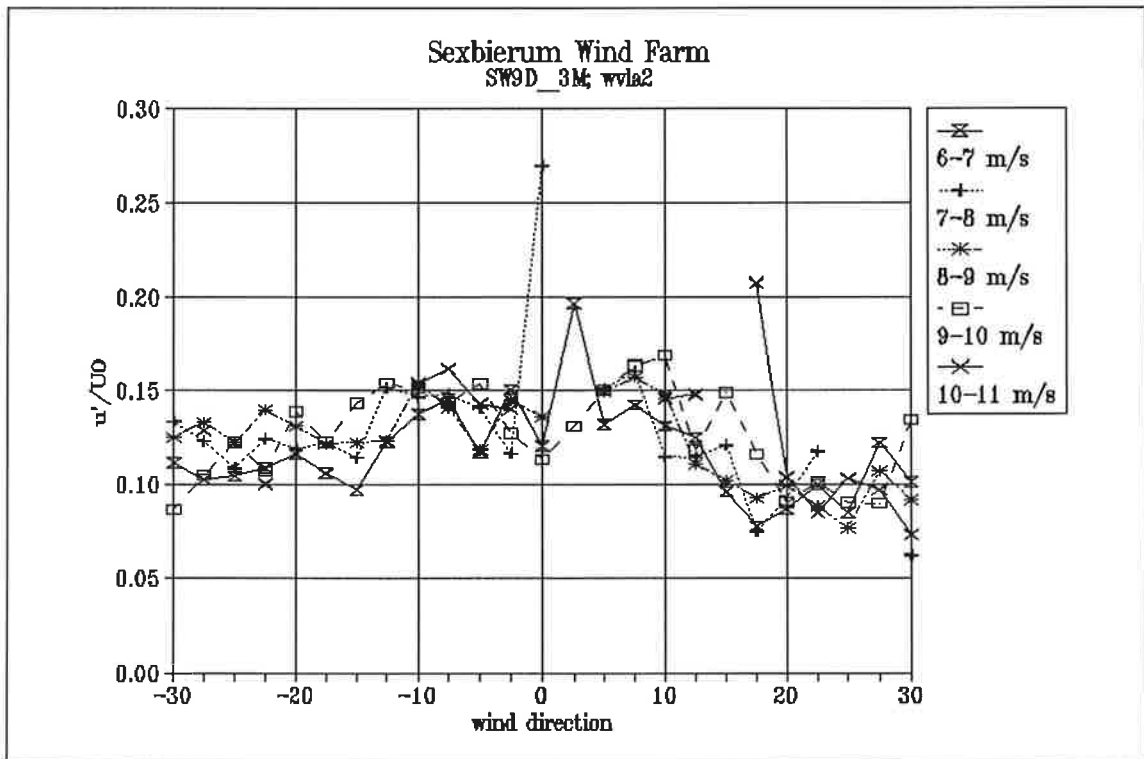


Figure 9 Non-dimensionalized longitudinal turbulent fluctuations  $u'/U_0$  as a function of wind direction and wind speed bin

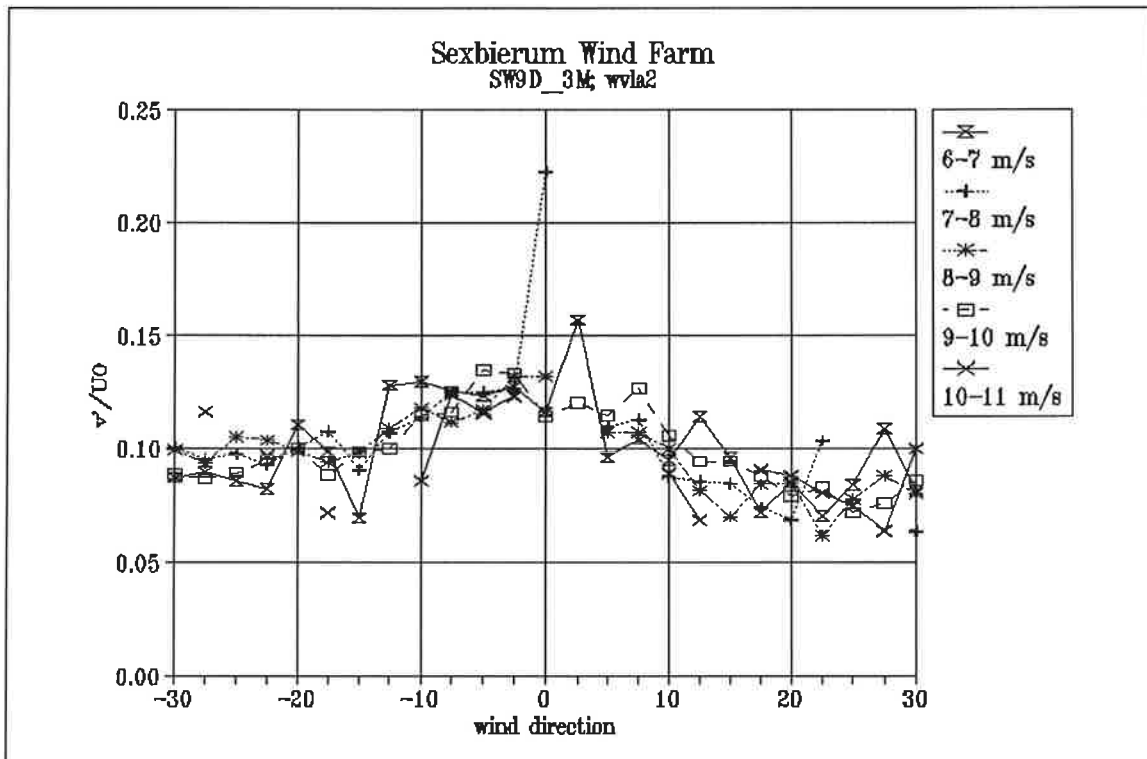


Figure 10 Non-dimensionalized lateral turbulent fluctuations  $v'/U_0$  as a function of wind direction and wind speed bin

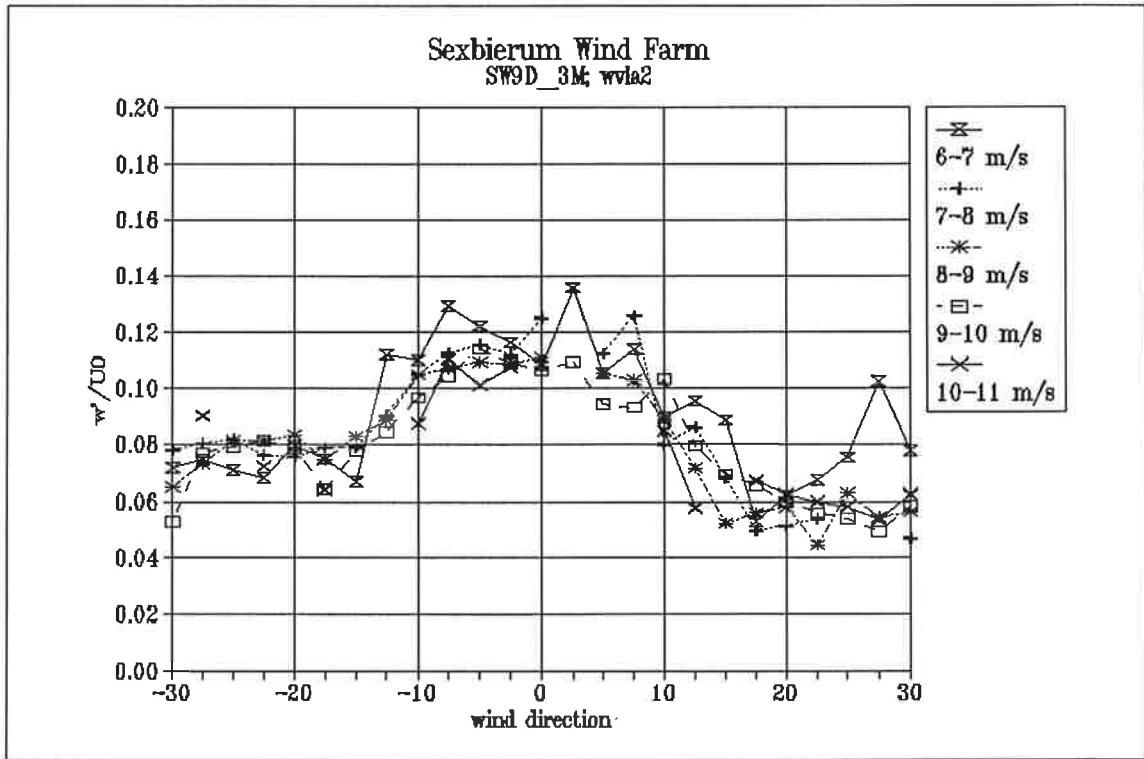


Figure 11 Non-dimensionalized vertical turbulent fluctuations  $w'/U_0$  as a function of wind direction and wind speed bin

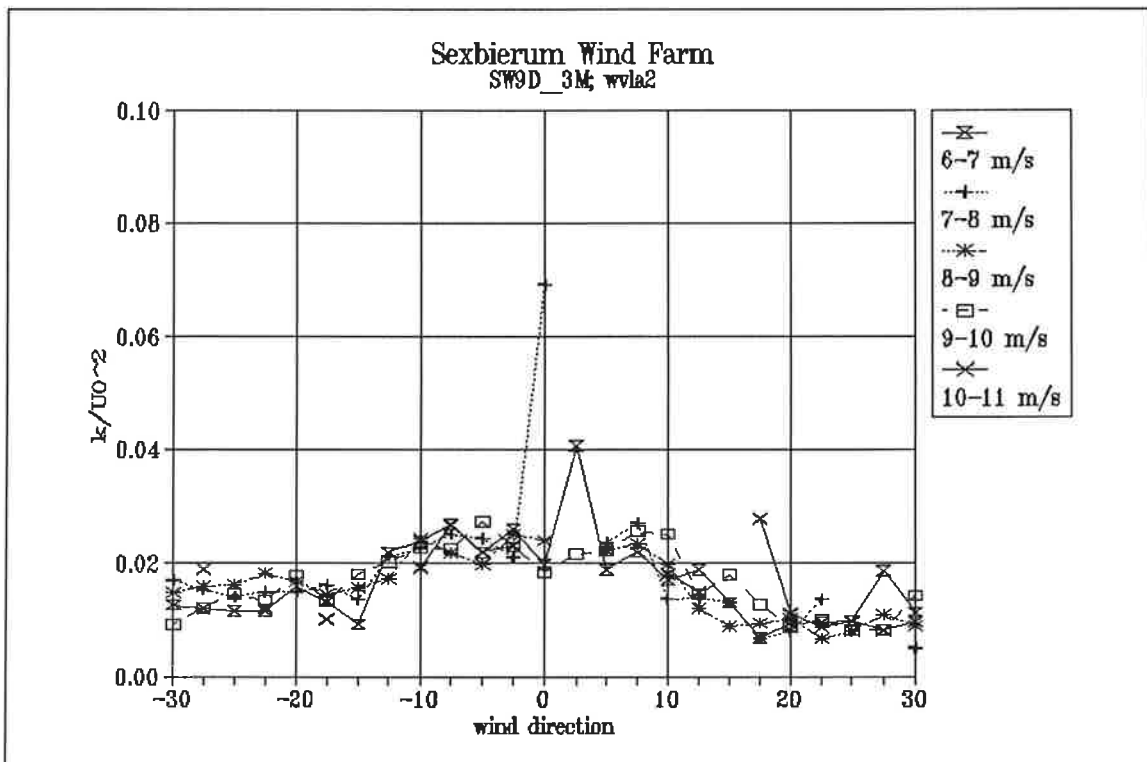


Figure 12 Non-dimensionalized turbulent kinetic energy  $k/U_0^2$  as a function of wind direction and wind speed bin

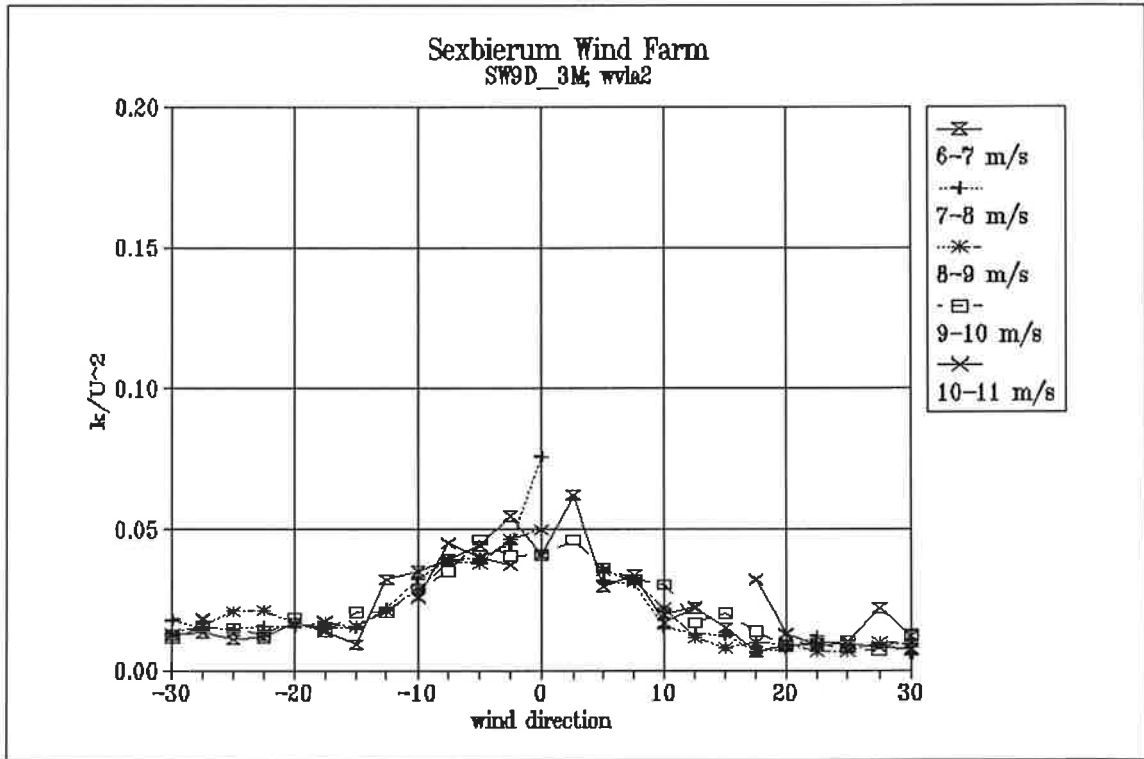


Figure 13 Non-dimensionalized turbulent kinetic energy  $k/U^2$  as a function of wind direction and wind speed bin

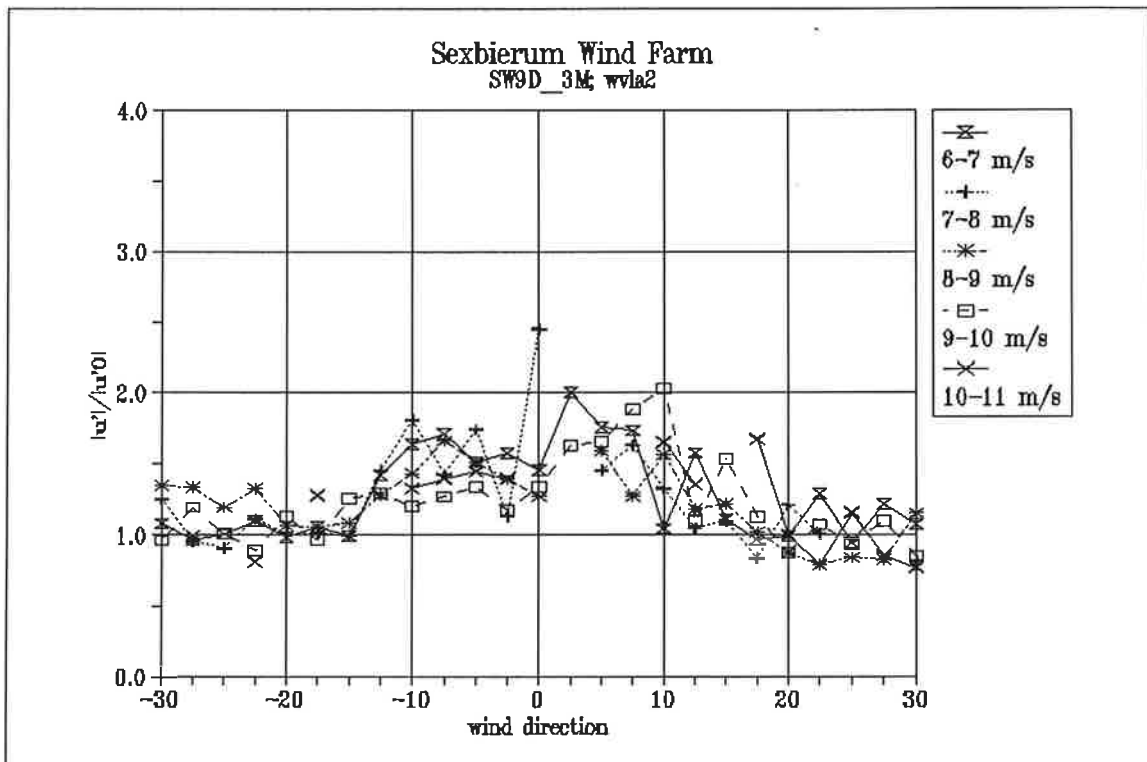


Figure 14 Longitudinal turbulence enhancement  $u'^2/u'0'$  as a function of wind direction and wind speed bin

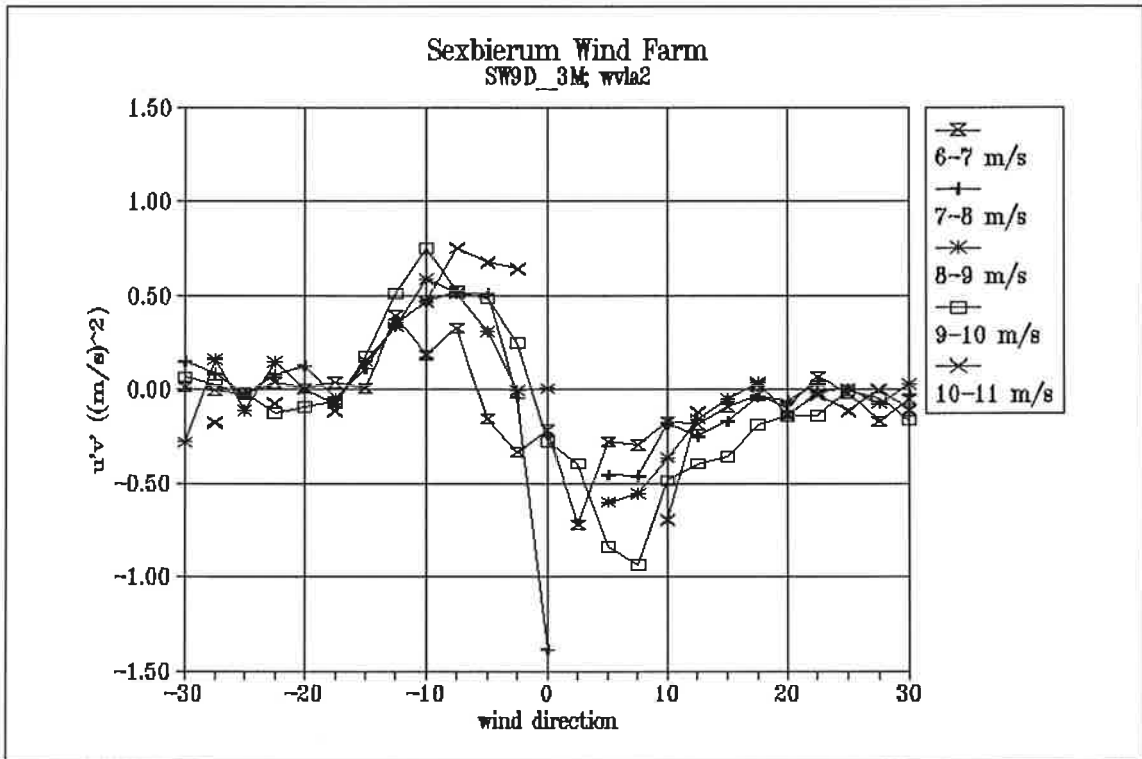


Figure 15 Shear stress  $u'v'$  as a function of wind direction and wind speed bin

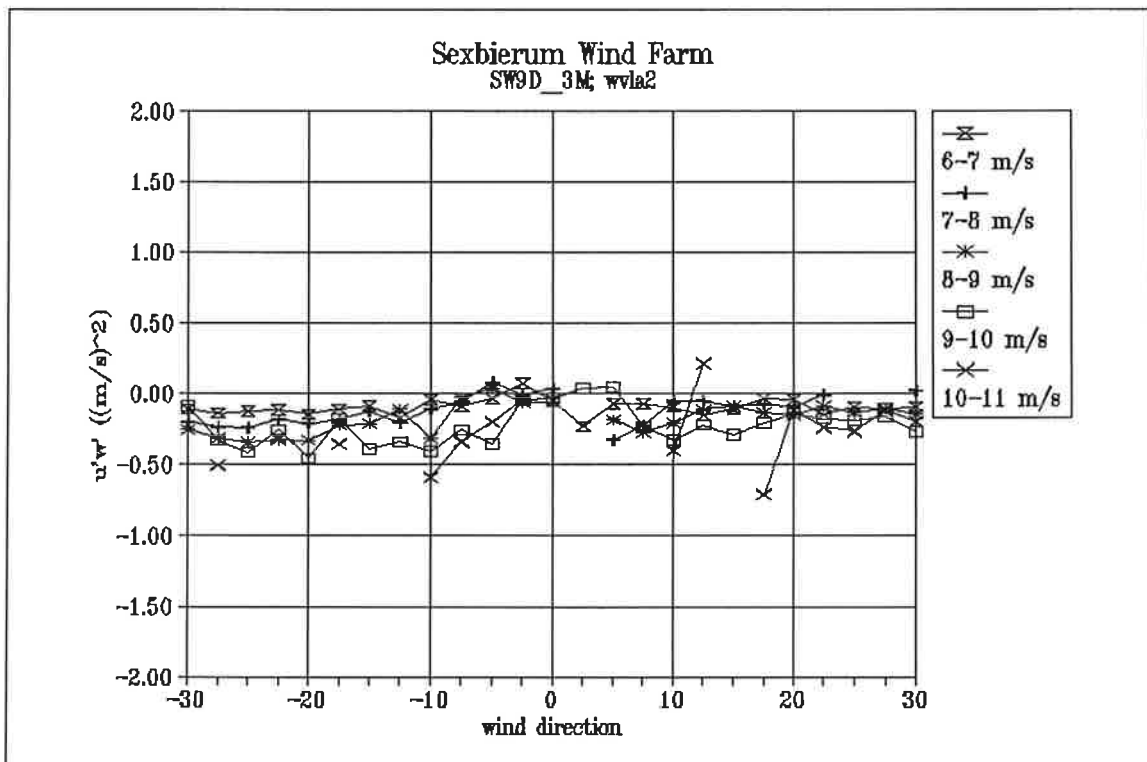


Figure 16 Shear stress  $u'w'$  as a function of wind direction and wind speed bin

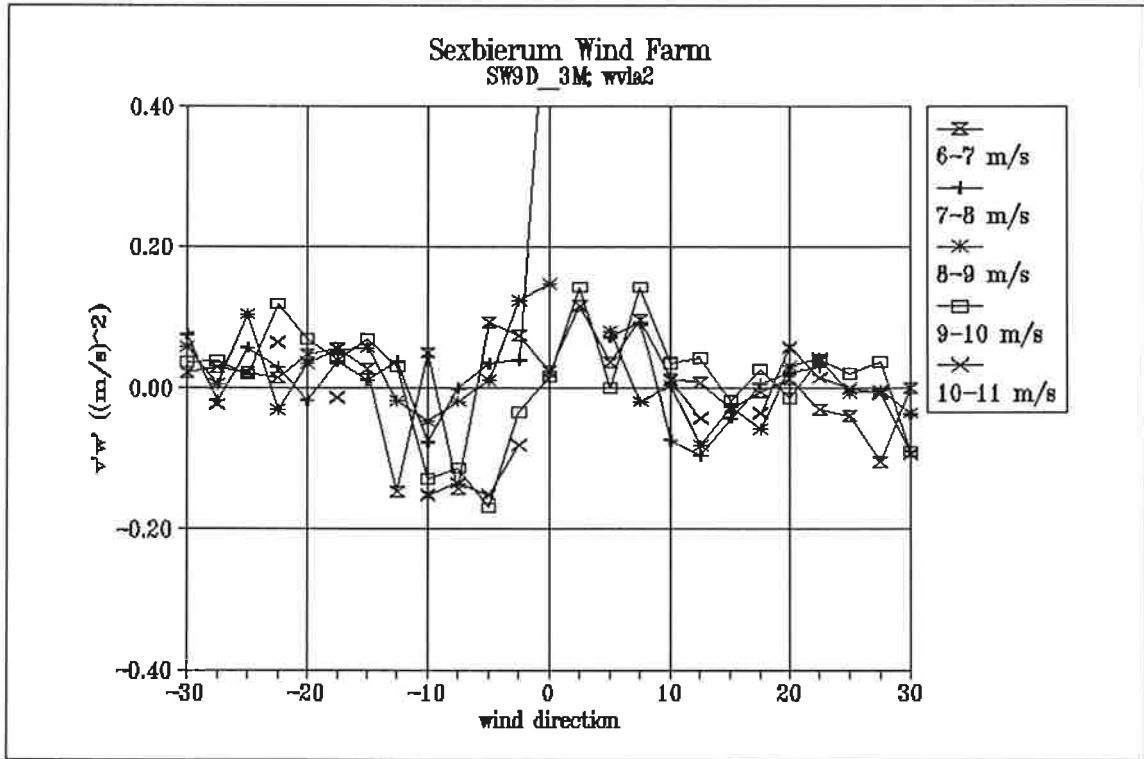


Figure 17 Shear stress  $v'w'$  as a function of wind direction and wind speed bin

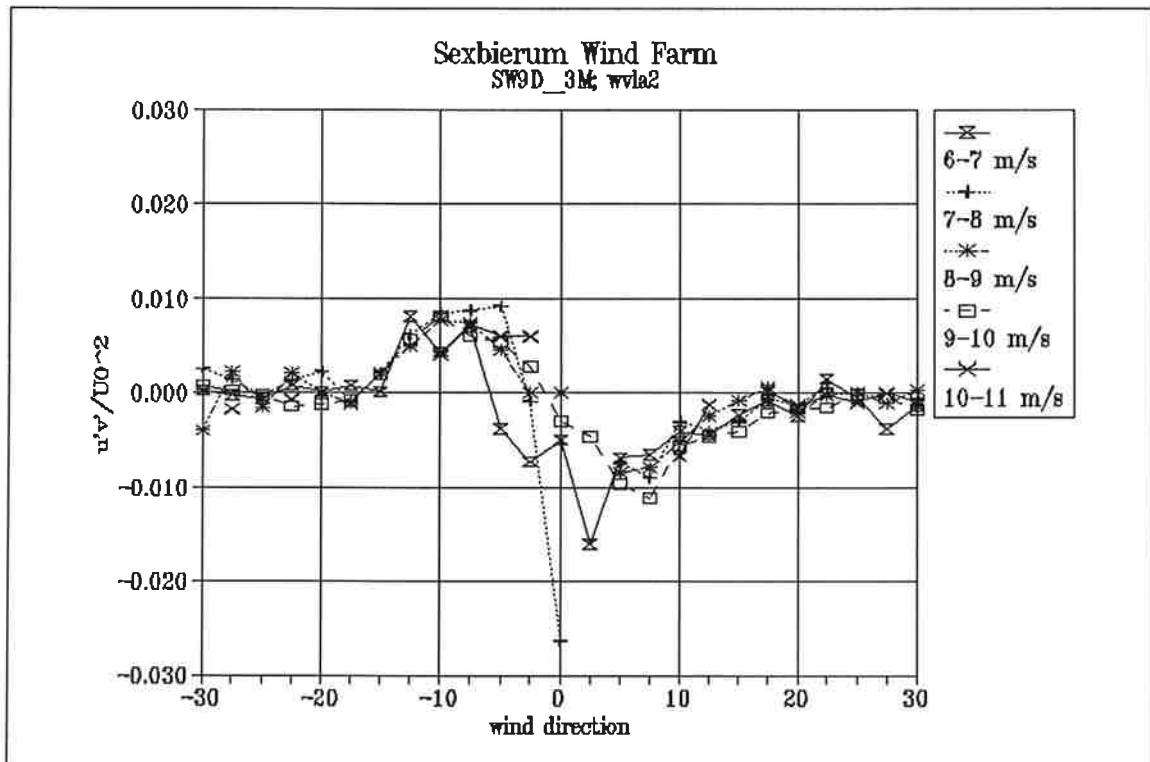


Figure 18 Non-dimensionalized shear stress  $u'v'/U_0^2$  as a function of wind direction and wind speed bin

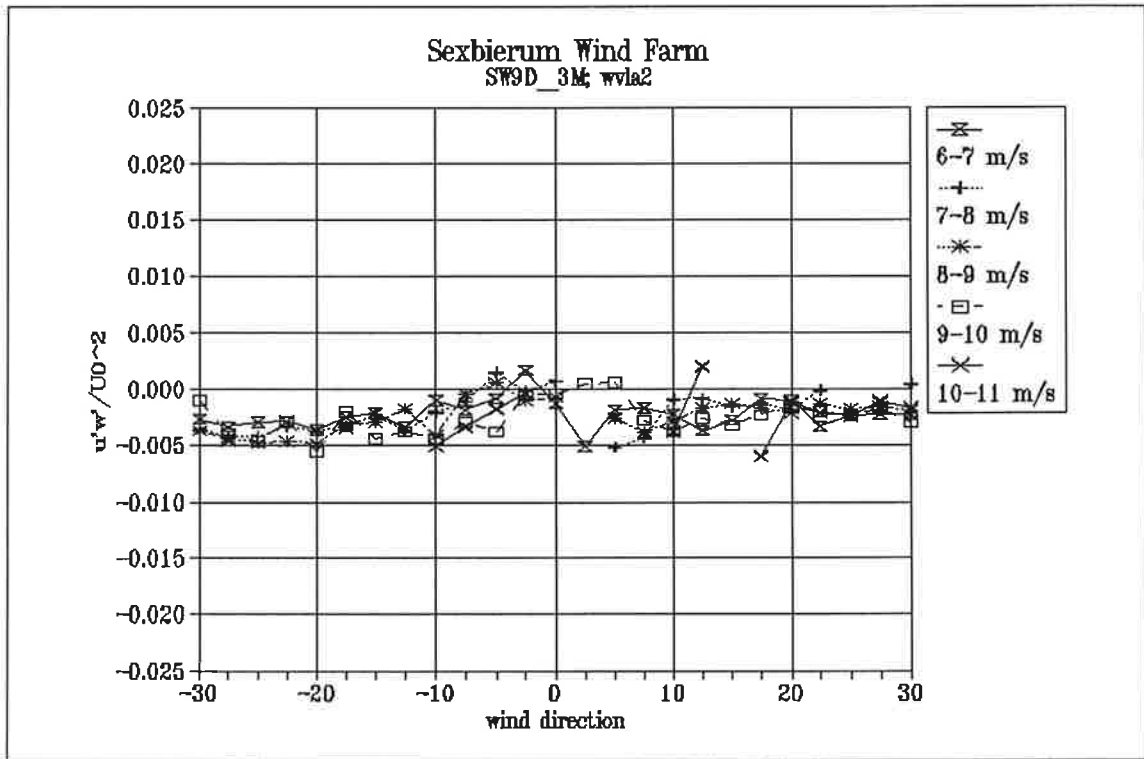


Figure 19 Non-dimensionalized shear stress  $u'w'/U_0^2$  as a function of wind direction and wind speed bin

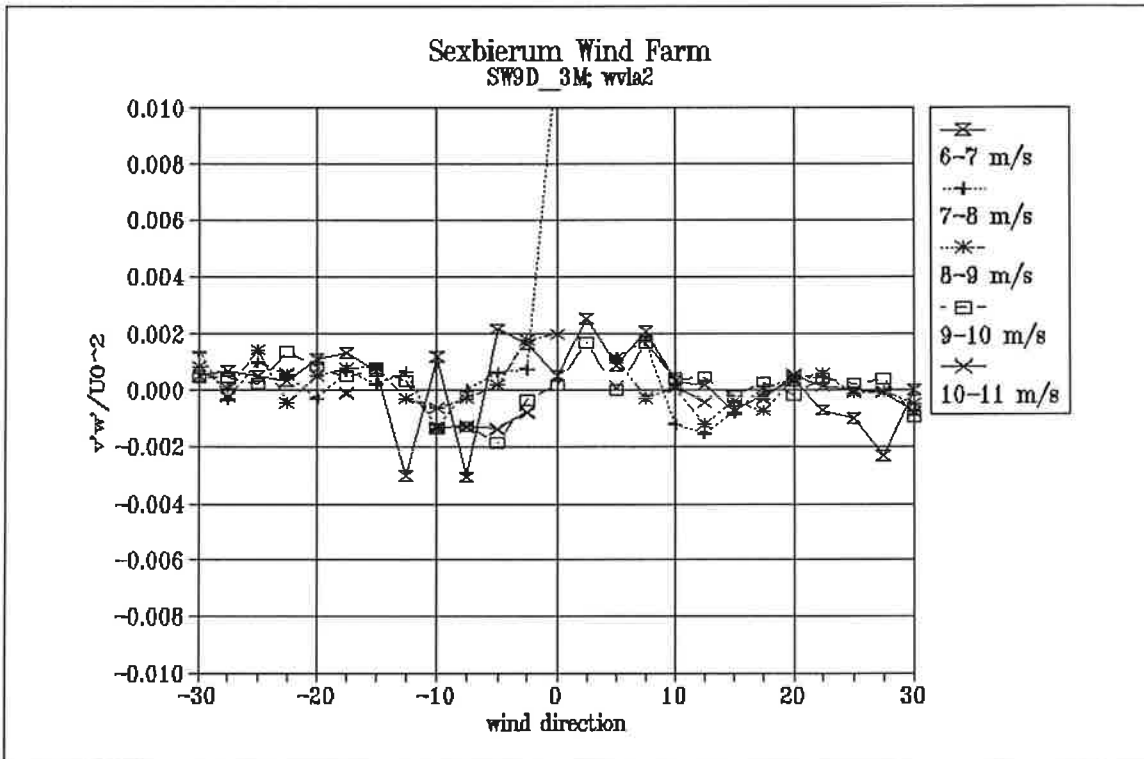


Figure 20 Non-dimensionalized shear stress  $v'w'/U_0^2$  as a function of wind direction and wind speed bin

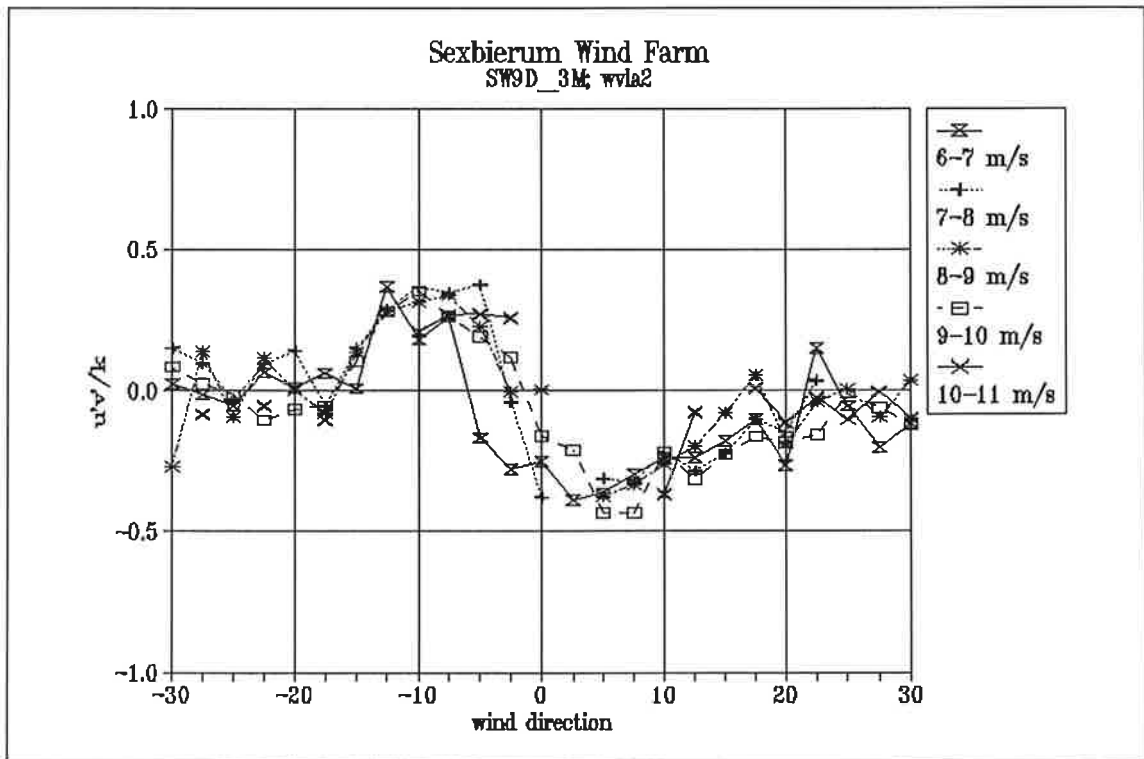


Figure 21 Non-dimensionalized shear stress  $u'v'/k$  as a function of wind direction and wind speed bin

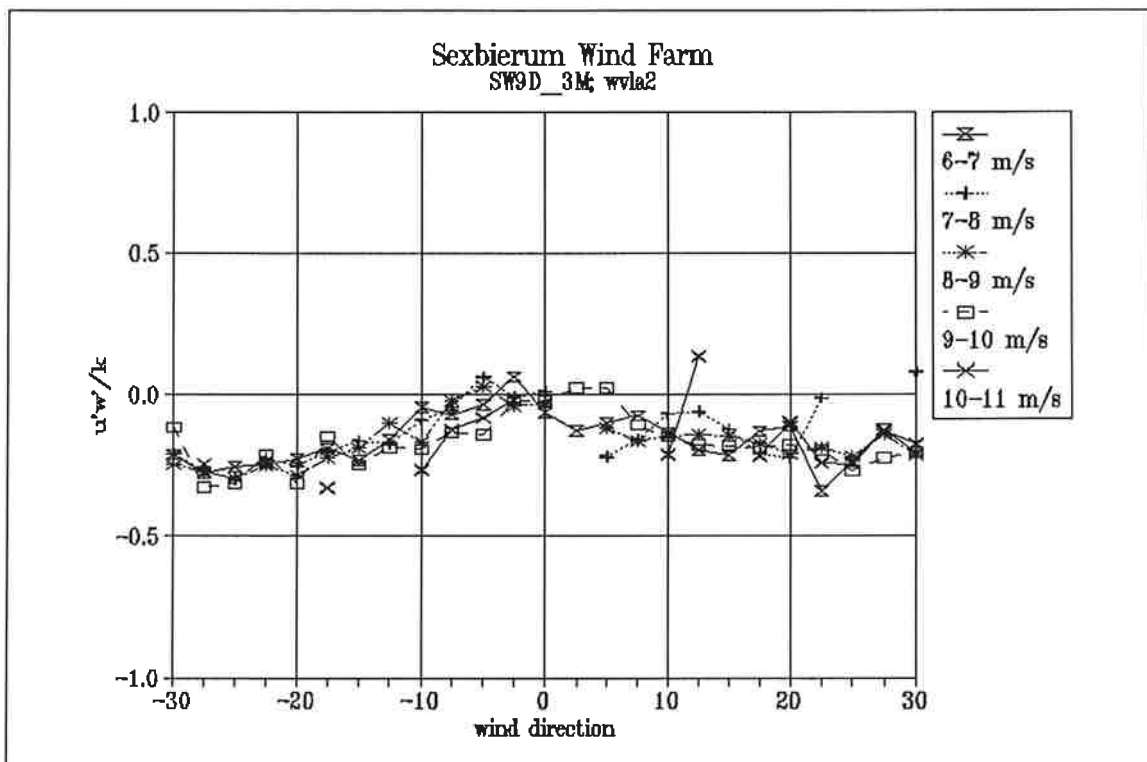


Figure 22 Non-dimensionalized shear stress  $u'w'/k$  as a function of wind direction and wind speed bin



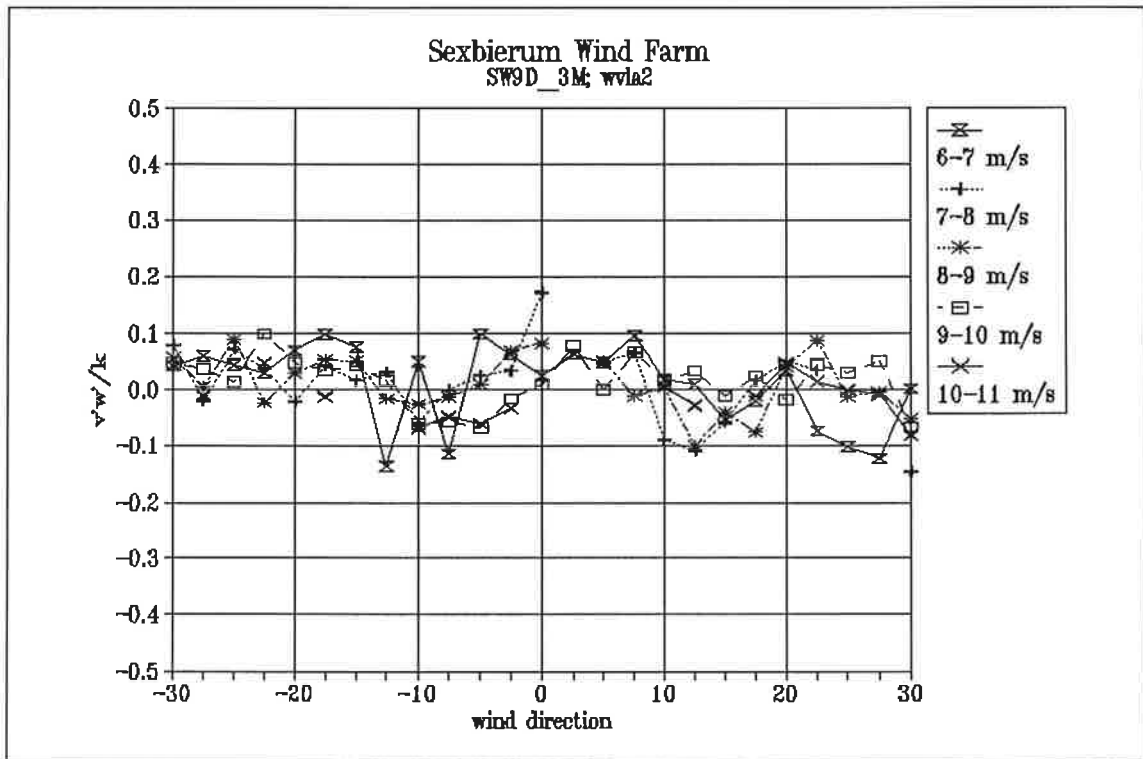


Figure 23 Non-dimensionalized shear stress  $v'w'/k$  as a function of wind direction and wind speed bin

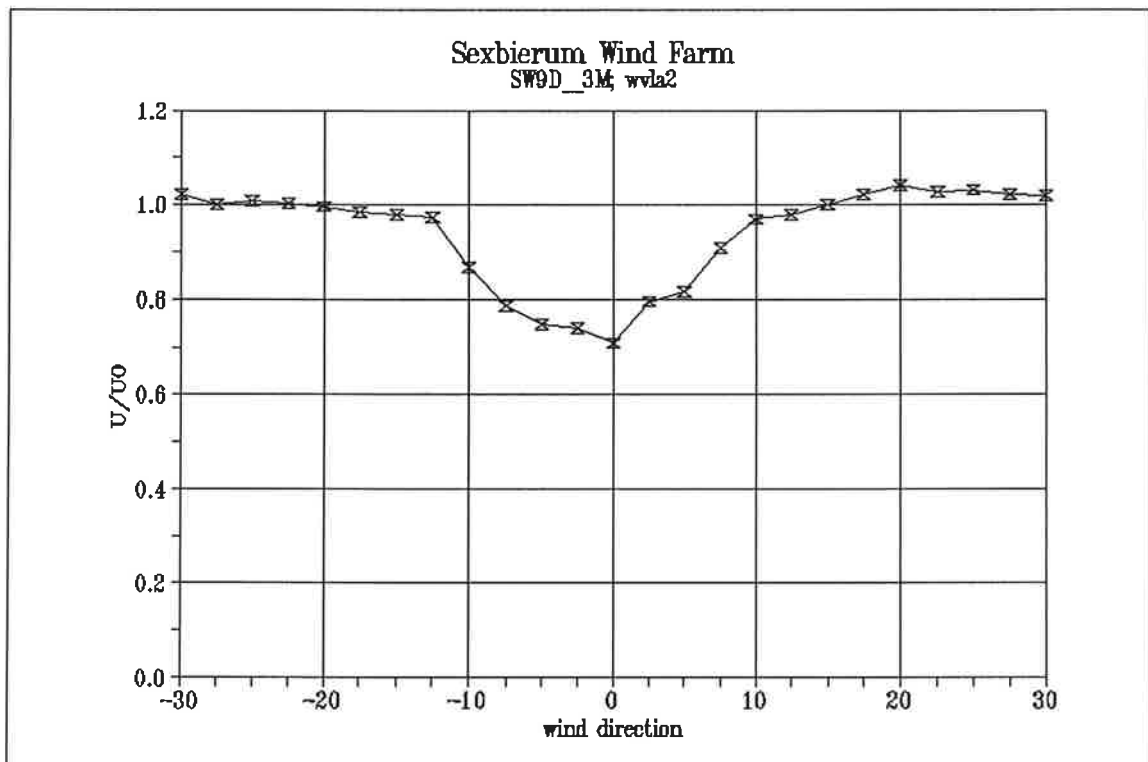


Figure 24 Wake deficit  $U/U_0$  as a function of wind direction in the wind speed bin 5-10 m/s

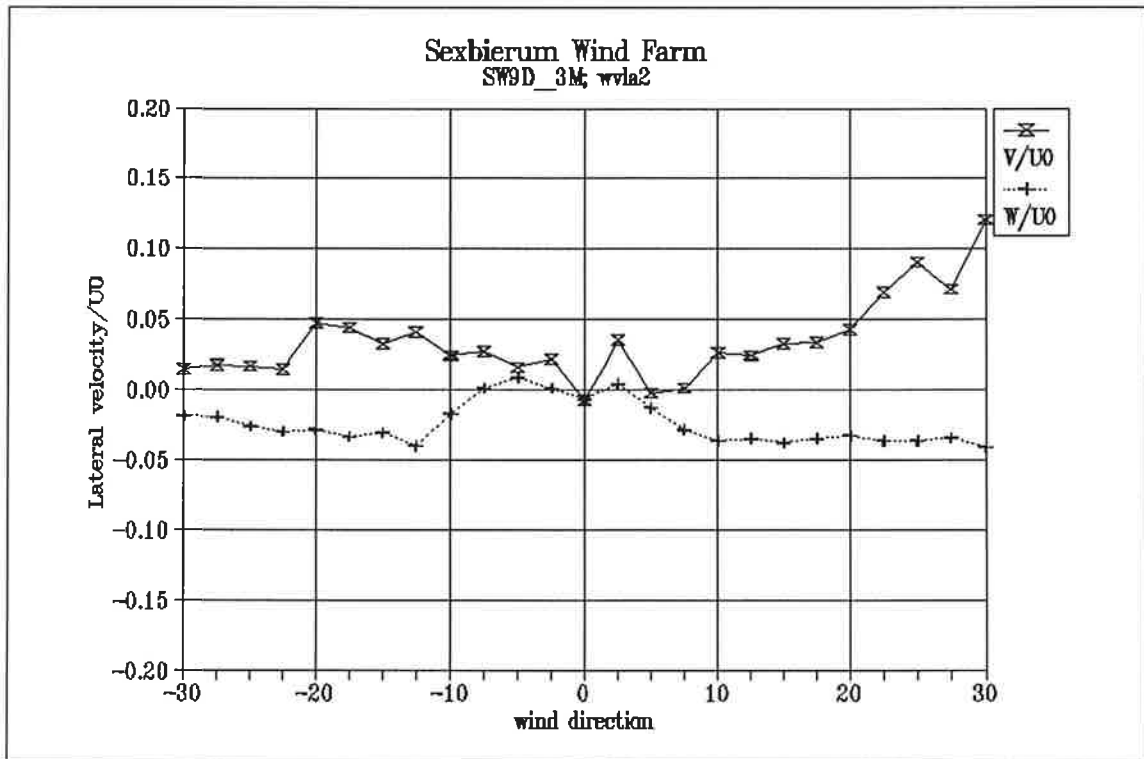


Figure 25 Lateral and vertical wind speed  $V/U_0$  and  $W/U_0$  as a function of wind direction in the wind speed bin 5-10 m/s

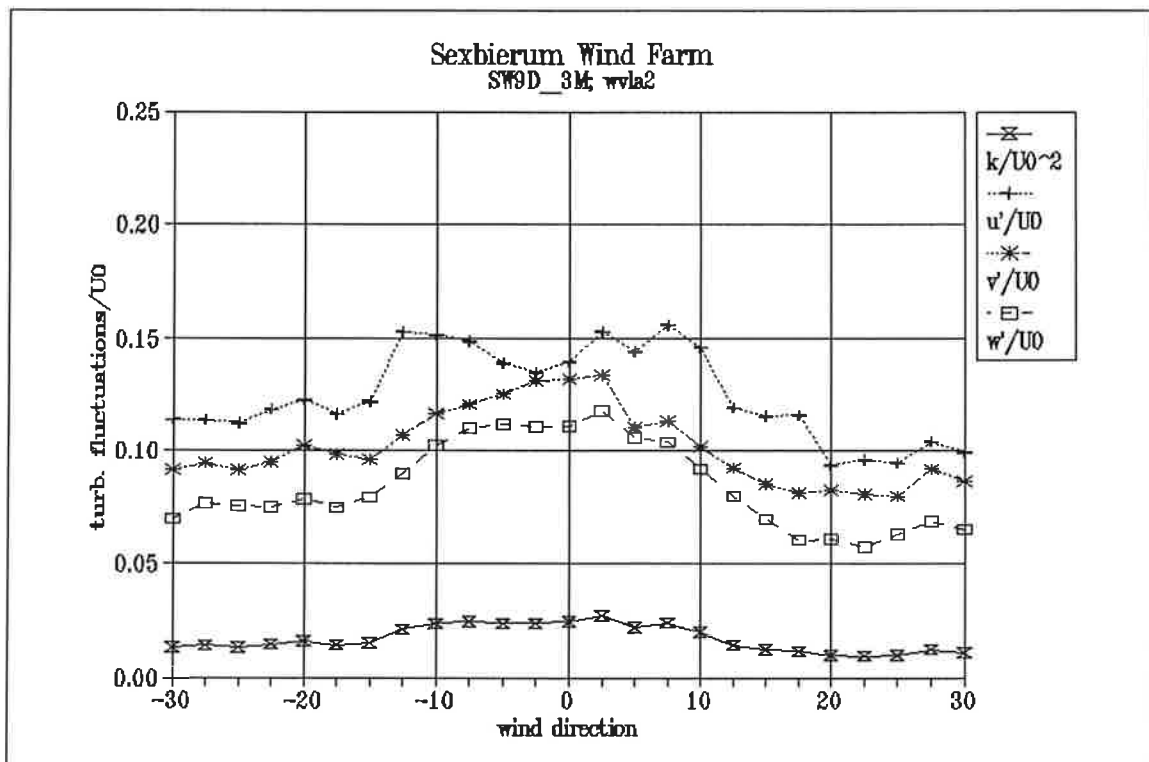


Figure 26 Turbulent fluctuations as a function of wind direction in the wind speed bin 5-10 m/s, non-dimensionalized with  $U_0$

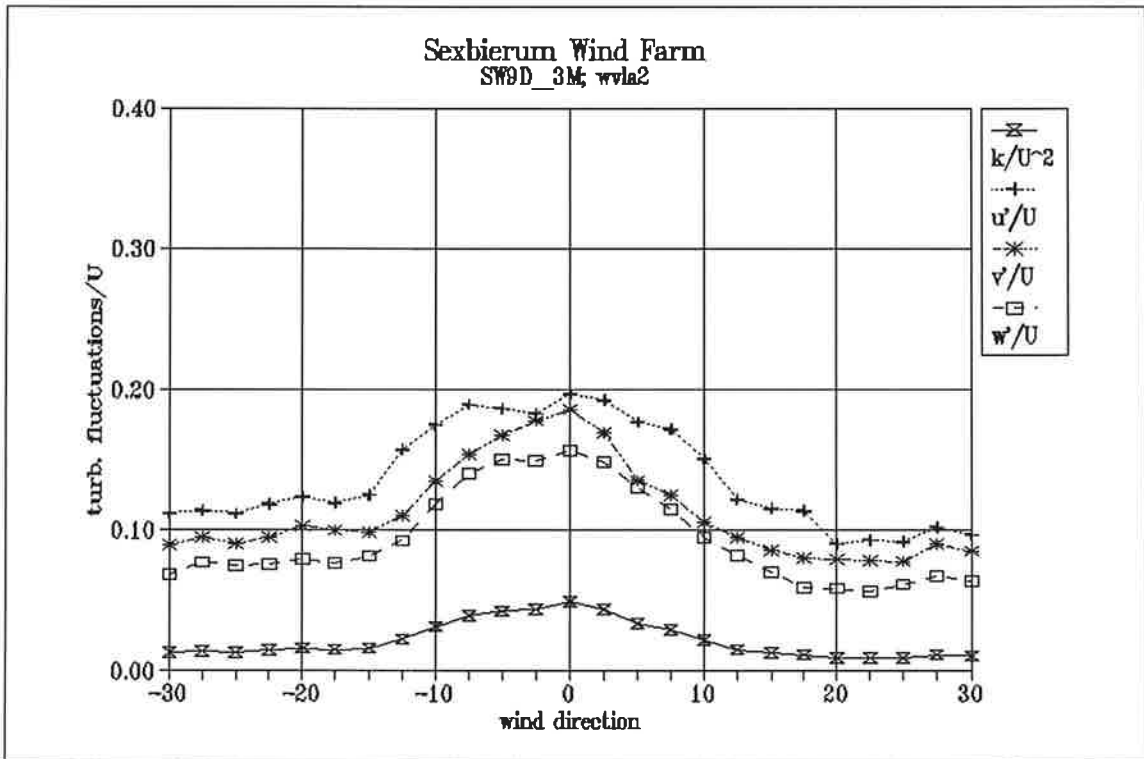


Figure 27 Turbulent fluctuations as a function of wind direction in the wind speed bin 5-10 m/s, non-dimensionalized with  $U$

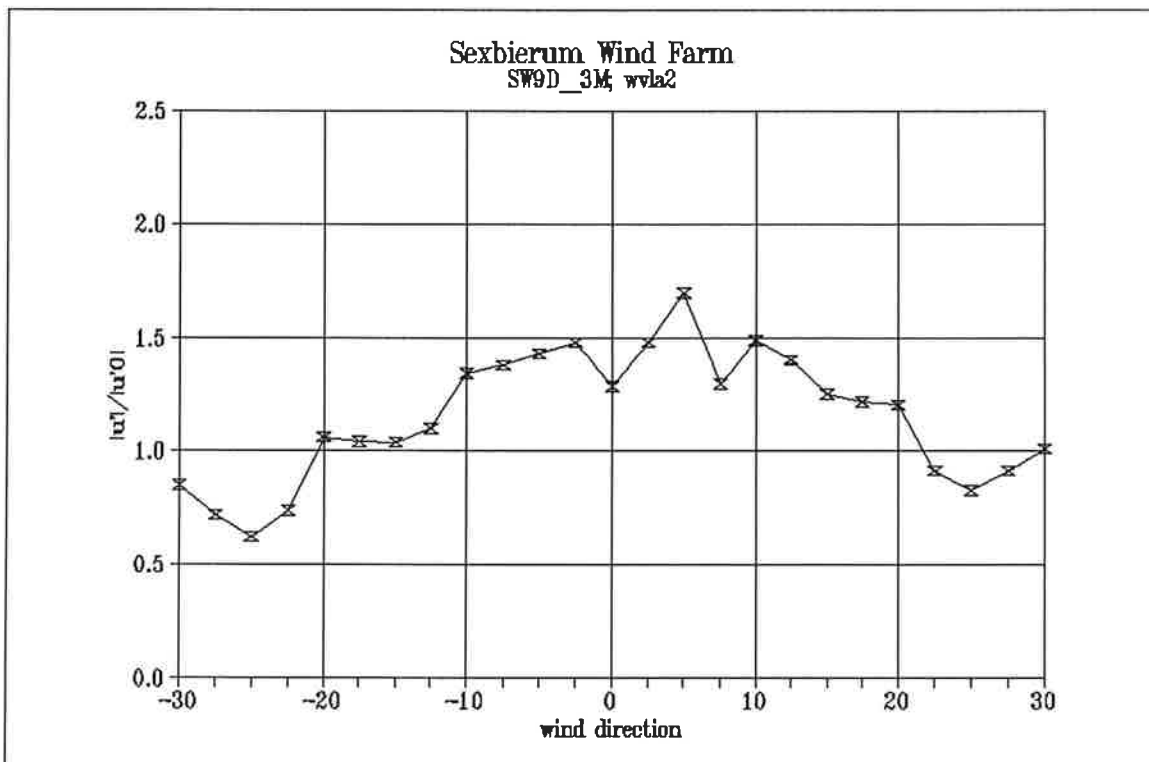


Figure 28 Longitudinal turbulence enhancement  $u'/u'_0$  as a function of wind direction in the wind speed bin 5-10 m/s

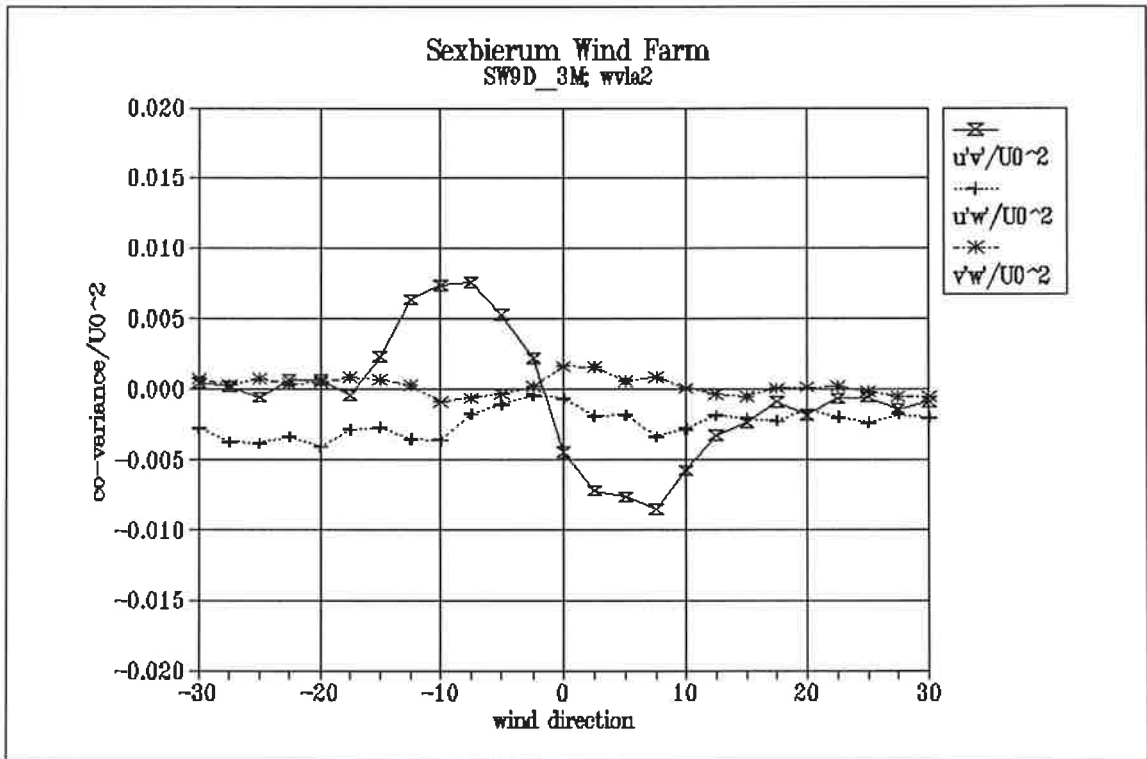


Figure 29 Non-dimensionalized shear stresses  $u'v'/U_0^2$ ;  $u'w'/U_0^2$ ;  $v'w'/U_0^2$  as a function of wind direction in the wind speed bin 5-10 m/s

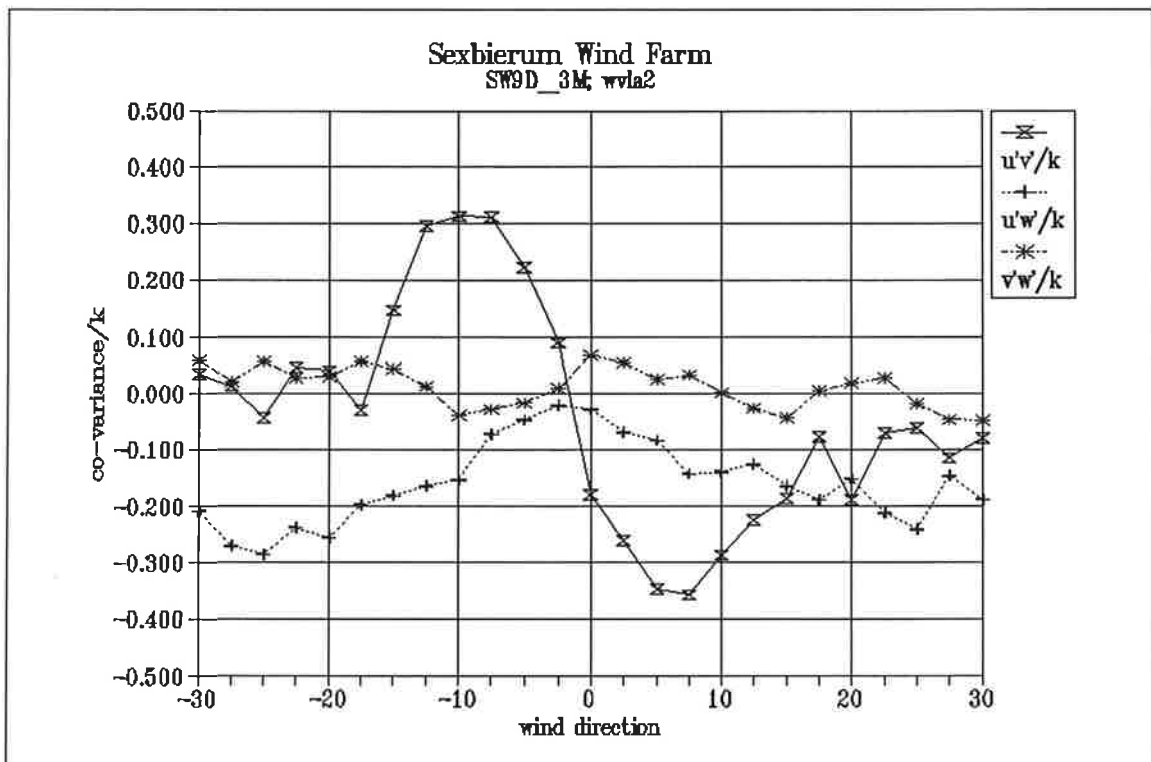


Figure 30 Non-dimensionalized shear stresses  $u'v'/k$ ;  $u'w'/k$ ;  $v'w'/k$  as a function of wind direction in the wind speed bin 5-10 m/s

*Results of Sexbierum Wind Farm; single wake measurements*

**A4.2 Sensor b1**

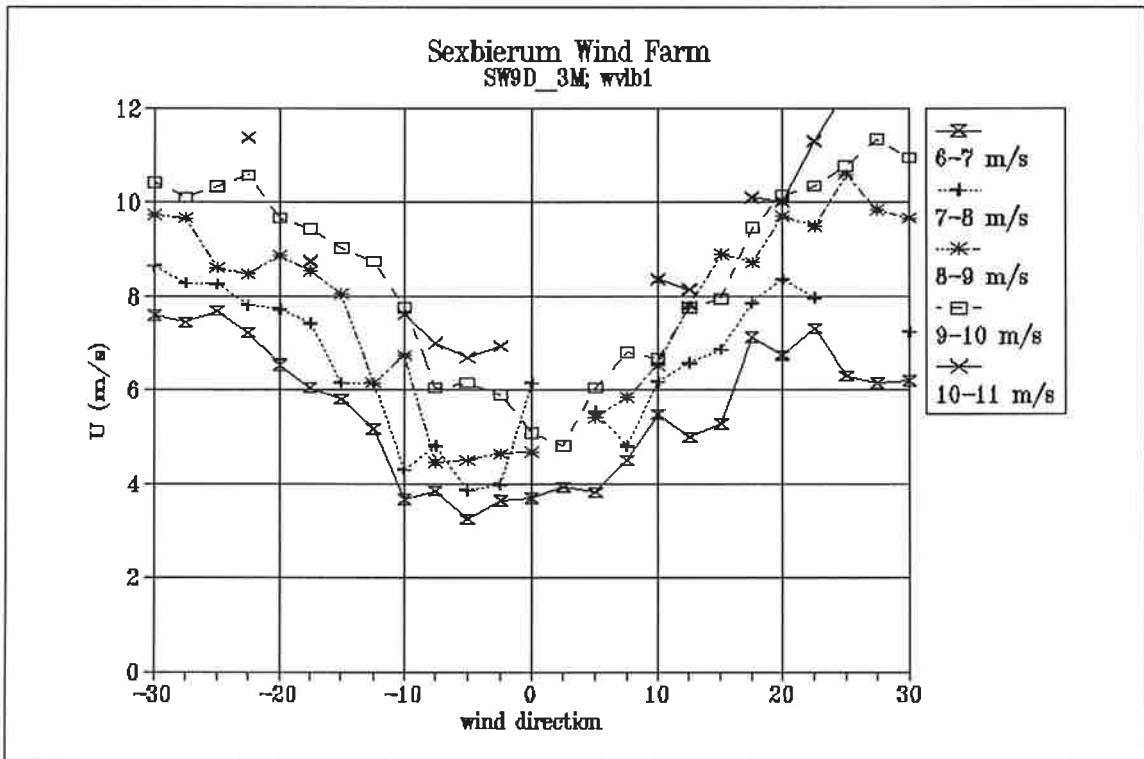


Figure 1 Horizontal wind speed  $U$  as a function of wind direction and wind speed bin

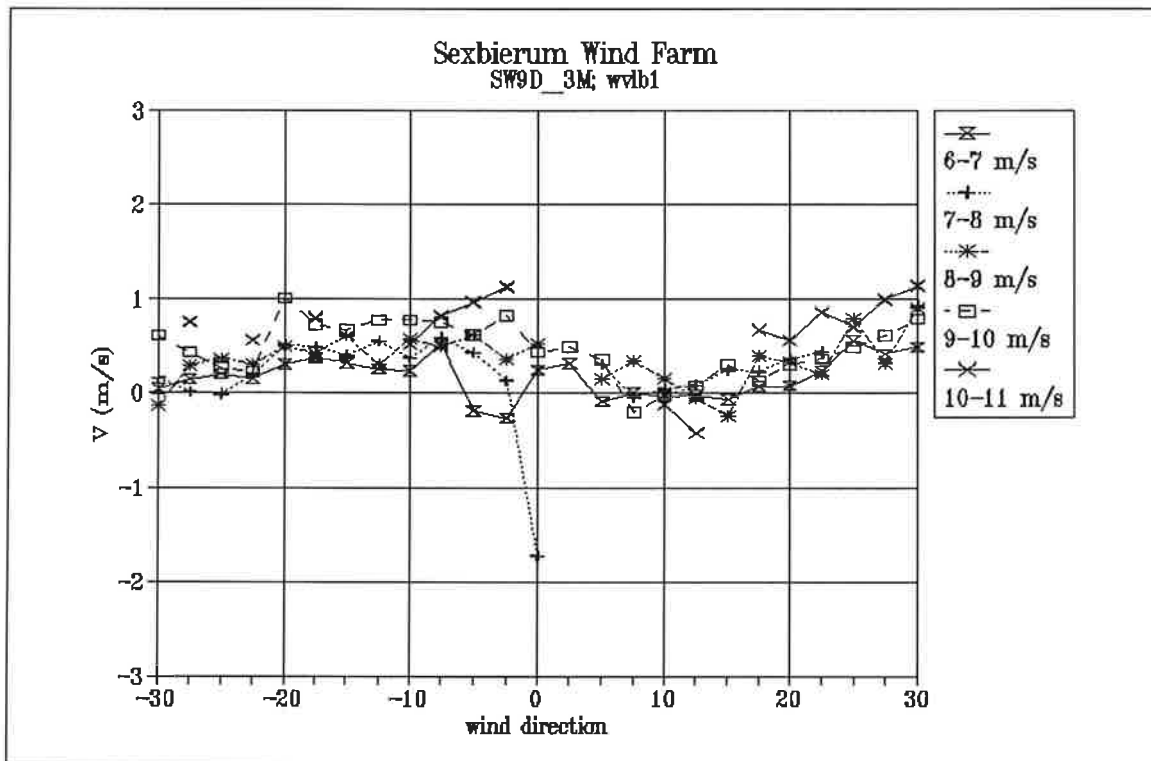


Figure 2 Lateral wind speed  $V$  as a function of wind direction and wind speed bin

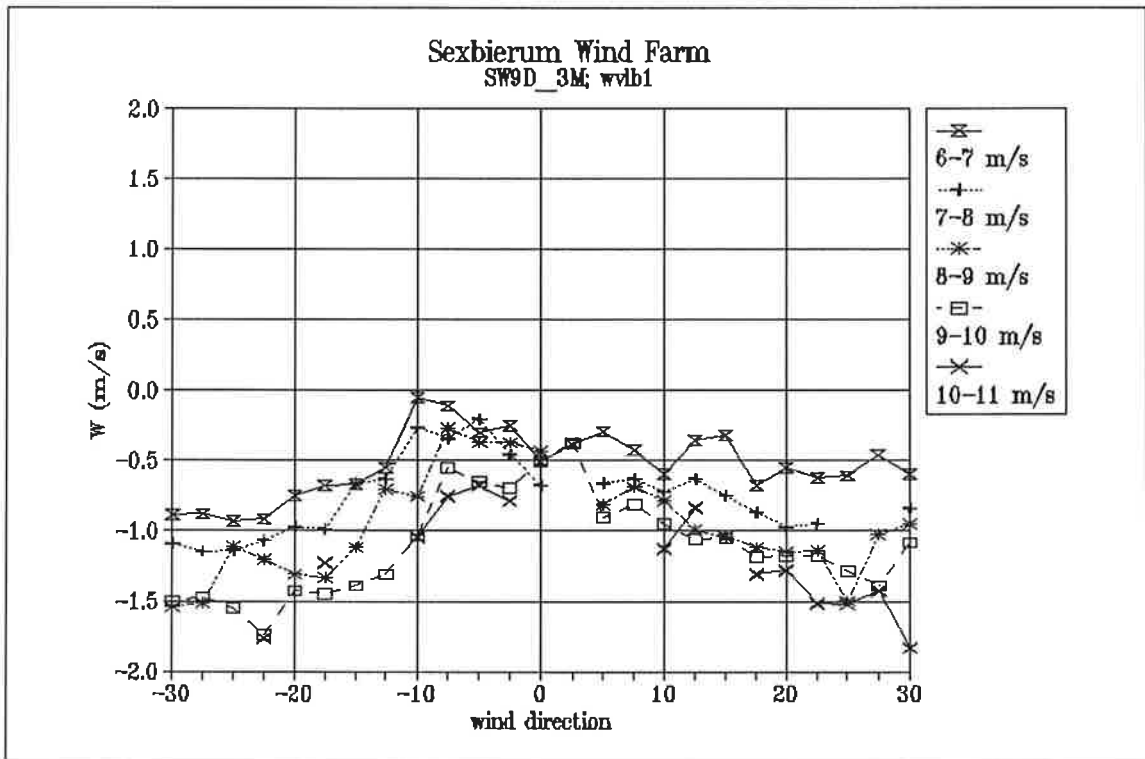


Figure 3 Vertical wind speed  $W$  as a function of wind direction and wind speed bin

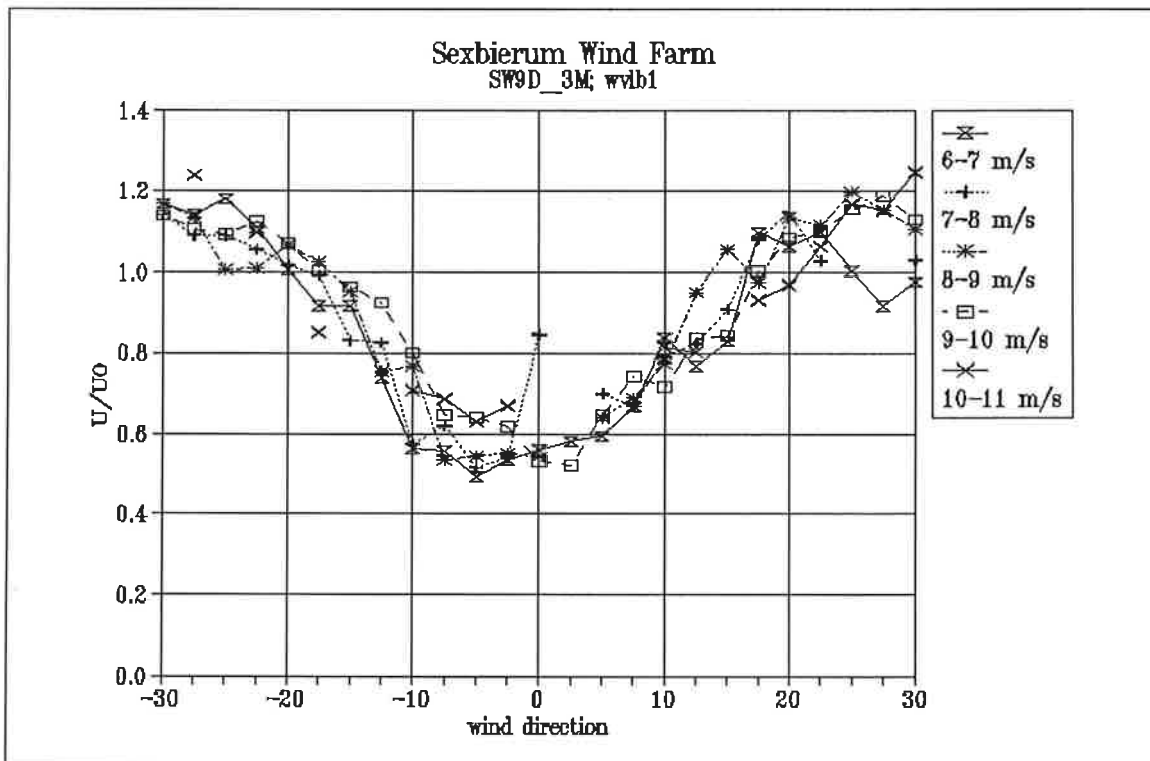


Figure 4 Wake deficit  $U/U_0$  as a function of wind direction and wind speed bin

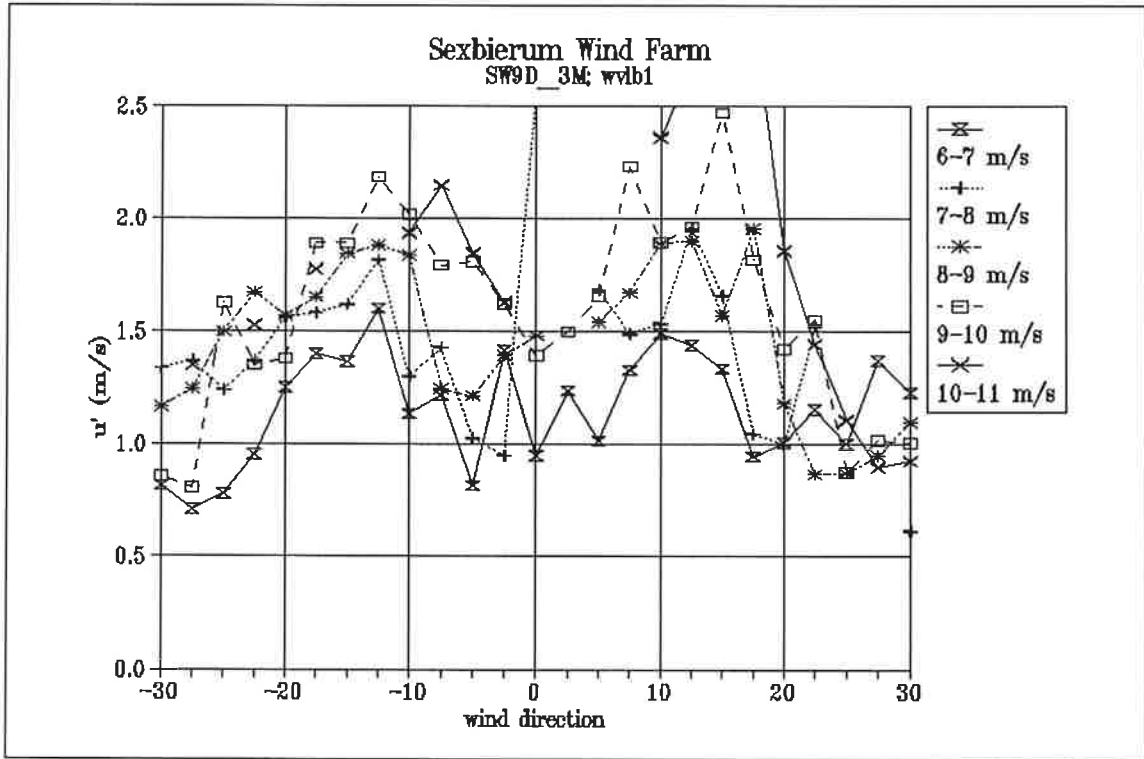


Figure 5 Longitudinal turbulent fluctuations  $u'$  as a function of wind direction and wind speed bin

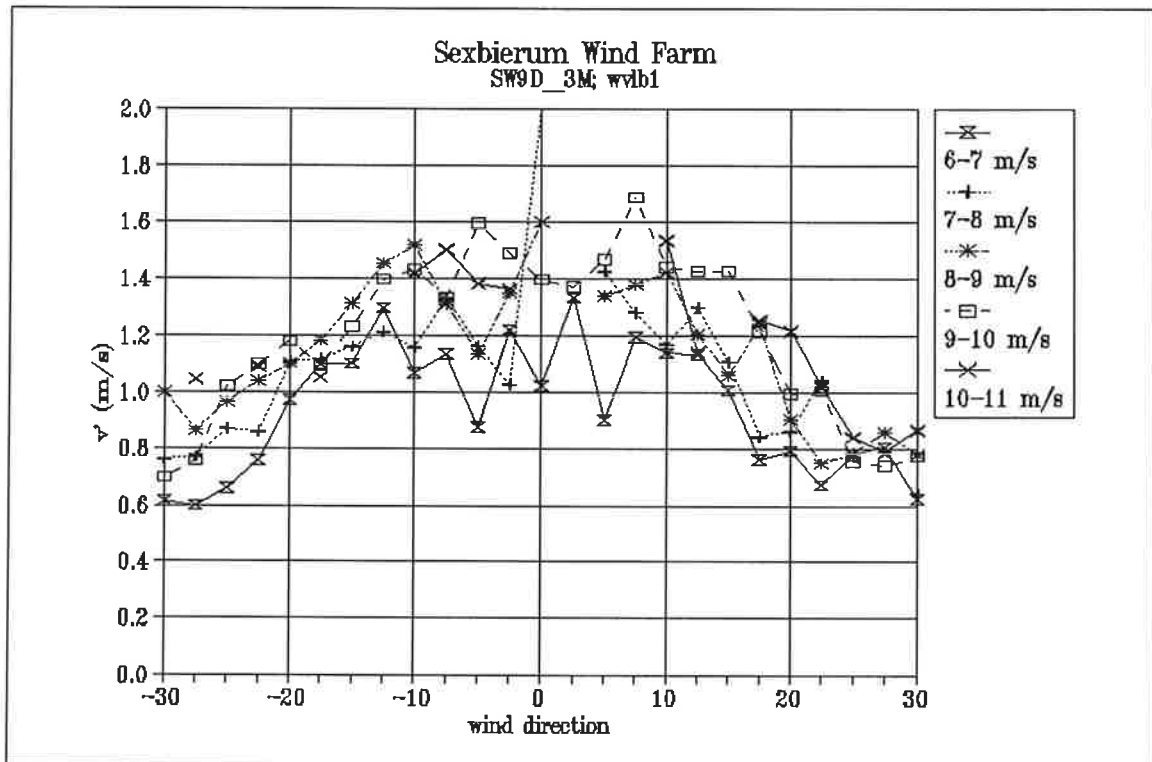


Figure 6 Lateral turbulent fluctuations  $v'$  as a function of wind direction and wind speed bin



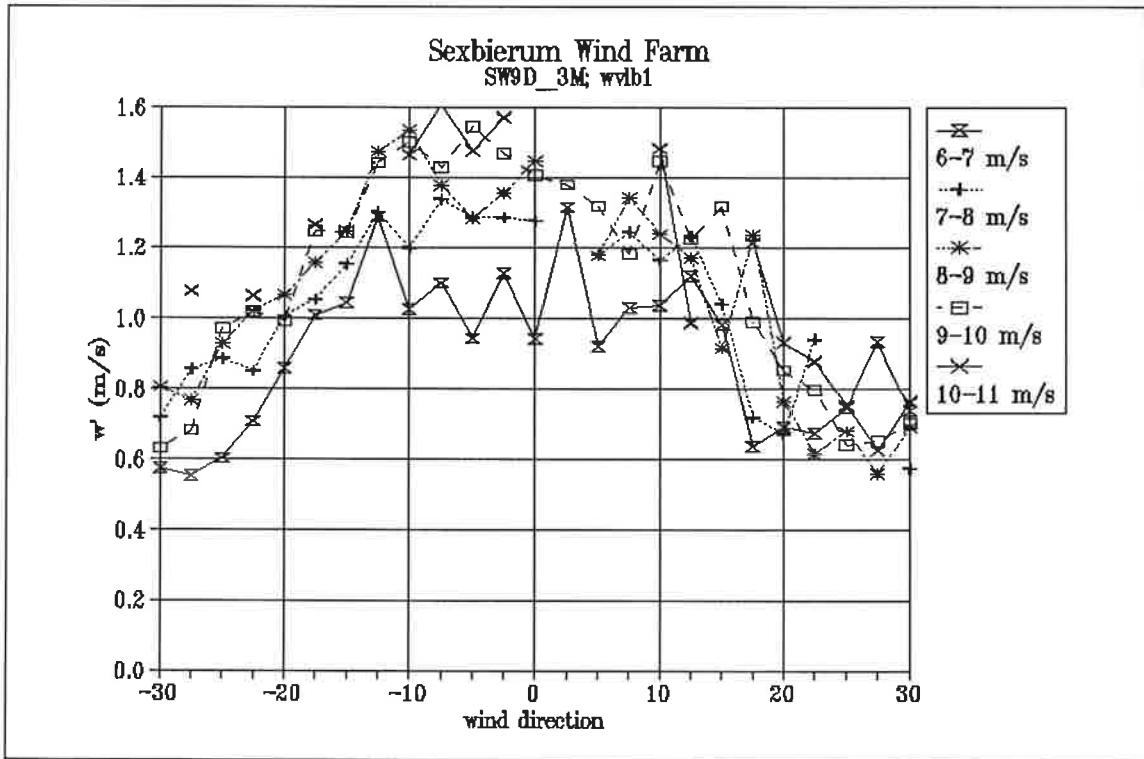


Figure 7 Vertical turbulent fluctuations  $w'$  as a function of wind direction and wind speed bin

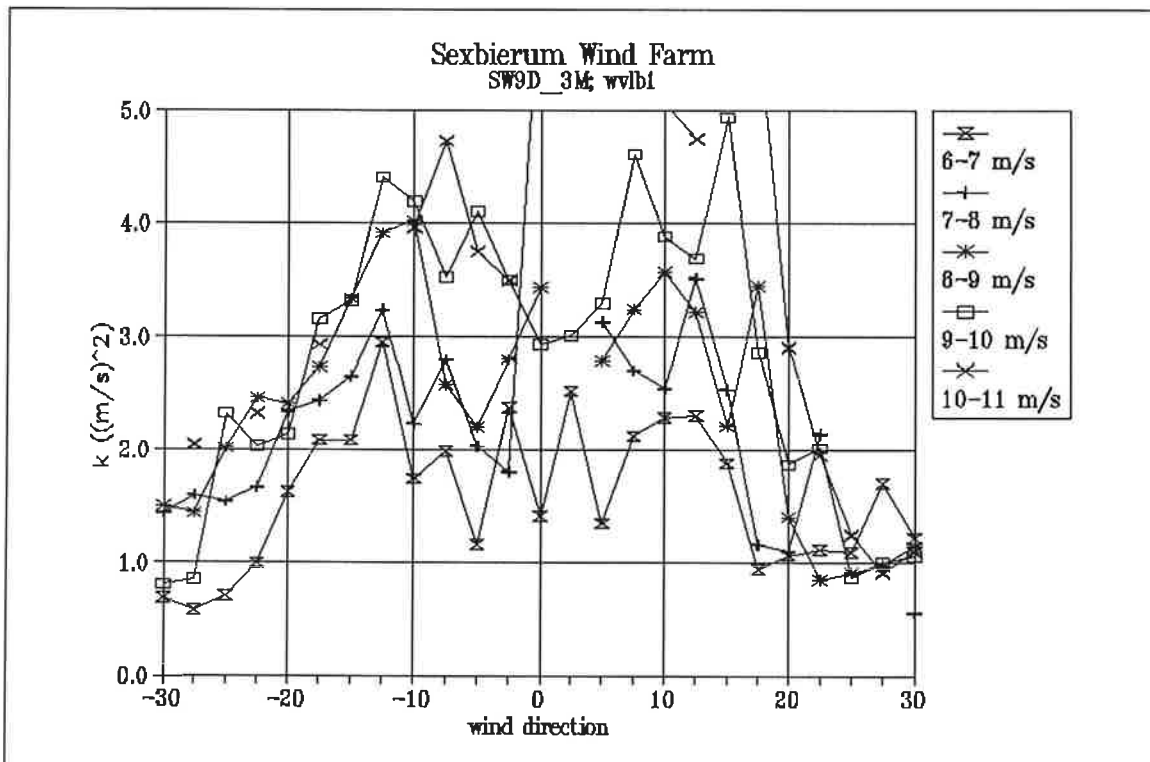


Figure 8 Turbulent kinetic energy per unit mass as a function of wind direction and wind speed bin

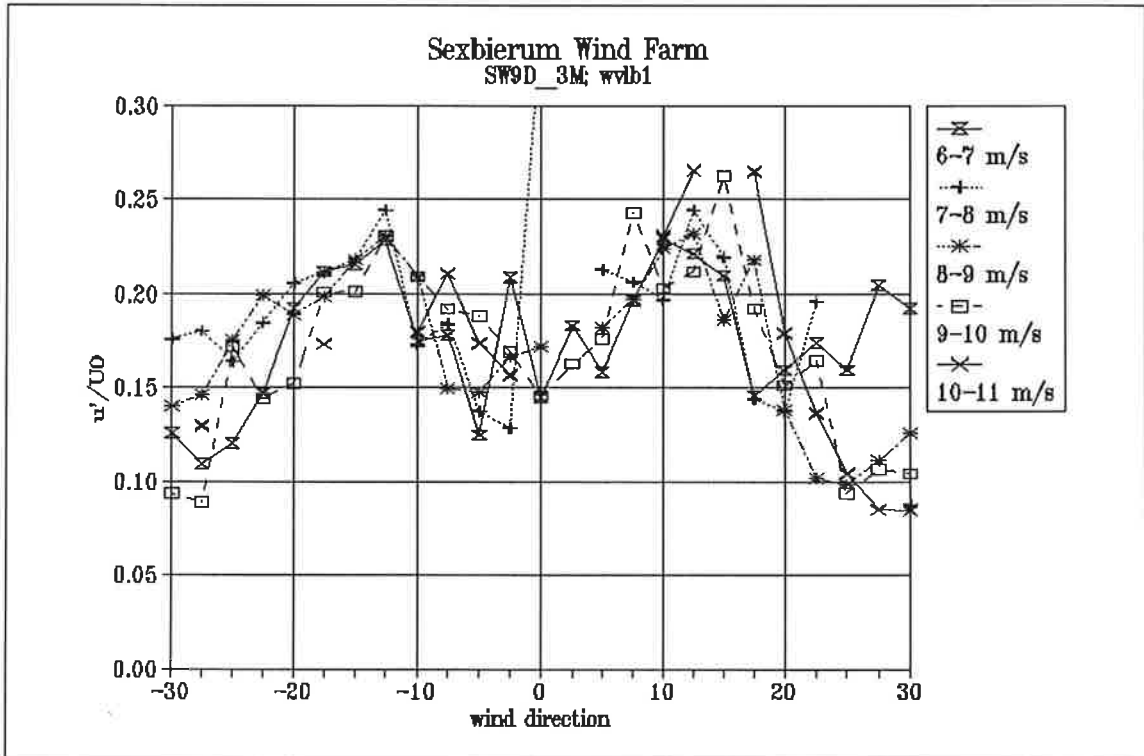


Figure 9 Non-dimensionalized longitudinal turbulent fluctuations  $u'/U_0$  as a function of wind direction and wind speed bin

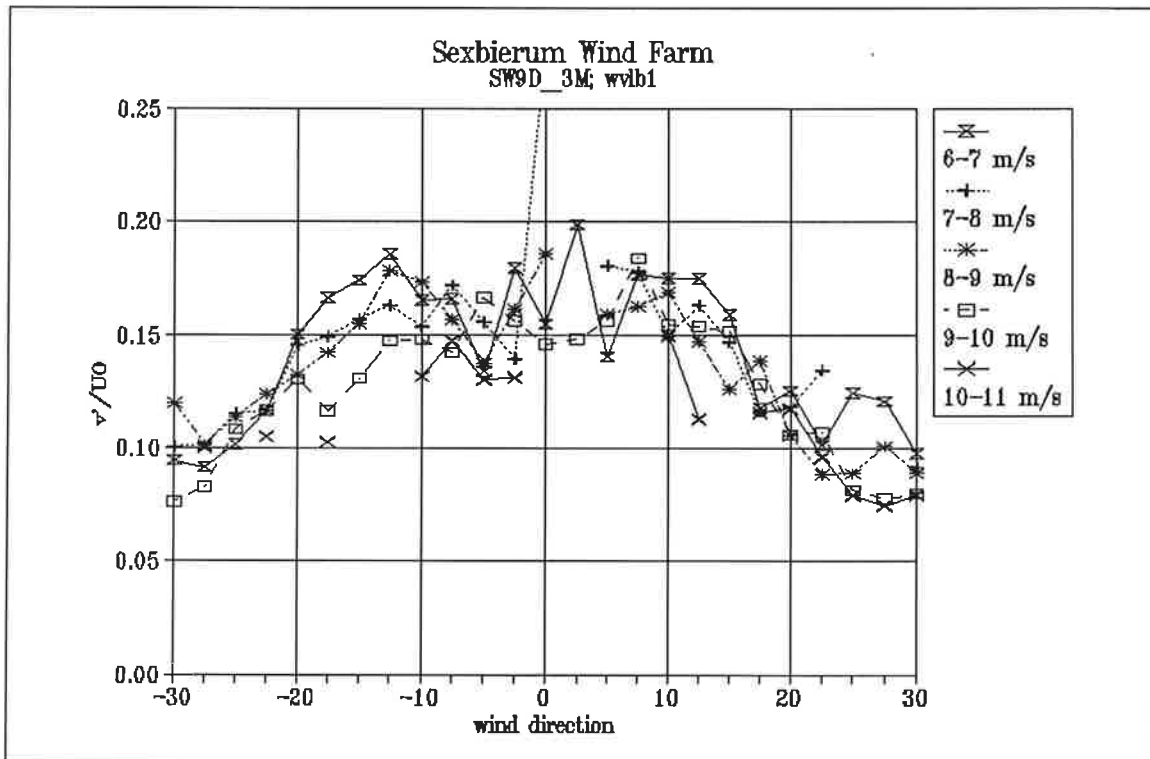


Figure 10 Non-dimensionalized lateral turbulent fluctuations  $v'/U_0$  as a function of wind direction and wind speed bin

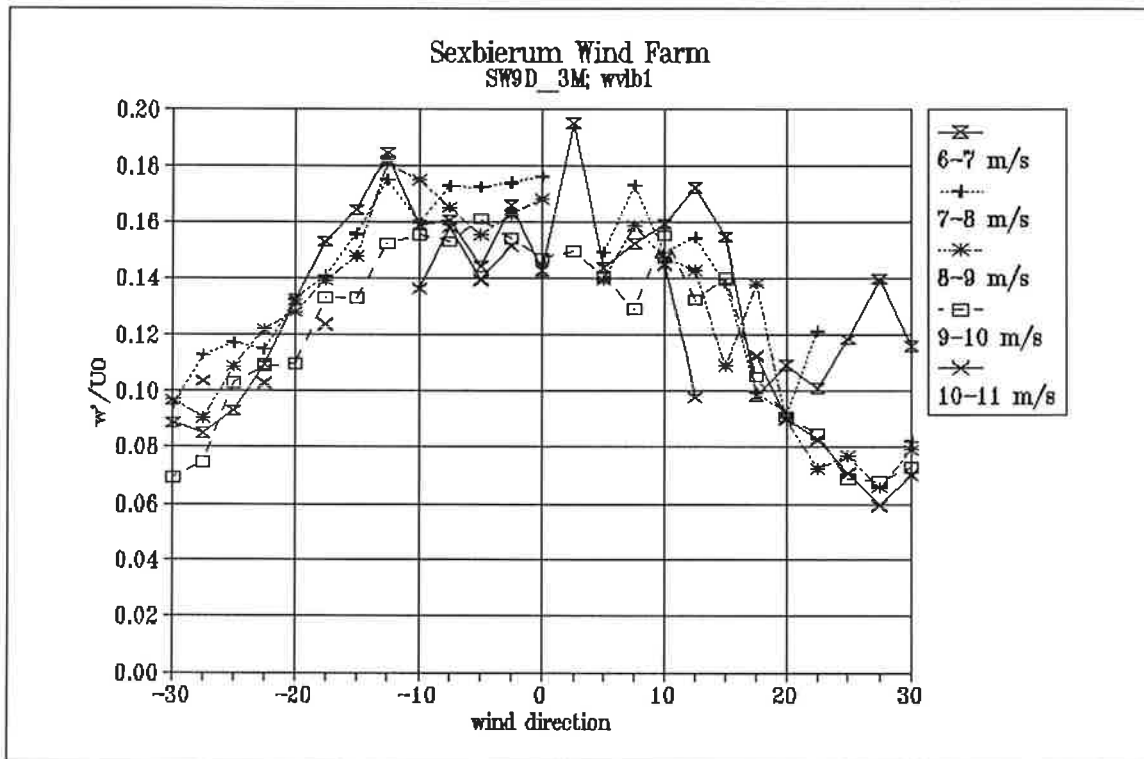


Figure 11 Non-dimensionalized vertical turbulent fluctuations  $w'/U_0$  as a function of wind direction and wind speed bin

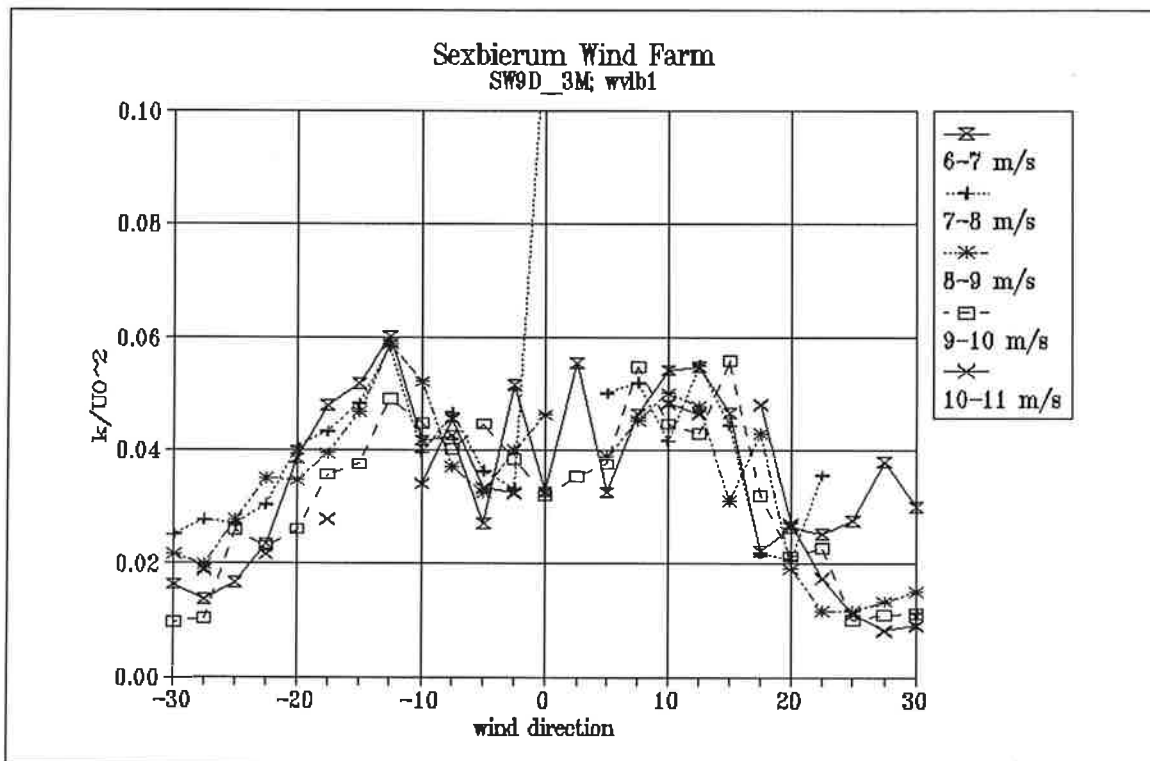


Figure 12 Non-dimensionalized turbulent kinetic energy  $k/U_0^2$  as a function of wind direction and wind speed bin

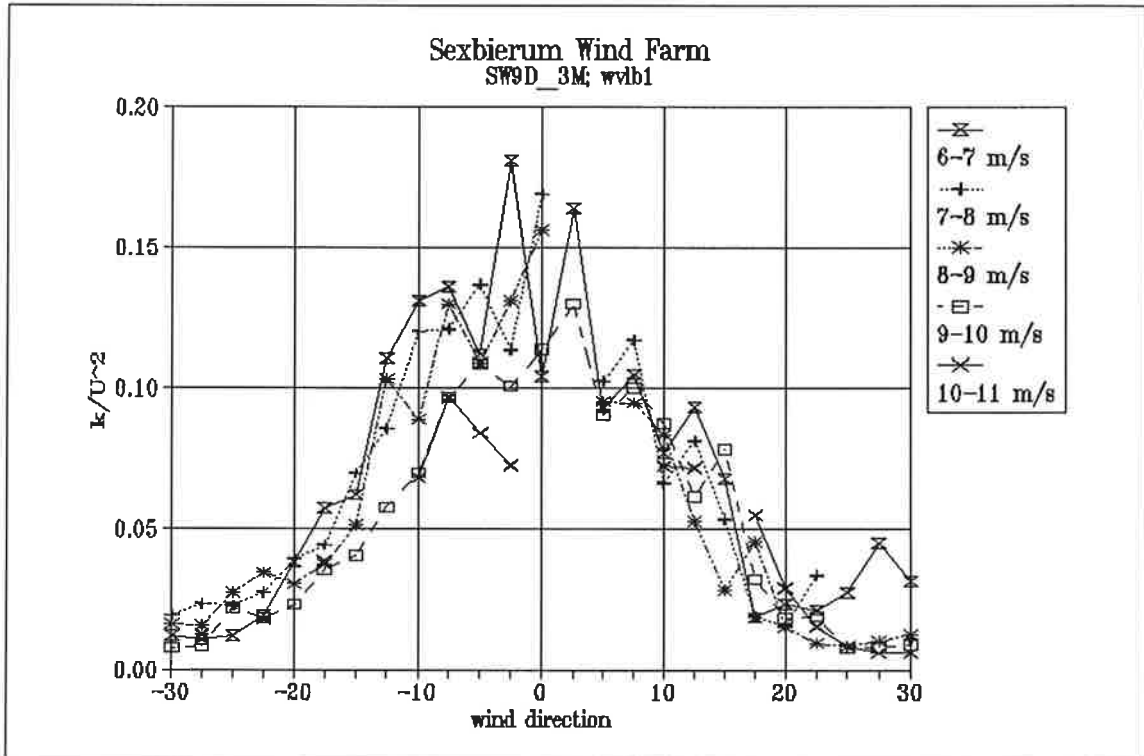


Figure 13 Non-dimensionalized turbulent kinetic energy  $k/U^2$  as a function of wind direction and wind speed bin

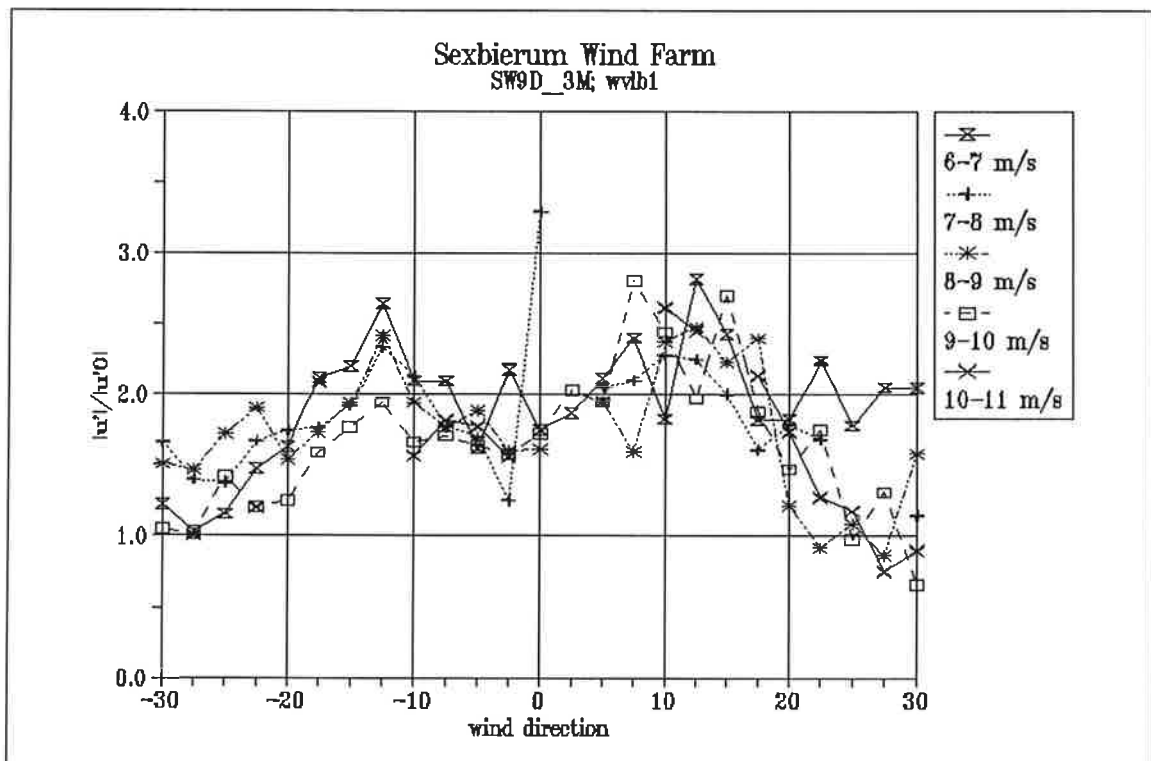


Figure 14 Longitudinal turbulence enhancement  $u' u'_0$  as a function of wind direction and wind speed bin

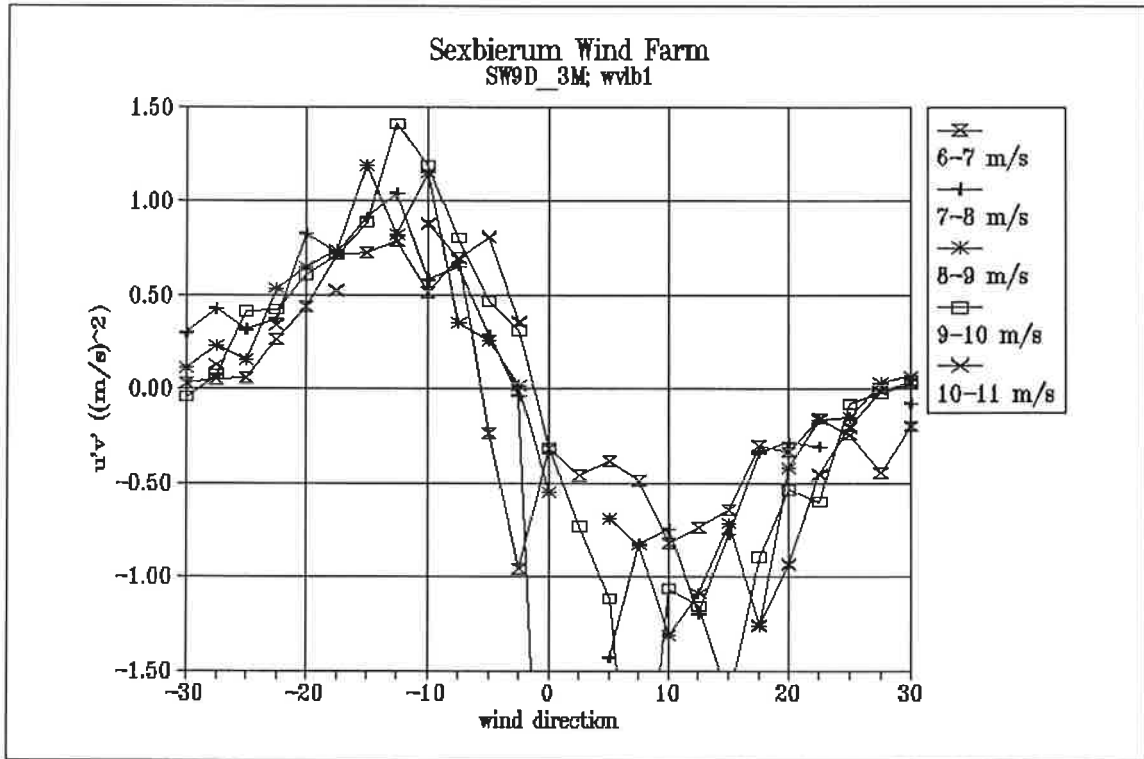


Figure 15 Shear stress  $u'v'$  as a function of wind direction and wind speed bin

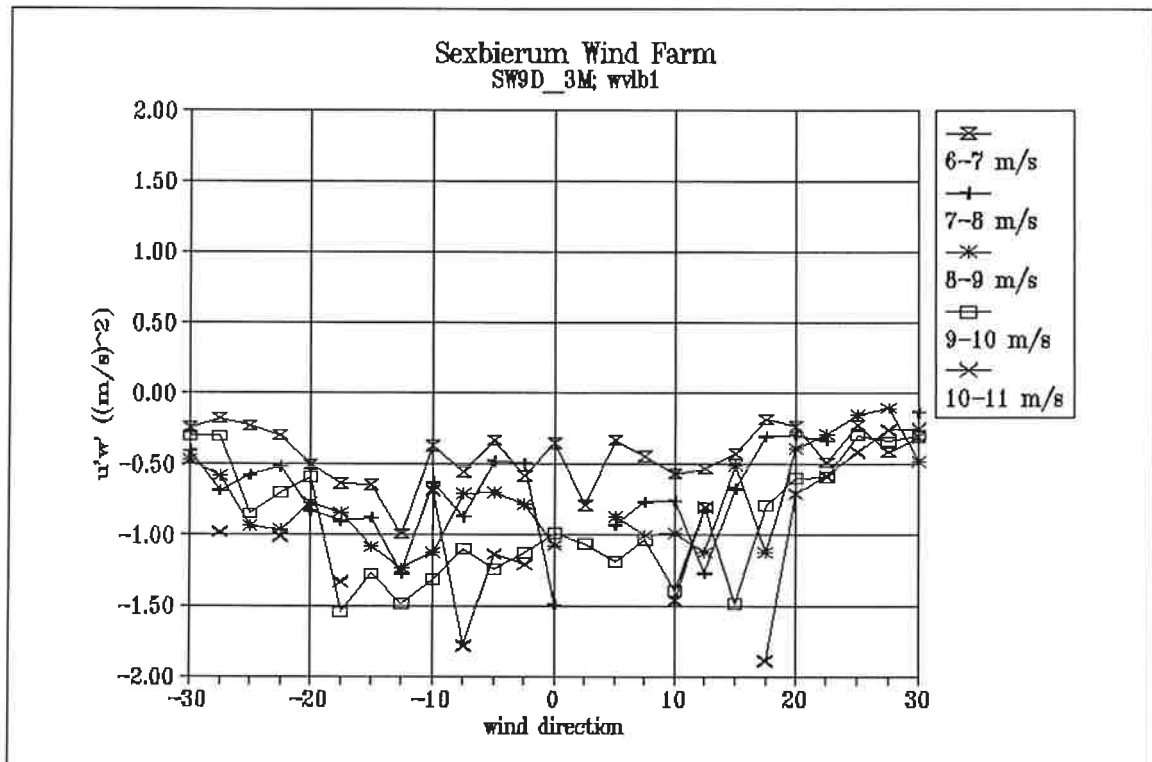


Figure 16 Shear stress  $u'w'$  as a function of wind direction and wind speed bin

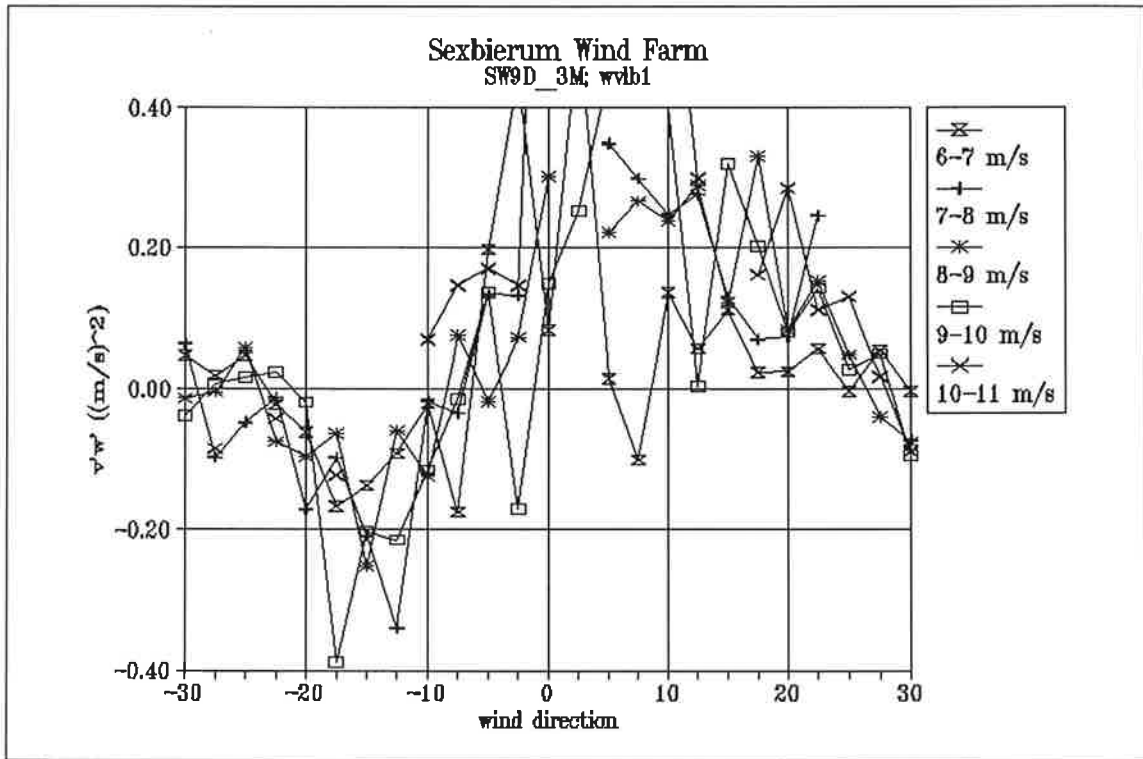


Figure 17 Shear stress  $v'w'$  as a function of wind direction and wind speed bin

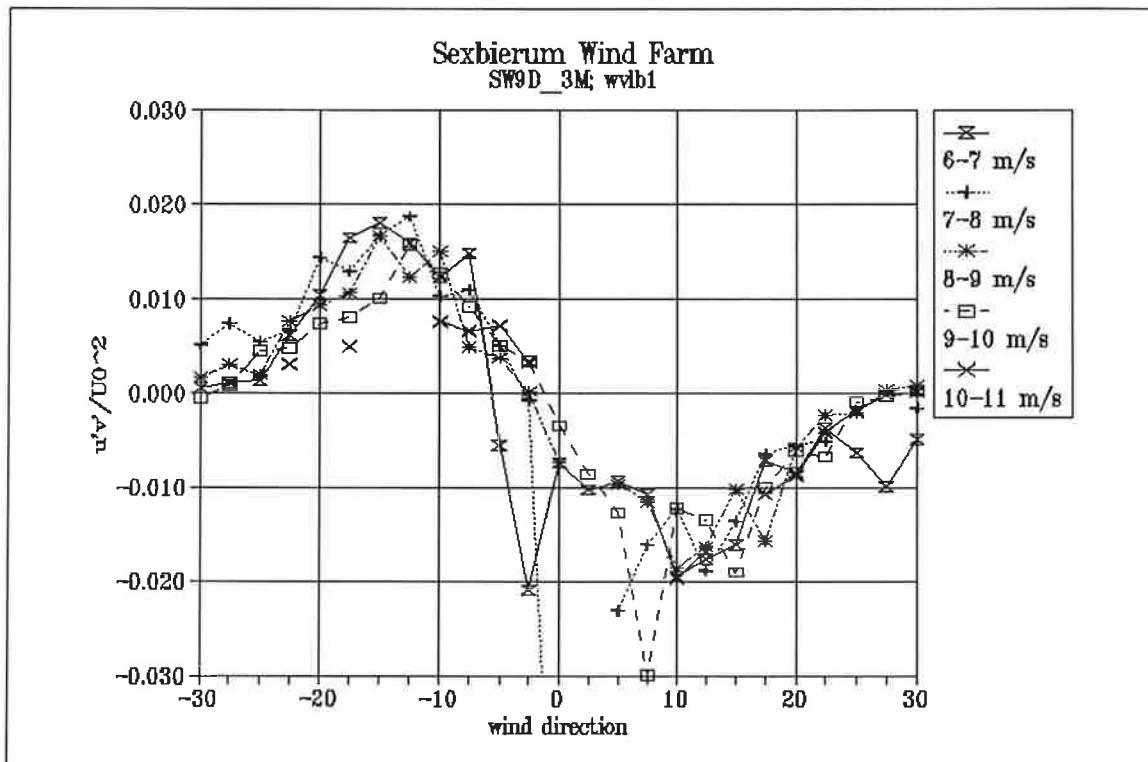


Figure 18 Non-dimensionalized shear stress  $u'v'/U_0^2$  as a function of wind direction and wind speed bin

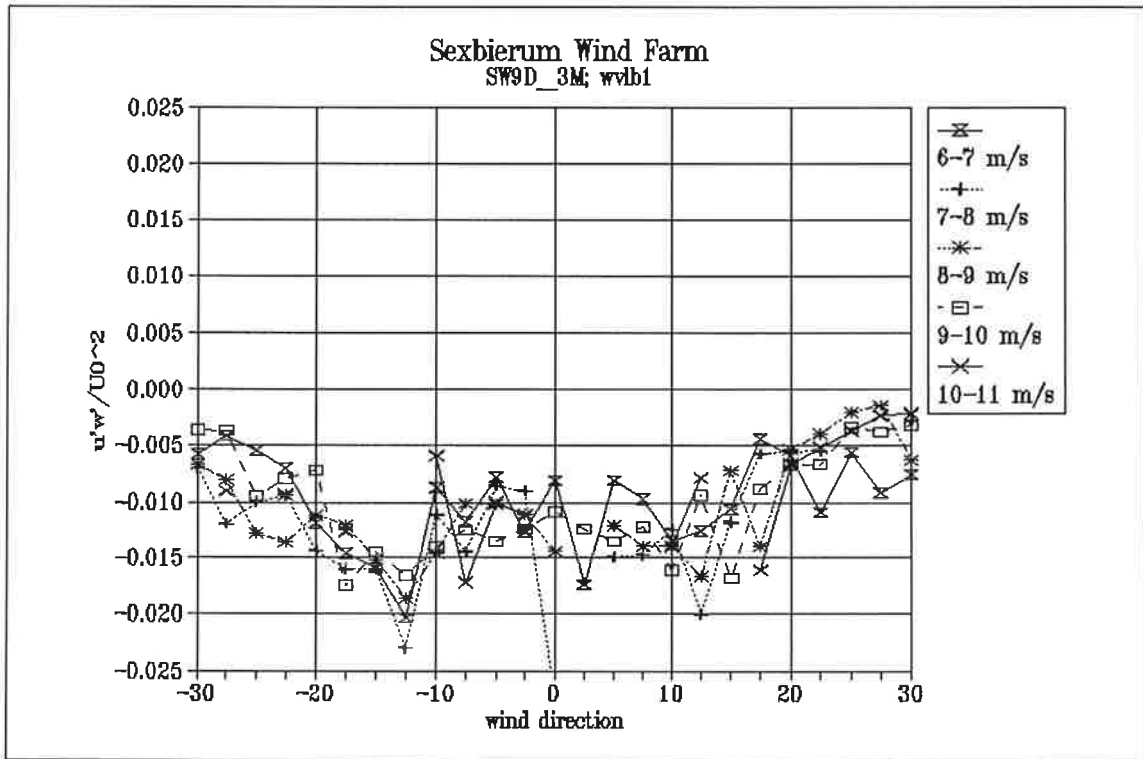


Figure 19 Non-dimensionalized shear stress  $u'w'/U_0^2$  as a function of wind direction and wind speed bin

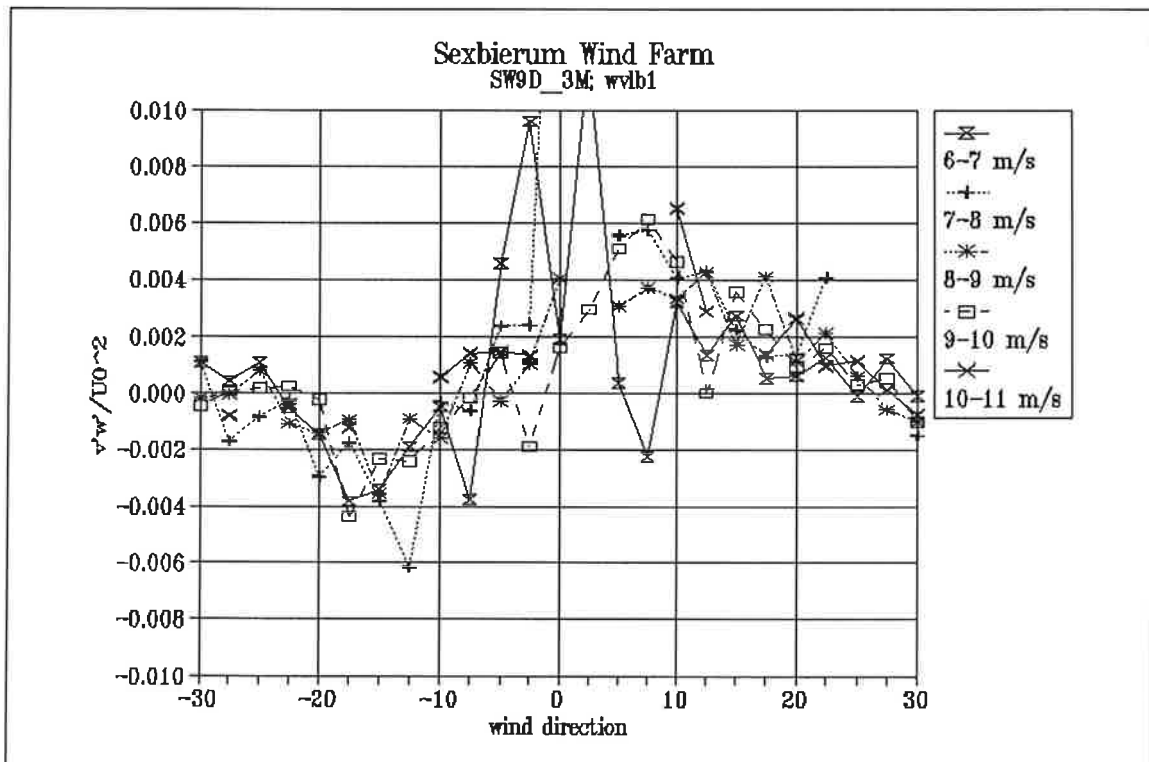


Figure 20 Non-dimensionalized shear stress  $v'w'/U_0^2$  as a function of wind direction and wind speed bin

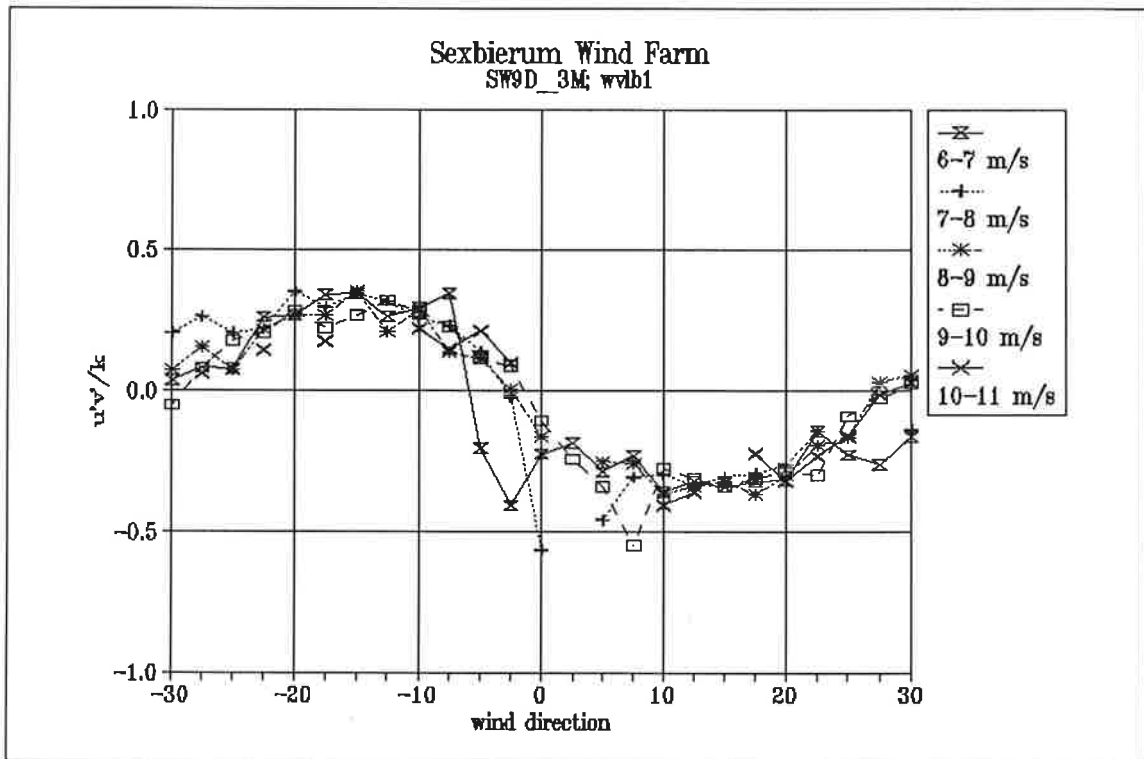


Figure 21 Non-dimensionalized shear stress  $u'v'/k$  as a function of wind direction and wind speed bin

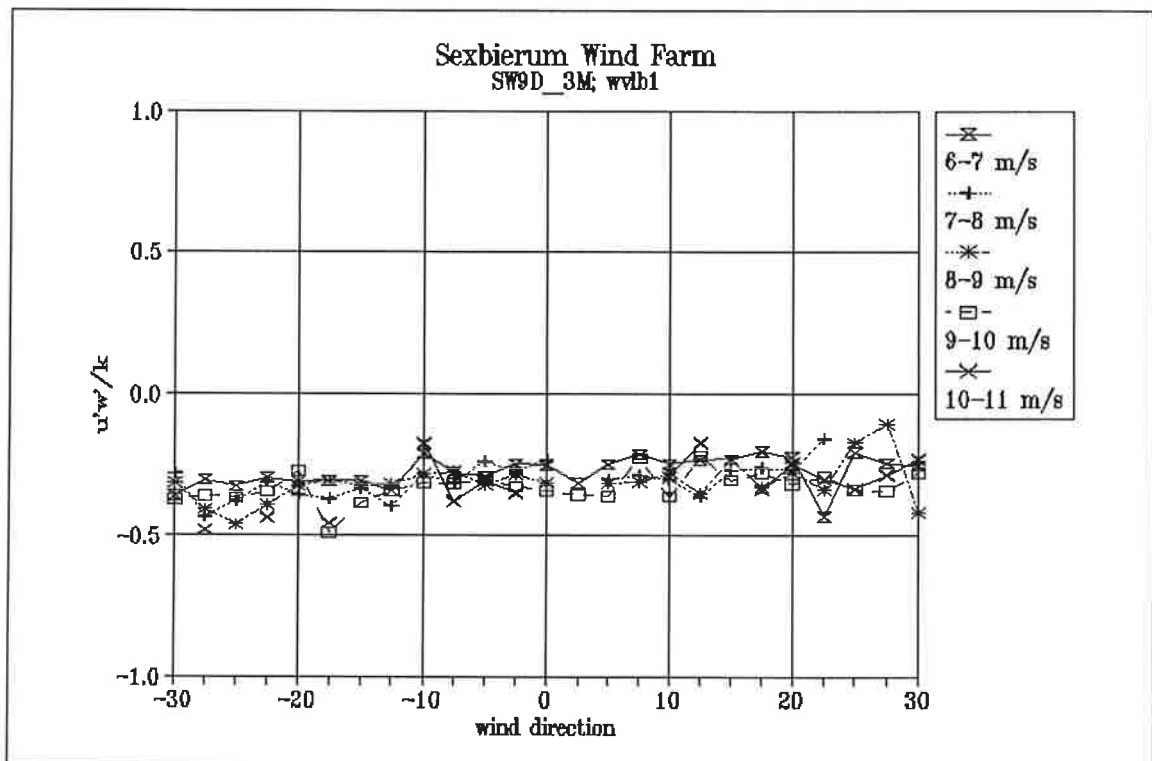


Figure 22 Non-dimensionalized shear stress  $u'w'/k$  as a function of wind direction and wind speed bin



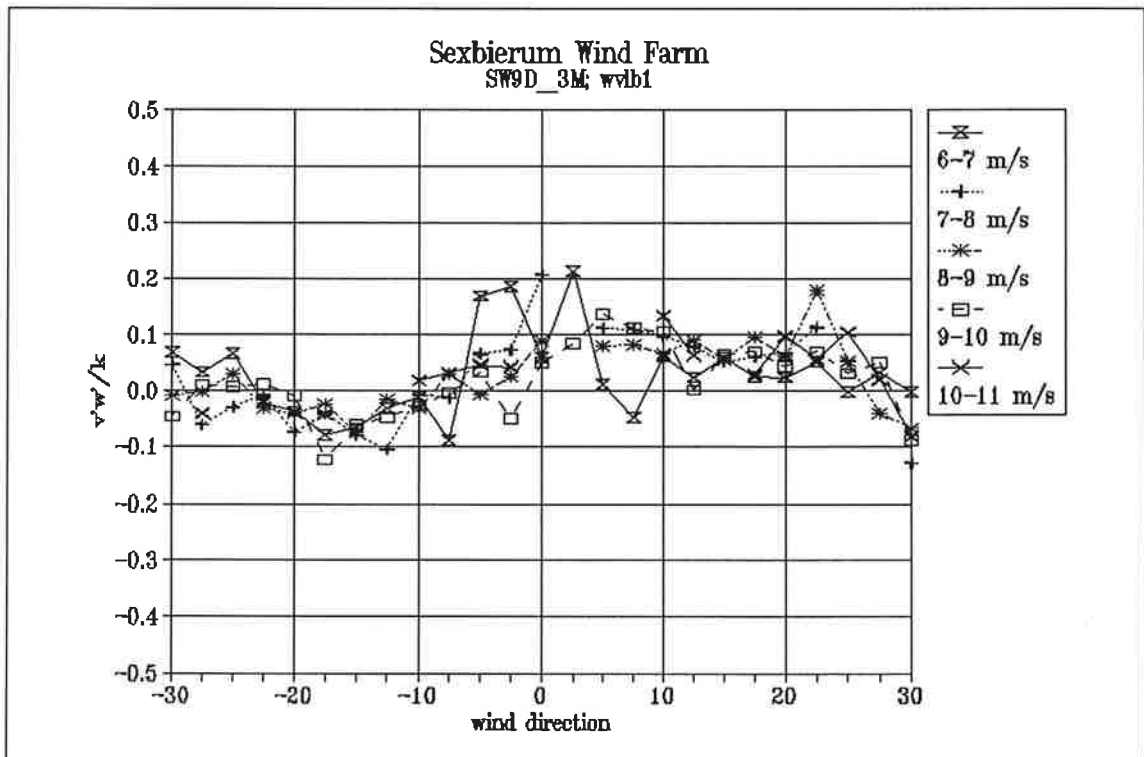


Figure 23 Non-dimensionalized shear stress  $v'w'/k$  as a function of wind direction and wind speed bin

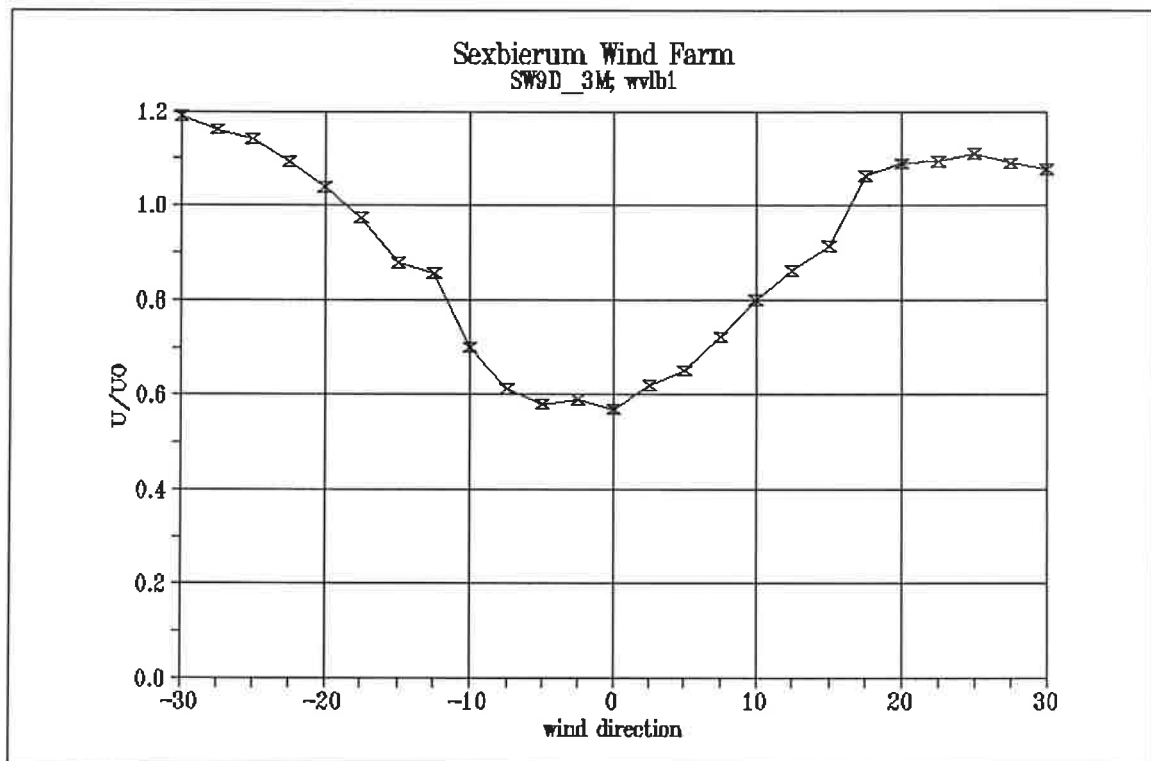


Figure 24 Wake deficit  $U/U_0$  as a function of wind direction in the wind speed bin 5-10 m/s

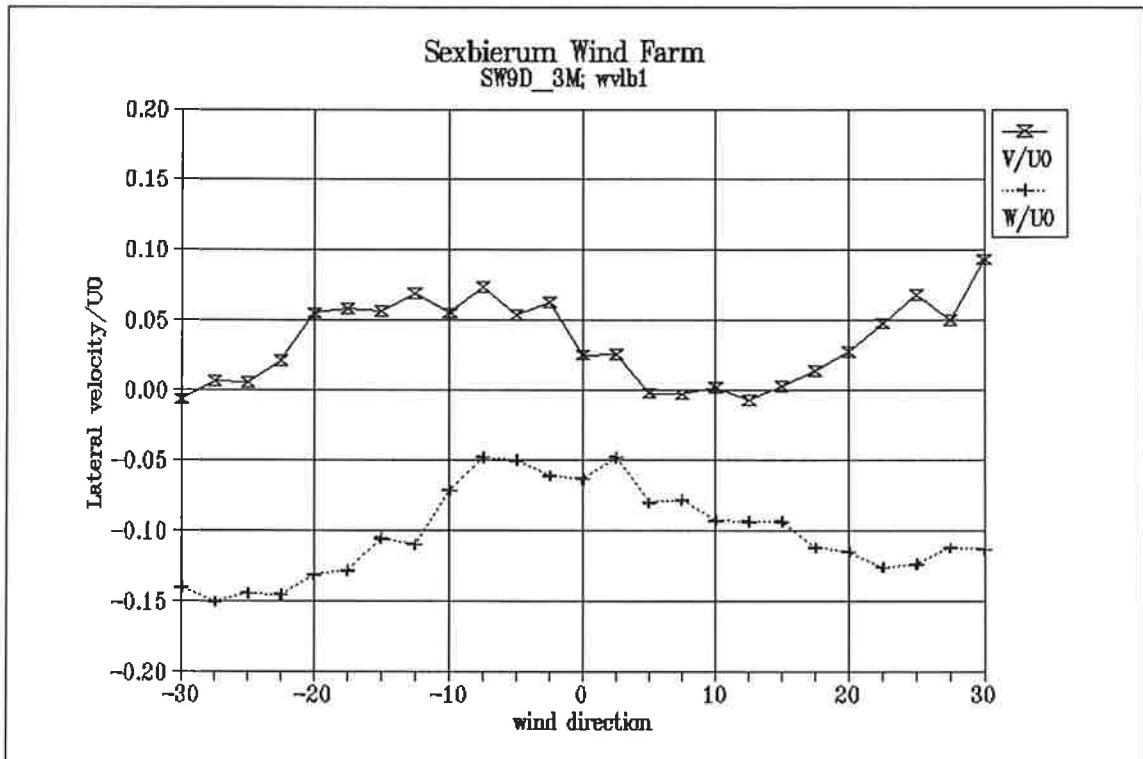


Figure 25 Lateral and vertical wind speed  $V/U_0$  and  $W/U_0$  as a function of wind direction in the wind speed bin 5-10 m/s

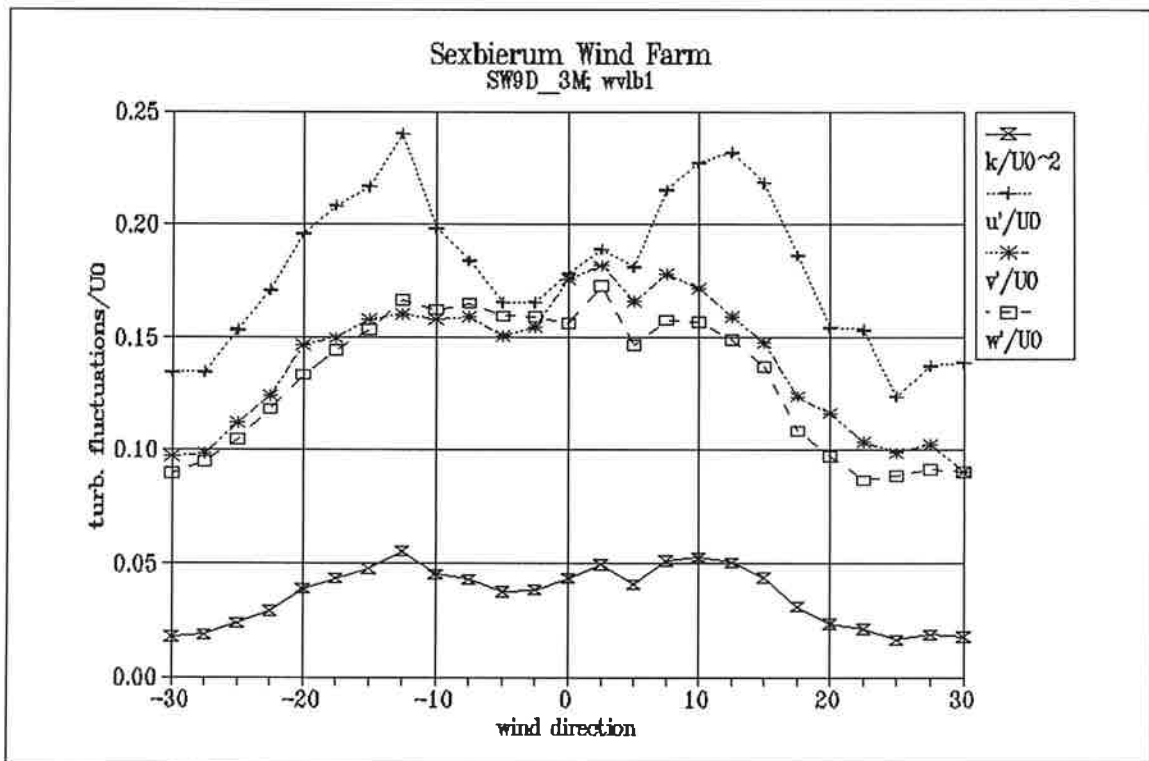


Figure 26 Turbulent fluctuations as a function of wind direction in the wind speed bin 5-10 m/s, non-dimensionalized with  $U_0$

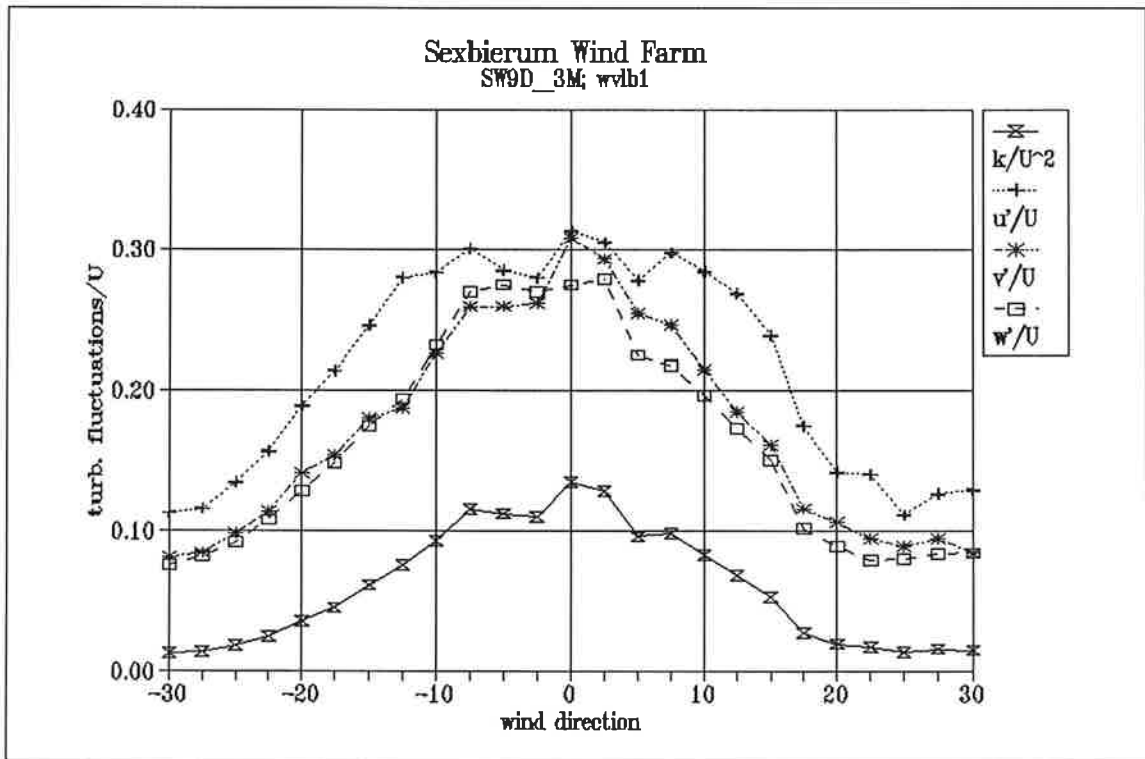


Figure 27 Turbulent fluctuations as a function of wind direction in the wind speed bin 5-10 m/s, non-dimensionalized with U

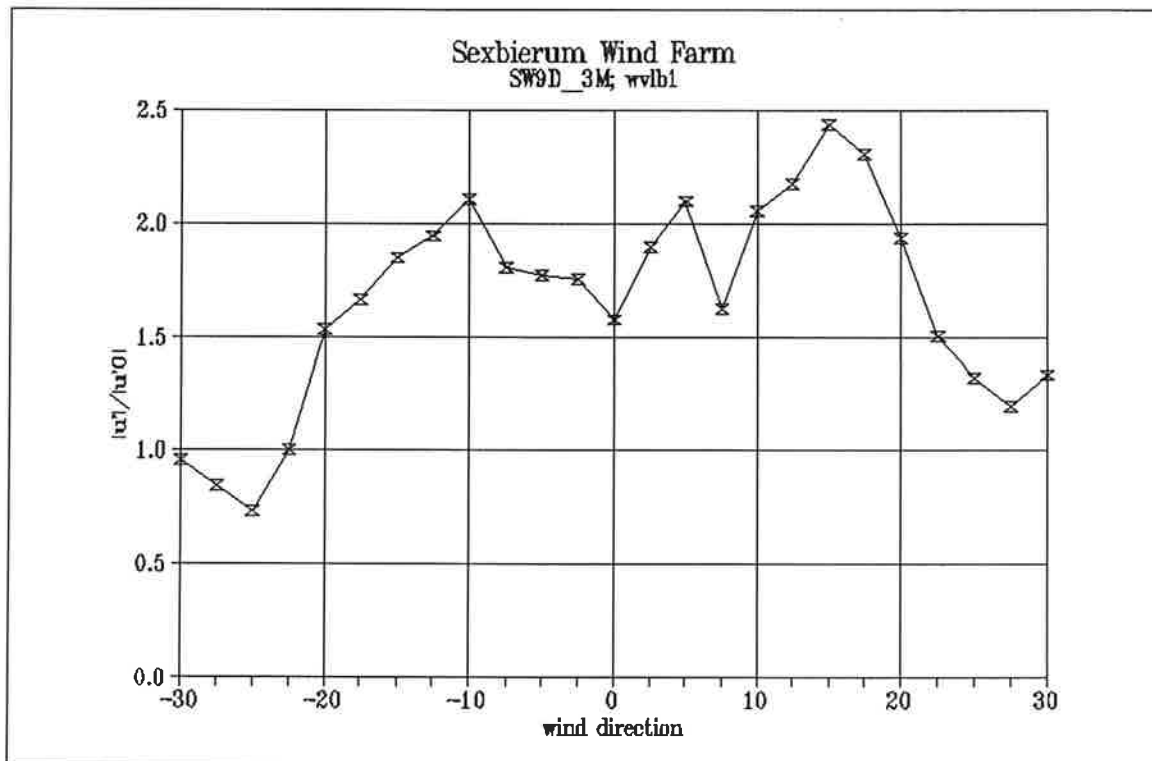


Figure 28 Longitudinal turbulence enhancement  $u'/u'_0$  as a function of wind direction in the wind speed bin 5-10 m/s

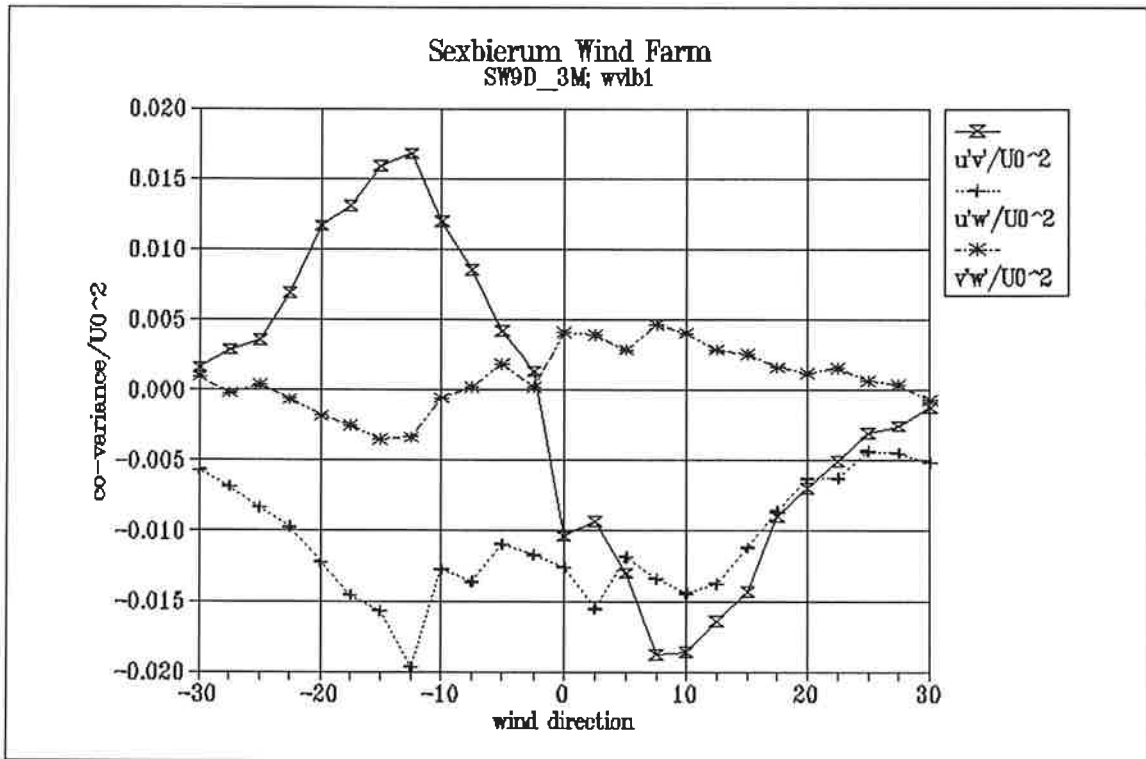


Figure 29 Non-dimensionalized shear stresses  $u'v'/U_0^2$ ;  $u'w'/U_0^2$ ;  $v'w'/U_0^2$  as a function of wind direction in the wind speed bin 5-10 m/s

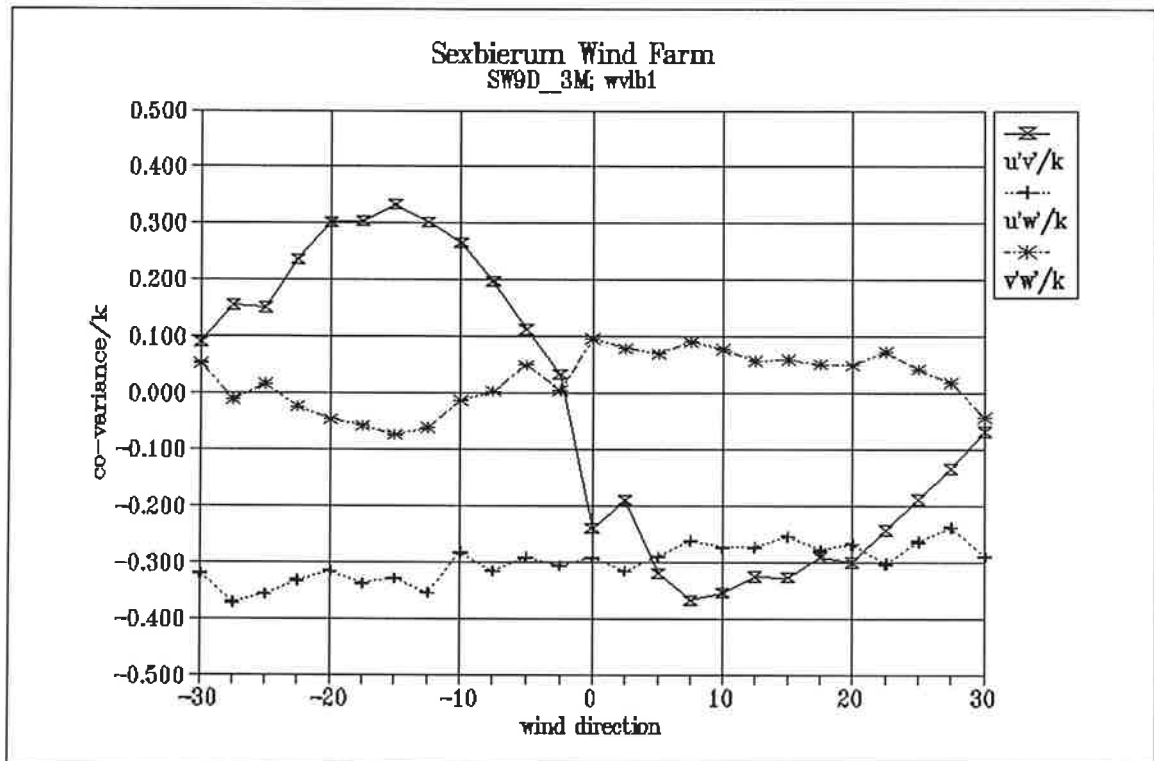


Figure 30 Non-dimensionalized shear stresses  $u'v'/k$ ;  $u'w'/k$ ;  $v'w'/k$  as a function of wind direction in the wind speed bin 5-10 m/s

*Results of Sexbierum Wind Farm; single wake measurements*

**A4.3 Sensor b2**

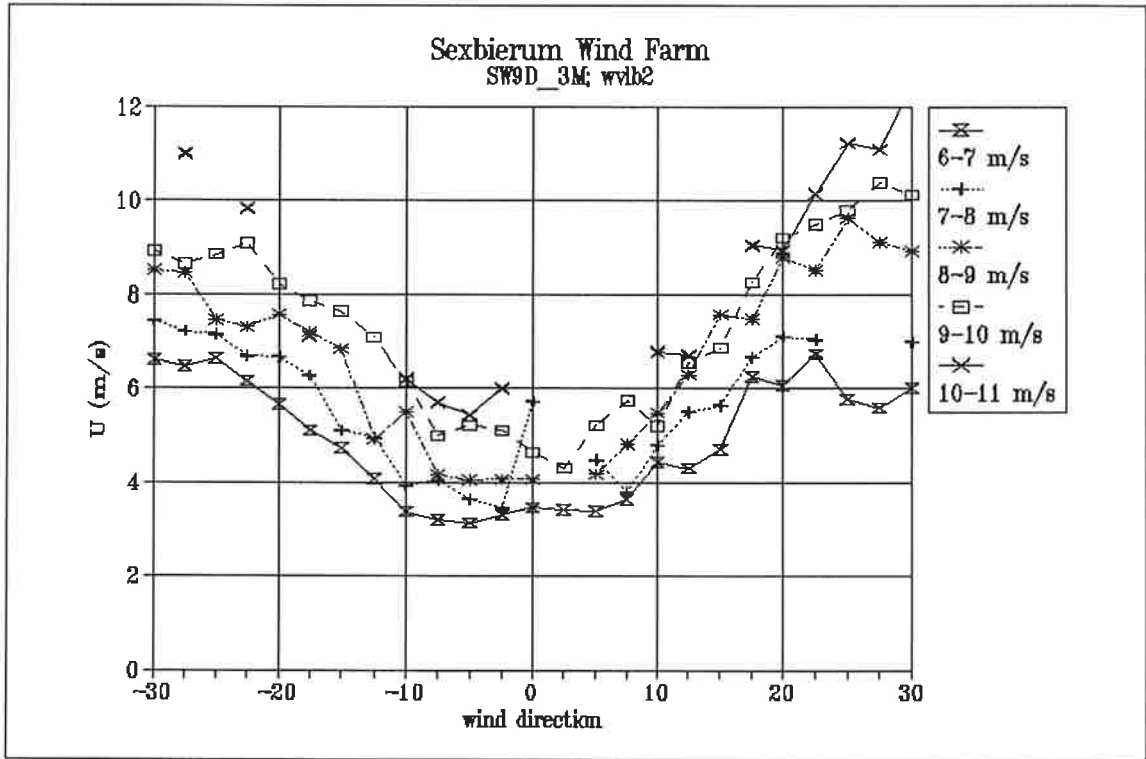


Figure 1 Horizontal wind speed  $U$  as a function of wind direction and wind speed bin

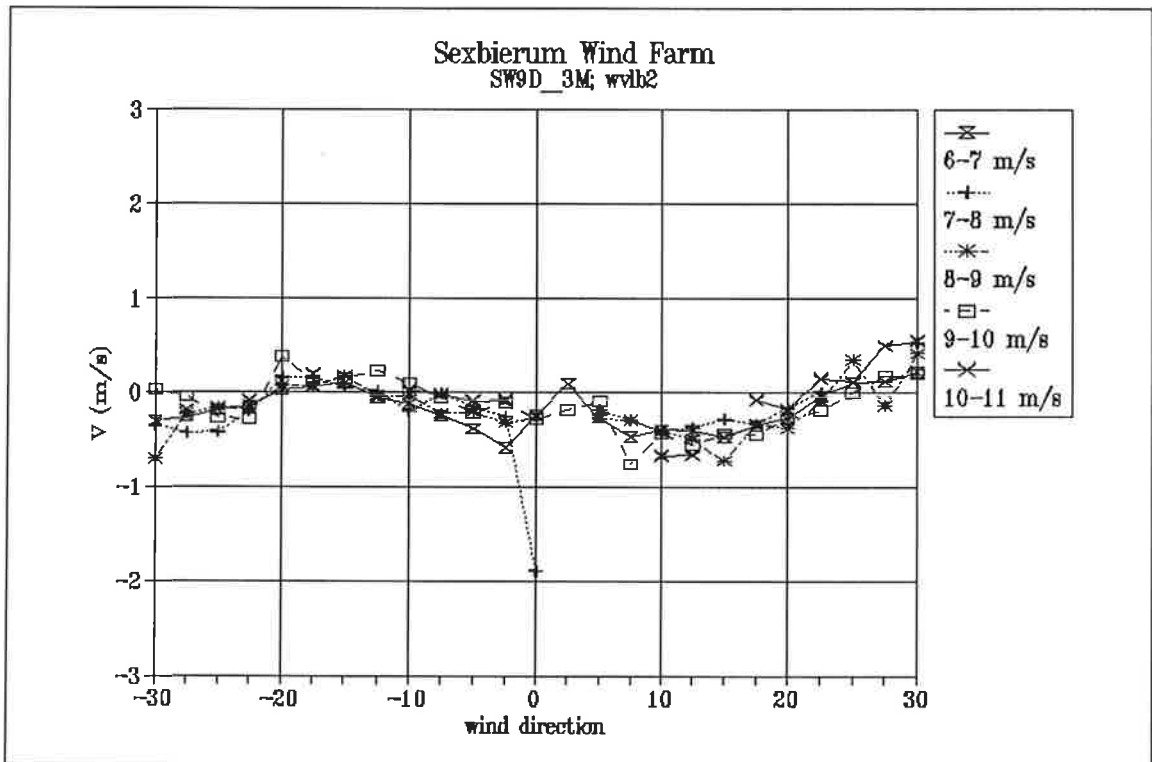


Figure 2 Lateral wind speed  $V$  as a function of wind direction and wind speed bin

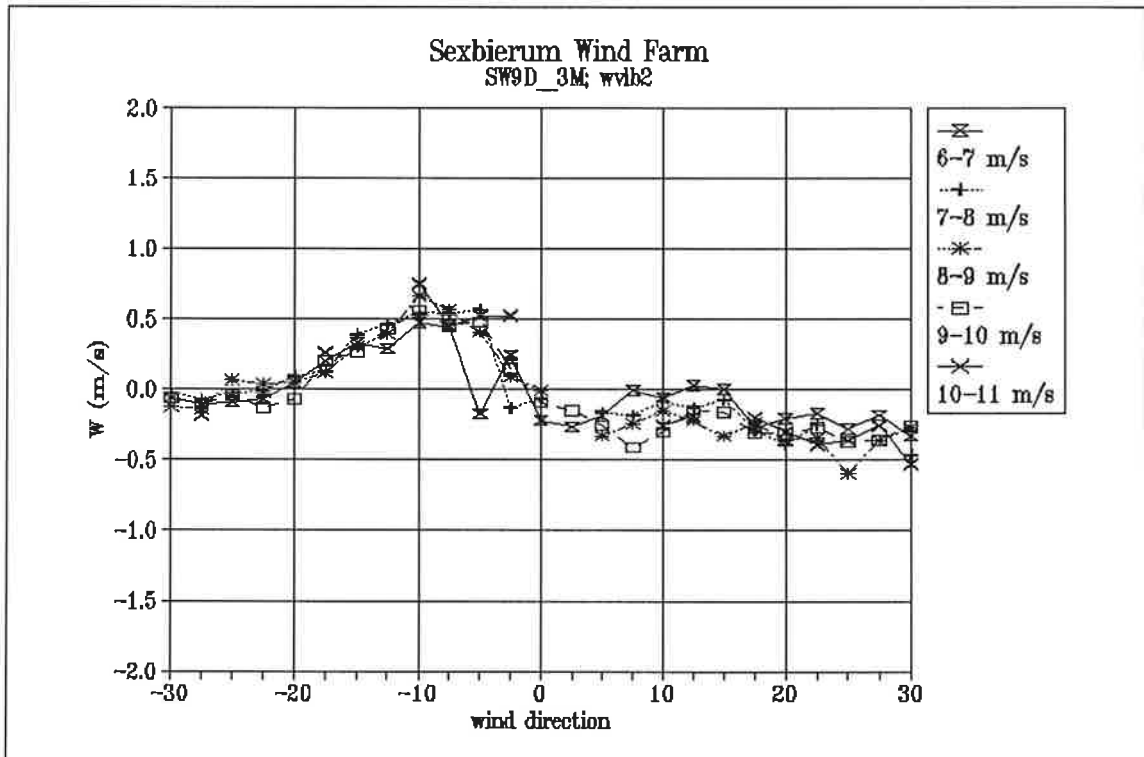


Figure 3 Vertical wind speed  $W$  as a function of wind direction and wind speed bin

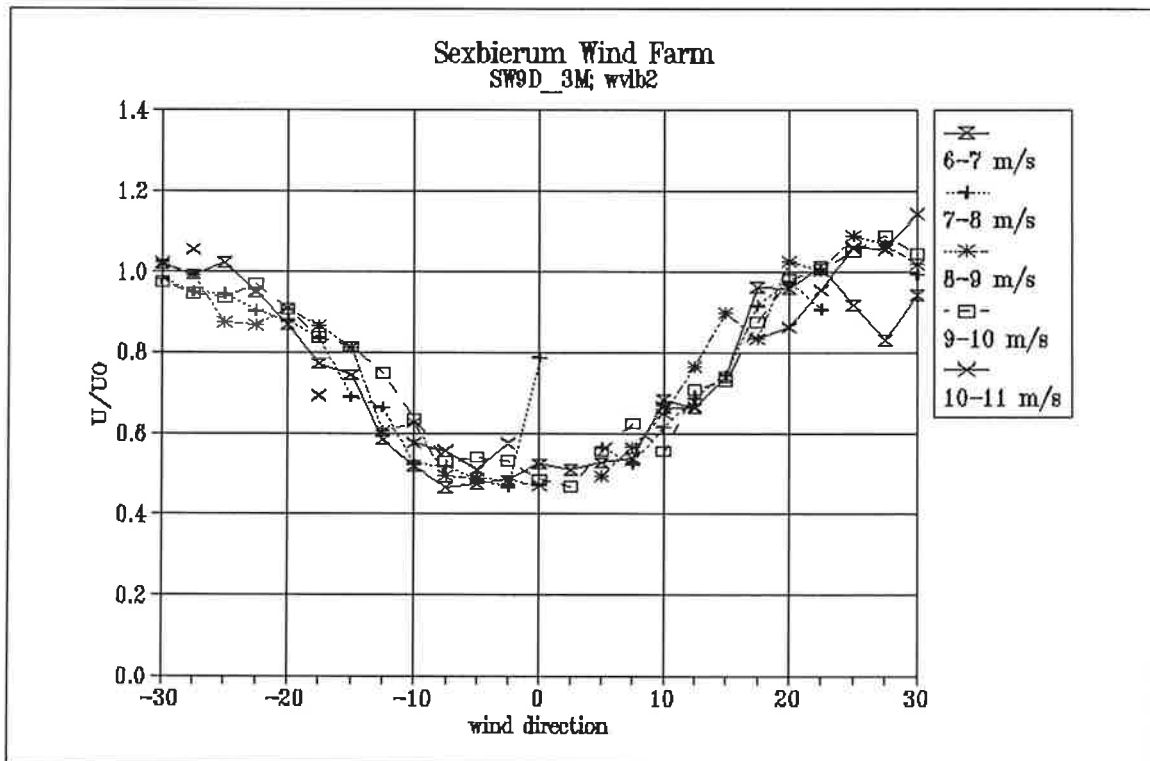


Figure 4 Wake deficit  $U/U_0$  as a function of wind direction and wind speed bin

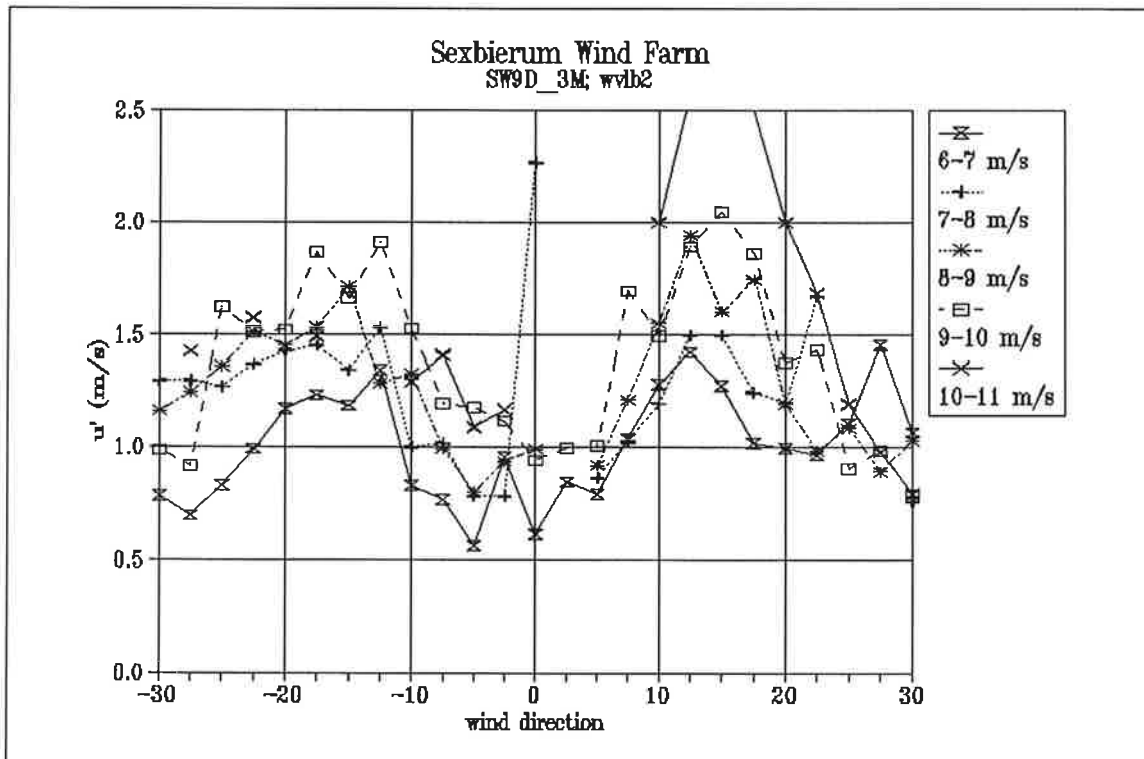


Figure 5 Longitudinal turbulent fluctuations  $u'$  as a function of wind direction and wind speed bin

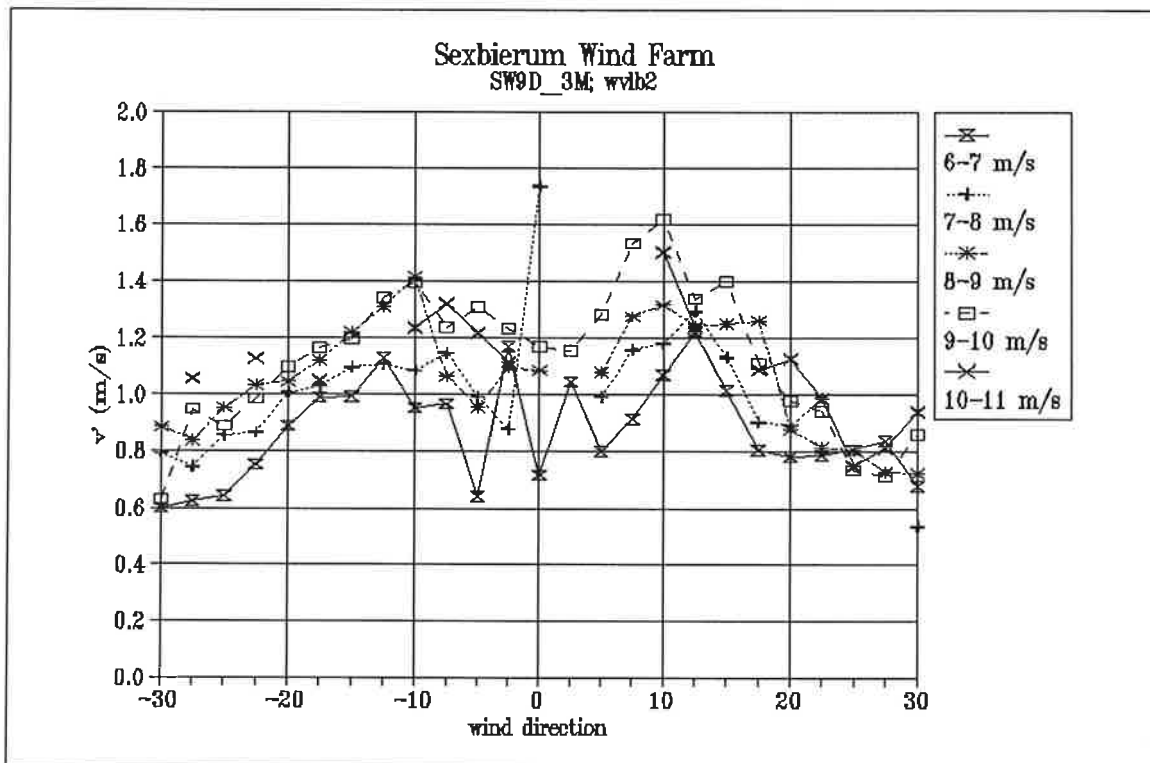


Figure 6 Lateral turbulent fluctuations  $v'$  as a function of wind direction and wind speed bin



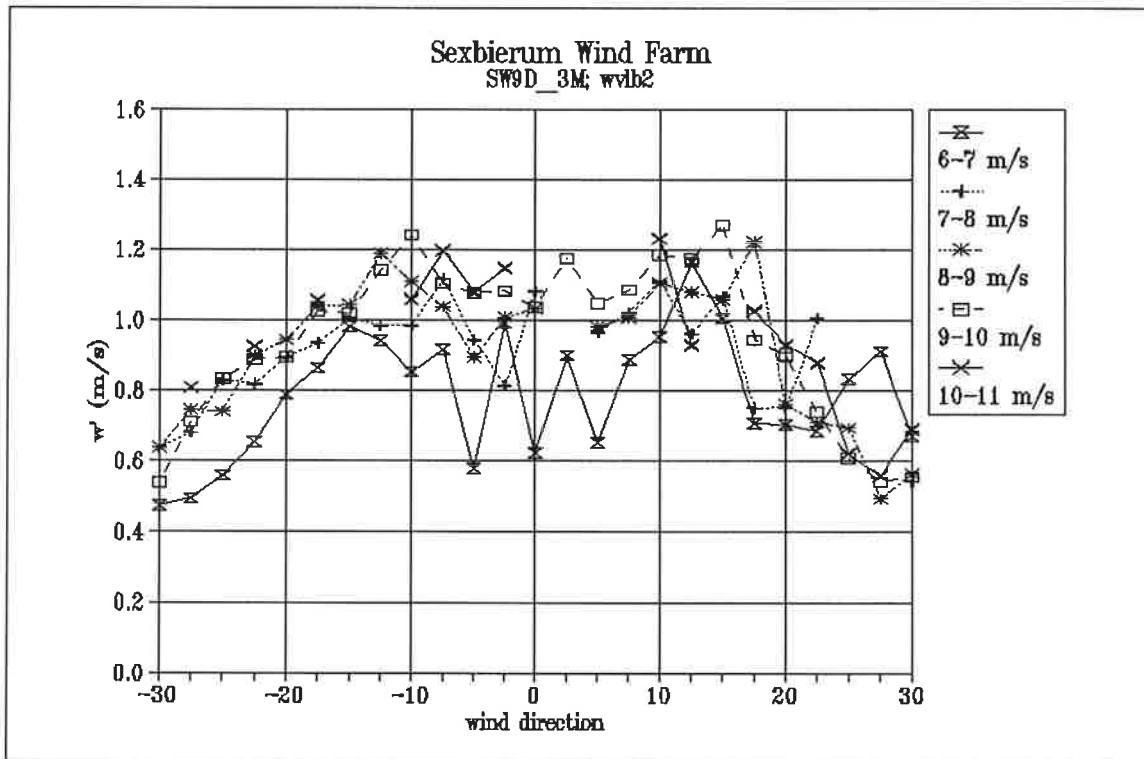


Figure 7 Vertical turbulent fluctuations  $w'$  as a function of wind direction and wind speed bin

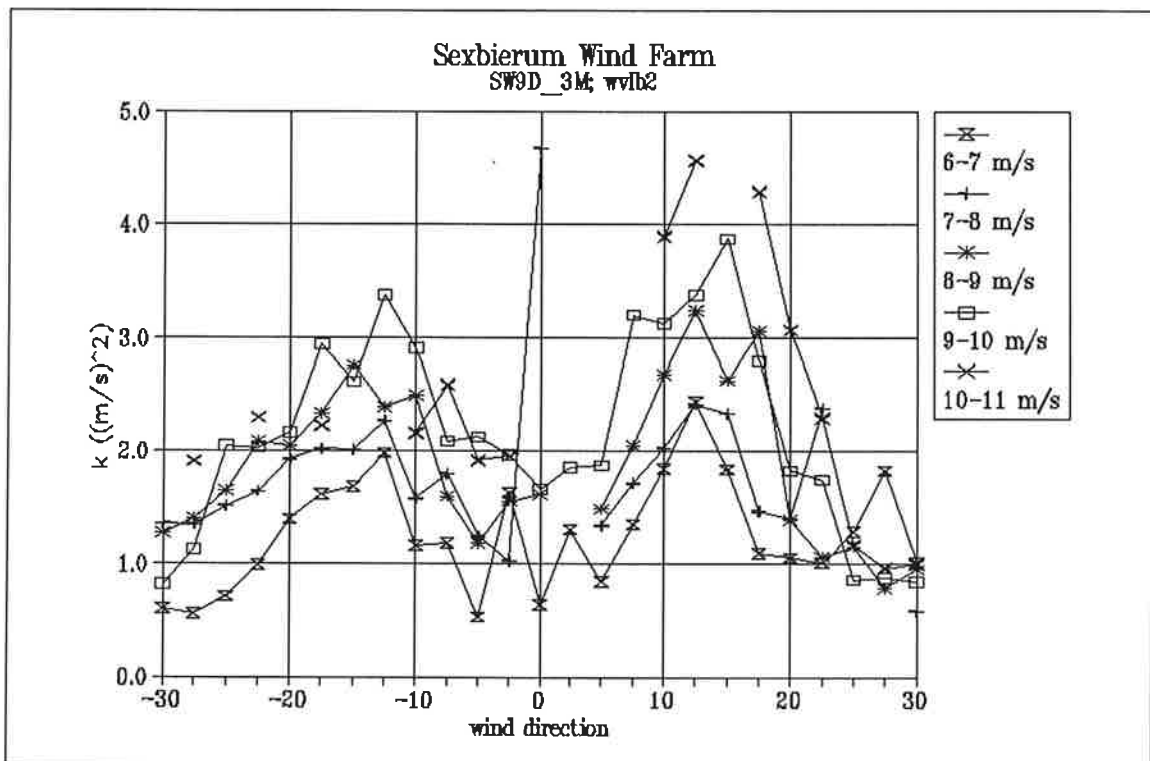


Figure 8 Turbulent kinetic energy per unit mass as a function of wind direction and wind speed bin

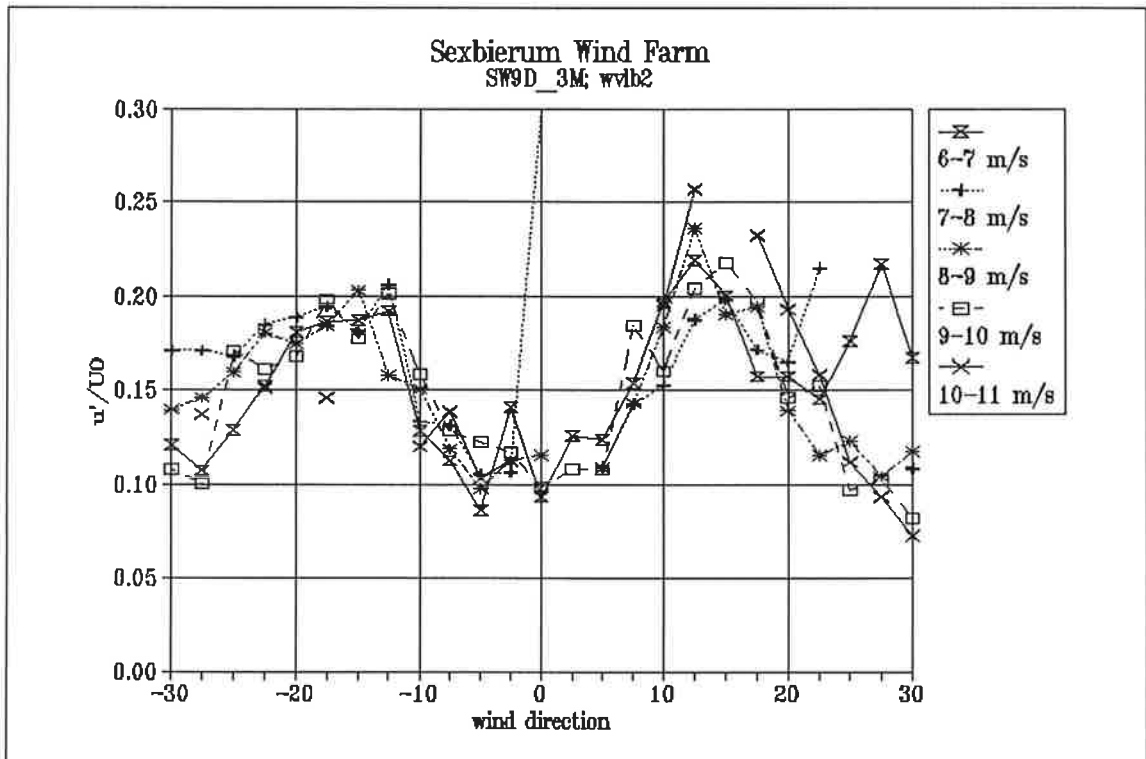


Figure 9 Non-dimensionalized longitudinal turbulent fluctuations  $u'/U_0$  as a function of wind direction and wind speed bin

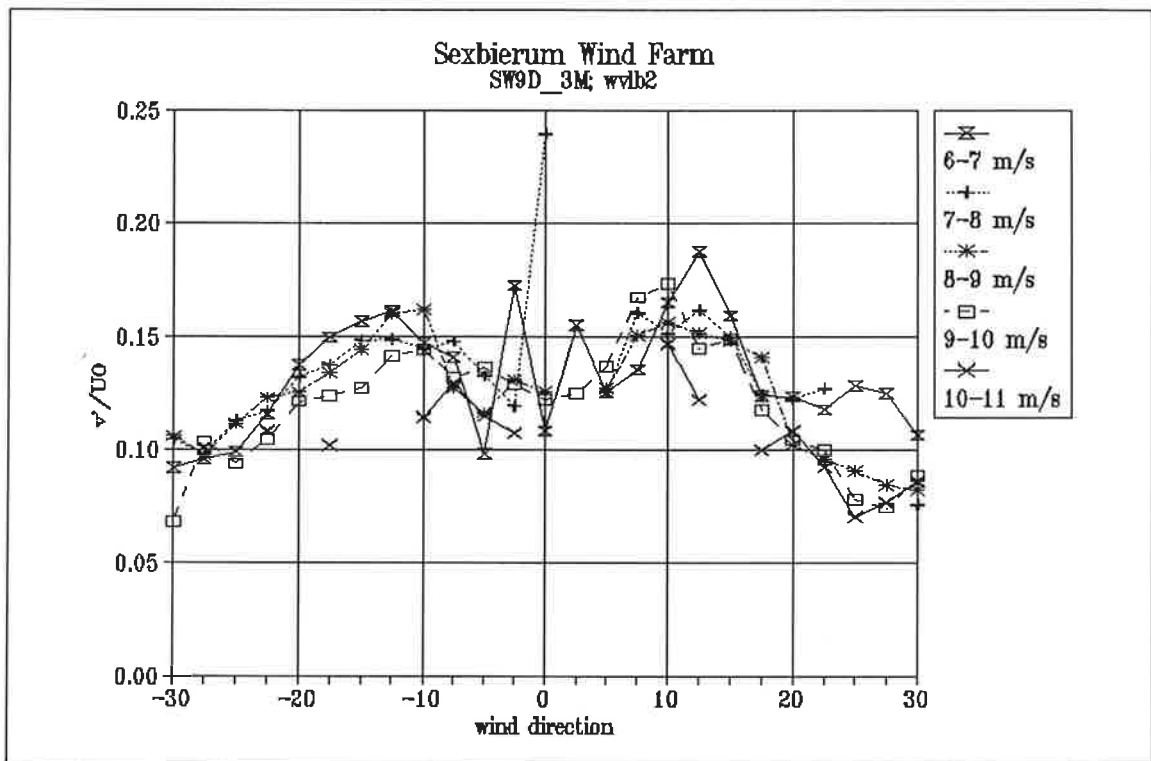


Figure 10 Non-dimensionalized lateral turbulent fluctuations  $v'/U_0$  as a function of wind direction and wind speed bin

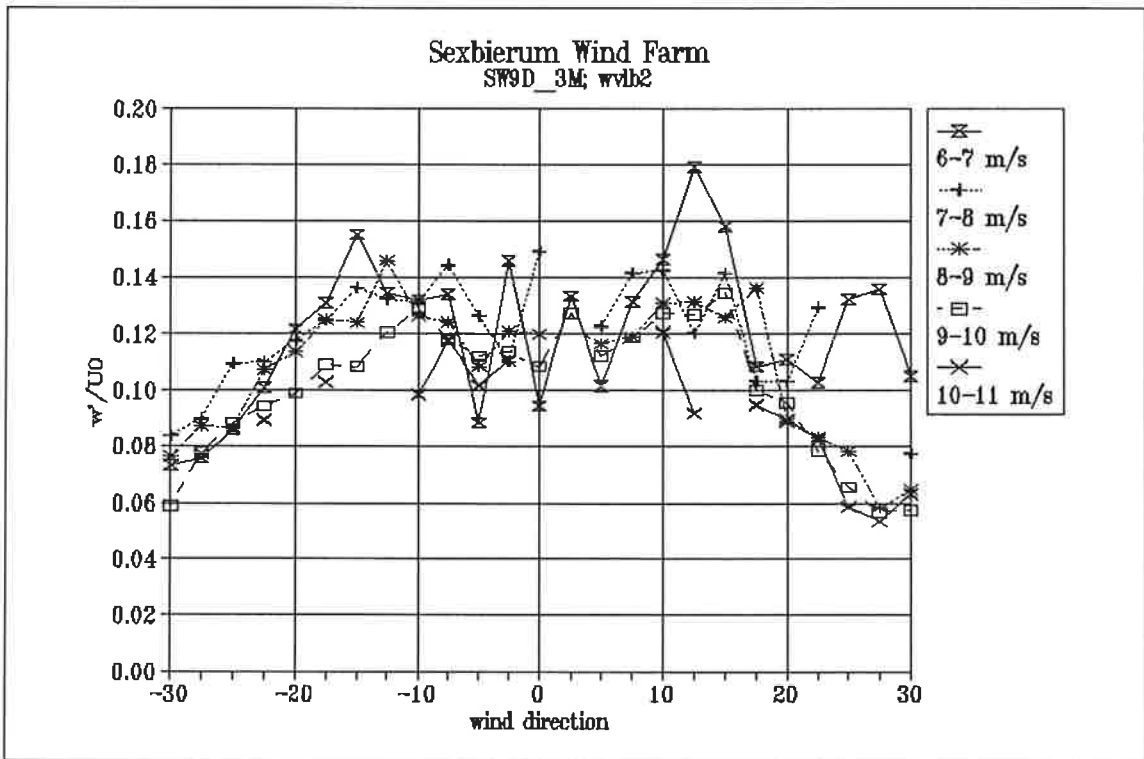


Figure 11 Non-dimensionalized vertical turbulent fluctuations  $w'/U_0$  as a function of wind direction and wind speed bin

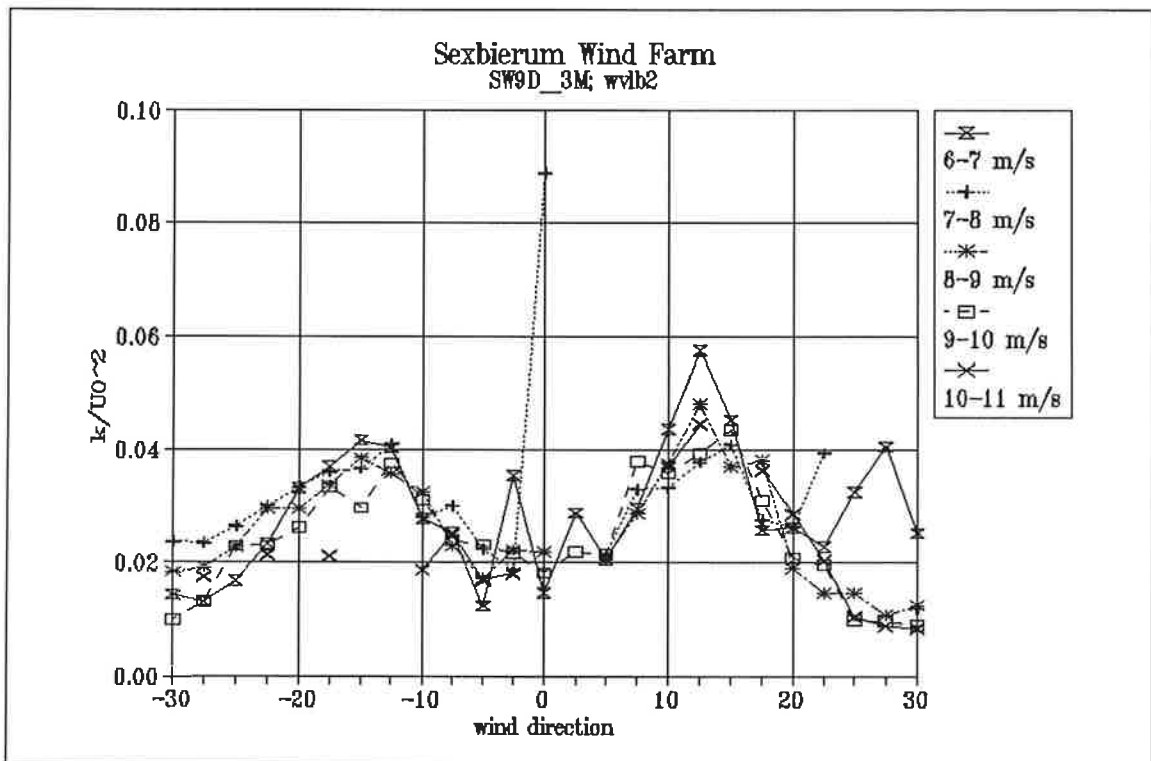


Figure 12 Non-dimensionalized turbulent kinetic energy  $k/U_0^2$  as a function of wind direction and wind speed bin

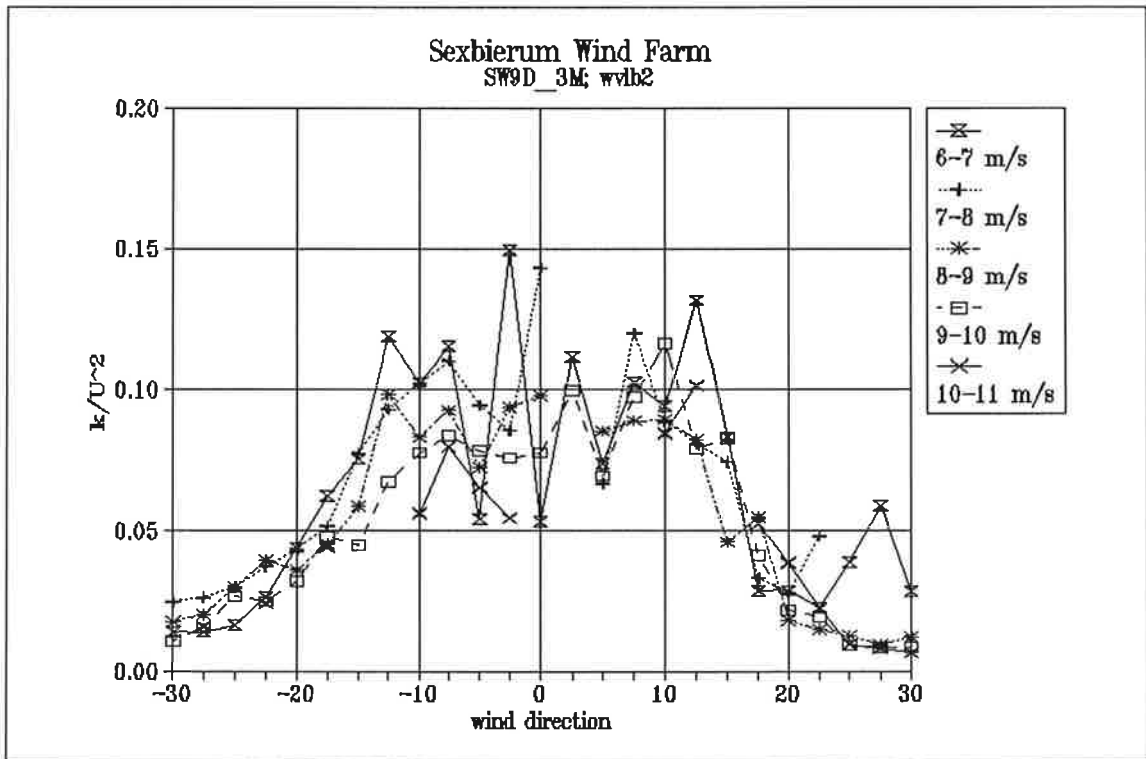


Figure 13 Non-dimensionalized turbulent kinetic energy  $k/U^2$  as a function of wind direction and wind speed bin

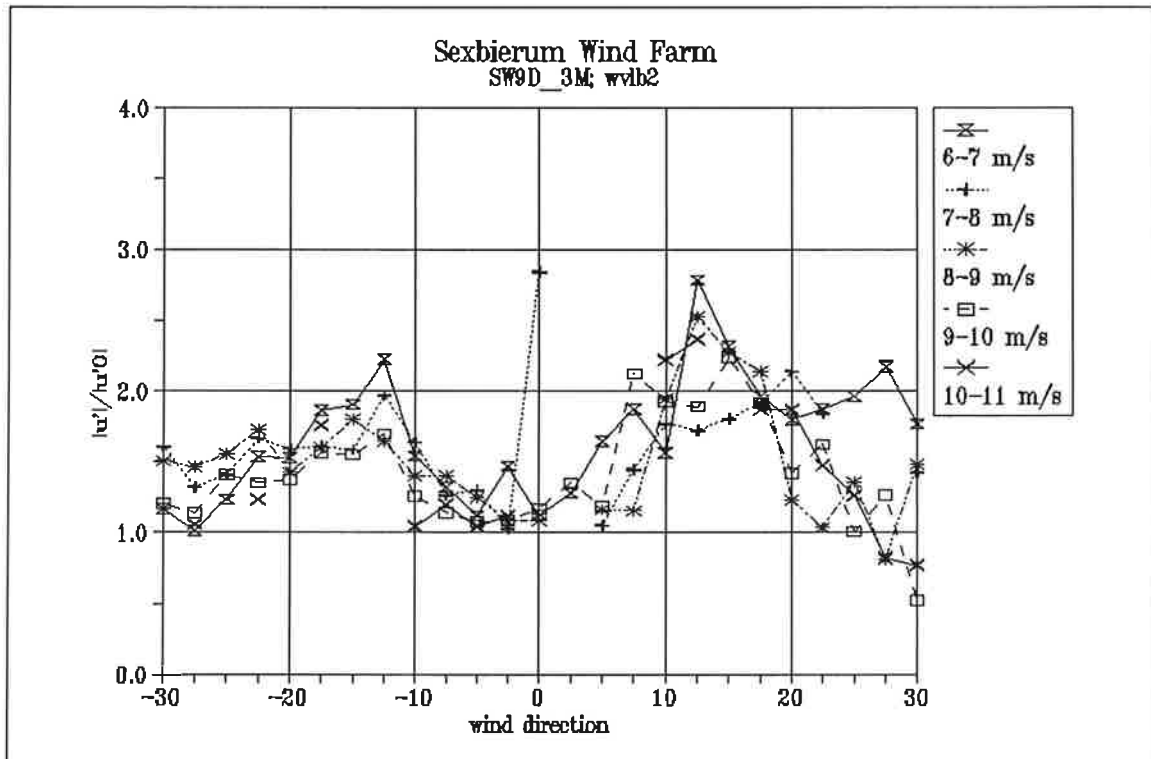


Figure 14 Longitudinal turbulence enhancement  $u'^2/u'01$  as a function of wind direction and wind speed bin

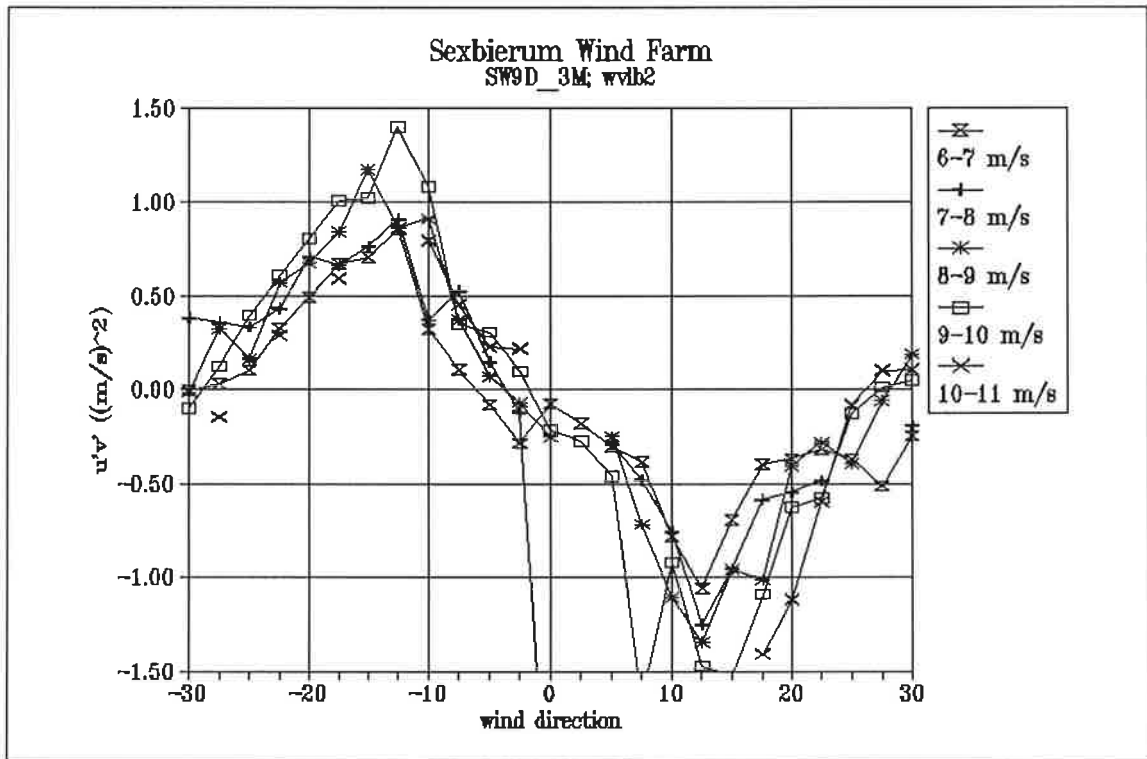


Figure 15 Shear stress  $u'v'$  as a function of wind direction and wind speed bin

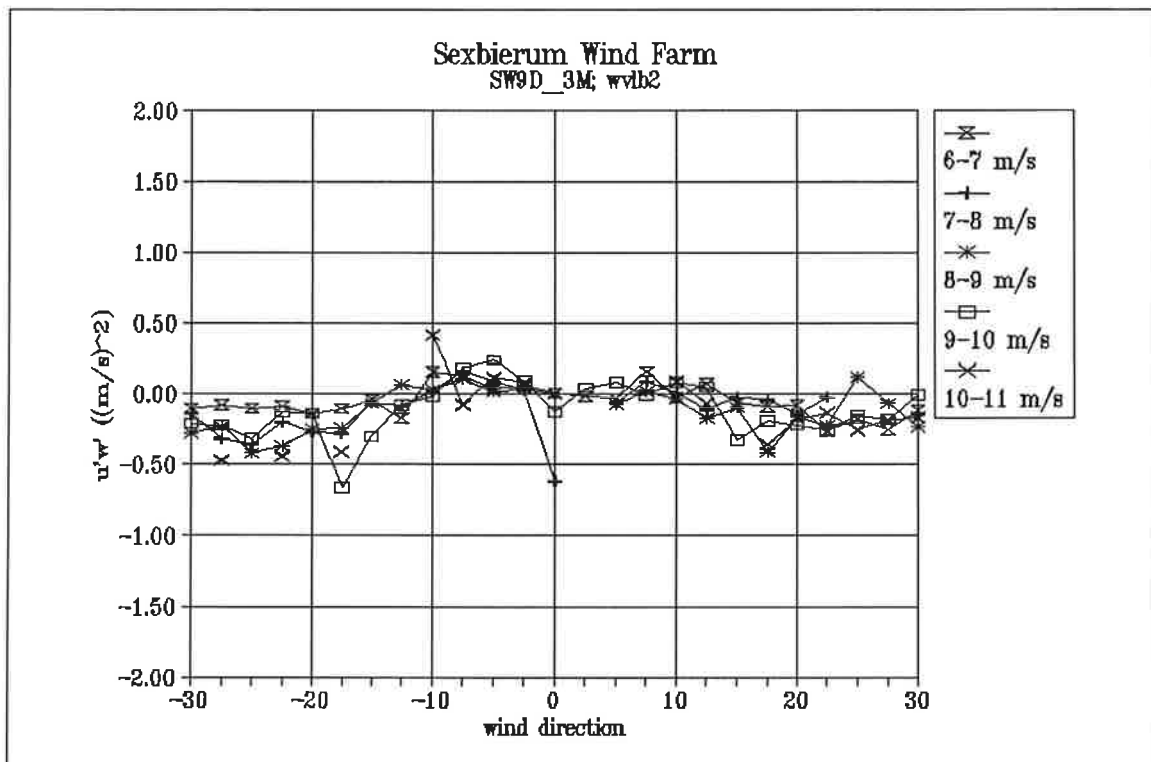


Figure 16 Shear stress  $u'w'$  as a function of wind direction and wind speed bin

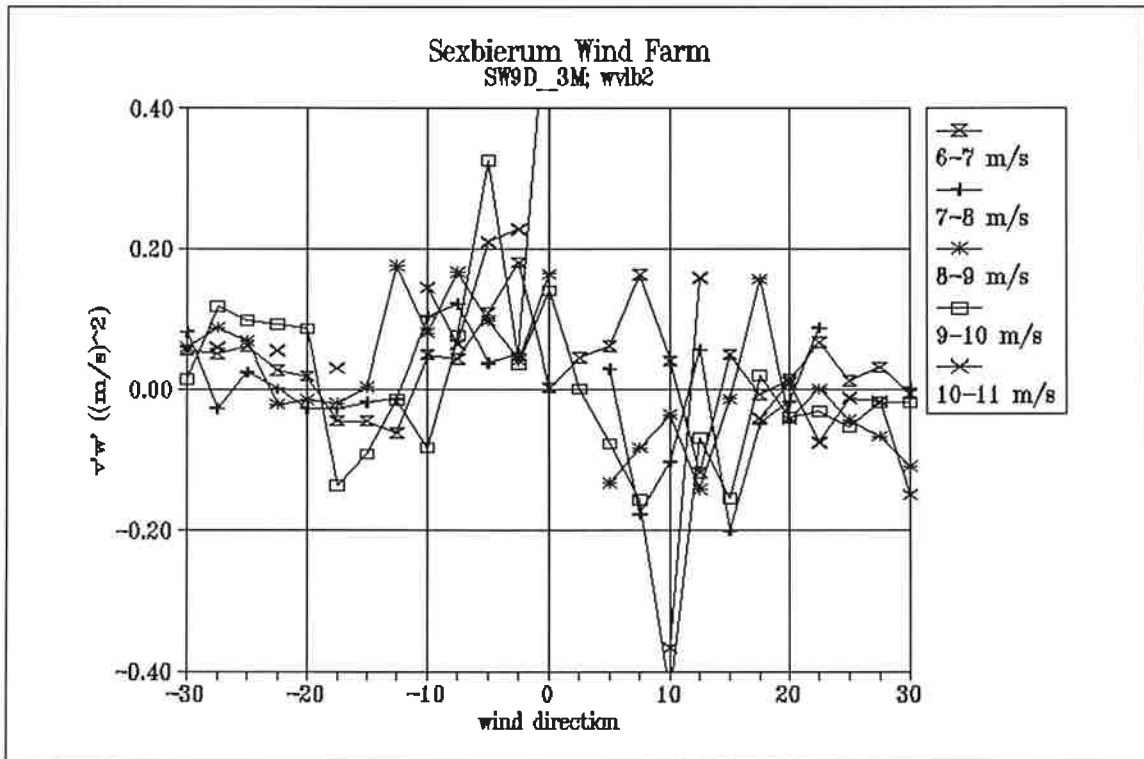


Figure 17 Shear stress  $v'w'$  as a function of wind direction and wind speed bin

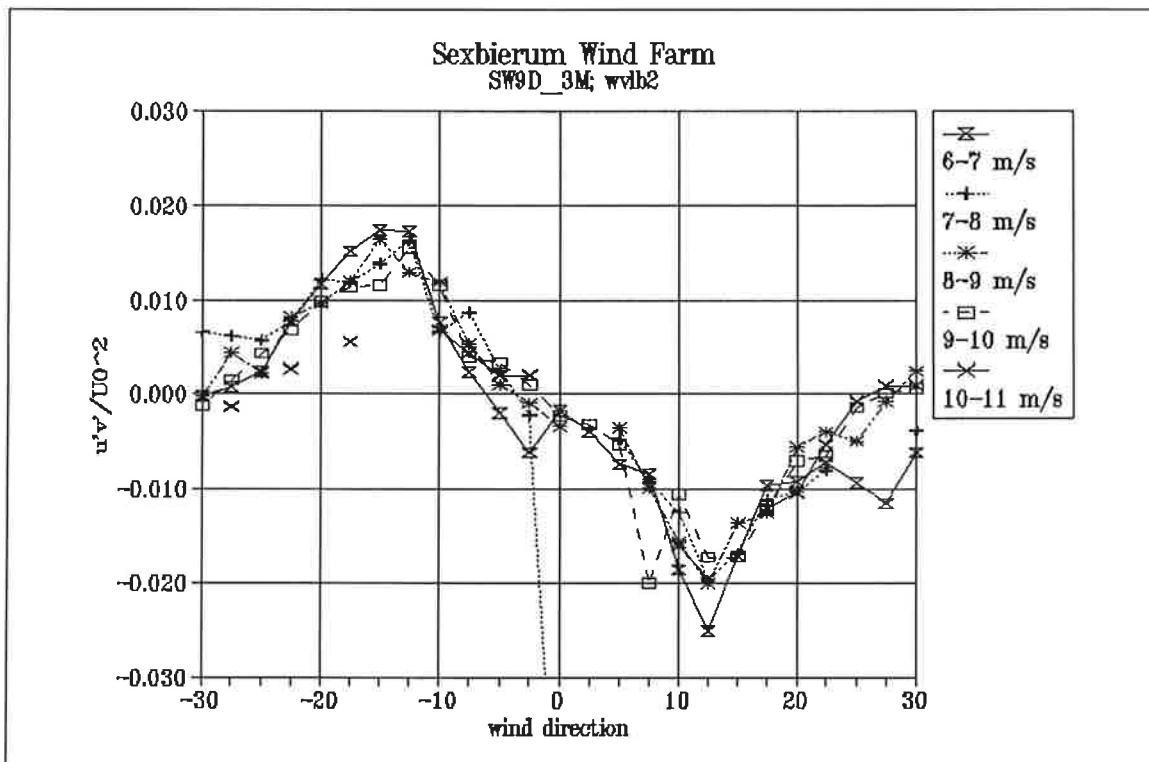


Figure 18 Non-dimensionalized shear stress  $u'v'/U_0^2$  as a function of wind direction and wind speed bin

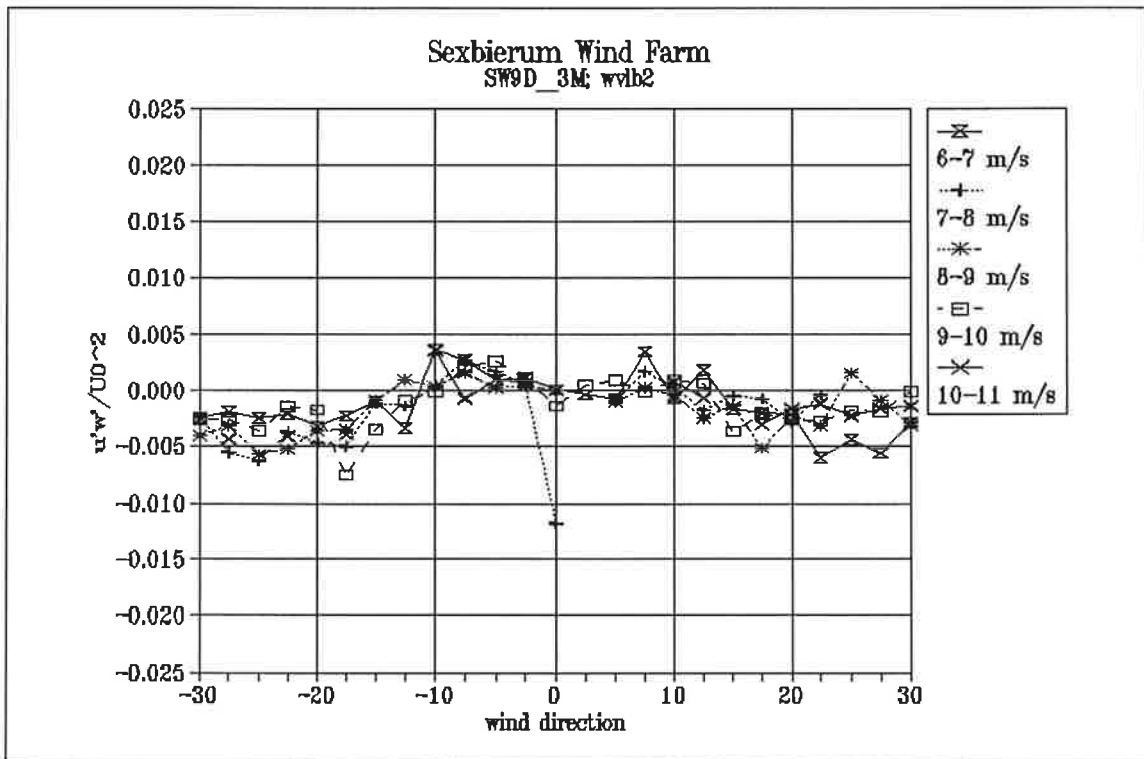


Figure 19 Non-dimensionalized shear stress  $u'w'/U_0^2$  as a function of wind direction and wind speed bin

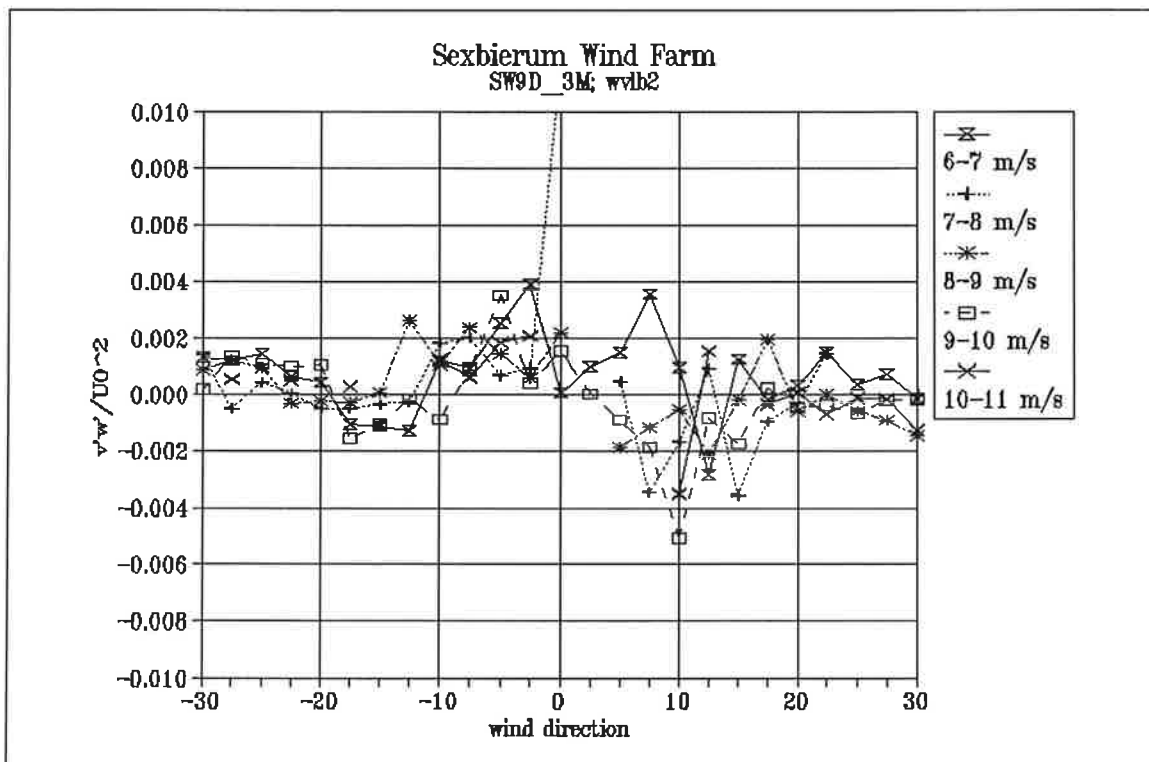


Figure 20 Non-dimensionalized shear stress  $v'w'/U_0^2$  as a function of wind direction and wind speed bin

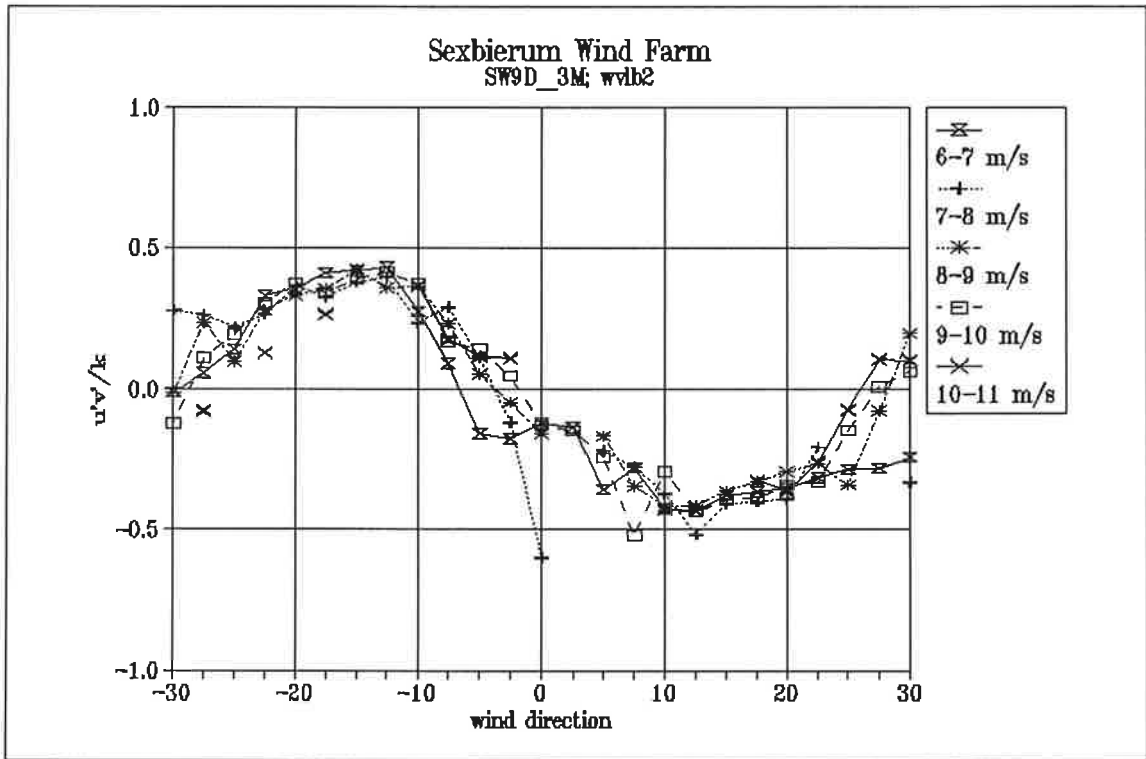


Figure 21 Non-dimensionalized shear stress  $u'v'/k$  as a function of wind direction and wind speed bin

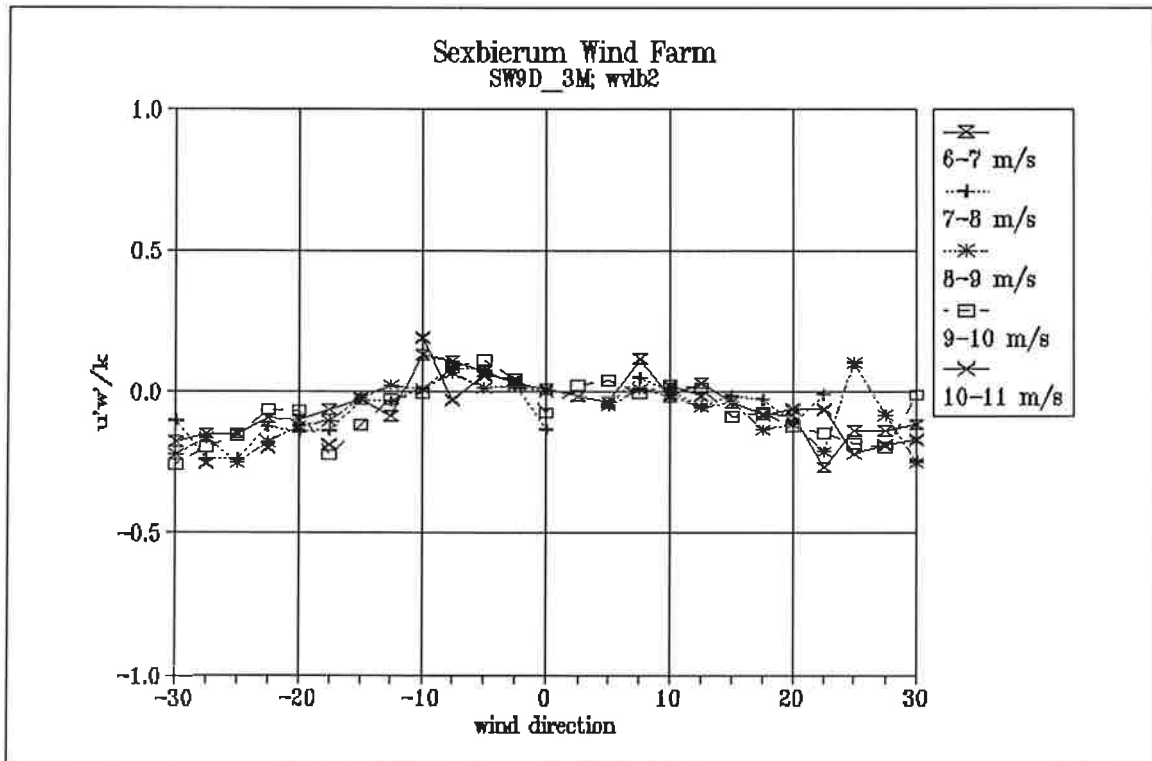


Figure 22 Non-dimensionalized shear stress  $u'w'/k$  as a function of wind direction and wind speed bin



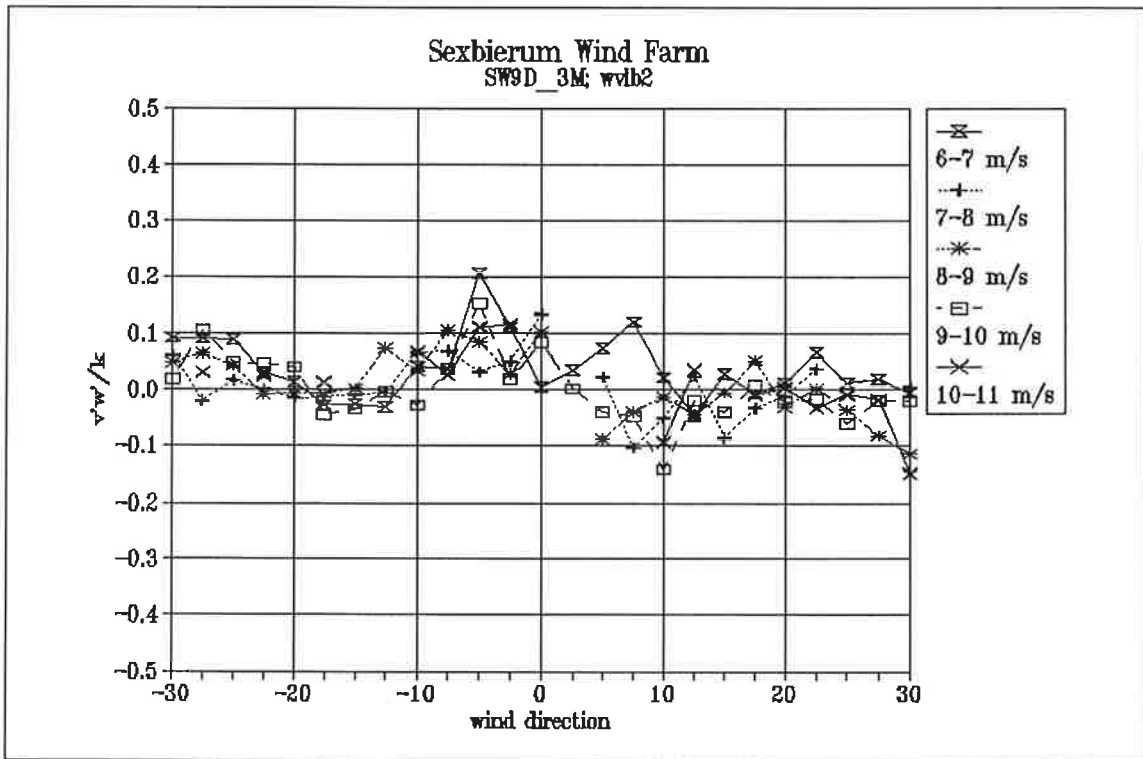


Figure 23 Non-dimensionalized shear stress  $v'w'/k$  as a function of wind direction and wind speed bin

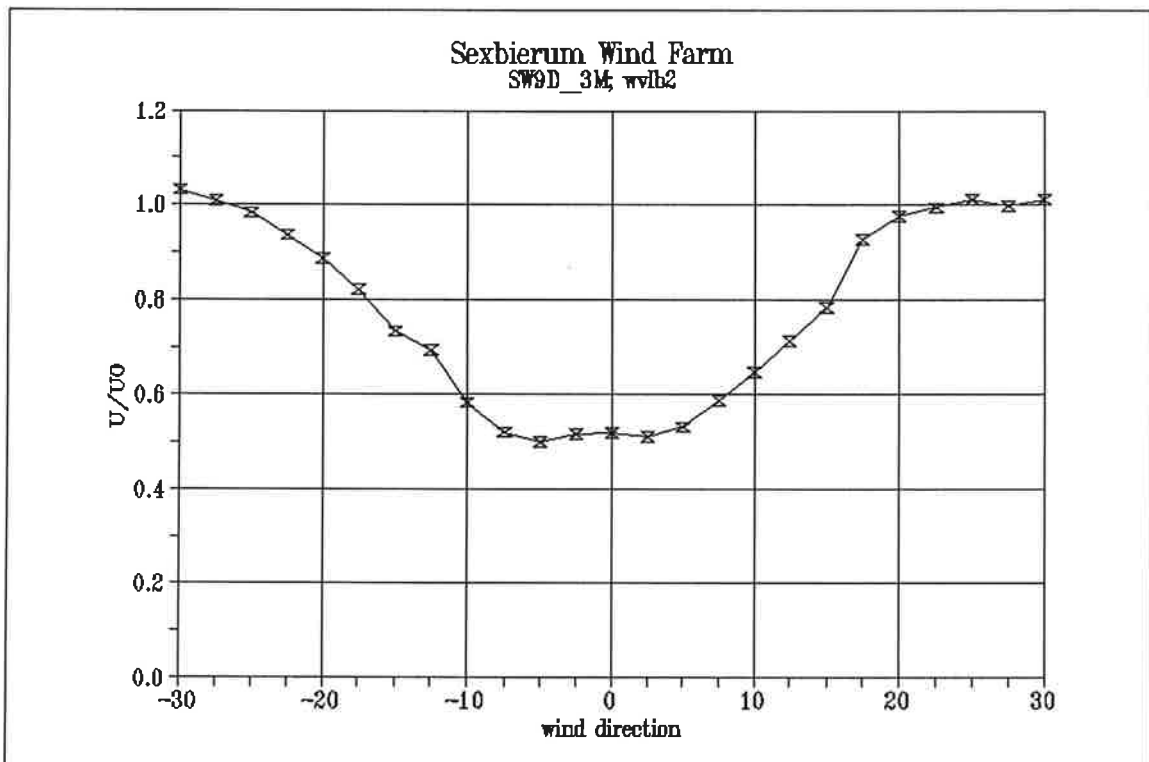


Figure 24 Wake deficit  $U/U_0$  as a function of wind direction in the wind speed bin 5-10 m/s

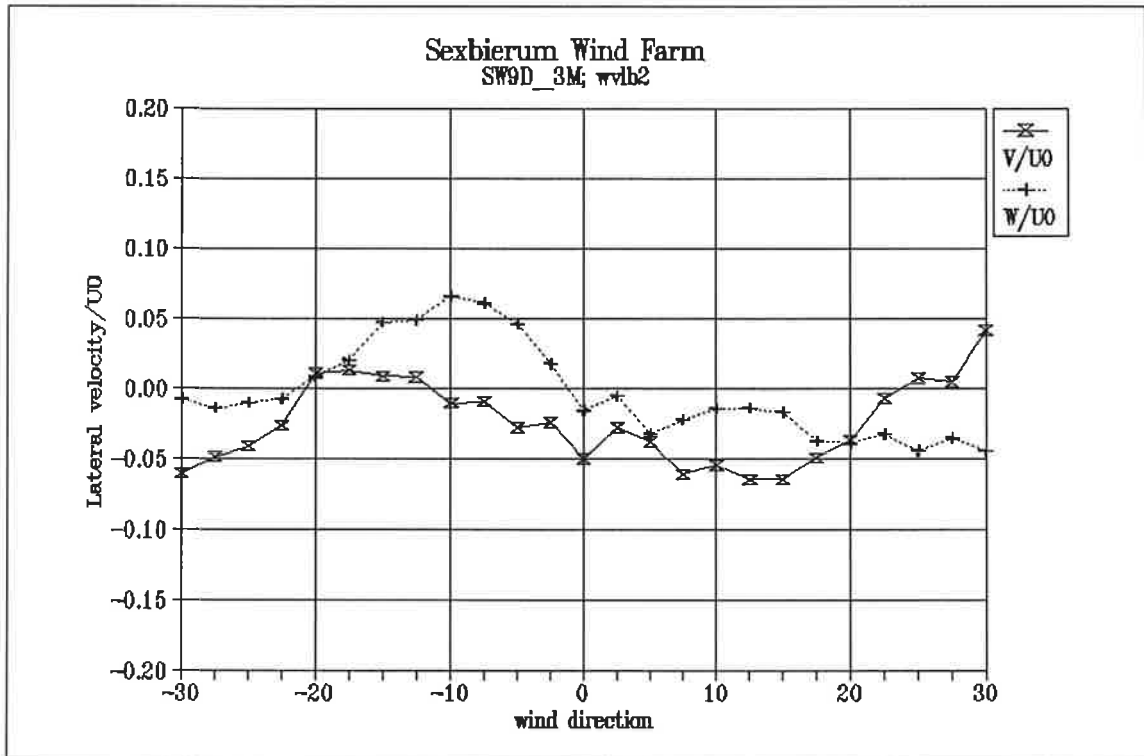


Figure 25 Lateral and vertical wind speed  $V/U_0$  and  $W/U_0$  as a function of wind direction in the wind speed bin 5-10 m/s

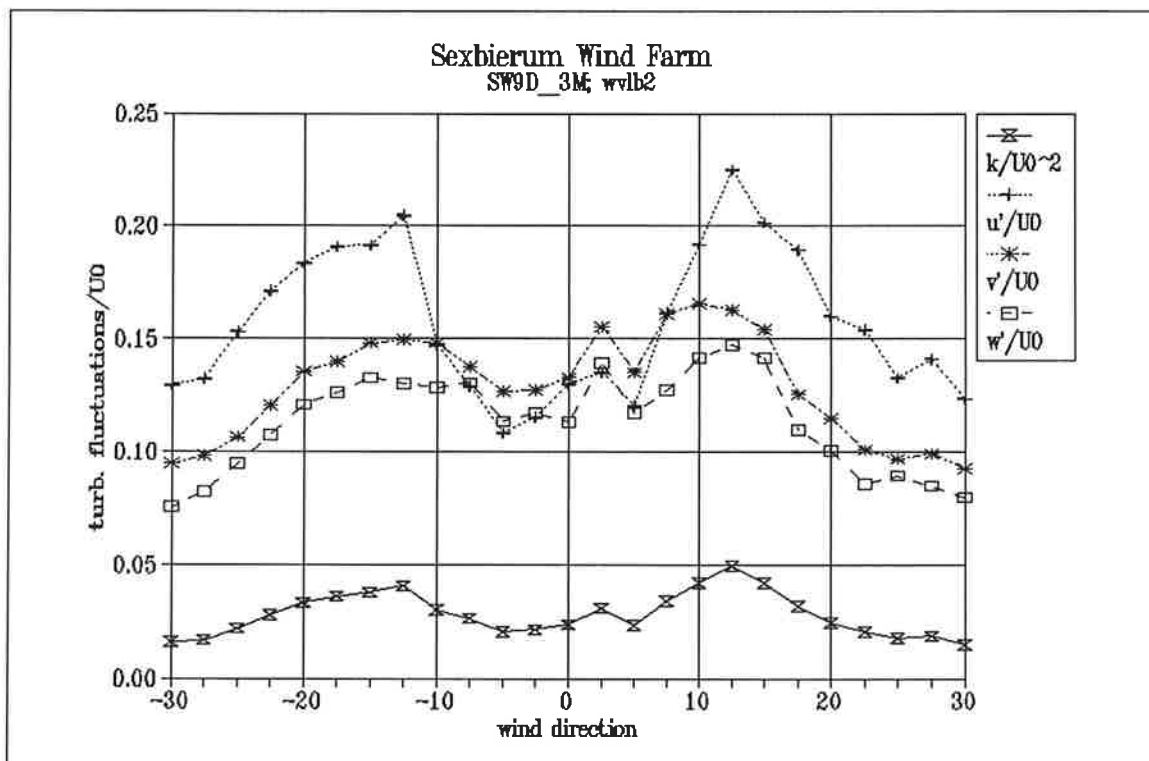


Figure 26 Turbulent fluctuations as a function of wind direction in the wind speed bin 5-10 m/s, non-dimensionalized with  $U_0$

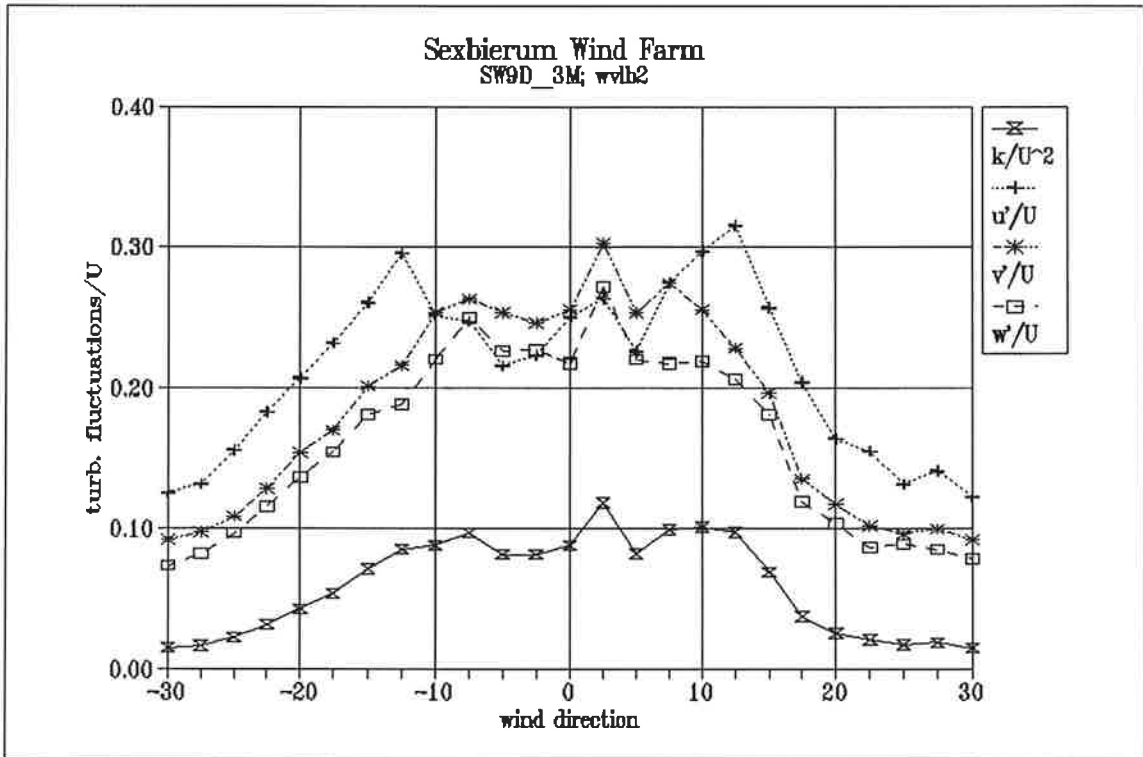


Figure 27 Turbulent fluctuations as a function of wind direction in the wind speed bin 5-10 m/s, non-dimensionalized with U

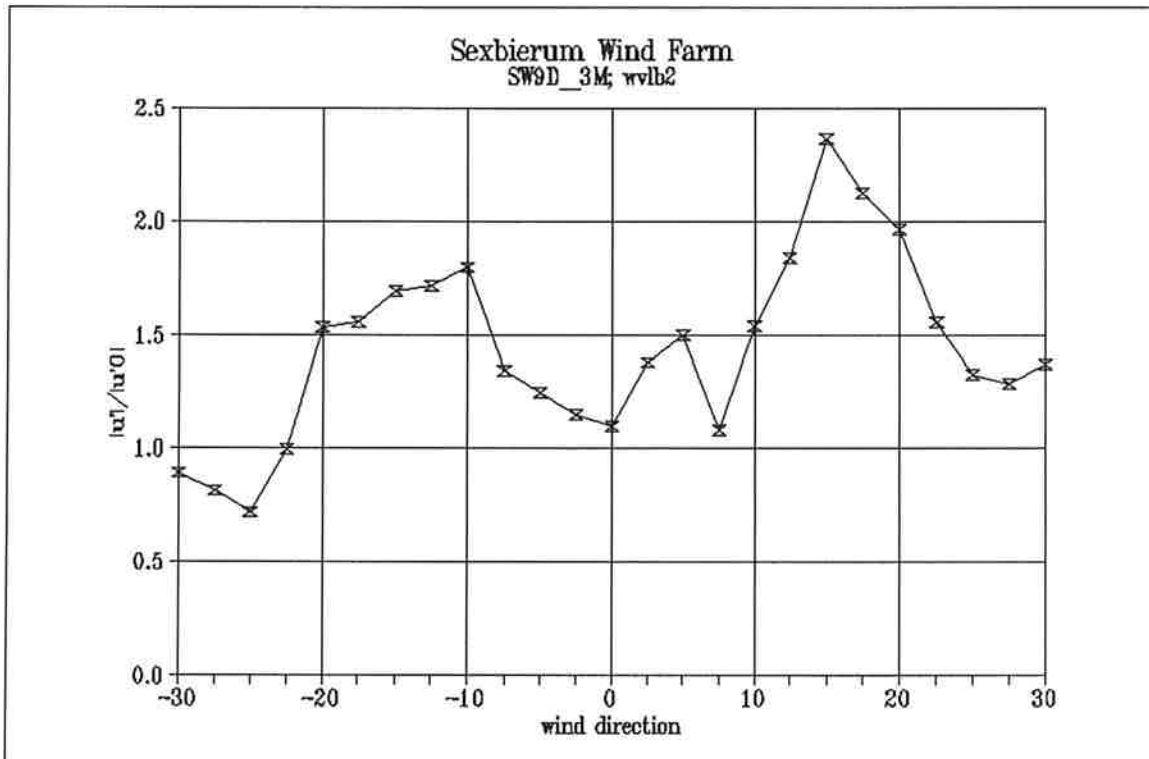


Figure 28 Longitudinal turbulence enhancement  $u'/u'_0$  as a function of wind direction in the wind speed bin 5-10 m/s

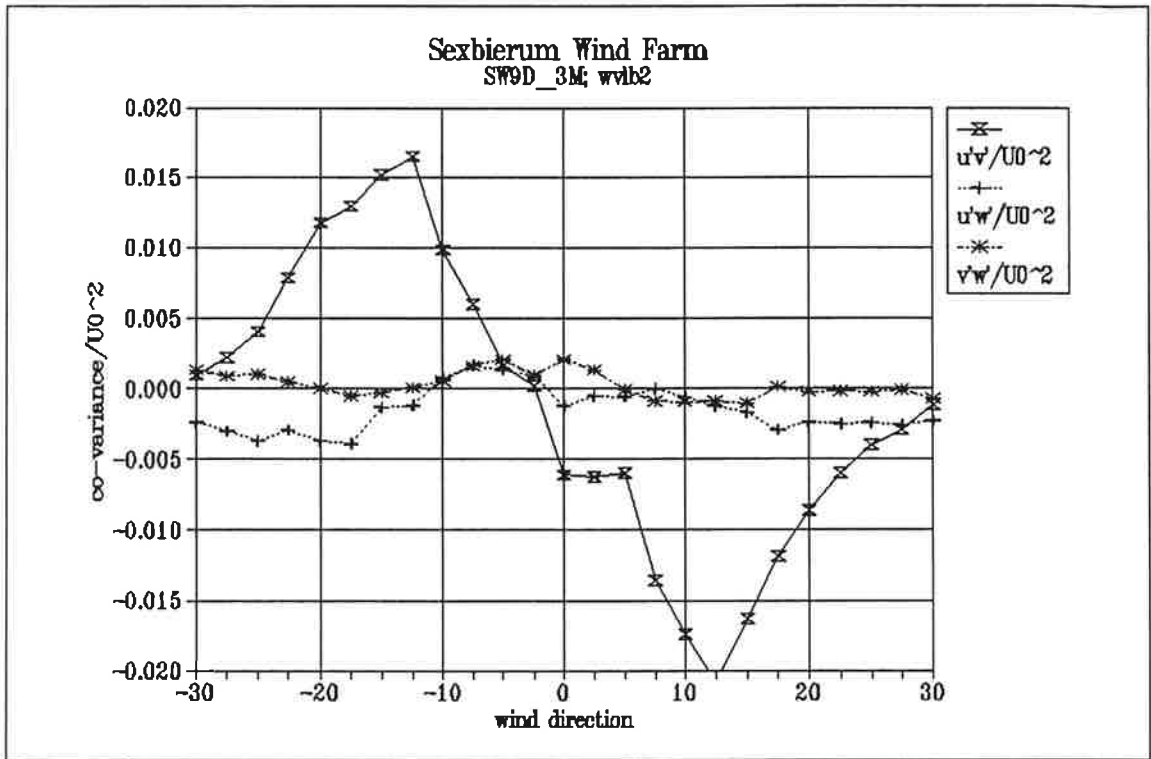


Figure 29 Non-dimensionalized shear stresses  $u'v'/U_0^2$ ;  $u'w'/U_0^2$ ;  $v'w'/U_0^2$  as a function of wind direction in the wind speed bin 5-10 m/s

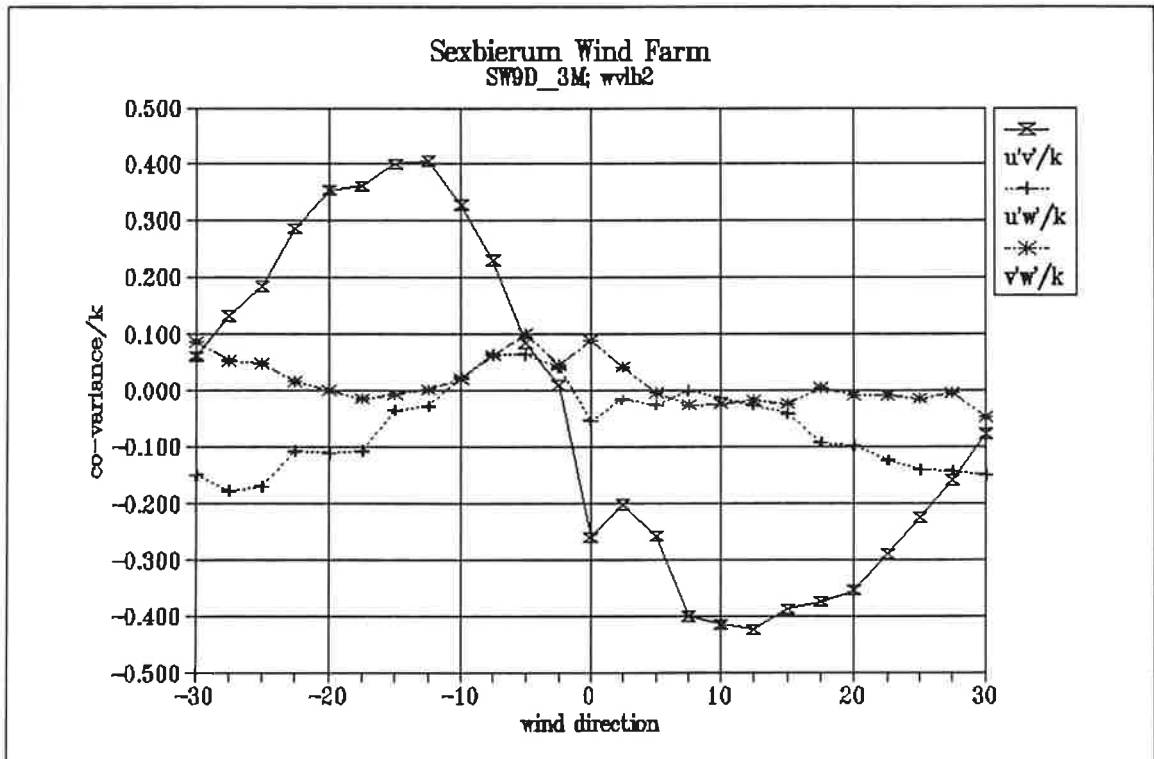


Figure 30 Non-dimensionalized shear stresses  $u'v'/k$ ;  $u'w'/k$ ;  $v'w'/k$  as a function of wind direction in the wind speed bin 5-10 m/s

*Results of Sexbierum Wind Farm; single wake measurements*

**A4.4 Sensor b3**

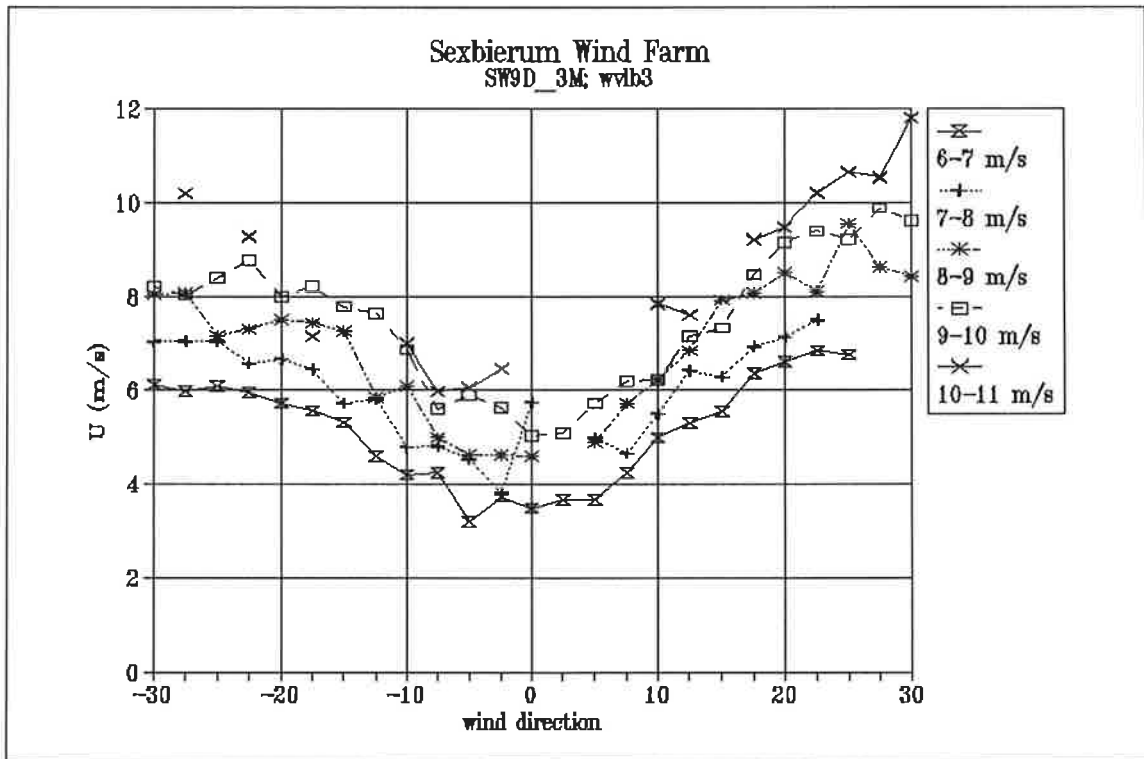


Figure 1 Horizontal wind speed  $U$  as a function of wind direction and wind speed bin

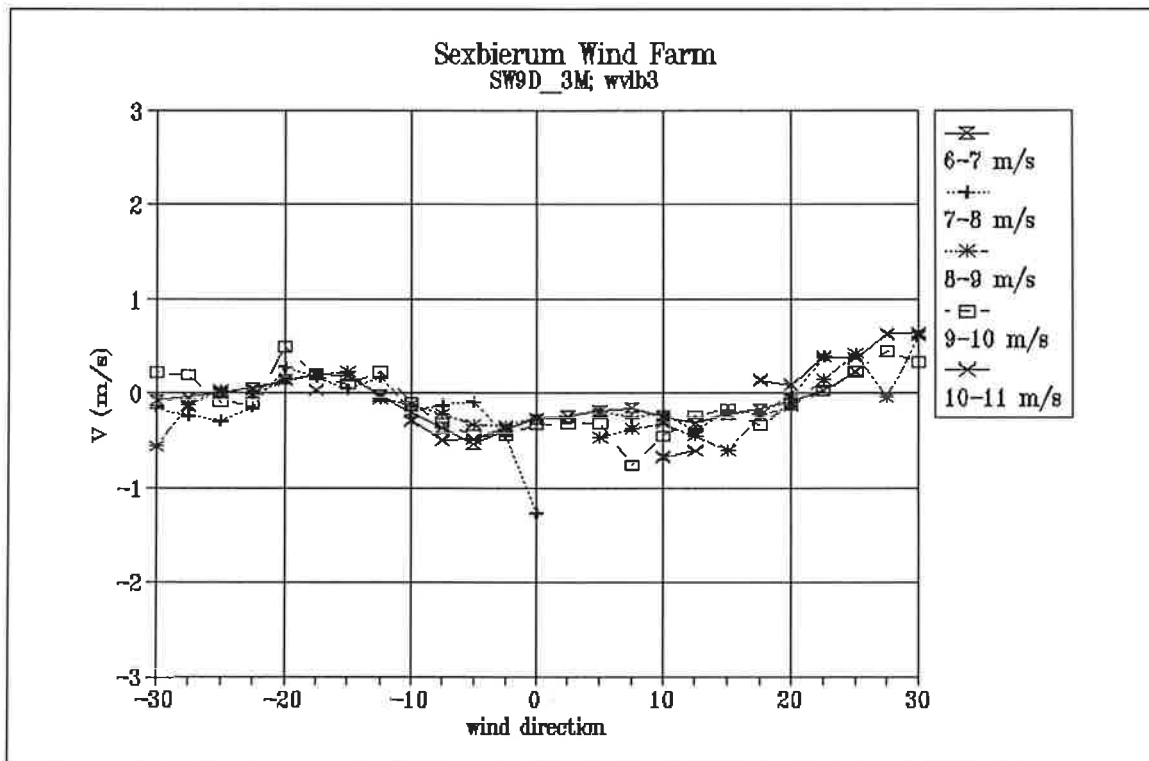


Figure 2 Lateral wind speed  $V$  as a function of wind direction and wind speed bin

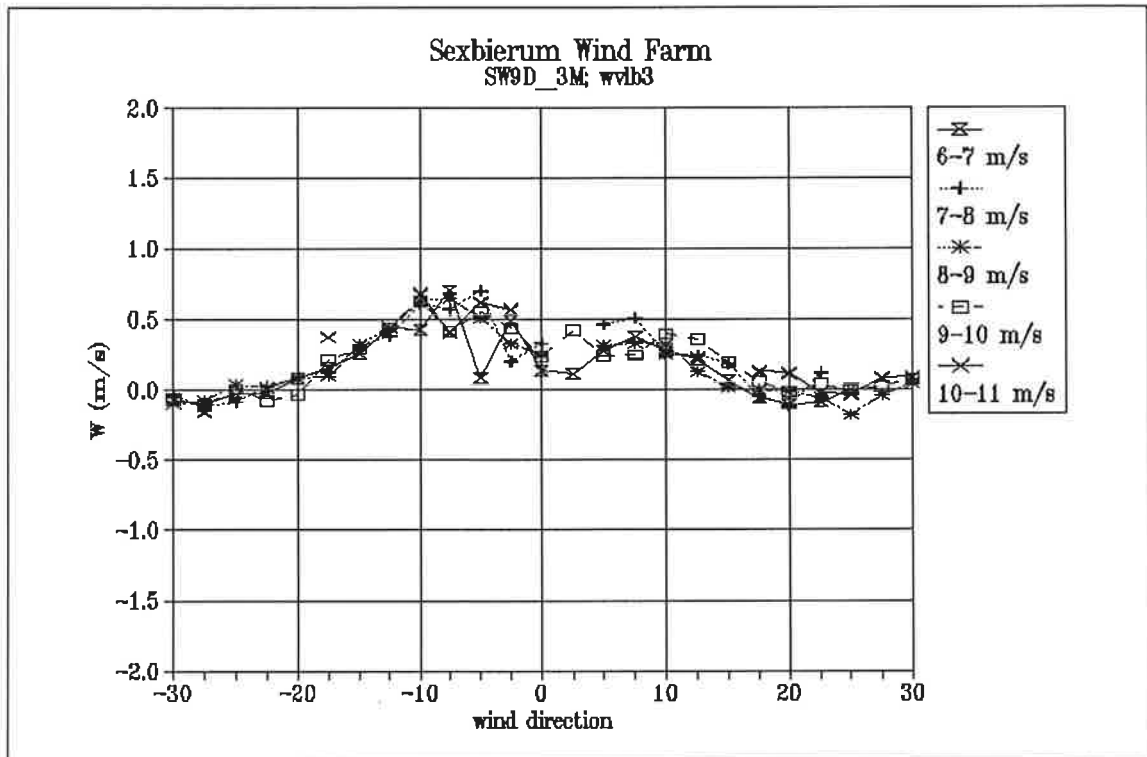


Figure 3 Vertical wind speed  $W$  as a function of wind direction and wind speed bin

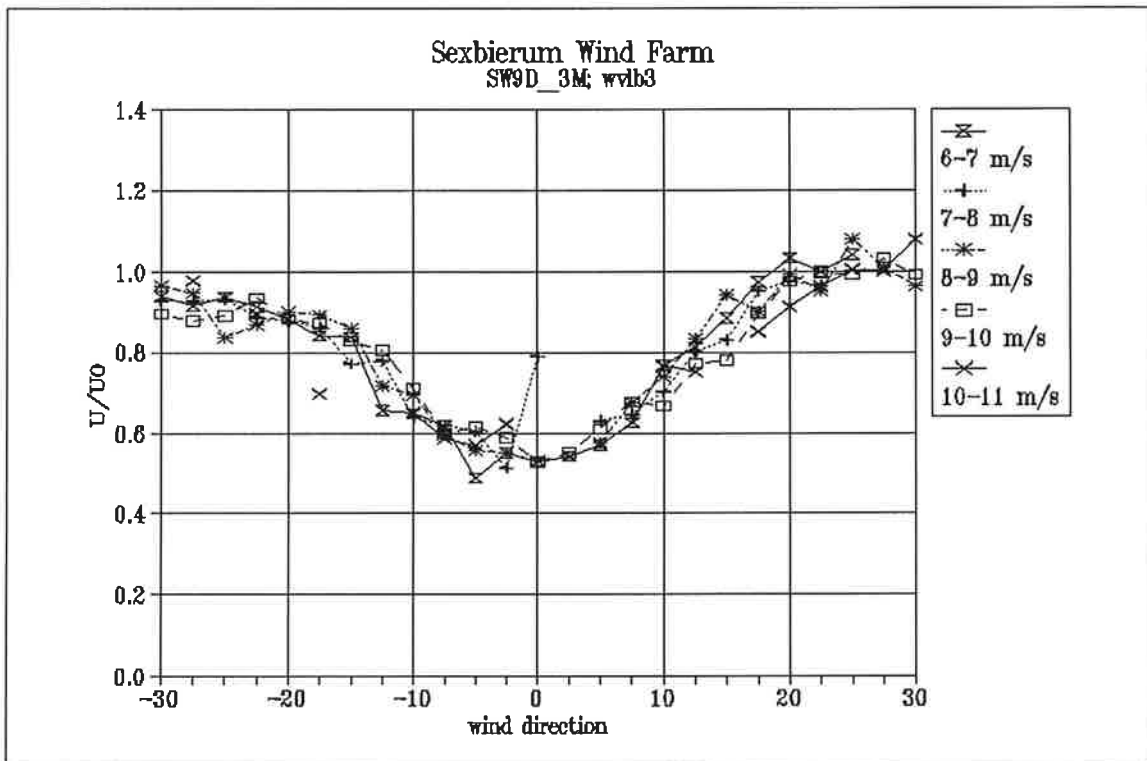


Figure 4 Wake deficit  $U/U_0$  as a function of wind direction and wind speed bin

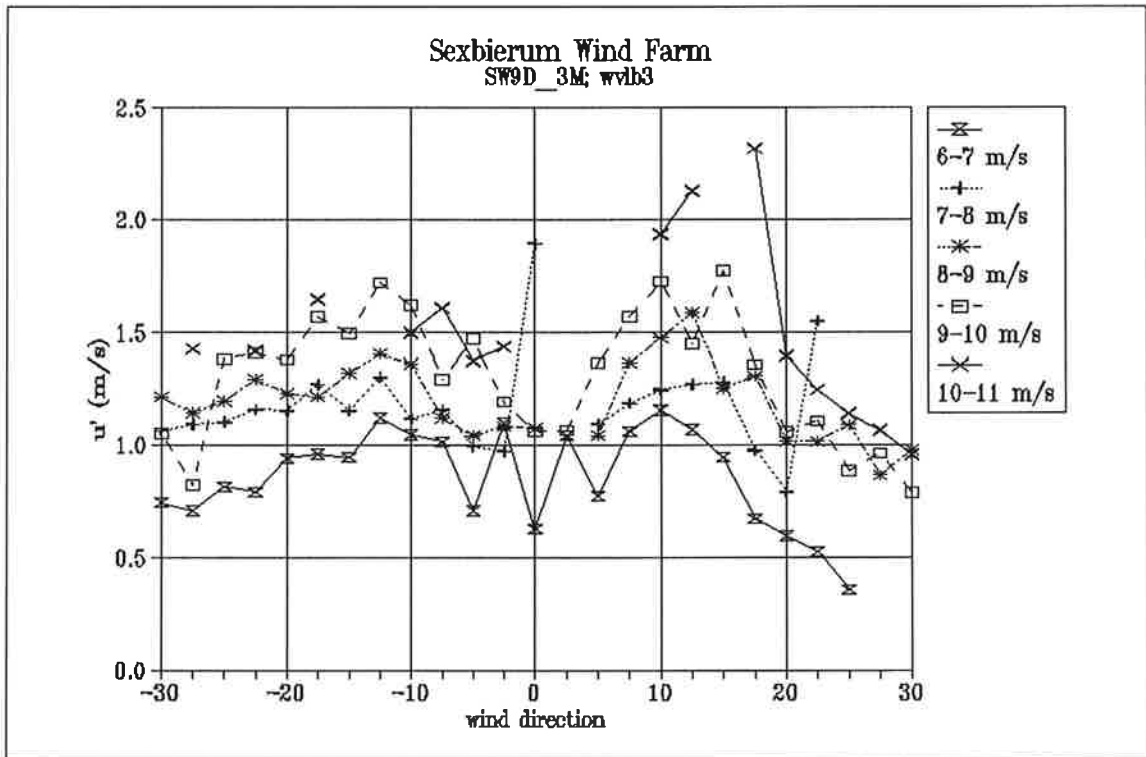


Figure 5 Longitudinal turbulent fluctuations  $u'$  as a function of wind direction and wind speed bin

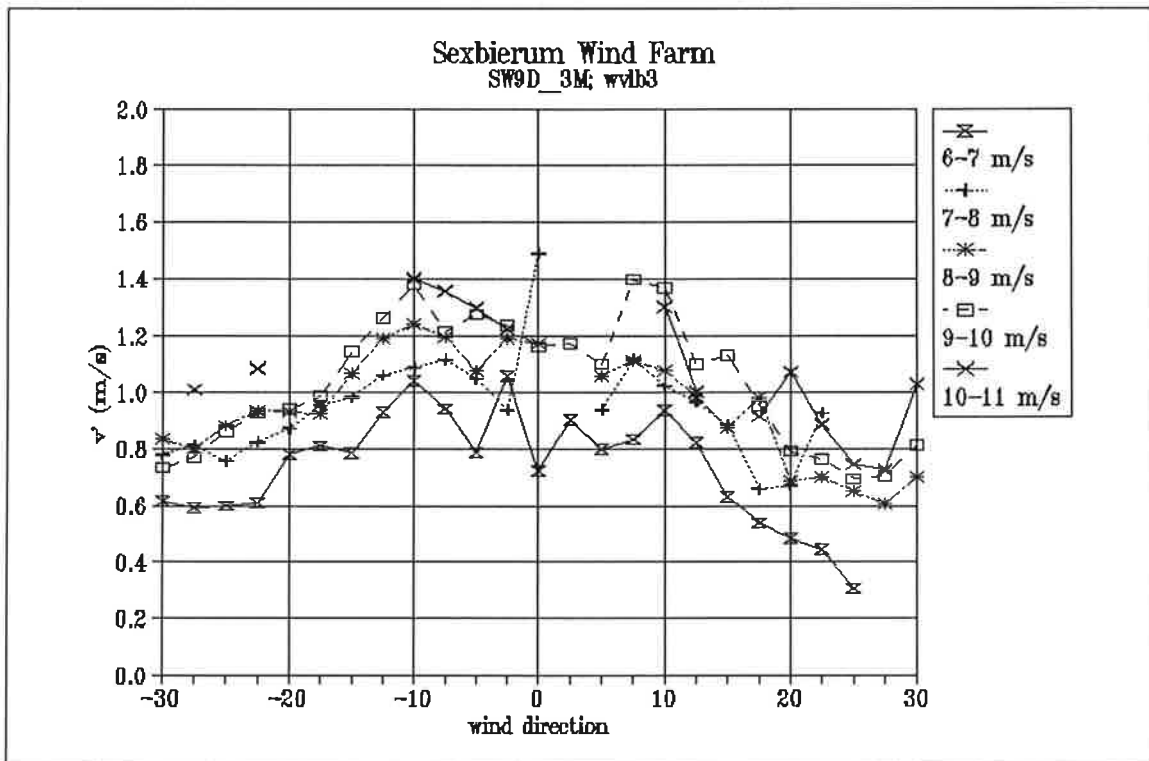


Figure 6 Lateral turbulent fluctuations  $v'$  as a function of wind direction and wind speed bin



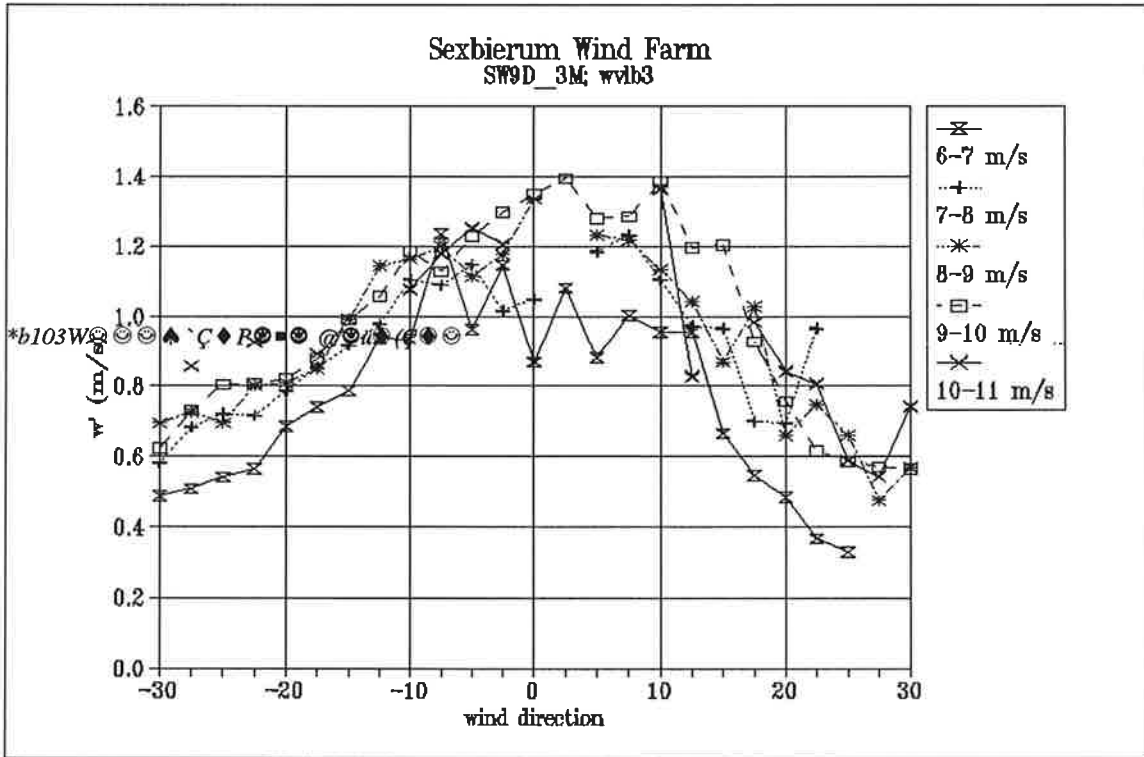


Figure 7 Vertical turbulent fluctuations  $w'$  as a function of wind direction and wind speed bin

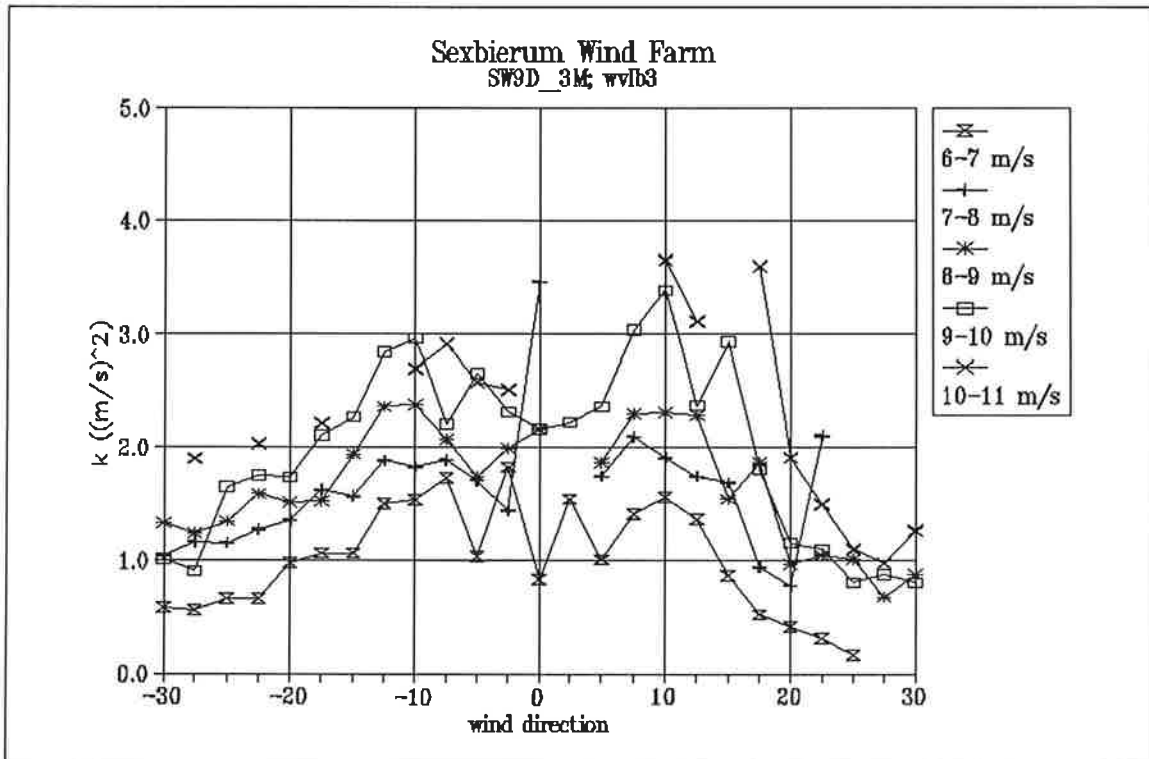


Figure 8 Turbulent kinetic energy per unit mass as a function of wind direction and wind speed bin

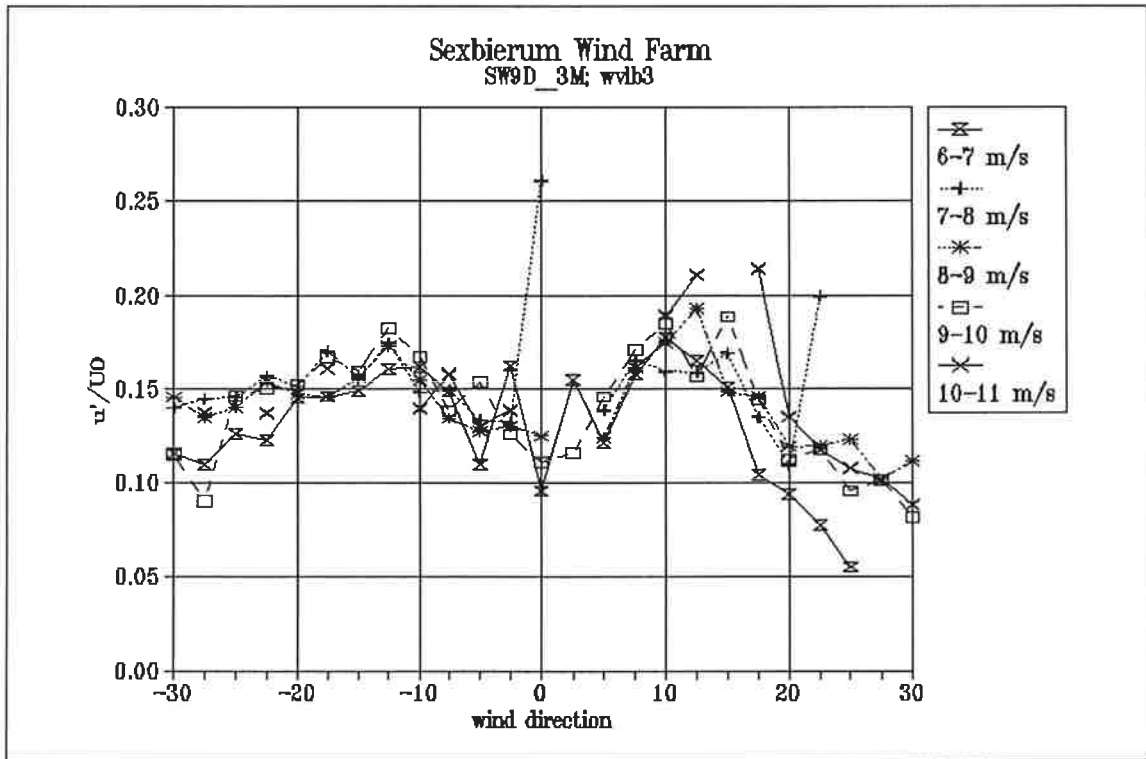


Figure 9 Non-dimensionalized longitudinal turbulent fluctuations  $u'/U_0$  as a function of wind direction and wind speed bin

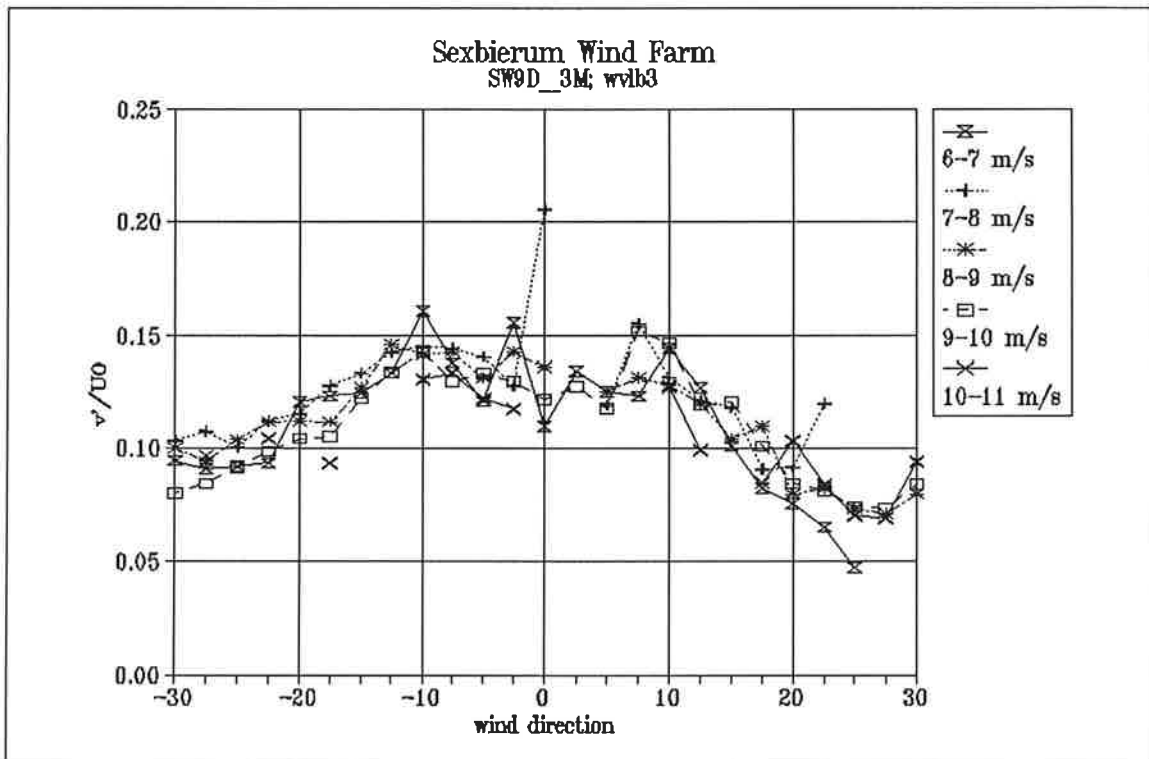


Figure 10 Non-dimensionalized lateral turbulent fluctuations  $v'/U_0$  as a function of wind direction and wind speed bin

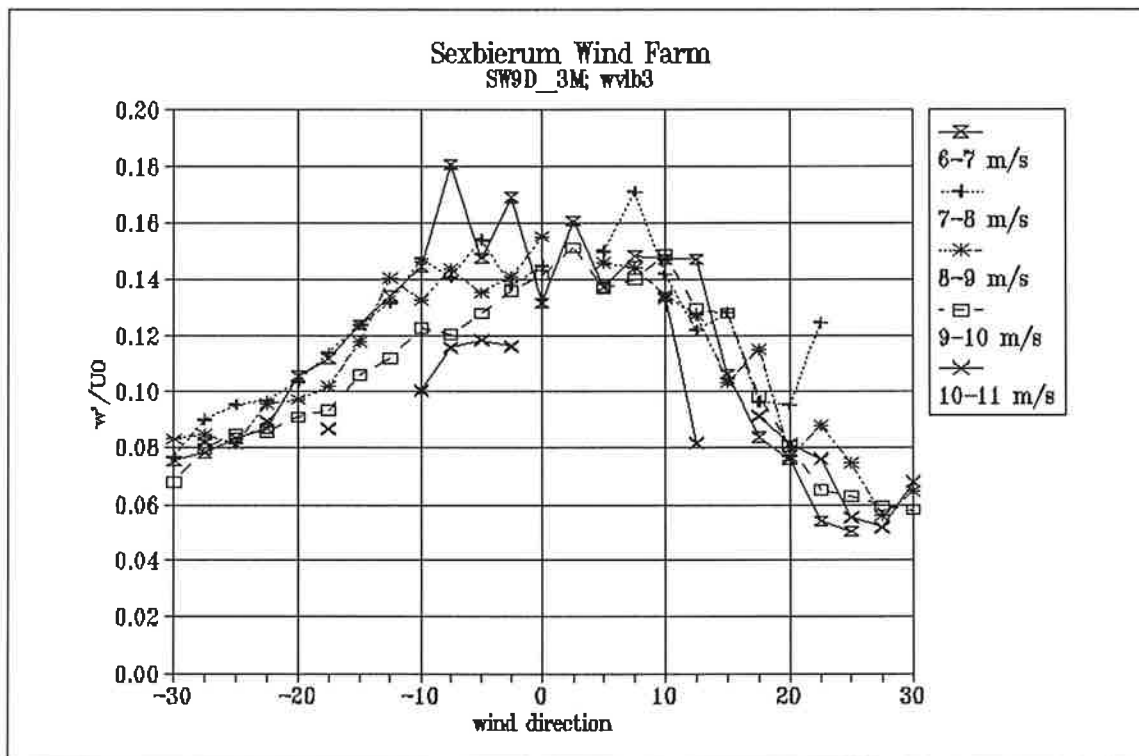


Figure 11 Non-dimensionalized vertical turbulent fluctuations  $w'/U_0$  as a function of wind direction and wind speed bin

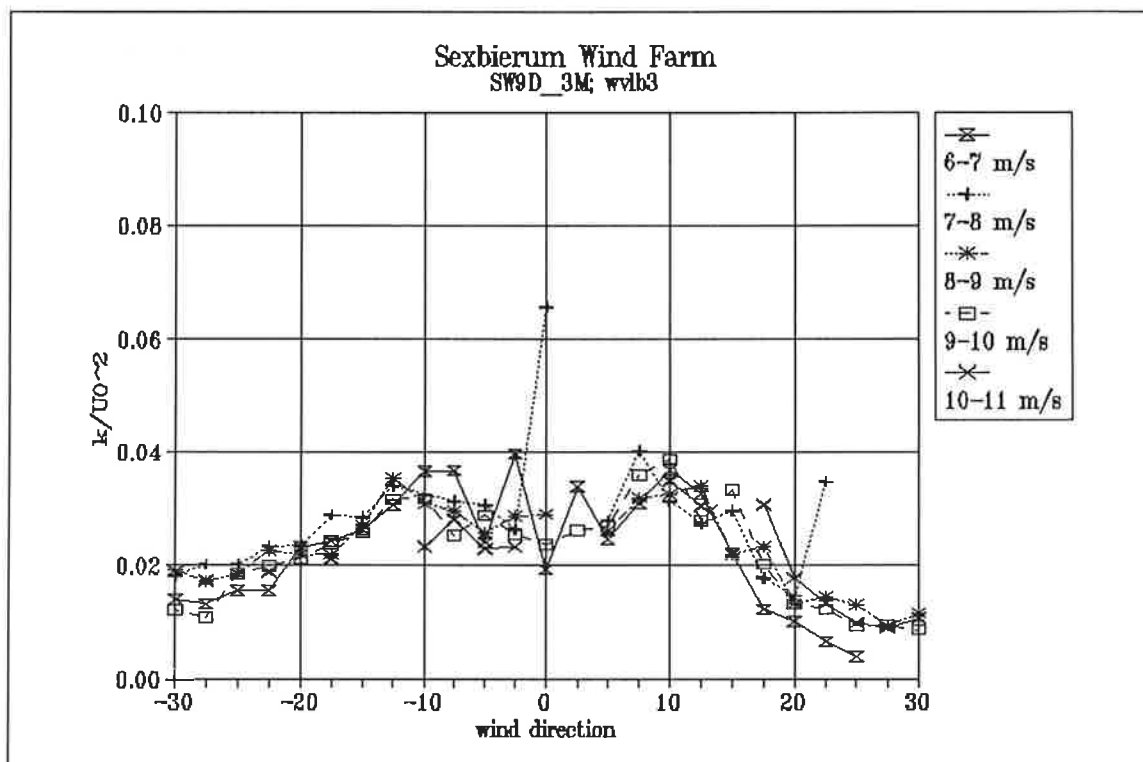


Figure 12 Non-dimensionalized turbulent kinetic energy  $k/U_0^2$  as a function of wind direction and wind speed bin

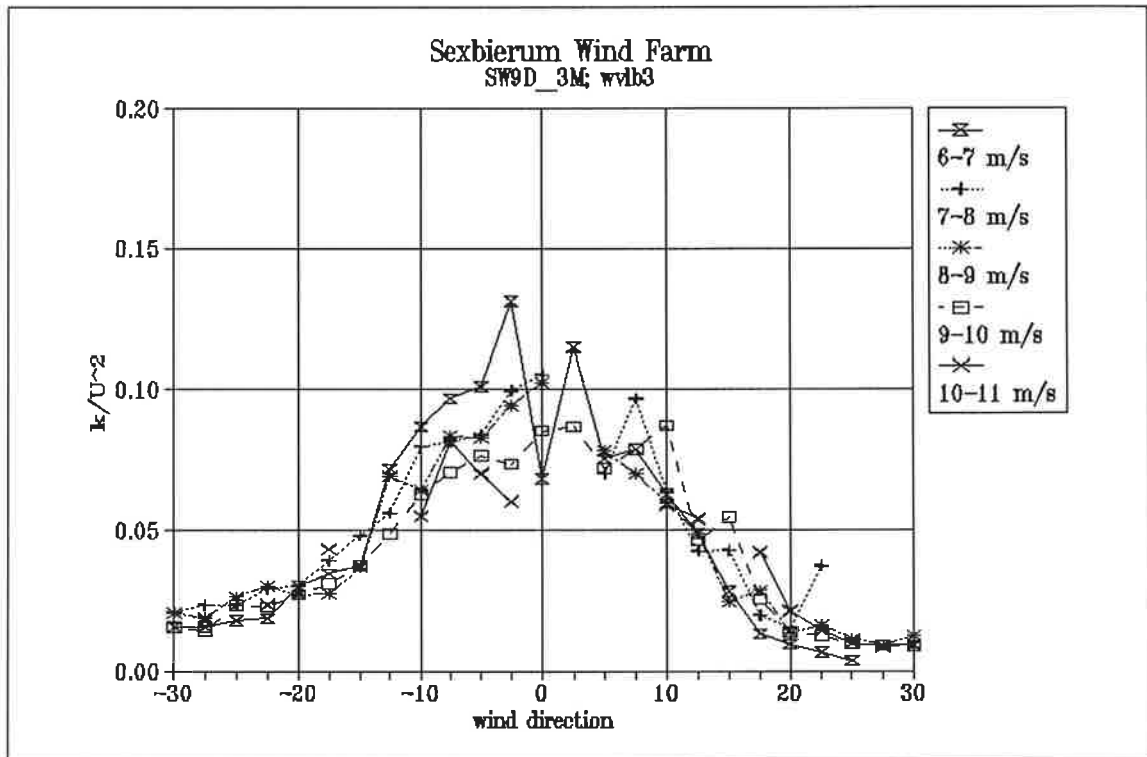


Figure 13 Non-dimensionalized turbulent kinetic energy  $k/U^2$  as a function of wind direction and wind speed bin

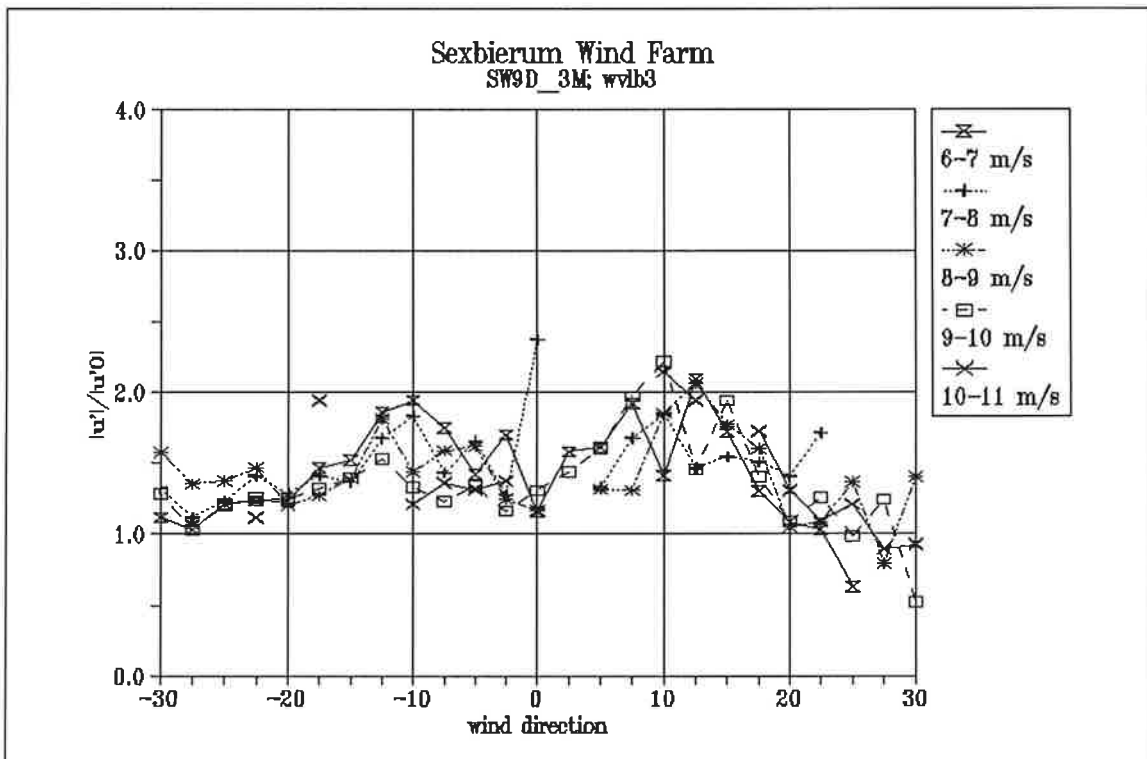


Figure 14 Longitudinal turbulence enhancement  $u'/u'_0$  as a function of wind direction and wind speed bin

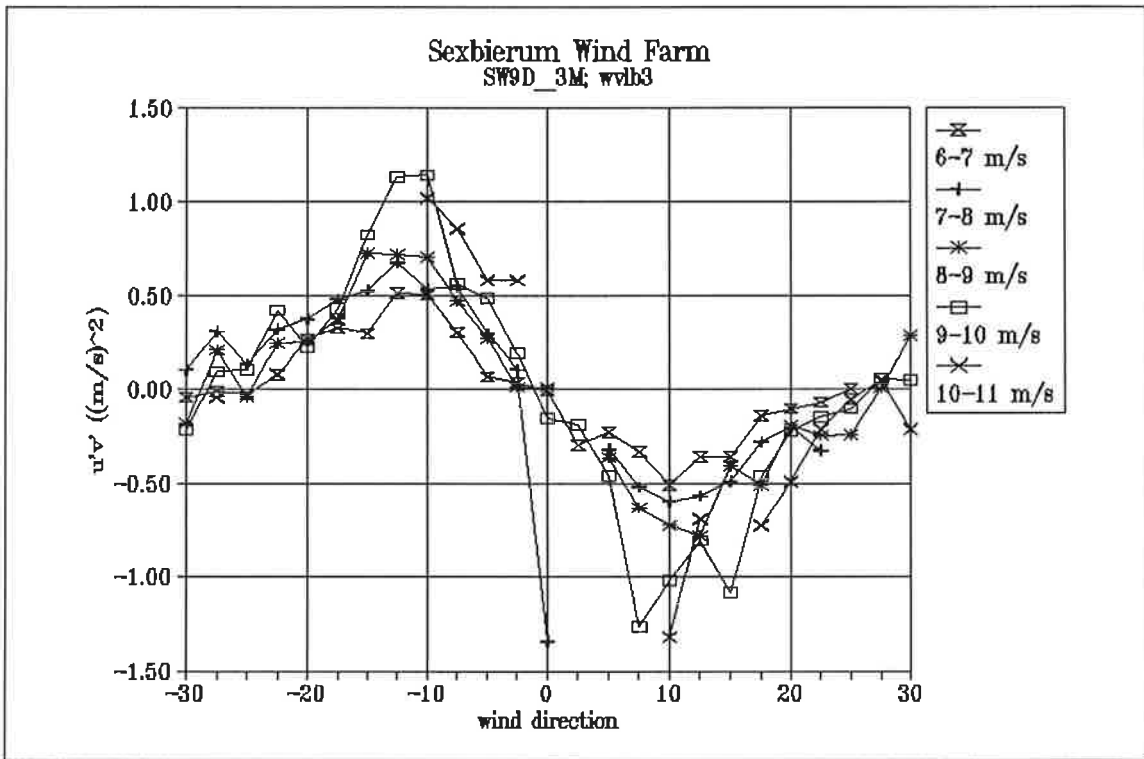


Figure 15 Shear stress  $u'v'$  as a function of wind direction and wind speed bin

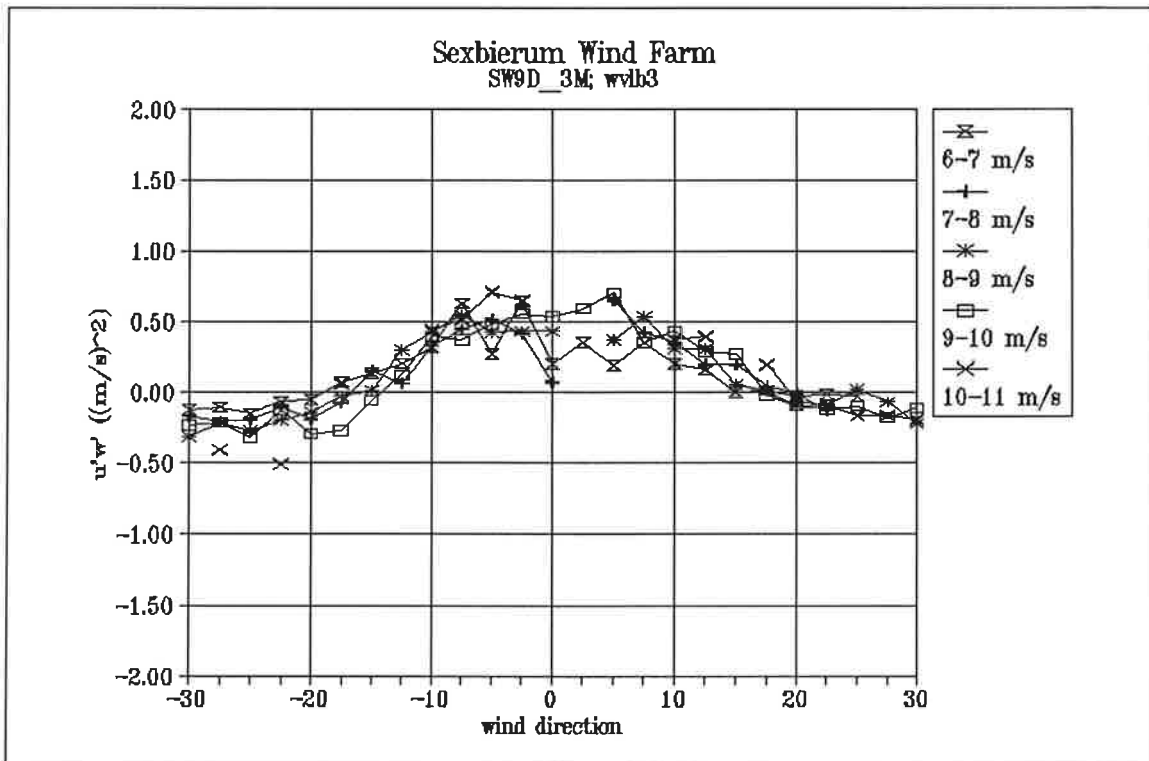


Figure 16 Shear stress  $u'w'$  as a function of wind direction and wind speed bin

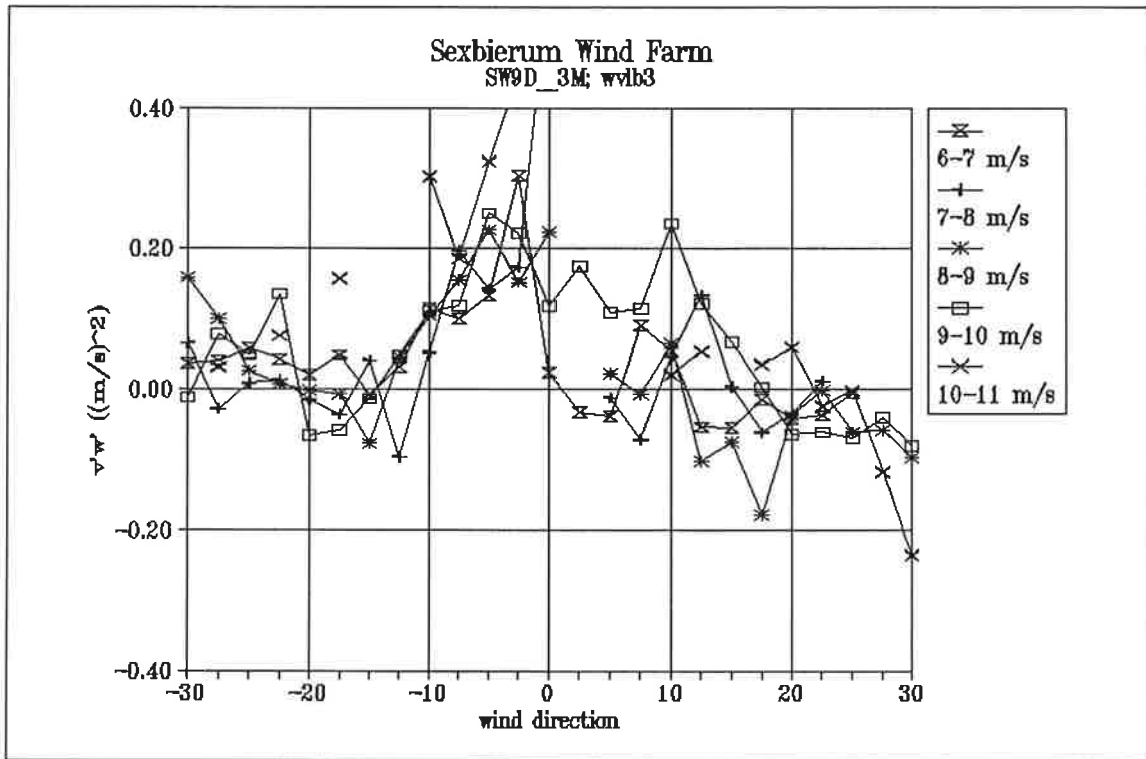


Figure 17 Shear stress  $v'w'$  as a function of wind direction and wind speed bin

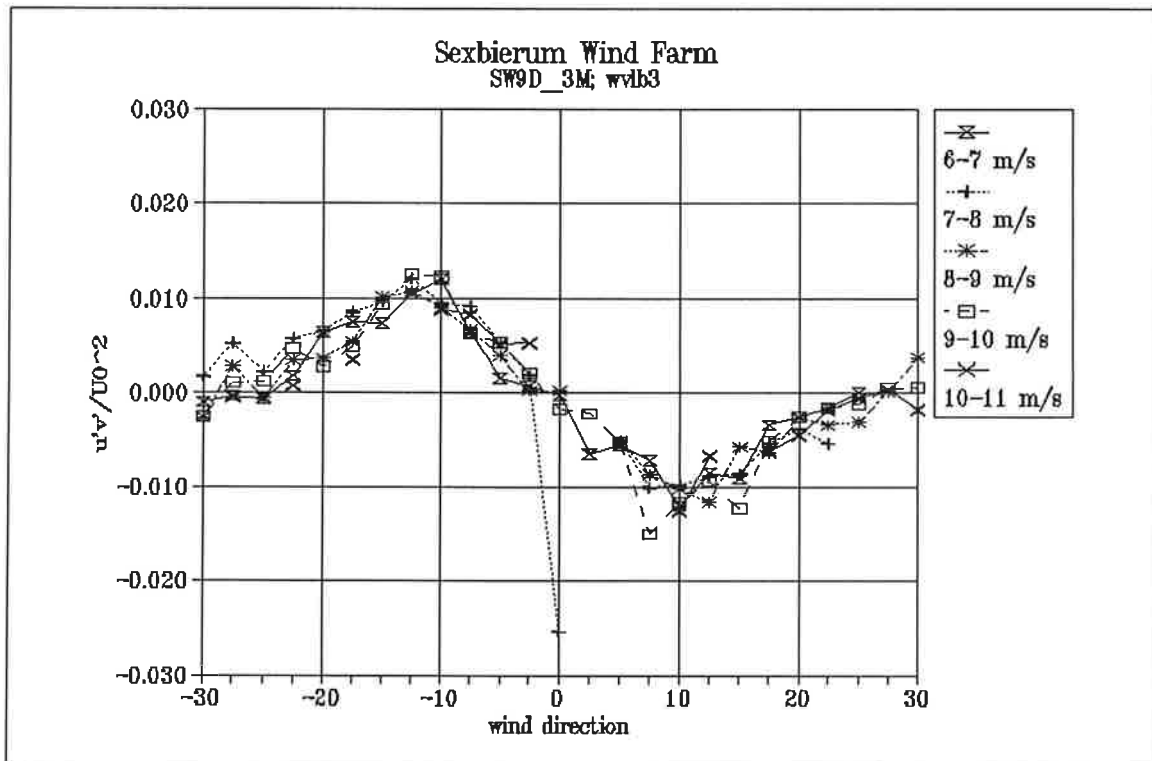


Figure 18 Non-dimensionalized shear stress  $u'v'/U_0^2$  as a function of wind direction and wind speed bin

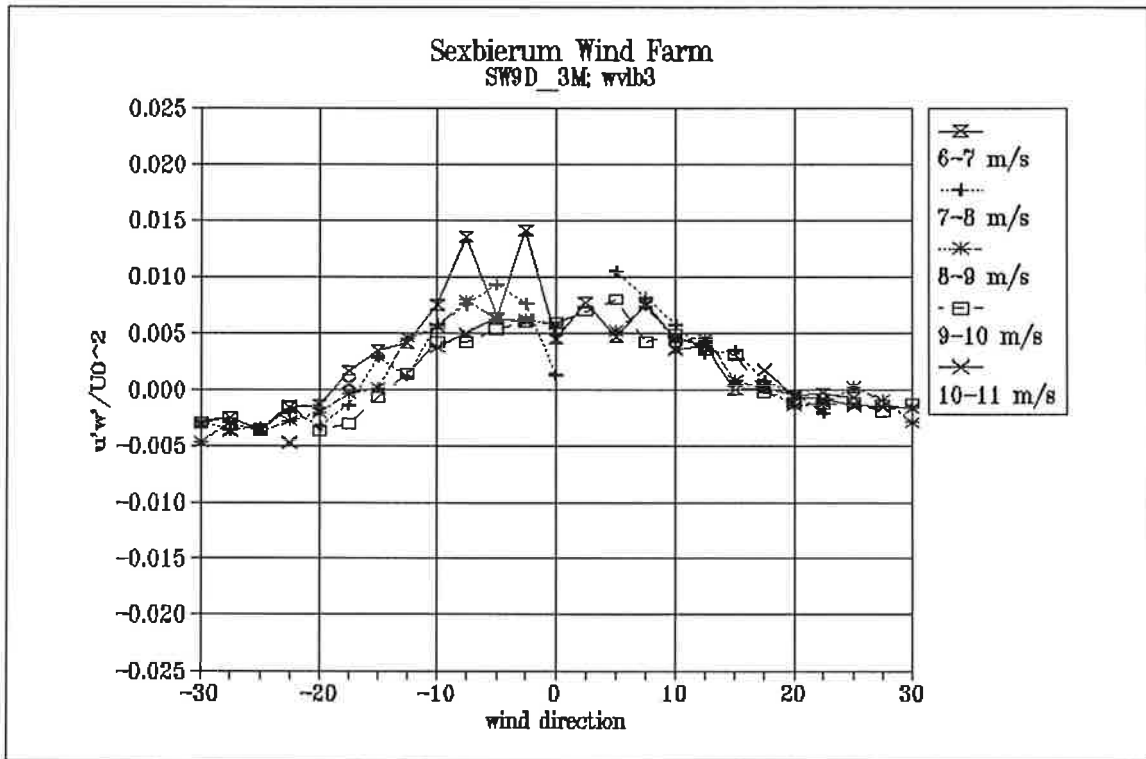


Figure 19 Non-dimensionalized shear stress  $u'w'/U_0^2$  as a function of wind direction and wind speed bin

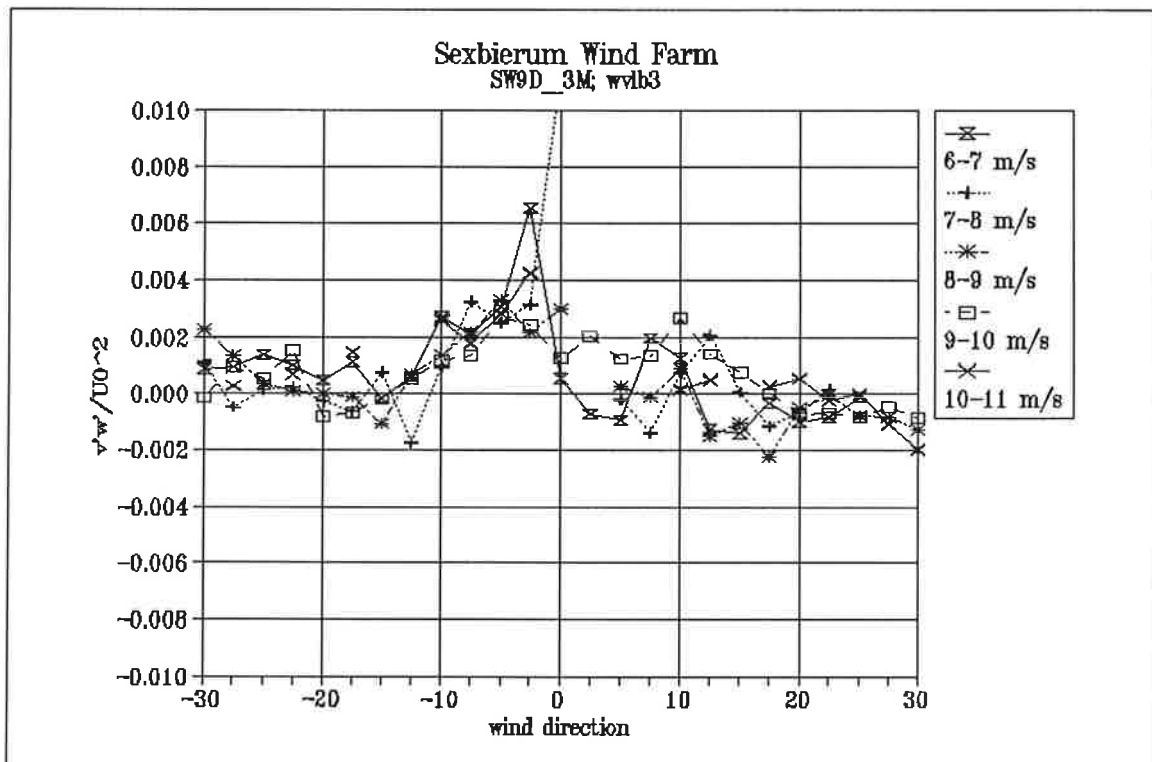


Figure 20 Non-dimensionalized shear stress  $v'w'/U_0^2$  as a function of wind direction and wind speed bin

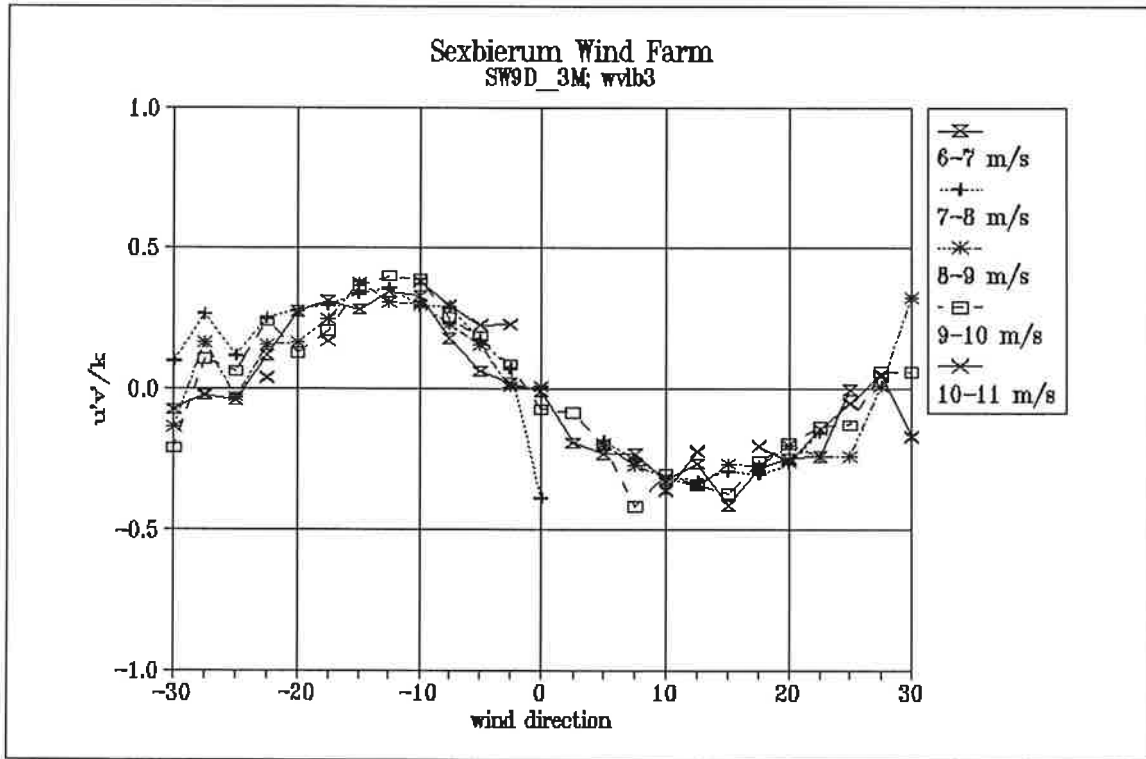


Figure 21 Non-dimensionalized shear stress  $u'v'/k$  as a function of wind direction and wind speed bin

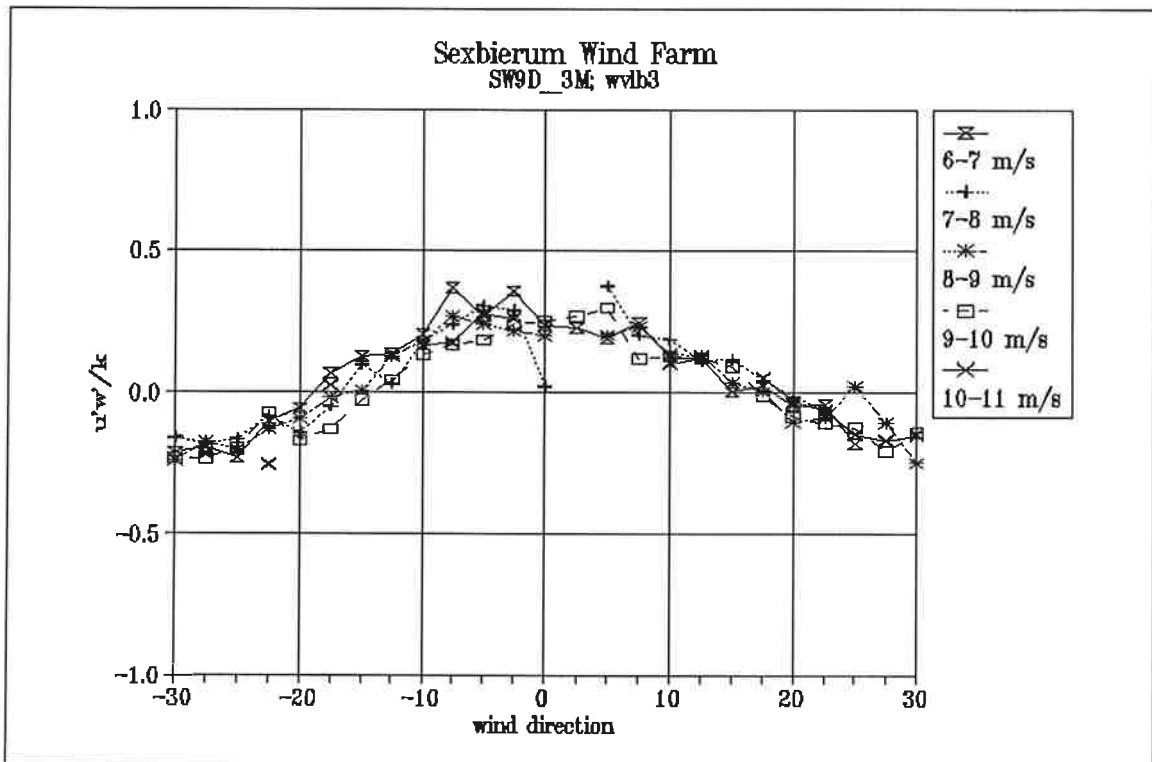


Figure 22 Non-dimensionalized shear stress  $u'w'/k$  as a function of wind direction and wind speed bin



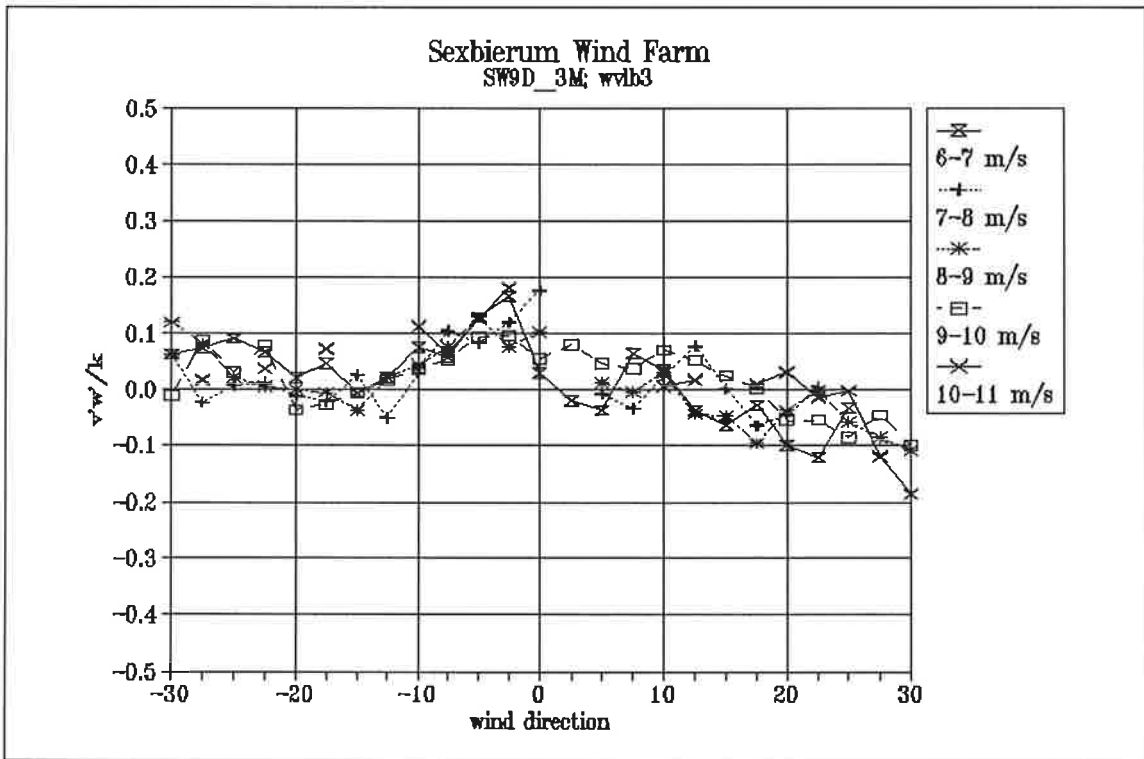


Figure 23 Non-dimensionalized shear stress  $v'w'/k$  as a function of wind direction and wind speed bin

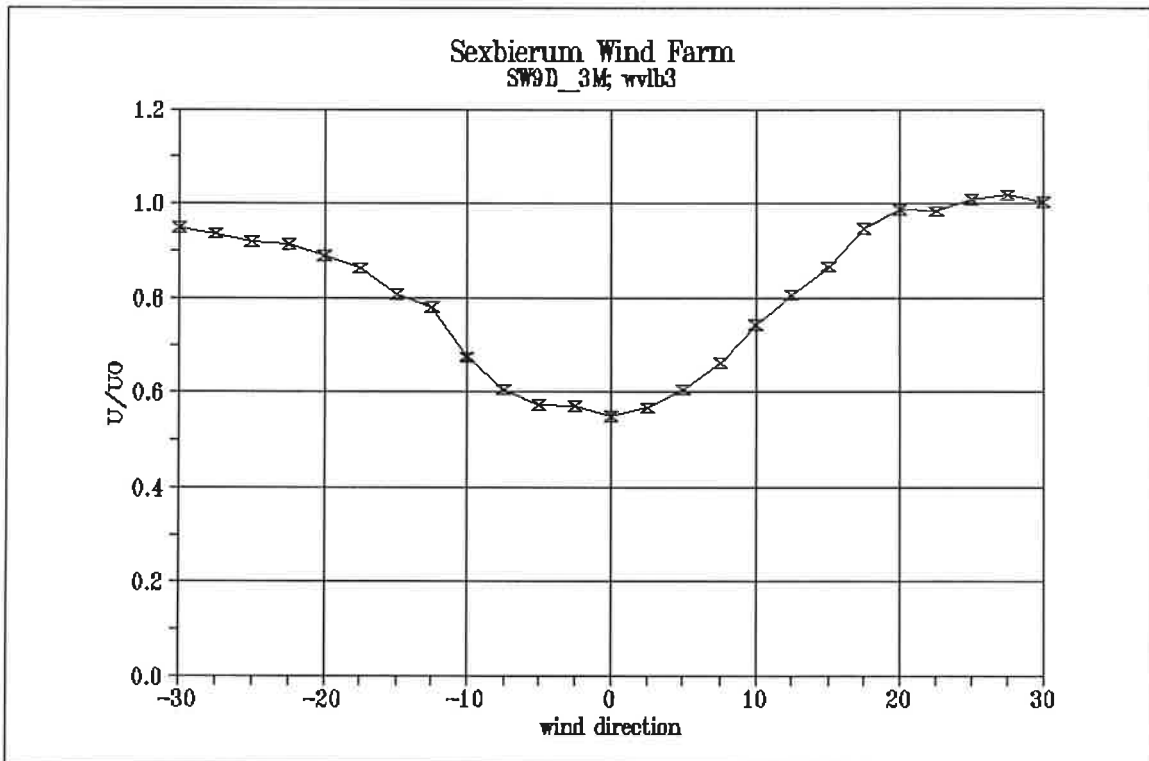


Figure 24 Wake deficit  $U/U_0$  as a function of wind direction in the wind speed bin 5-10 m/s

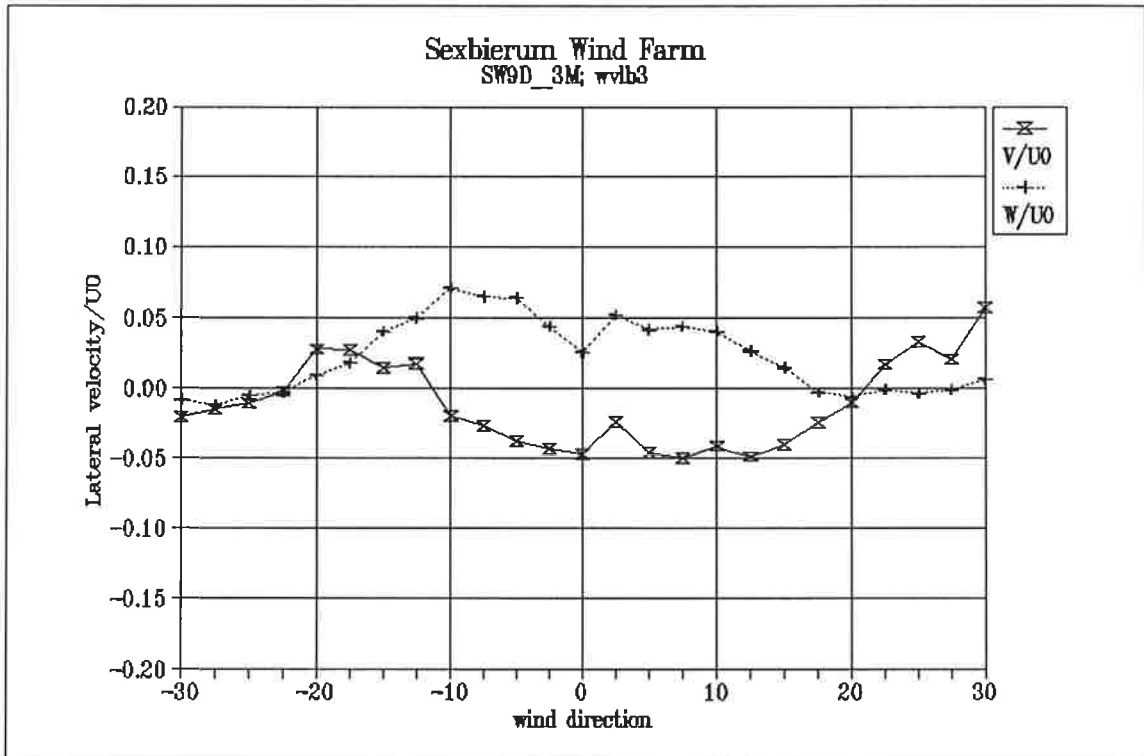


Figure 25 Lateral and vertical wind speed  $V/U_0$  and  $W/U_0$  as a function of wind direction in the wind speed bin 5-10 m/s

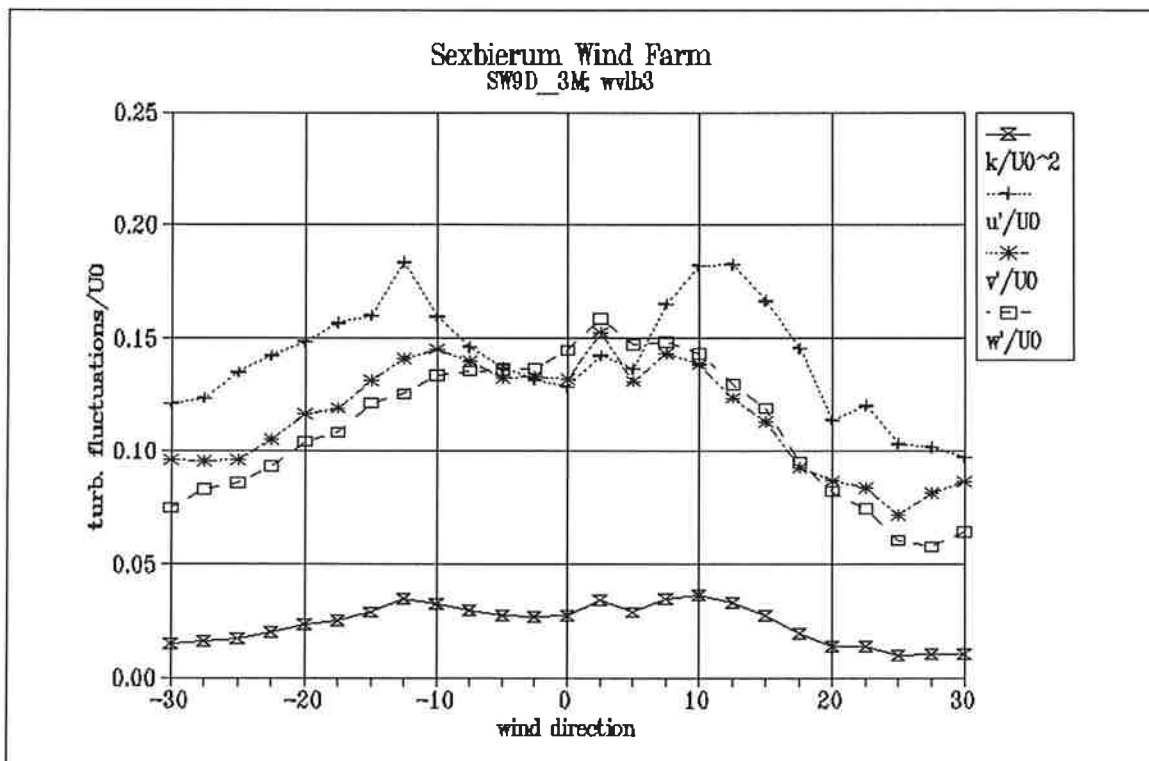


Figure 26 Turbulent fluctuations as a function of wind direction in the wind speed bin 5-10 m/s, non-dimensionalized with  $U_0$

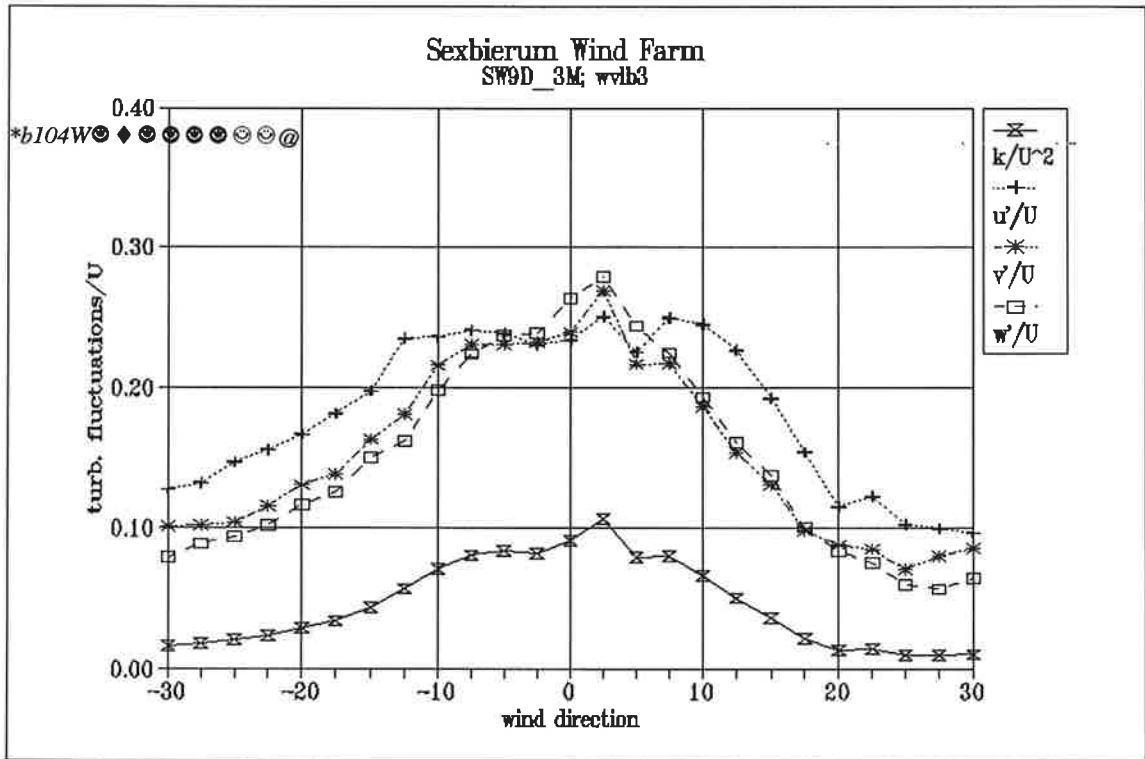


Figure 27 Turbulent fluctuations as a function of wind direction in the wind speed bin 5-10 m/s, non-dimensionalized with  $U$

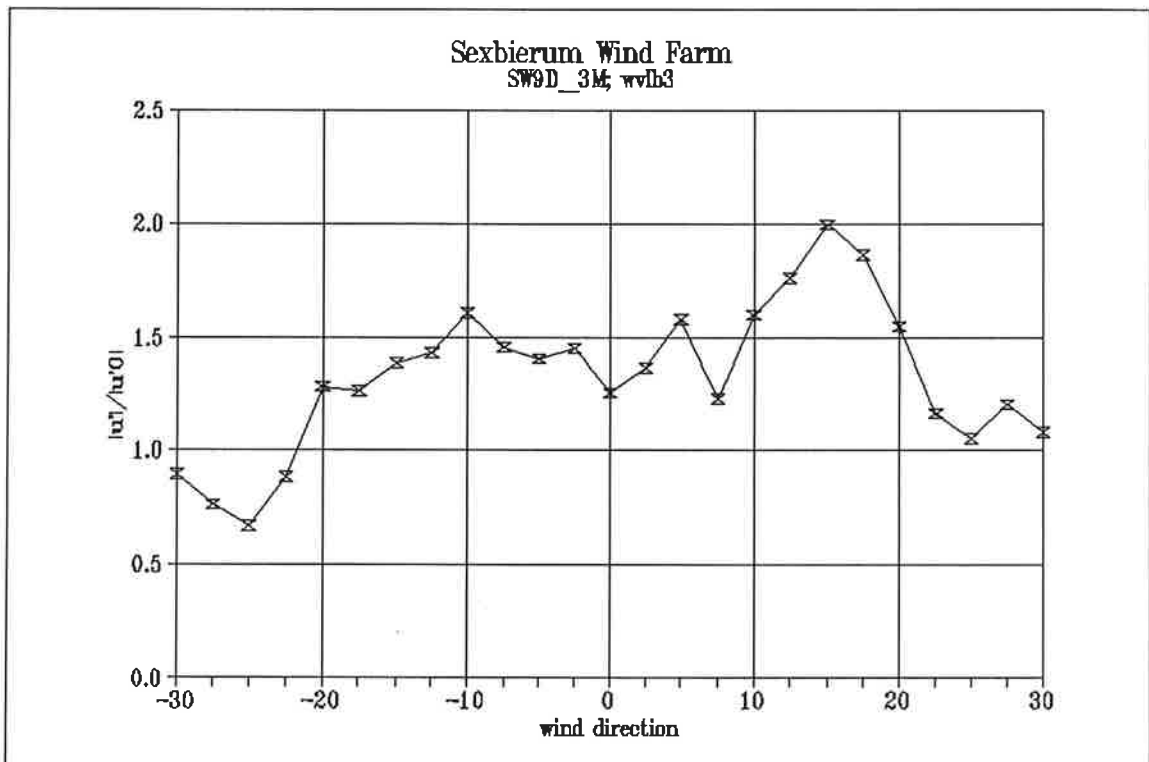


Figure 28 Longitudinal turbulence enhancement  $u'u'_0$  as a function of wind direction in the wind speed bin 5-10 m/s

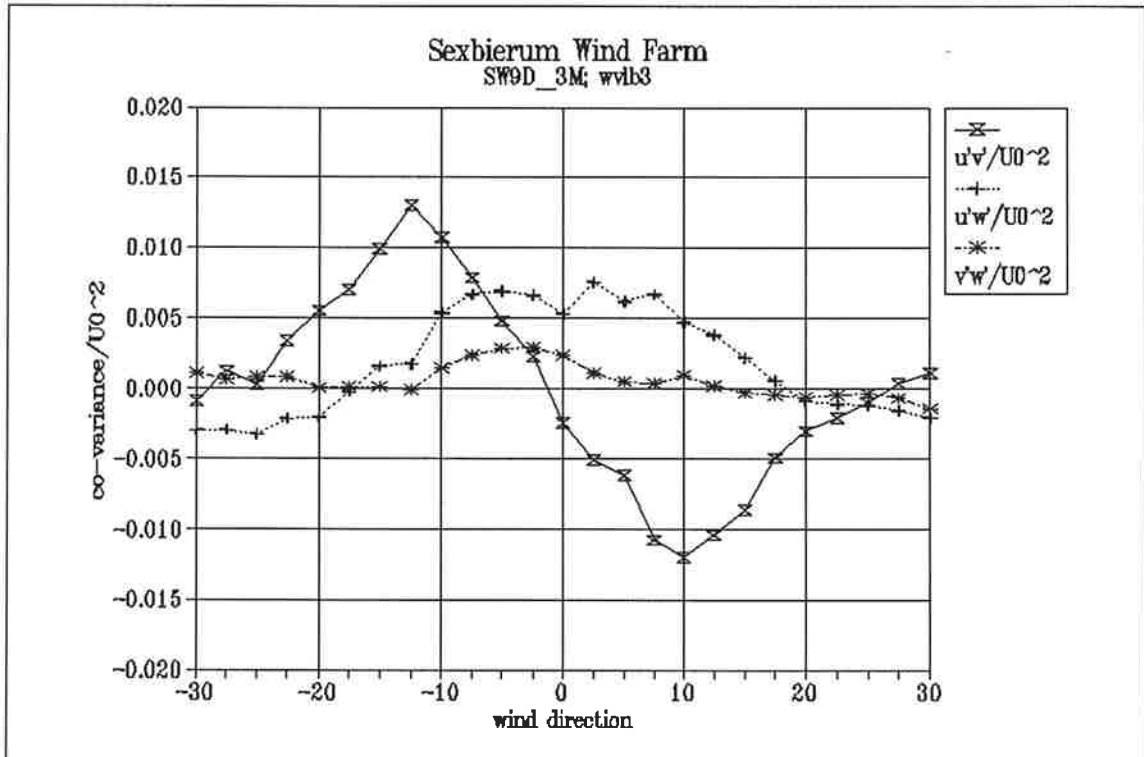


Figure 29 Non-dimensionalized shear stresses  $u'v'/U_0^2$ ;  $u'w'/U_0^2$ ;  $v'w'/U_0^2$  as a function of wind direction in the wind speed bin 5-10 m/s

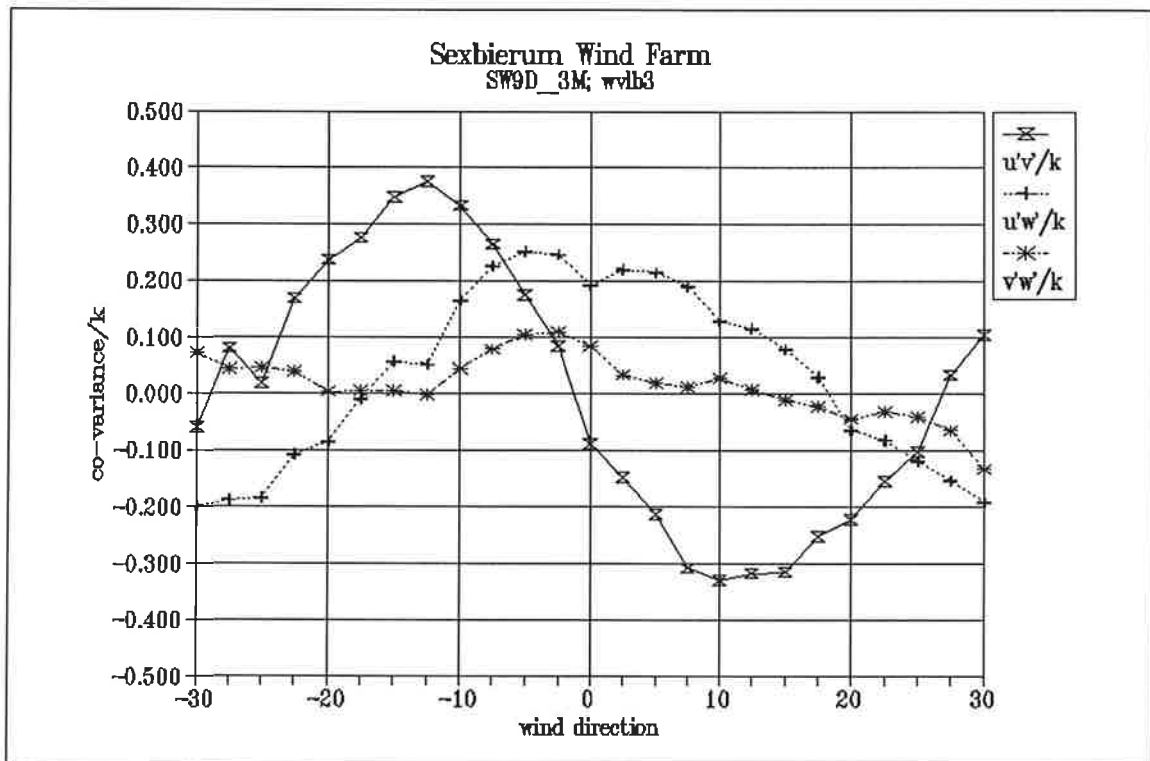


Figure 30 Non-dimensionalized shear stresses  $u'v'/k$ ;  $u'w'/k$ ;  $v'w'/k$  as a function of wind direction in the wind speed bin 5-10 m/s

*Results of Sexbierum Wind Farm; single wake measurements*

**A4.5 Sensor c2**

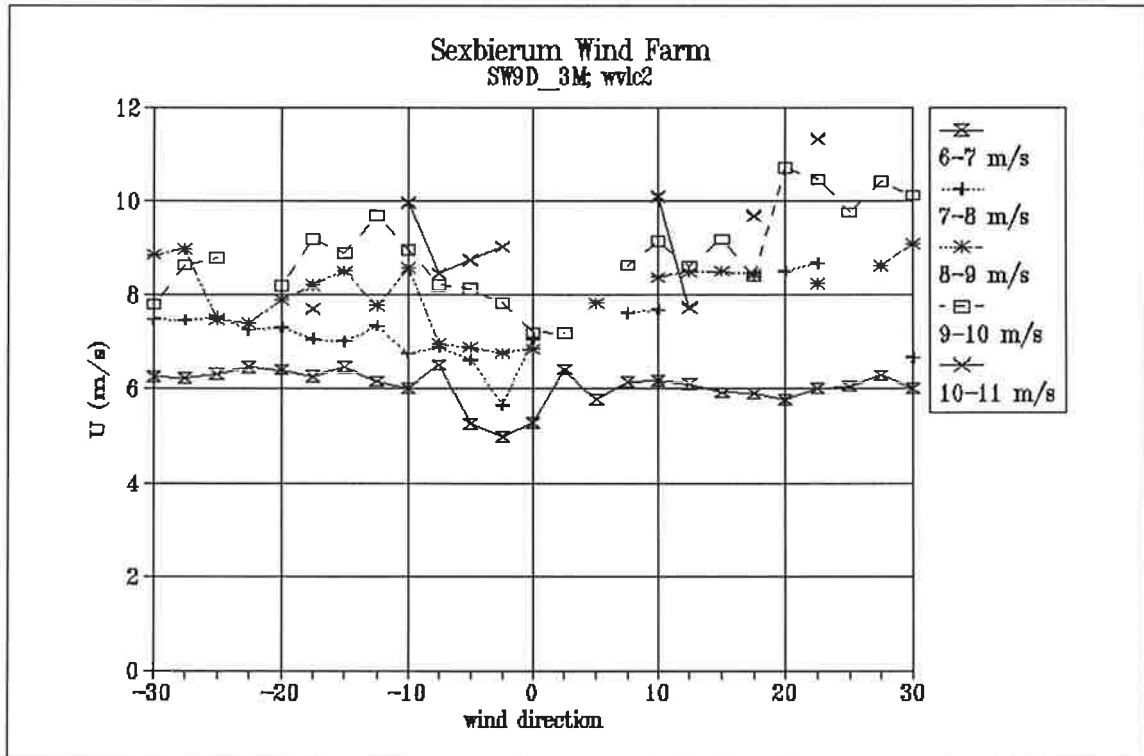


Figure 1 Horizontal wind speed  $U$  as a function of wind direction and wind speed bin

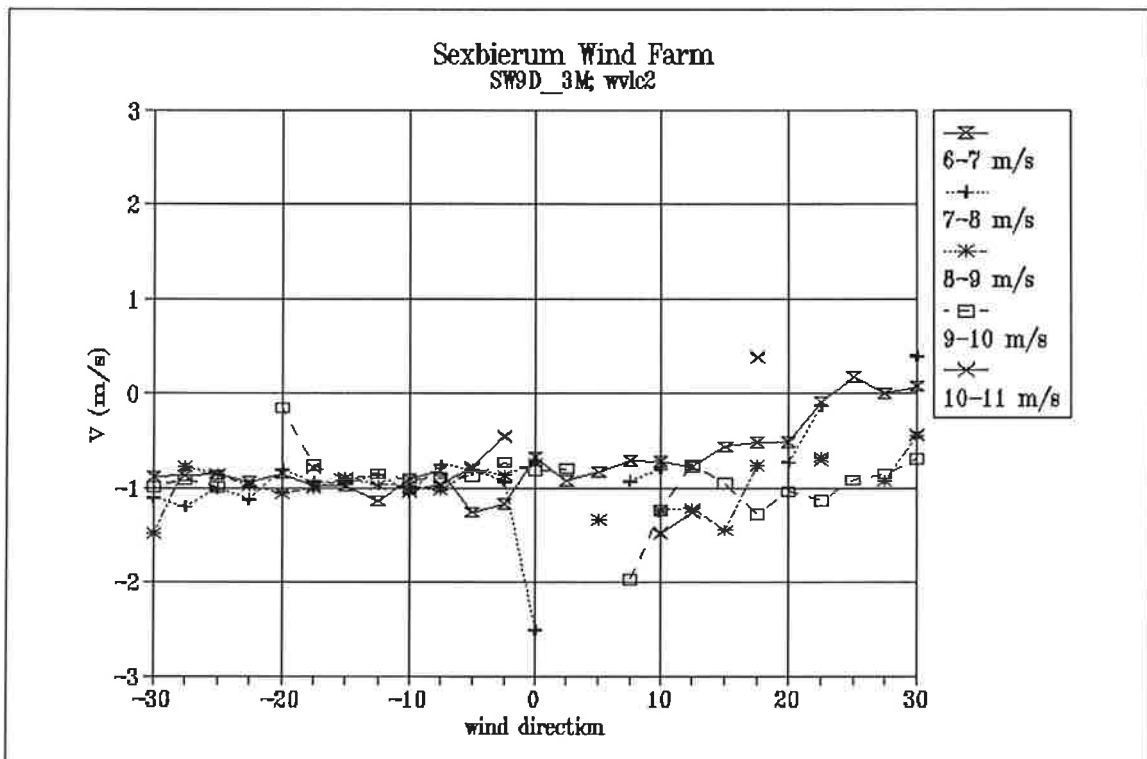


Figure 2 Lateral wind speed  $V$  as a function of wind direction and wind speed bin

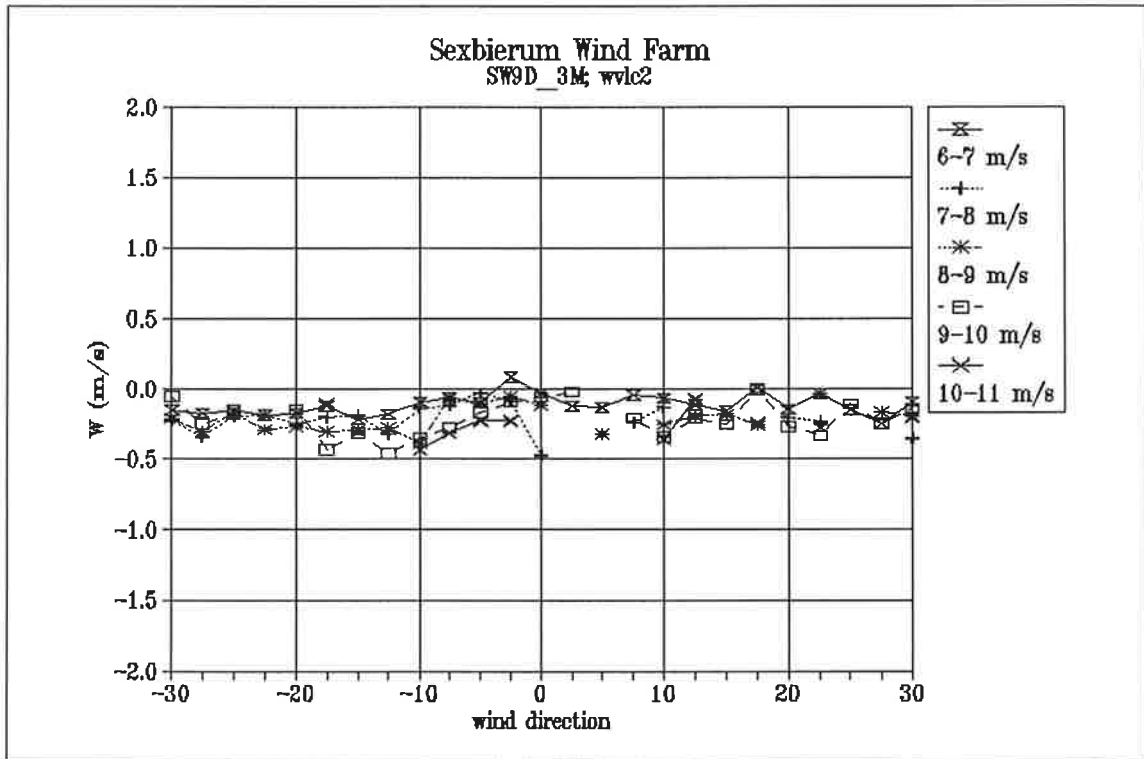


Figure 3 Vertical wind speed  $W$  as a function of wind direction and wind speed bin

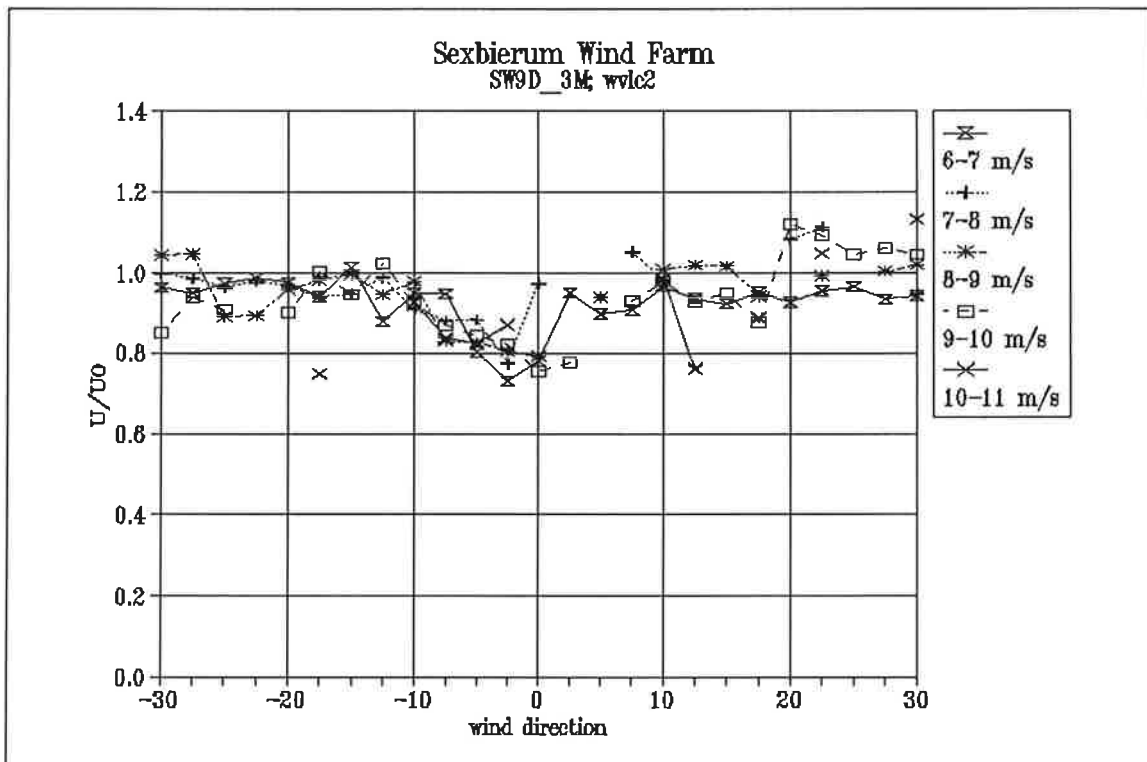


Figure 4 Wake deficit  $U/U_0$  as a function of wind direction and wind speed bin

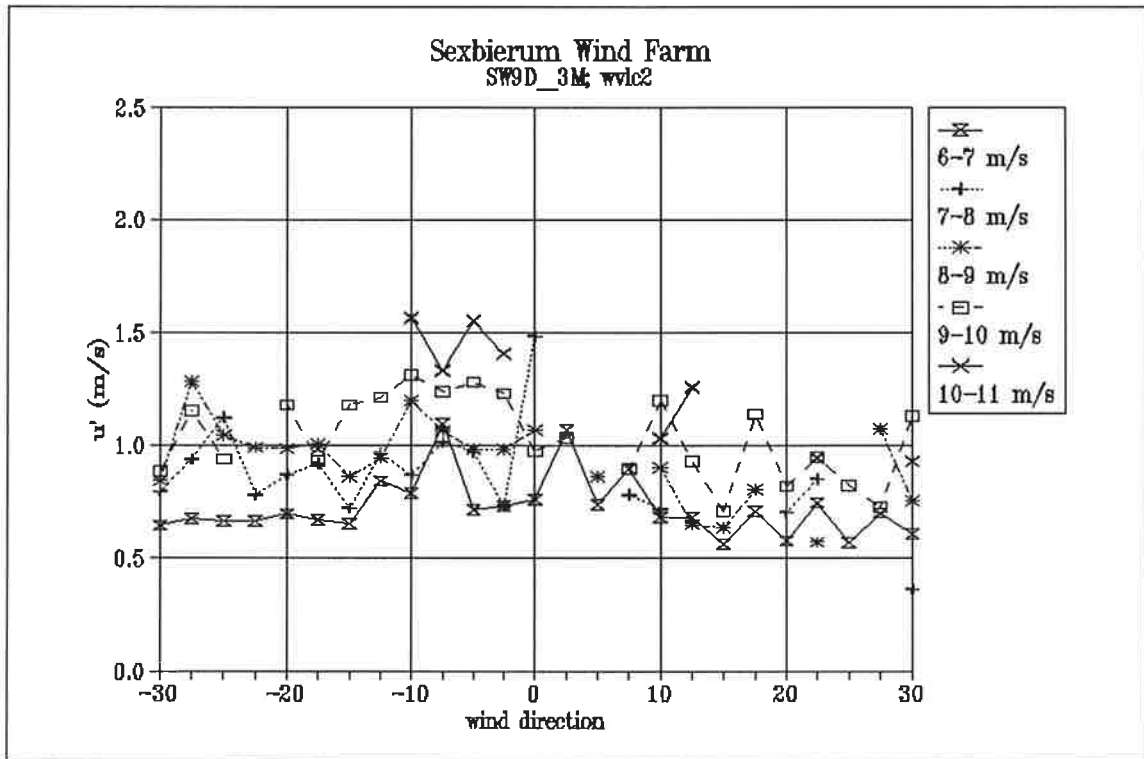


Figure 5 Longitudinal turbulent fluctuations  $u'$  as a function of wind direction and wind speed bin

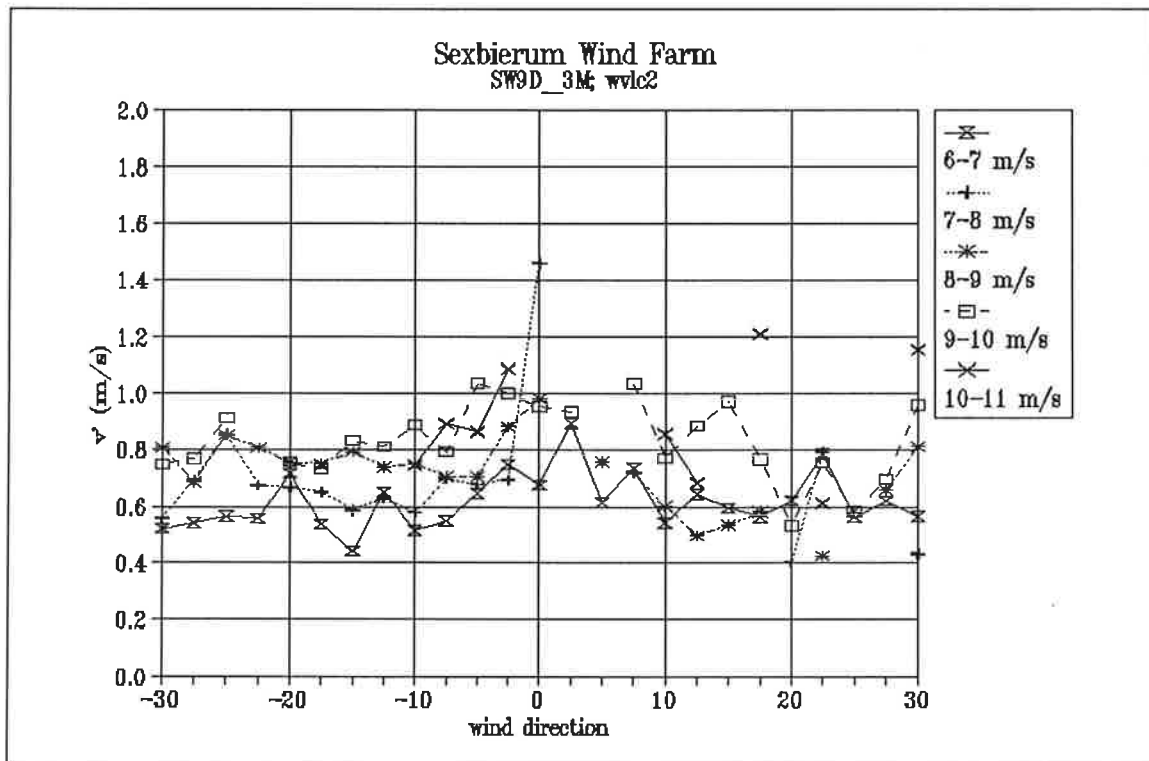


Figure 6 Lateral turbulent fluctuations  $v'$  as a function of wind direction and wind speed bin



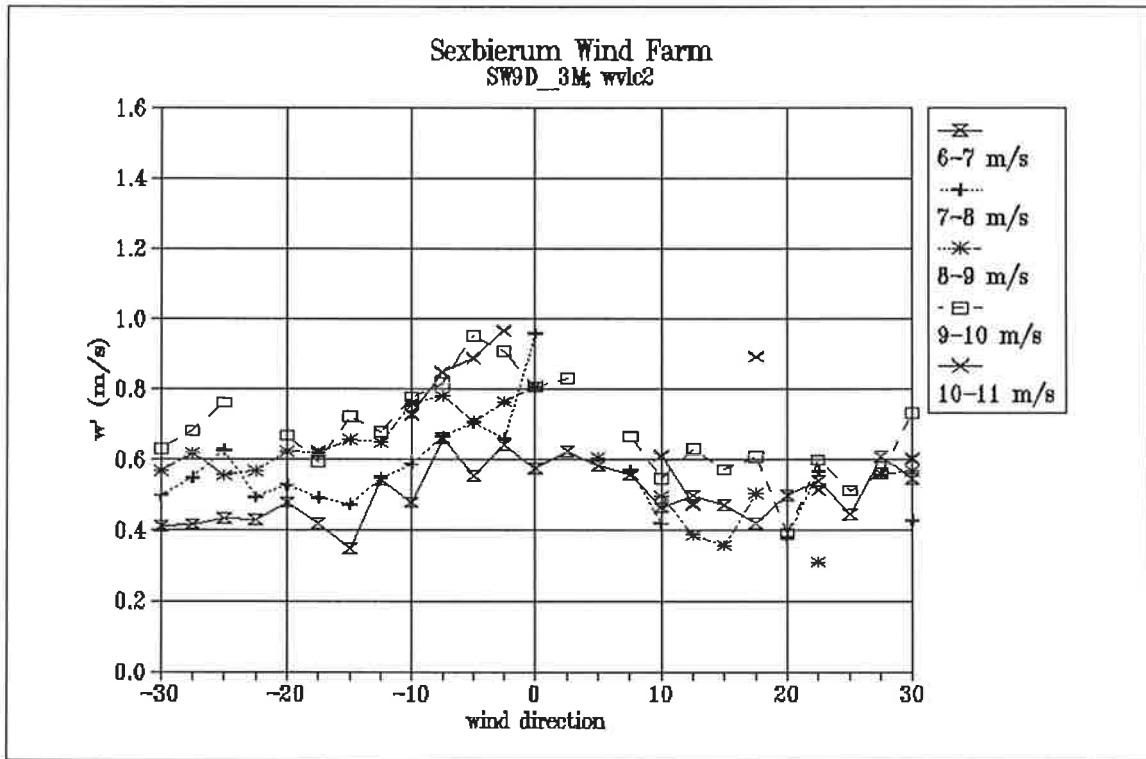


Figure 7 Vertical turbulent fluctuations  $w'$  as a function of wind direction and wind speed bin

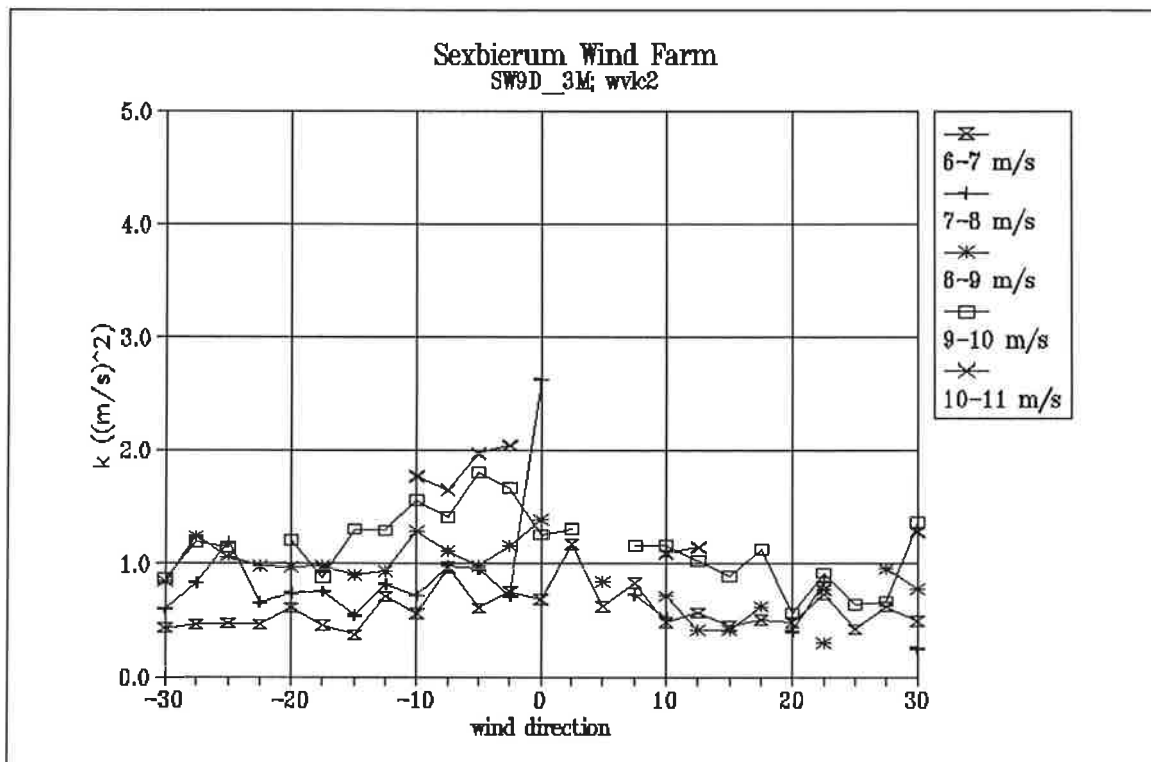


Figure 8 Turbulent kinetic energy per unit mass as a function of wind direction and wind speed bin

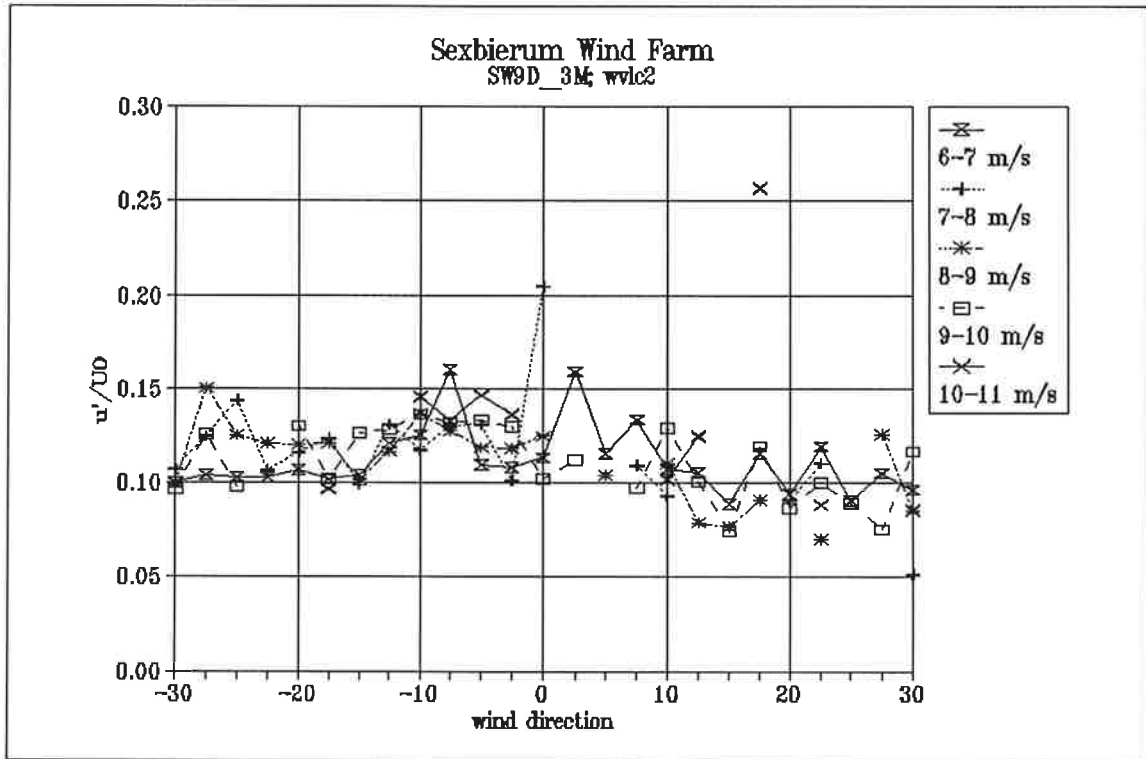


Figure 9 Non-dimensionalized longitudinal turbulent fluctuations  $u'/U_0$  as a function of wind direction and wind speed bin

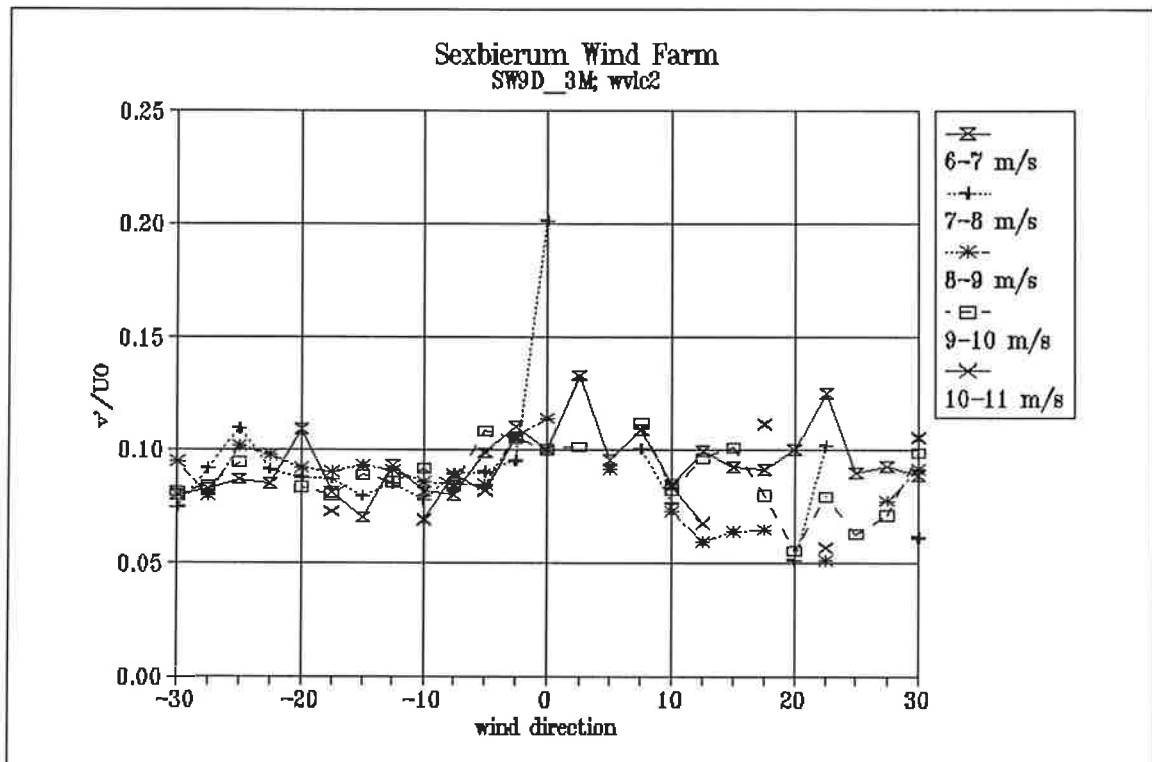


Figure 10 Non-dimensionalized lateral turbulent fluctuations  $v'/U_0$  as a function of wind direction and wind speed bin

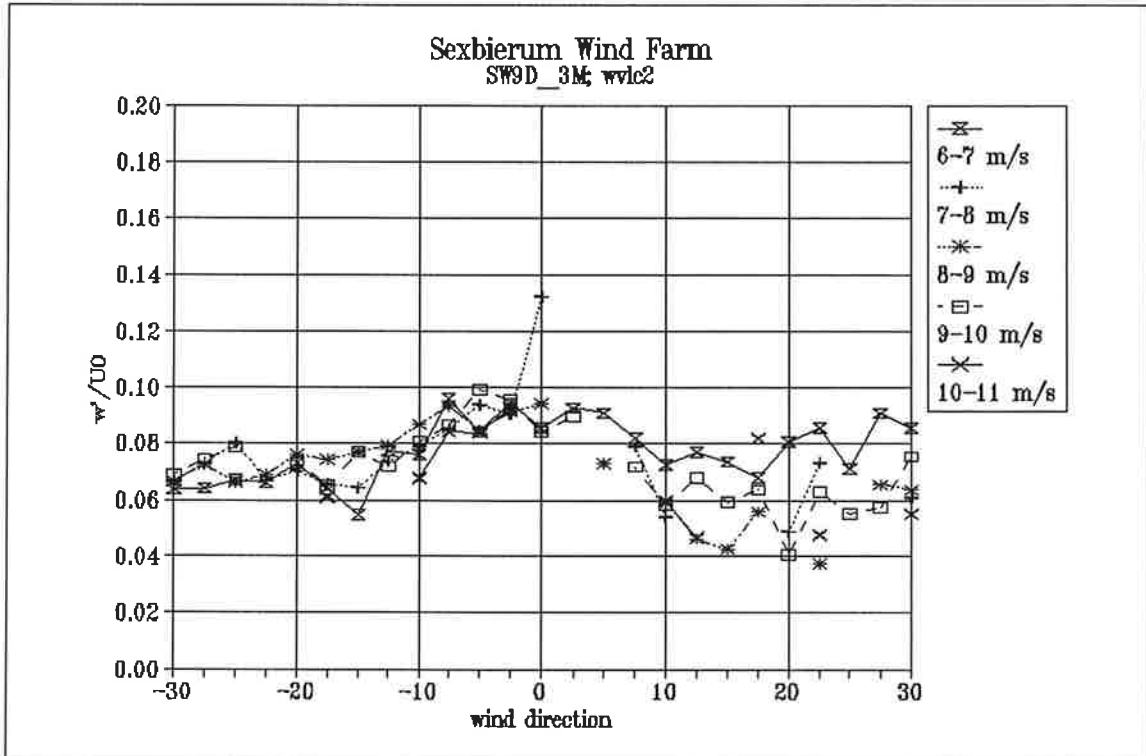


Figure 11 Non-dimensionalized vertical turbulent fluctuations  $w'/U_0$  as a function of wind direction and wind speed bin

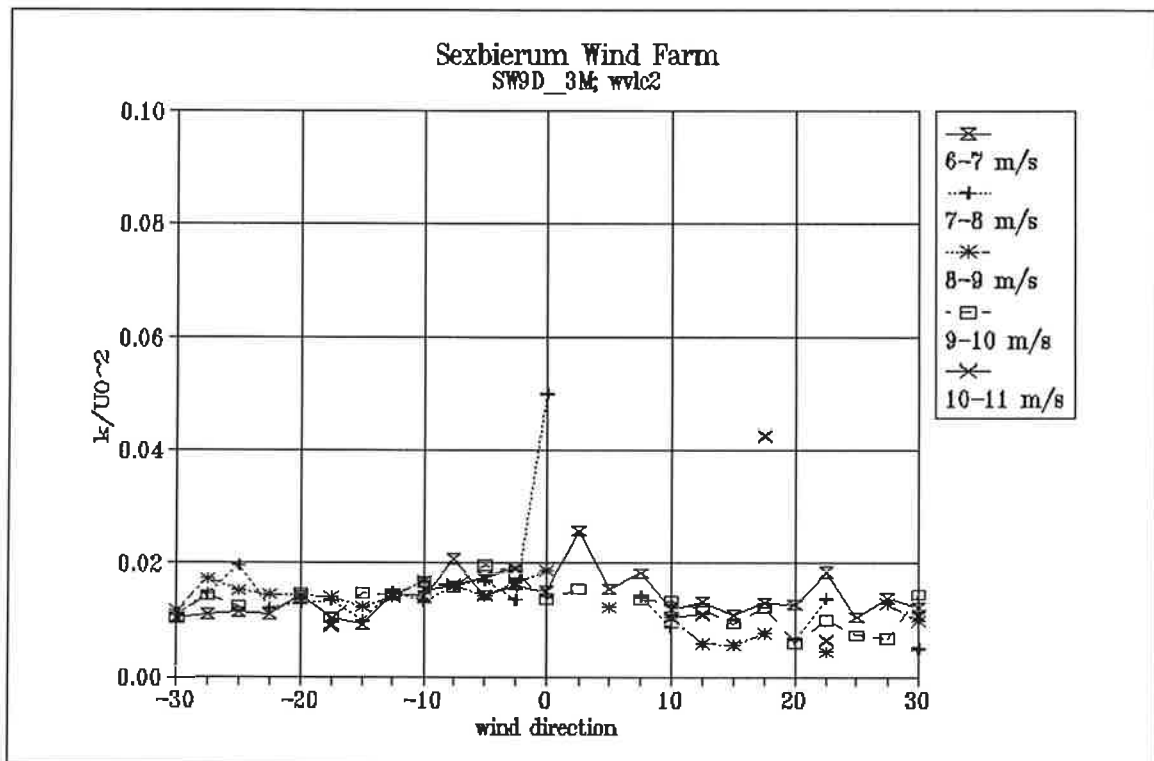


Figure 12 Non-dimensionalized turbulent kinetic energy  $k/U_0^2$  as a function of wind direction and wind speed bin

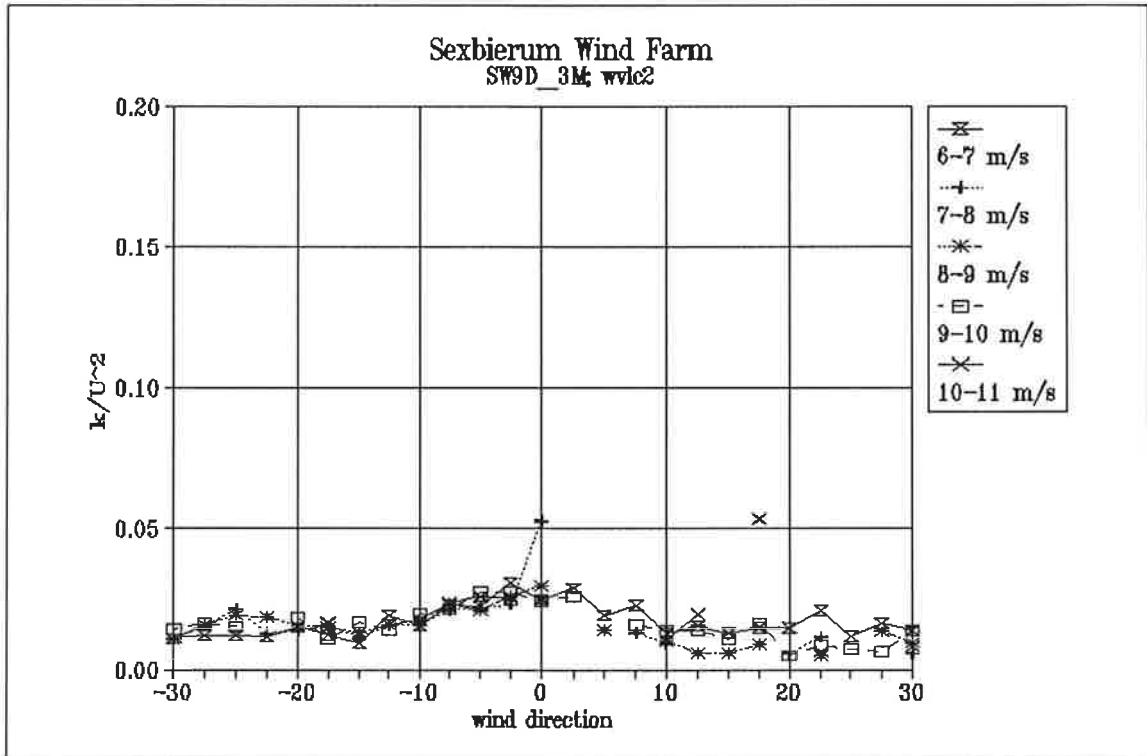


Figure 13 Non-dimensionalized turbulent kinetic energy  $k/U^2$  as a function of wind direction and wind speed bin

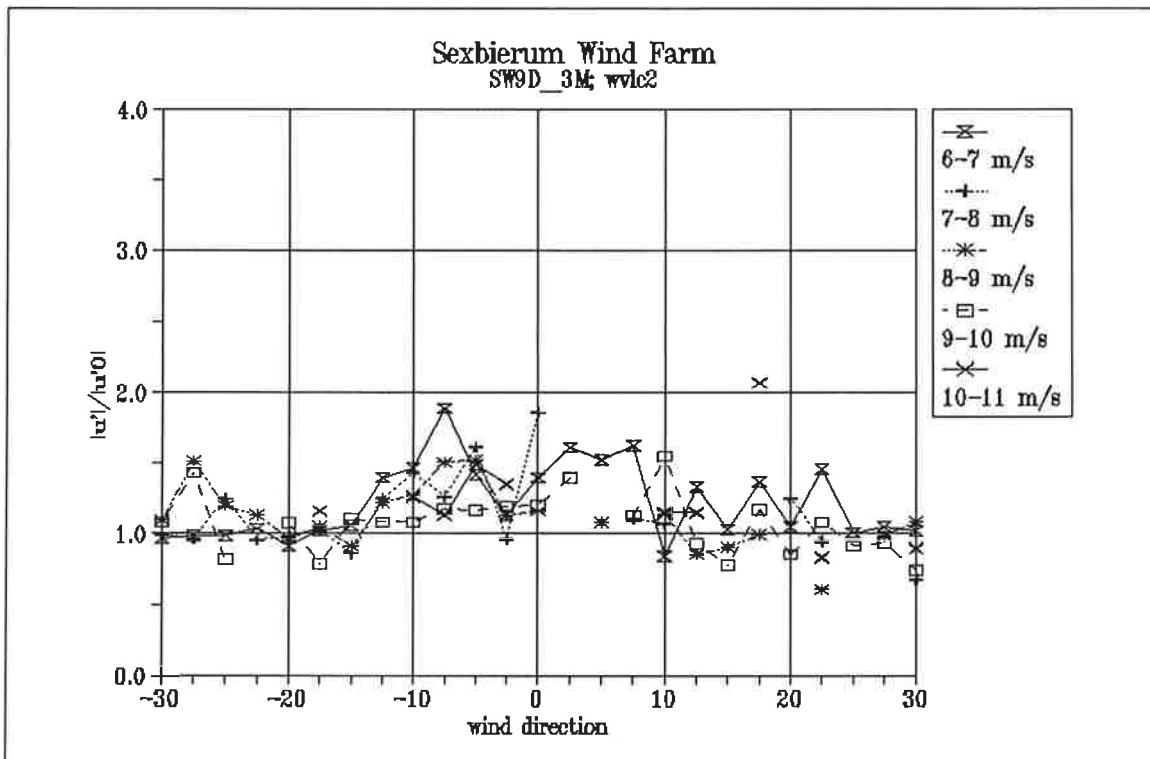


Figure 14 Longitudinal turbulence enhancement  $u^2/u_0'$  as a function of wind direction and wind speed bin

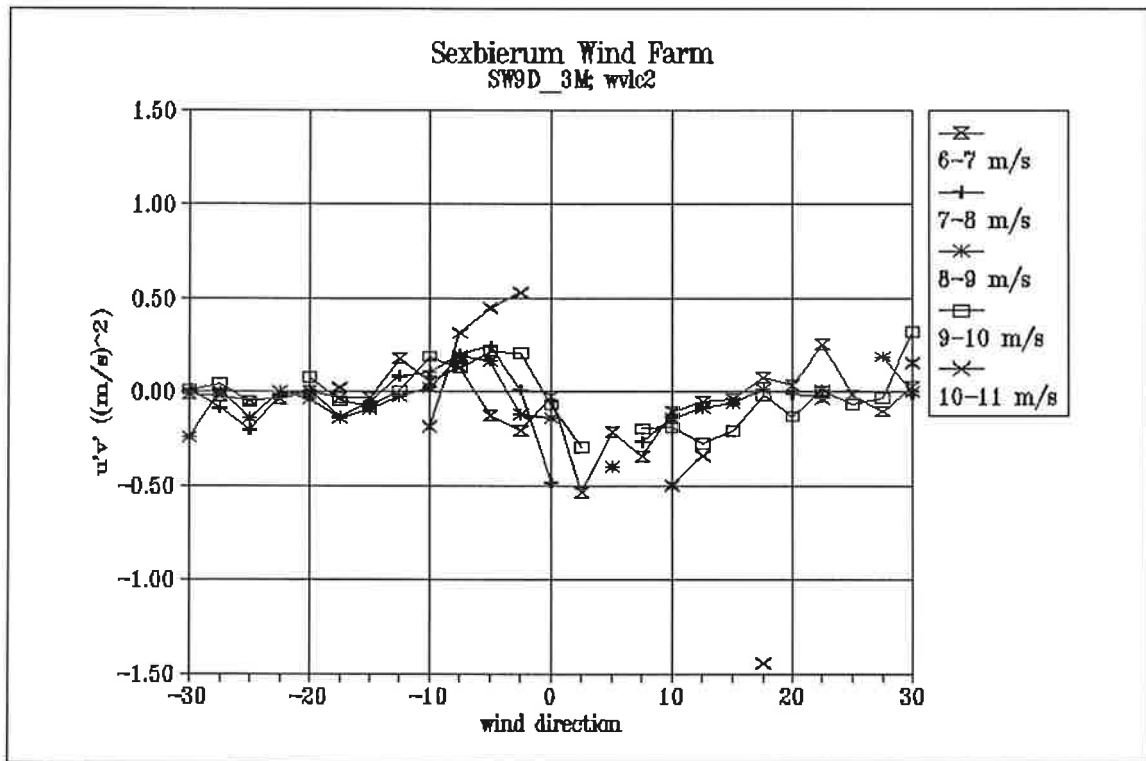


Figure 15 Shear stress  $u'v'$  as a function of wind direction and wind speed bin

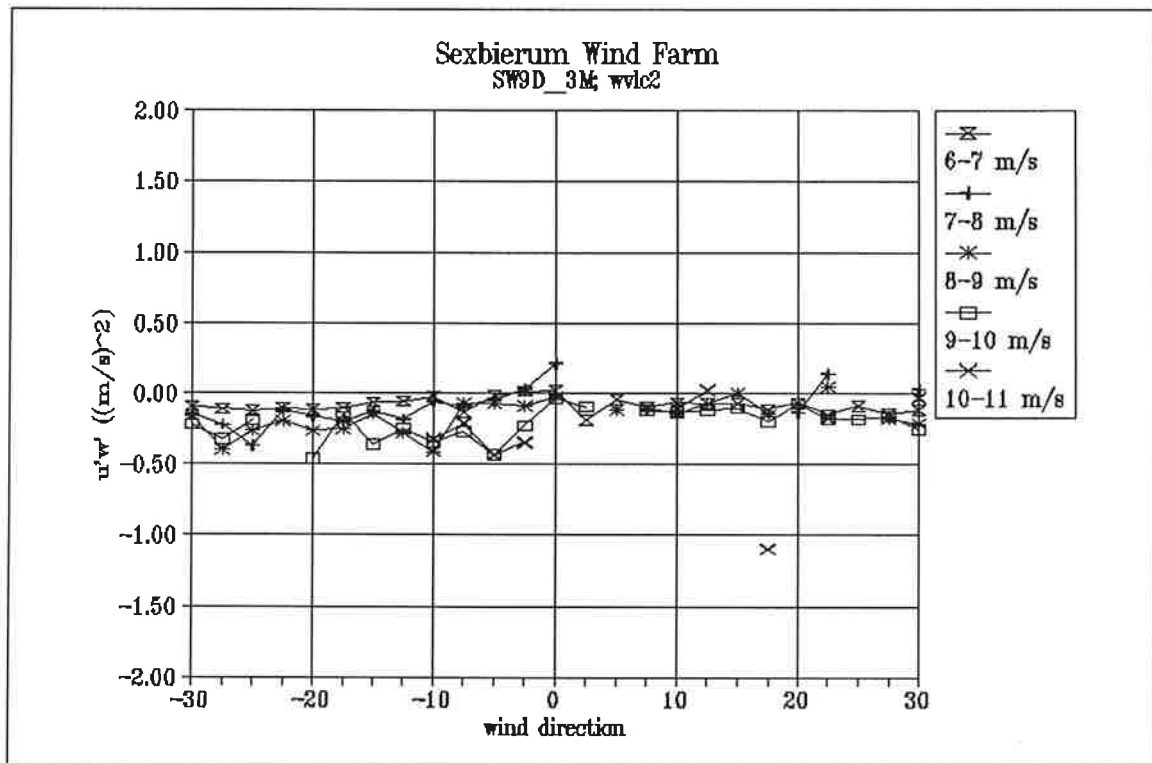


Figure 16 Shear stress  $u'w'$  as a function of wind direction and wind speed bin

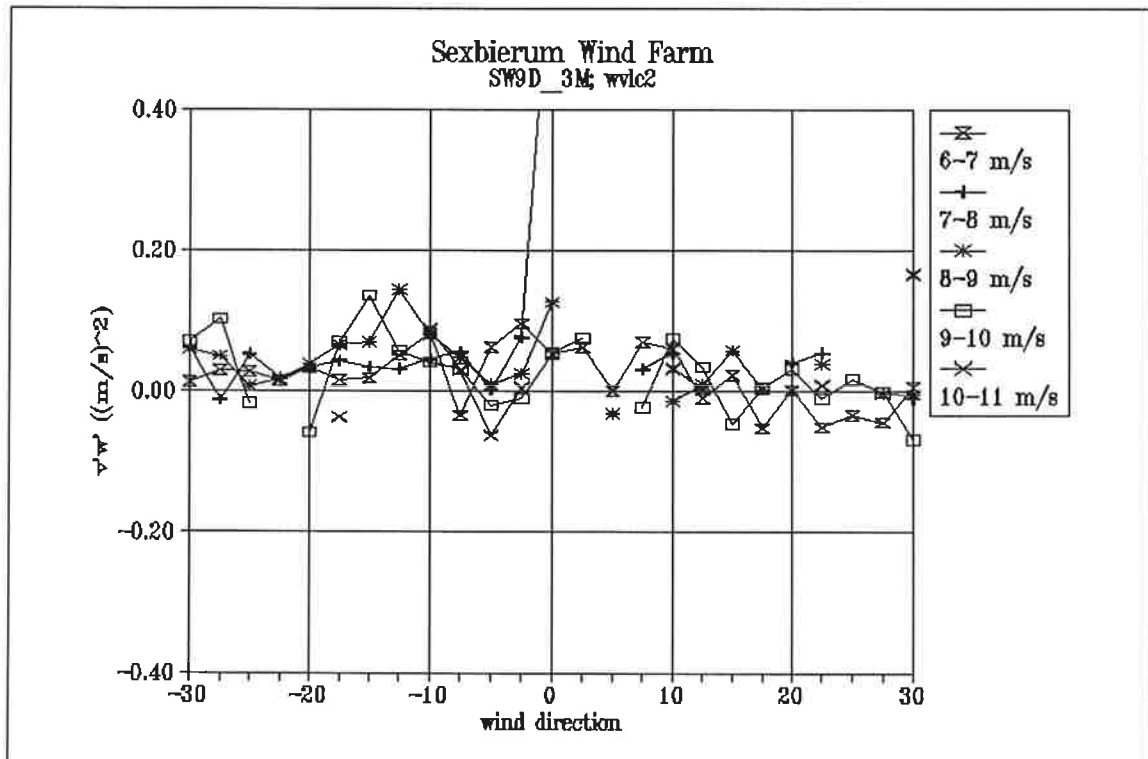


Figure 17 Shear stress  $v'w'$  as a function of wind direction and wind speed bin

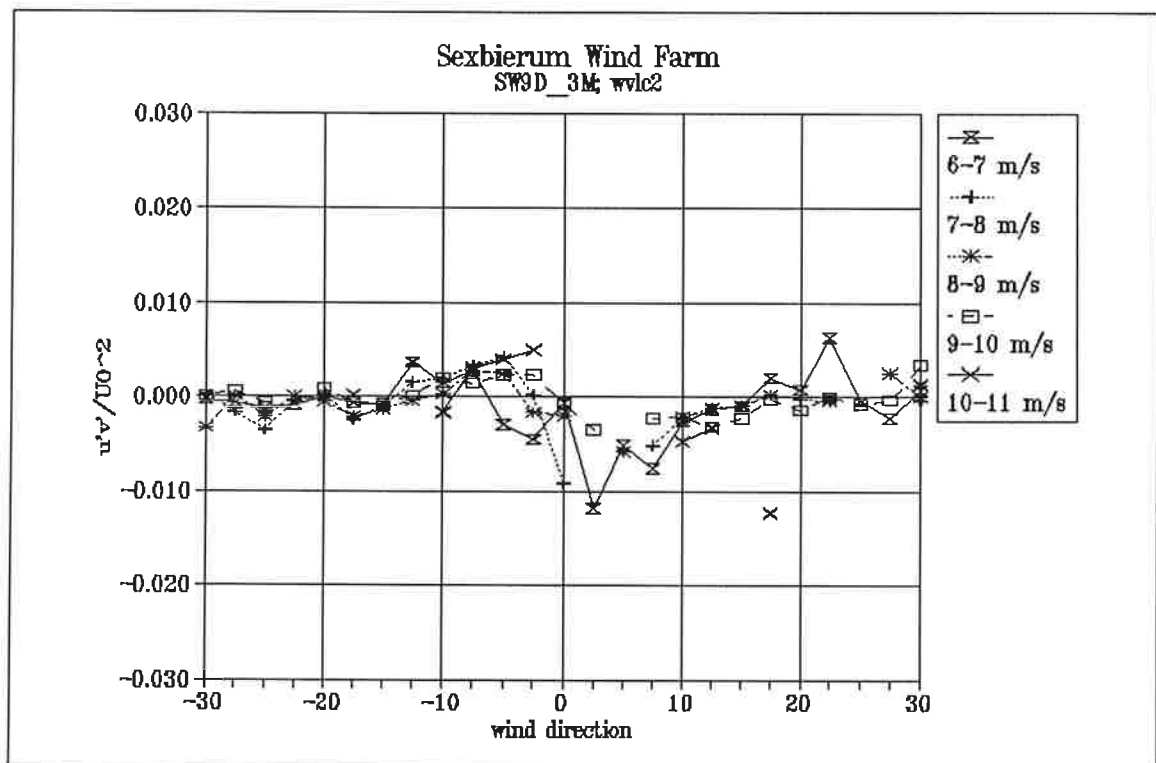


Figure 18 Non-dimensionalized shear stress  $u'v'/U_0^2$  as a function of wind direction and wind speed bin

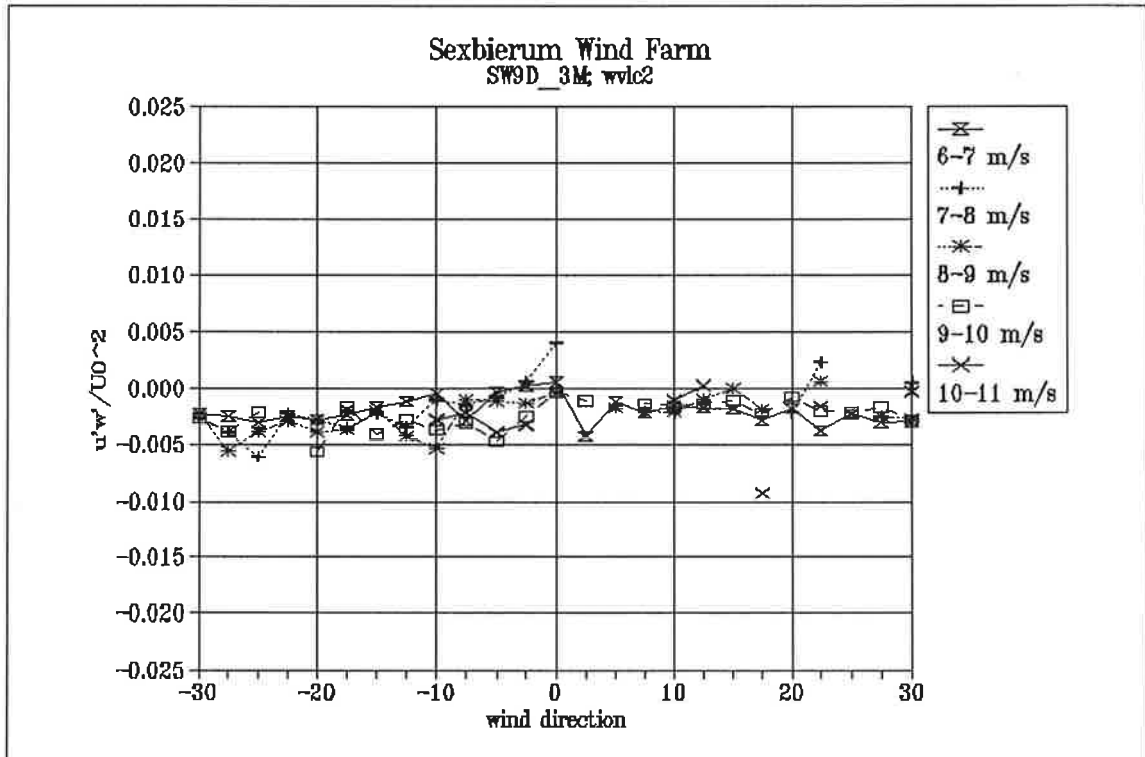


Figure 19 Non-dimensionalized shear stress  $u'w'/U_0^2$  as a function of wind direction and wind speed bin

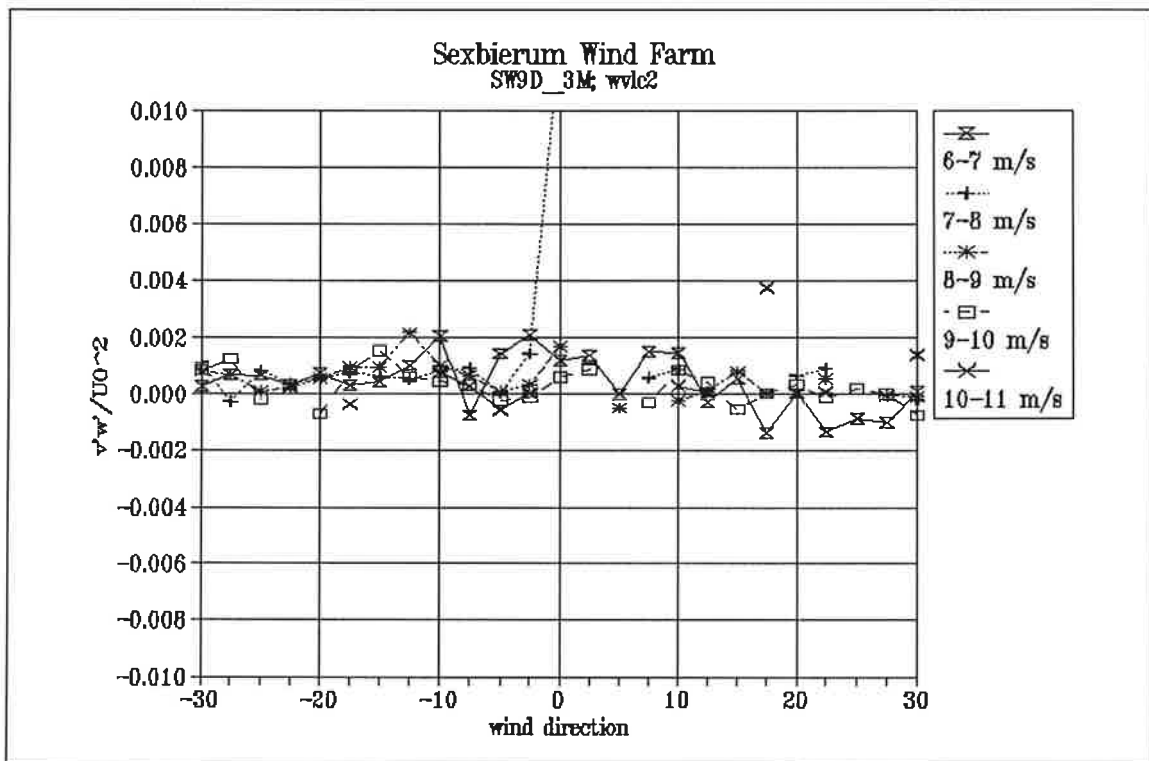


Figure 20 Non-dimensionalized shear stress  $v'w'/U_0^2$  as a function of wind direction and wind speed bin

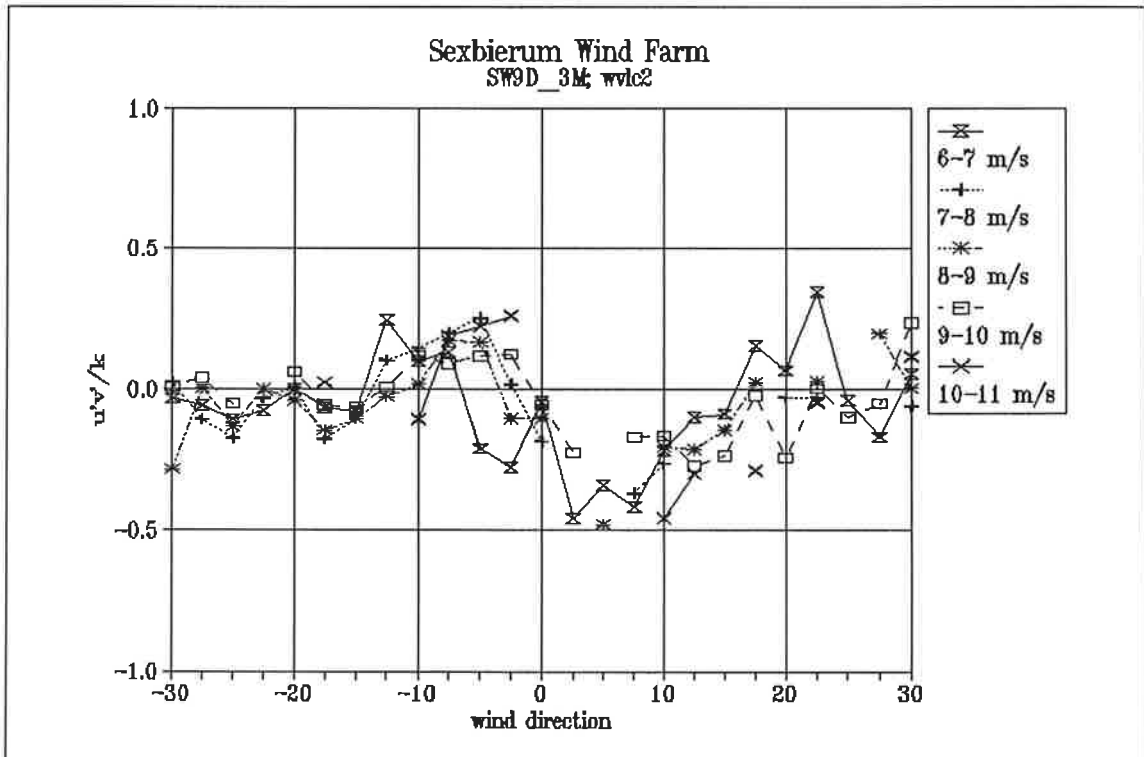


Figure 21 Non-dimensionalized shear stress  $u'v'/k$  as a function of wind direction and wind speed bin

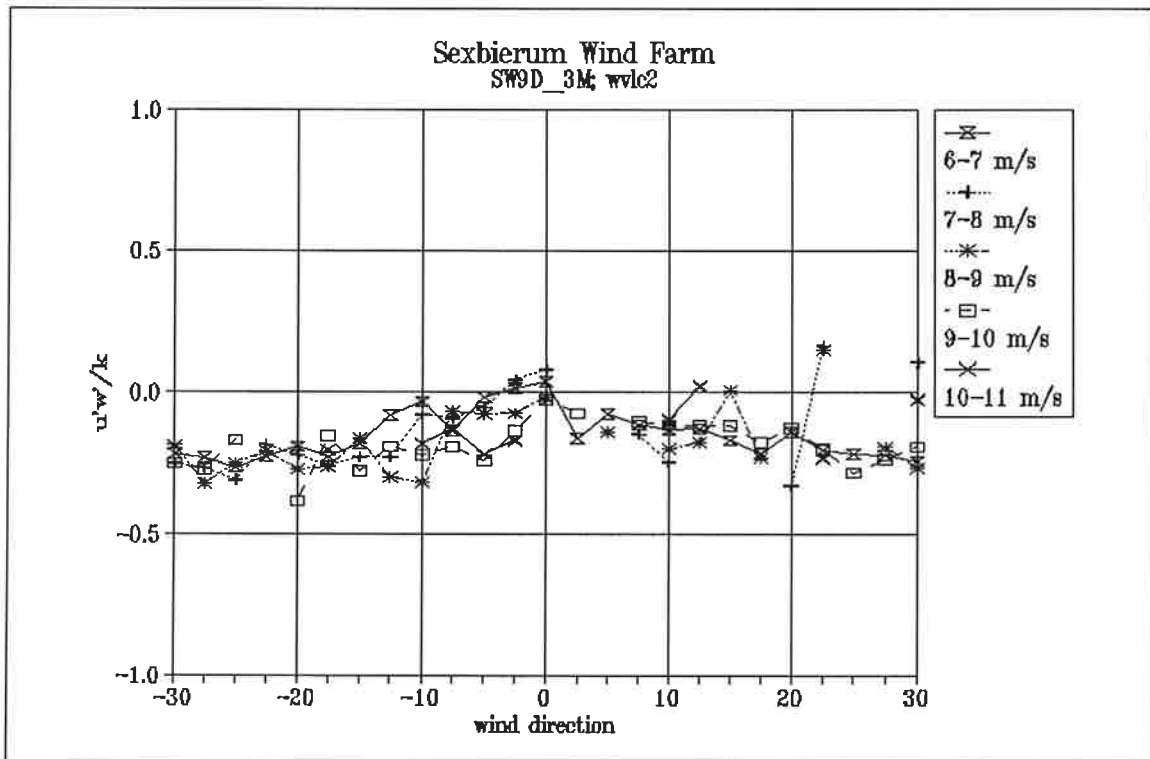


Figure 22 Non-dimensionalized shear stress  $u'w'/k$  as a function of wind direction and wind speed bin



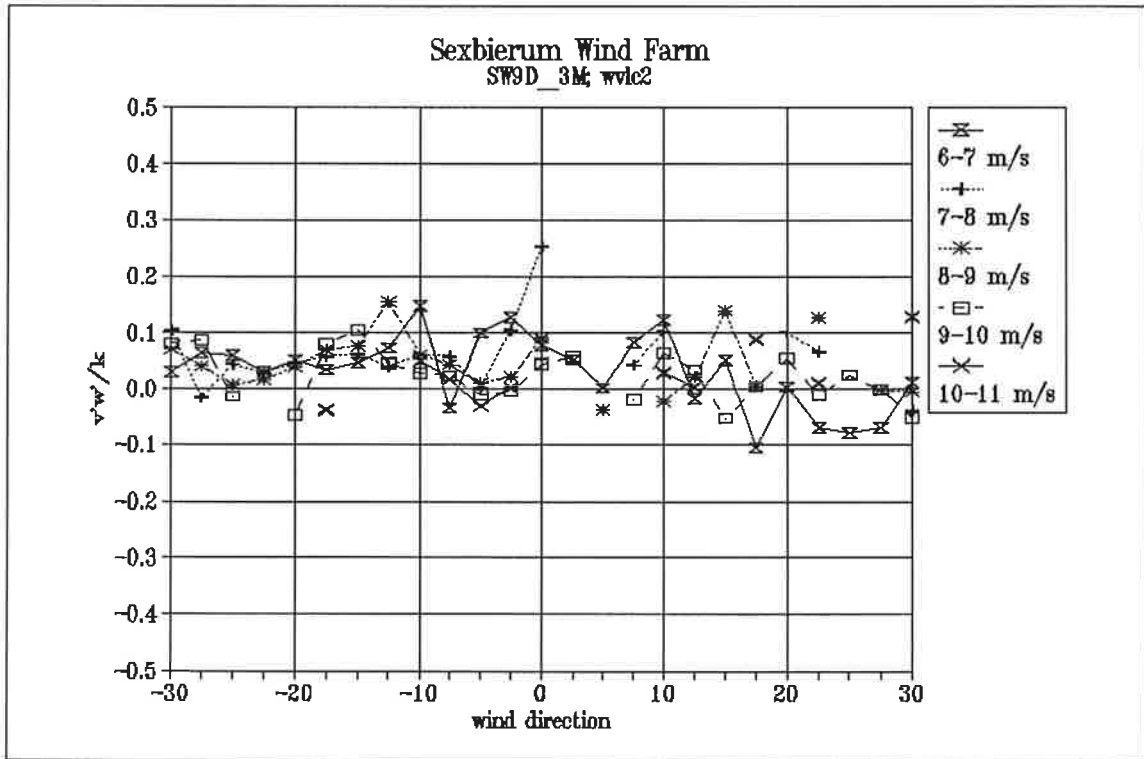


Figure 23 Non-dimensionalized shear stress  $v'w'/k$  as a function of wind direction and wind speed bin

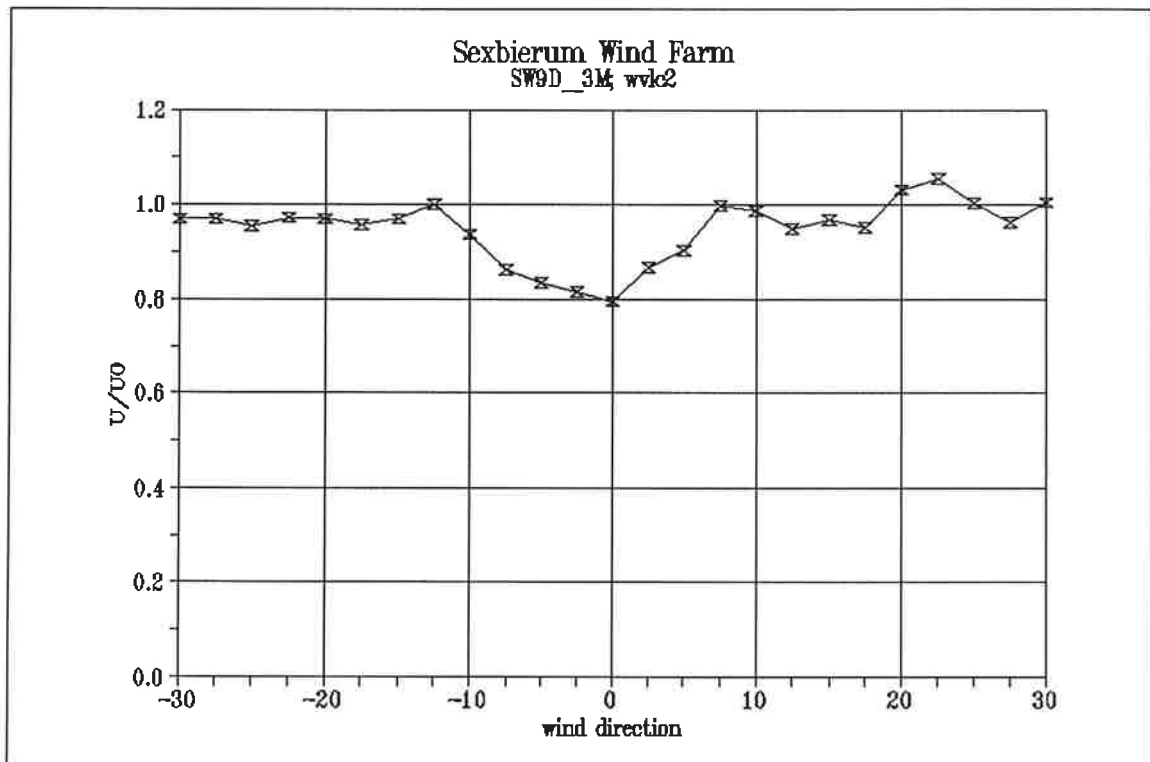


Figure 24 Wake deficit  $U/U_0$  as a function of wind direction in the wind speed bin 5-10 m/s

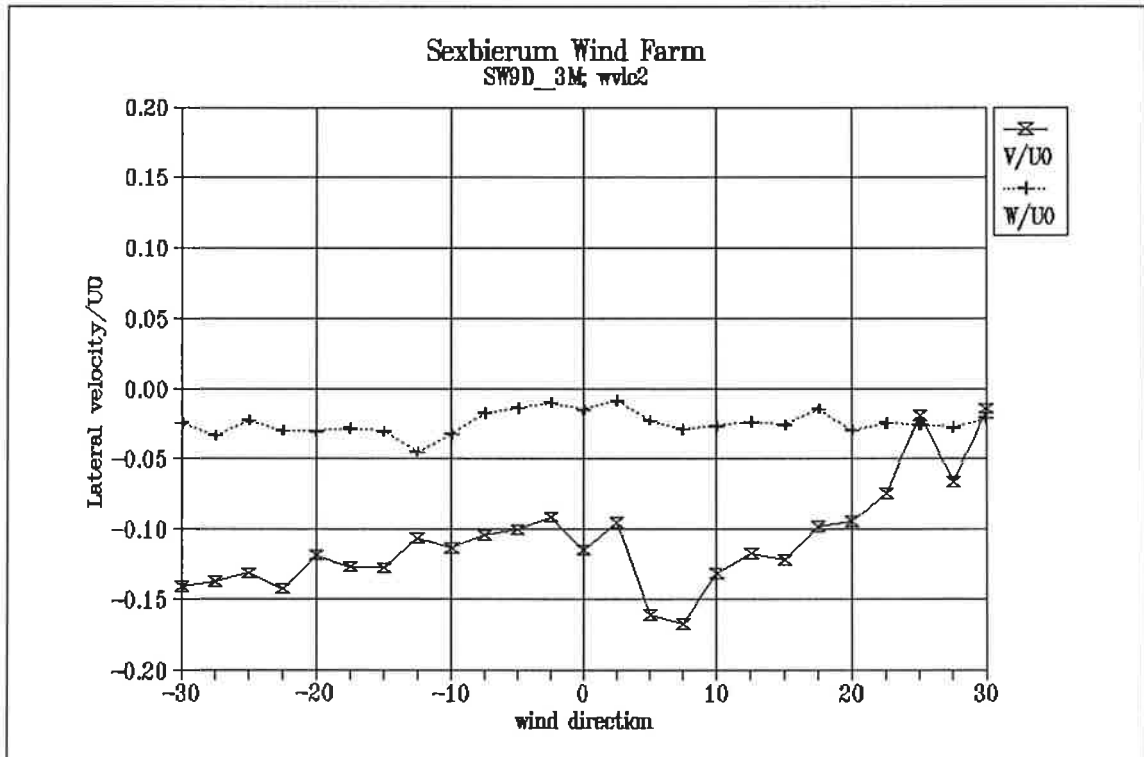


Figure 25 Lateral and vertical wind speed  $V/U_0$  and  $W/U_0$  as a function of wind direction in the wind speed bin 5-10 m/s

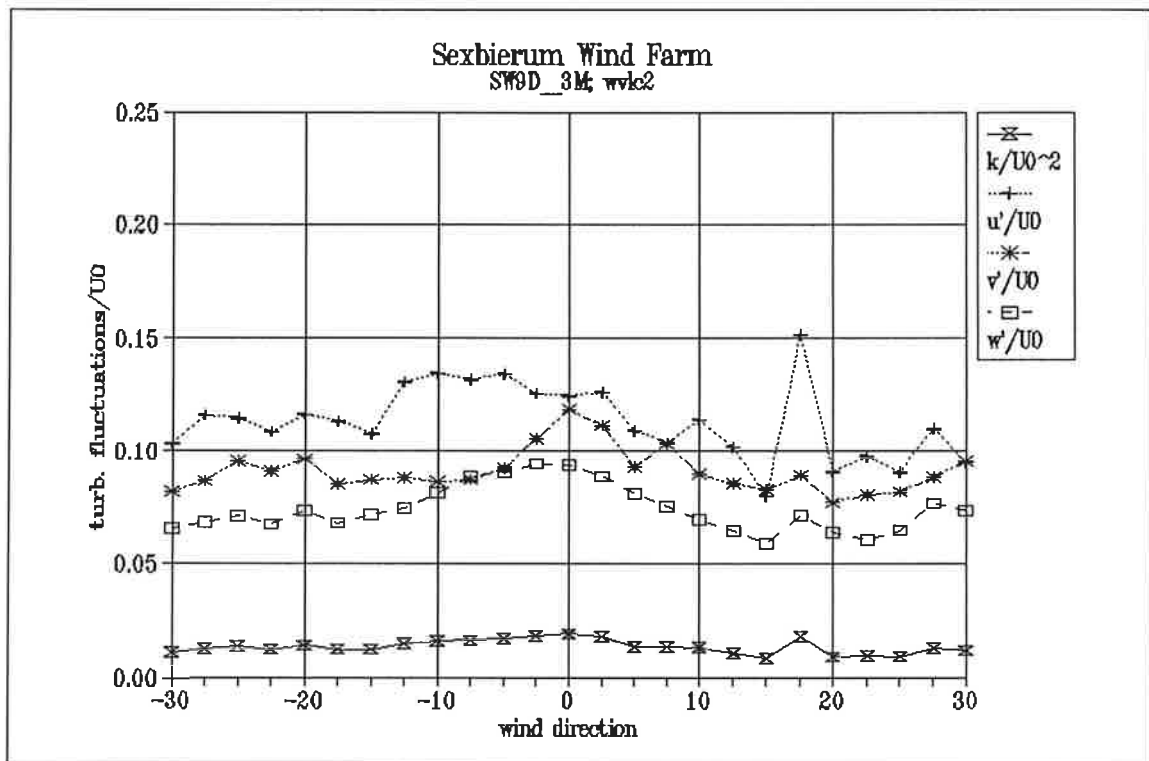


Figure 26 Turbulent fluctuations as a function of wind direction in the wind speed bin 5-10 m/s, non-dimensionalized with  $U_0$

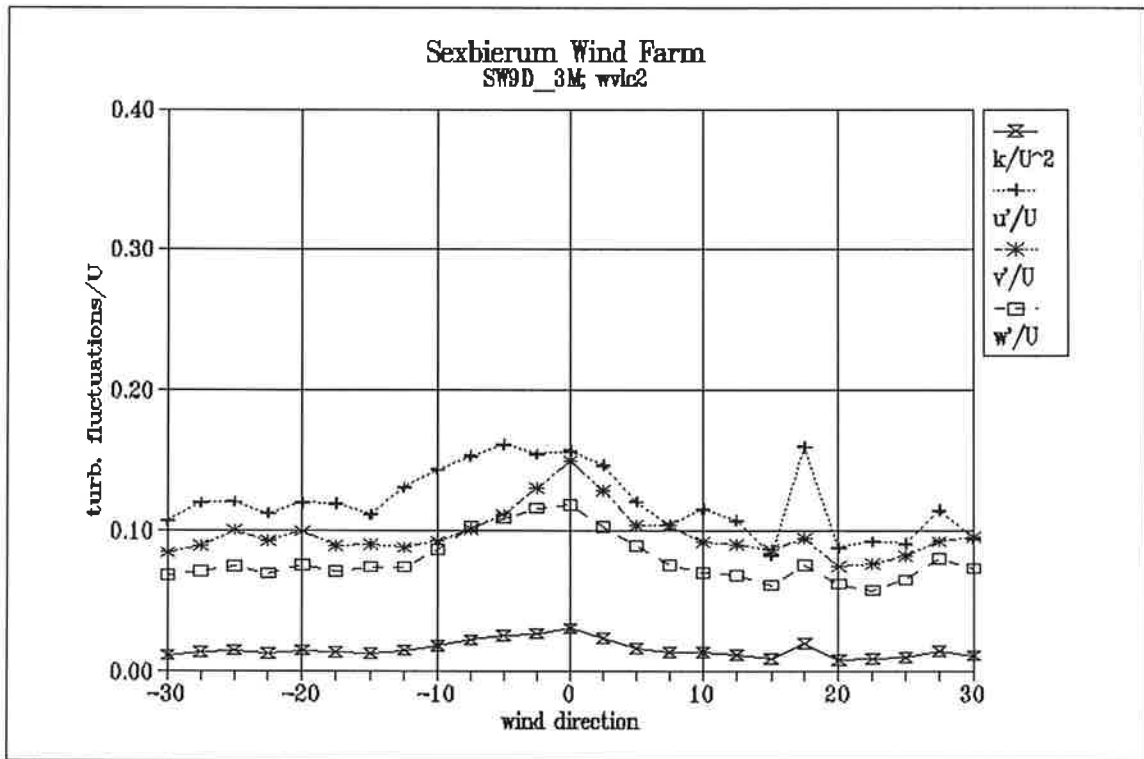


Figure 27 Turbulent fluctuations as a function of wind direction in the wind speed bin 5-10 m/s, non-dimensionalized with  $U$

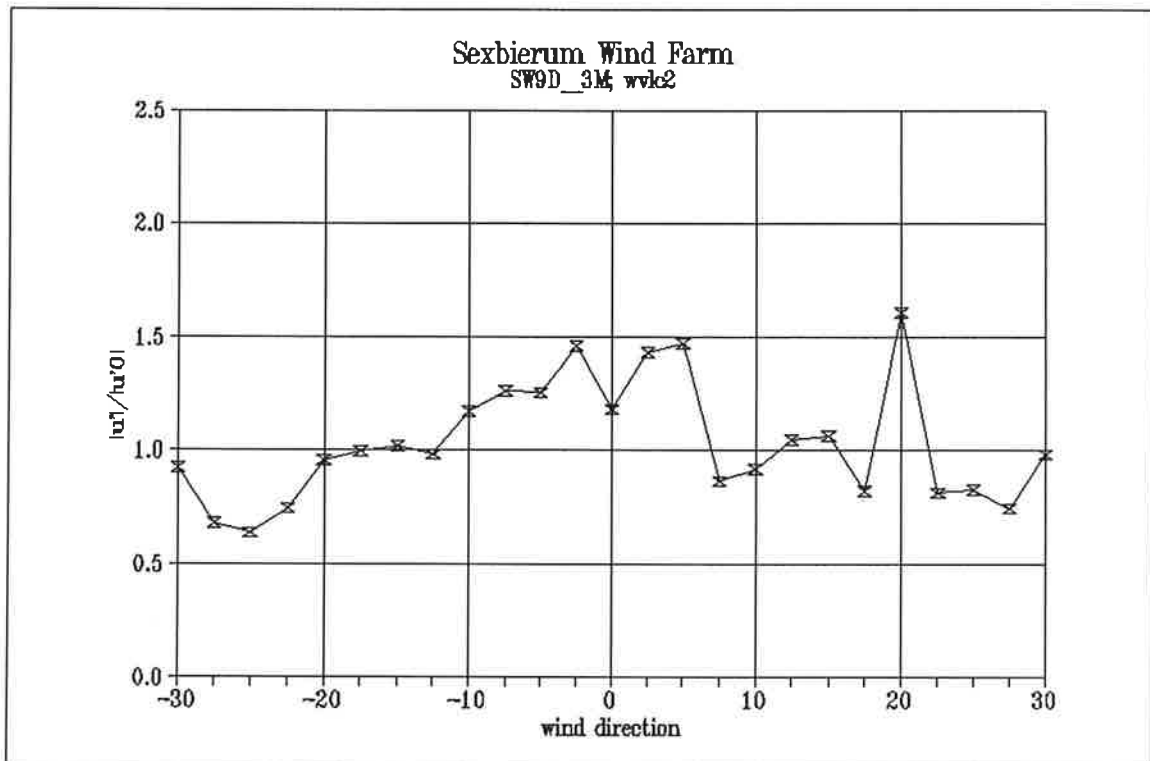


Figure 28 Longitudinal turbulence enhancement  $u'/u'_0$  as a function of wind direction in the wind speed bin 5-10 m/s

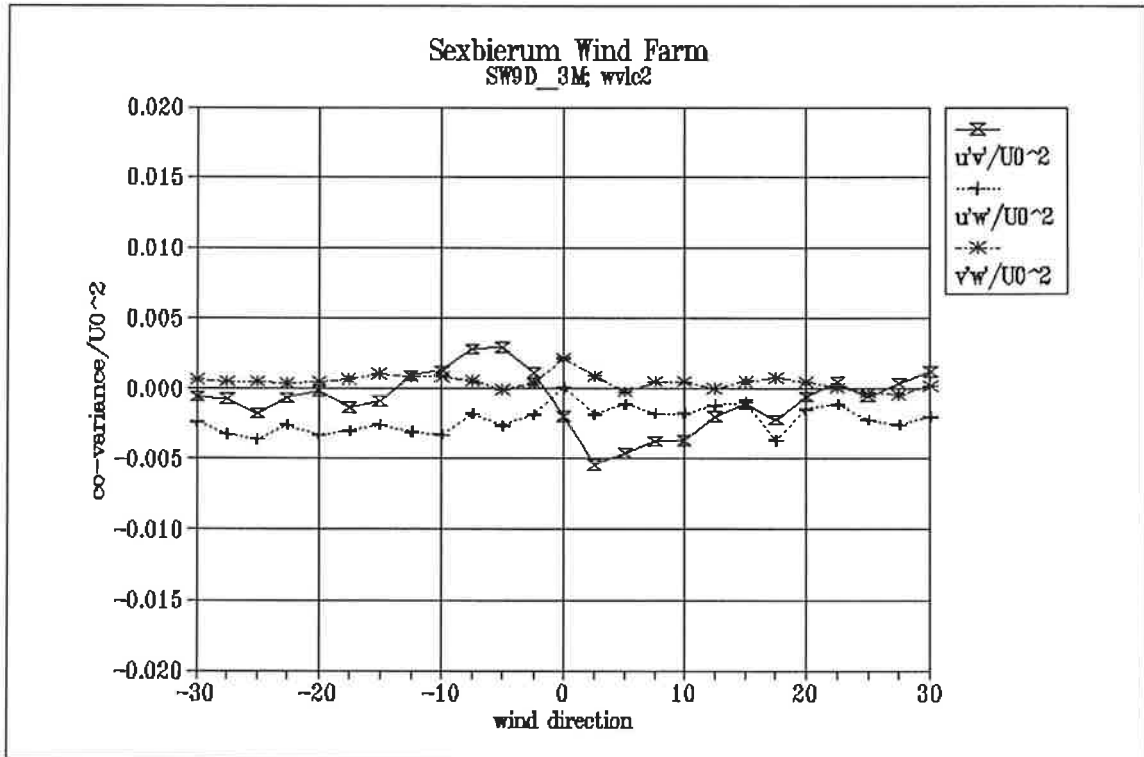


Figure 29 Non-dimensionalized shear stresses  $u'v'/U_0^2$ ;  $u'w'/U_0^2$ ;  $v'w'/U_0^2$  as a function of wind direction in the wind speed bin 5-10 m/s

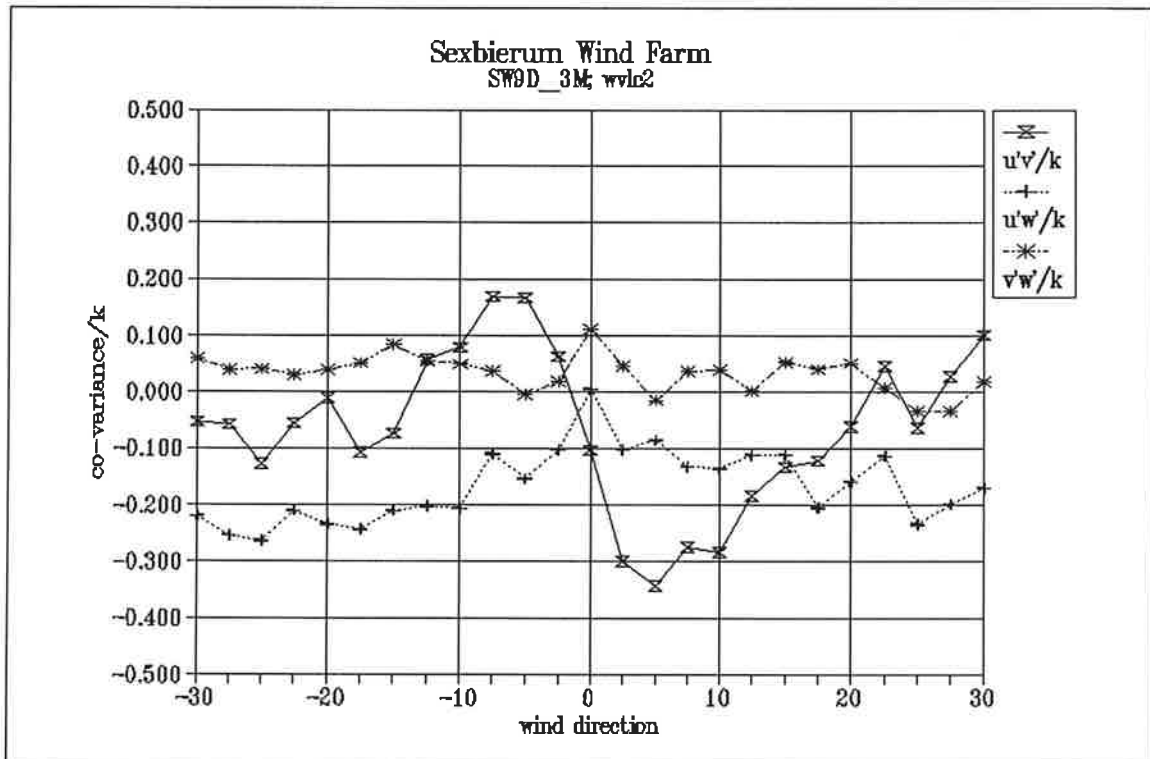


Figure 30 Non-dimensionalized shear stresses  $u'v'/k$ ;  $u'w'/k$ ;  $v'w'/k$  as a function of wind direction in the wind speed bin 5-10 m/s

## **A4.6 Vertical profiles**

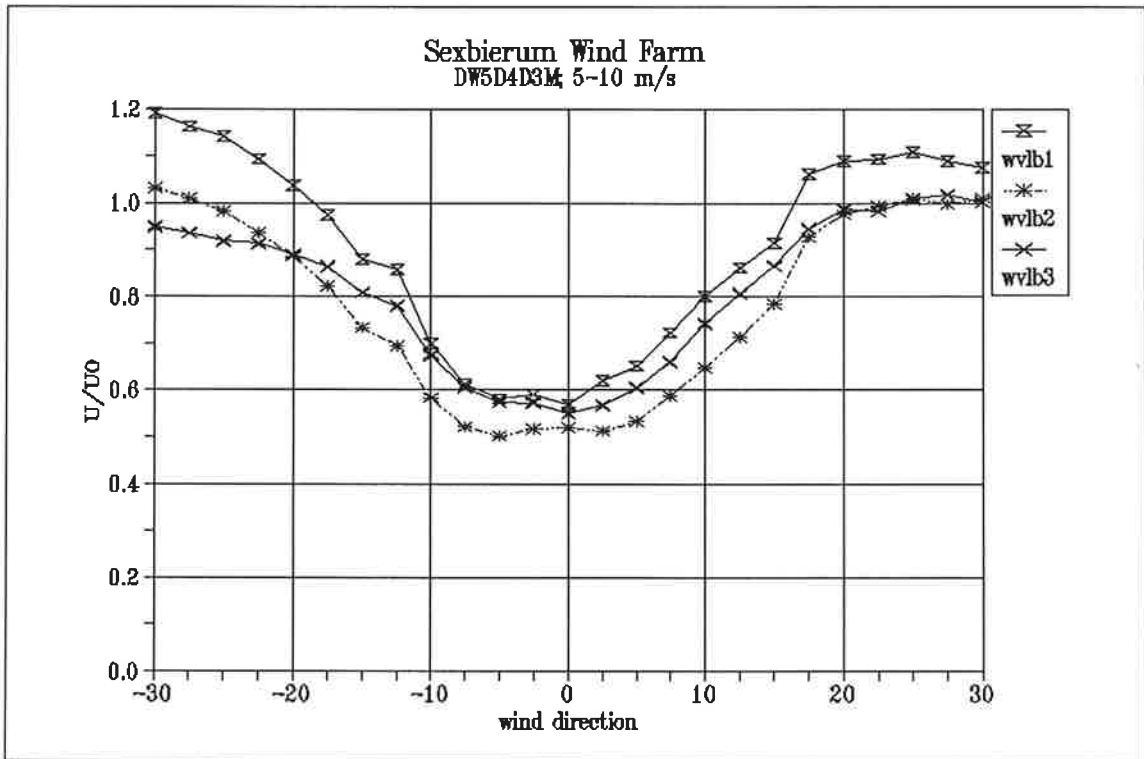


Figure 1 Wake deficit  $U/U_0$  as a function of wind direction in the wind speed bin 5-10 m/s

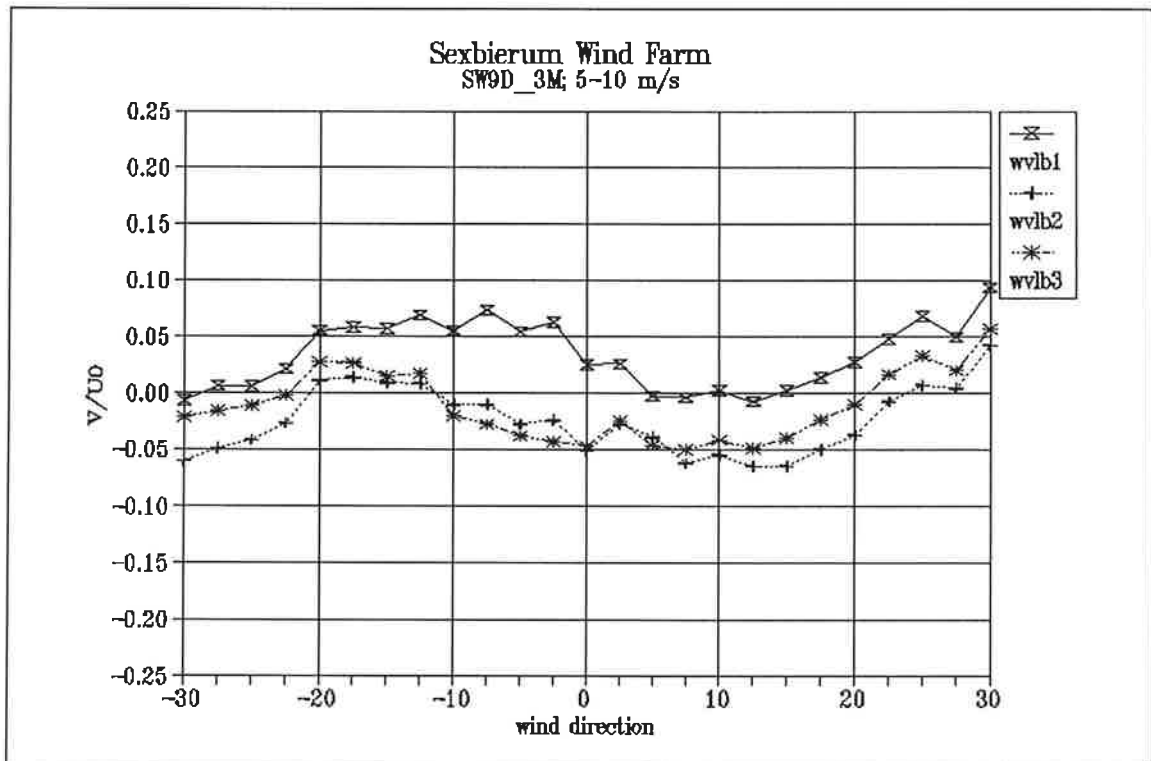


Figure 2 Lateral wind speed  $V/U_0$  as a function of wind direction in the wind speed bin 5-10 m/s

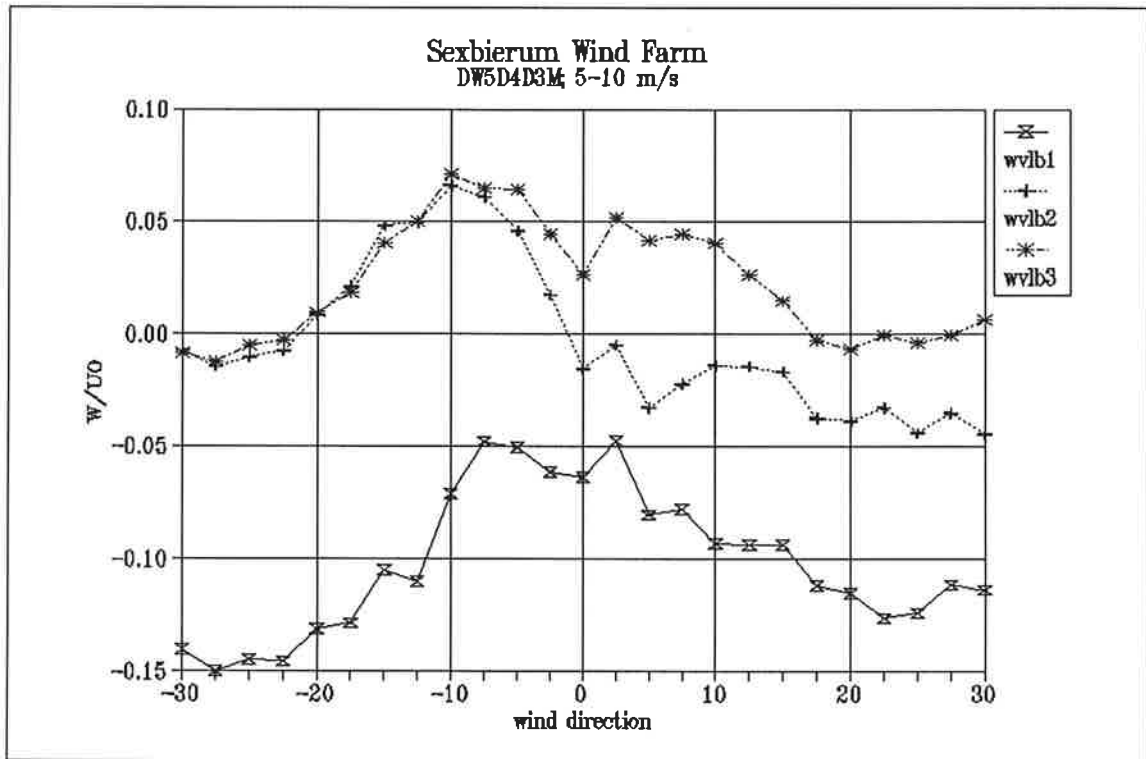


Figure 3 Vertical wind speed  $W/U_0$  as a function of wind direction in the wind speed bin 5-10 m/s

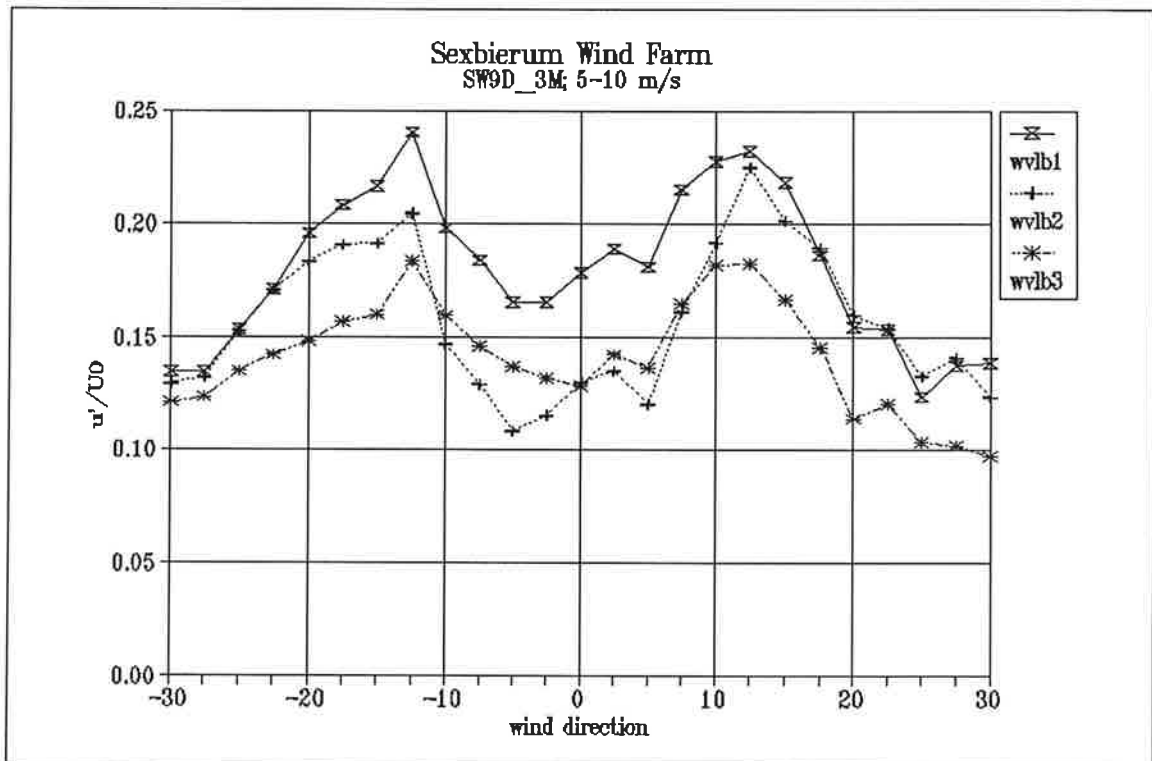


Figure 4 Non-dimensionalized longitudinal turbulent fluctuations  $u'/U_0$  as a function of wind direction in the wind speed bin 5-10 m/s

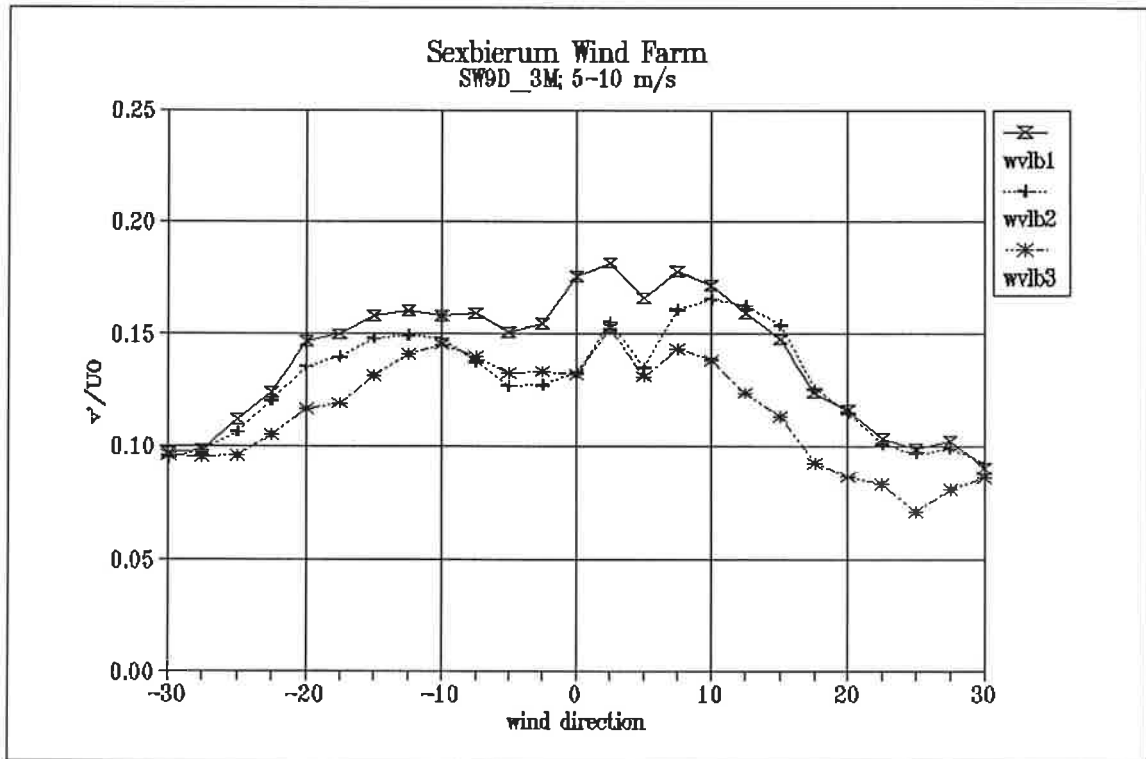


Figure 5 Non-dimensionalized lateral turbulent fluctuations  $v'/U_0$  as a function of wind direction in the wind speed bin 5-10 m/s

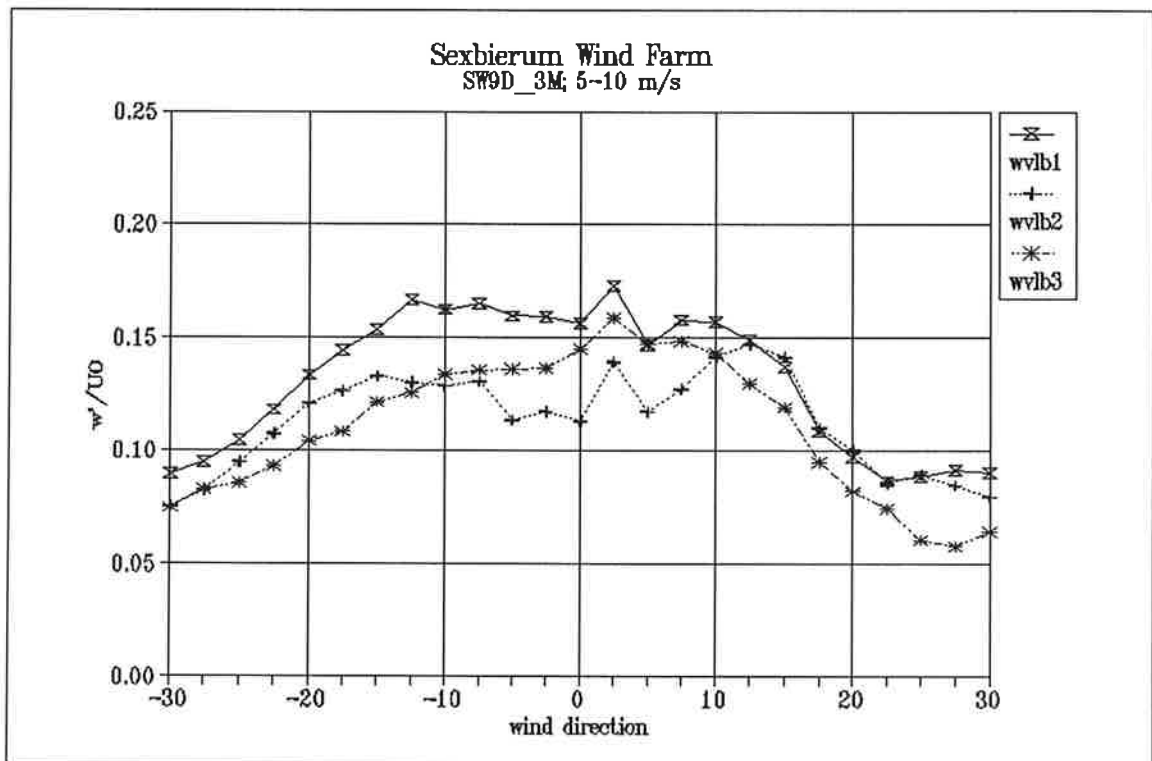


Figure 6 Non-dimensionalized vertical turbulent fluctuations  $w'/U_0$  as a function of wind direction in the wind speed bin 5-10 m/s



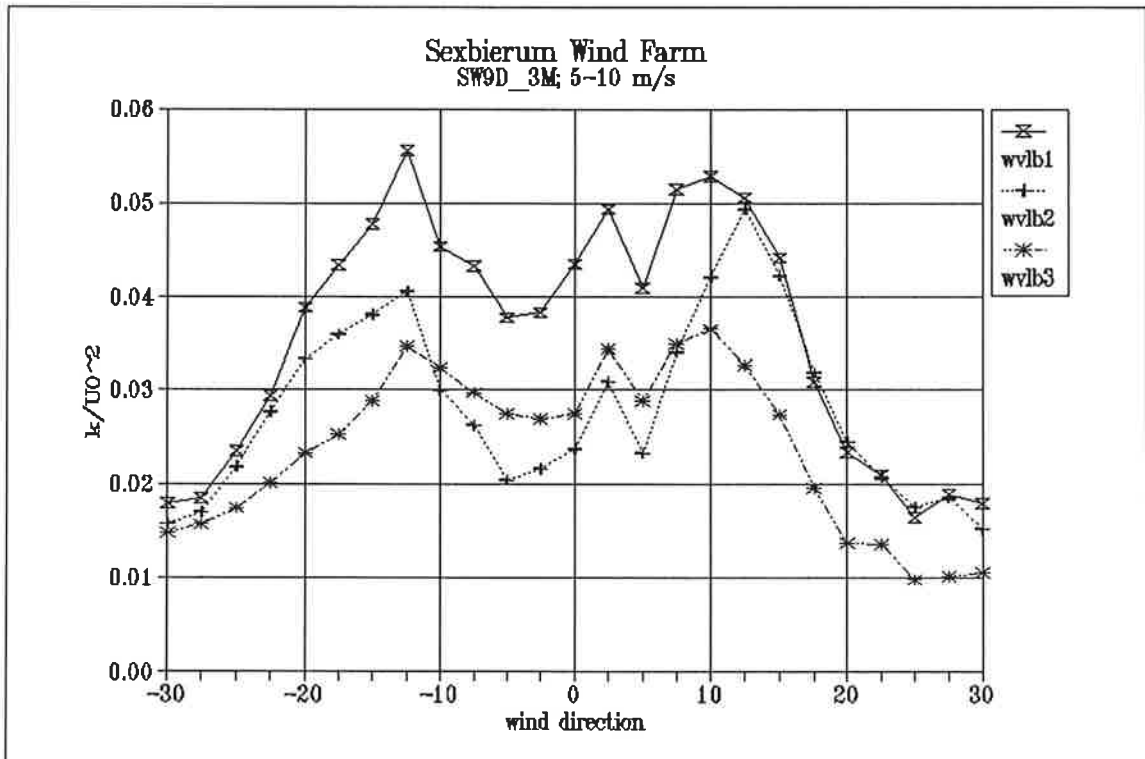


Figure 7 Non-dimensionalized turbulent kinetic energy  $k/U_0^2$  as a function of wind direction in the wind speed bin 5-10 m/s

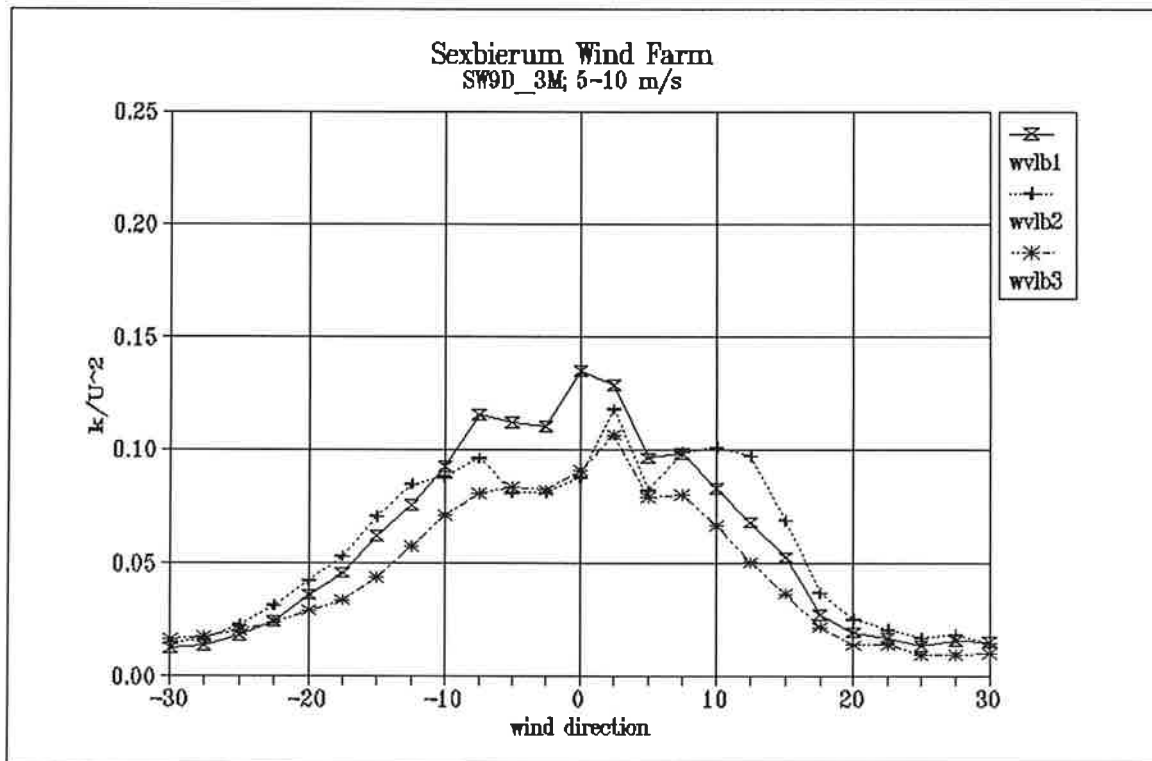


Figure 8 Non-dimensionalized turbulent kinetic energy  $k/U^2$  as a function of wind direction in the wind speed bin 5-10 m/s

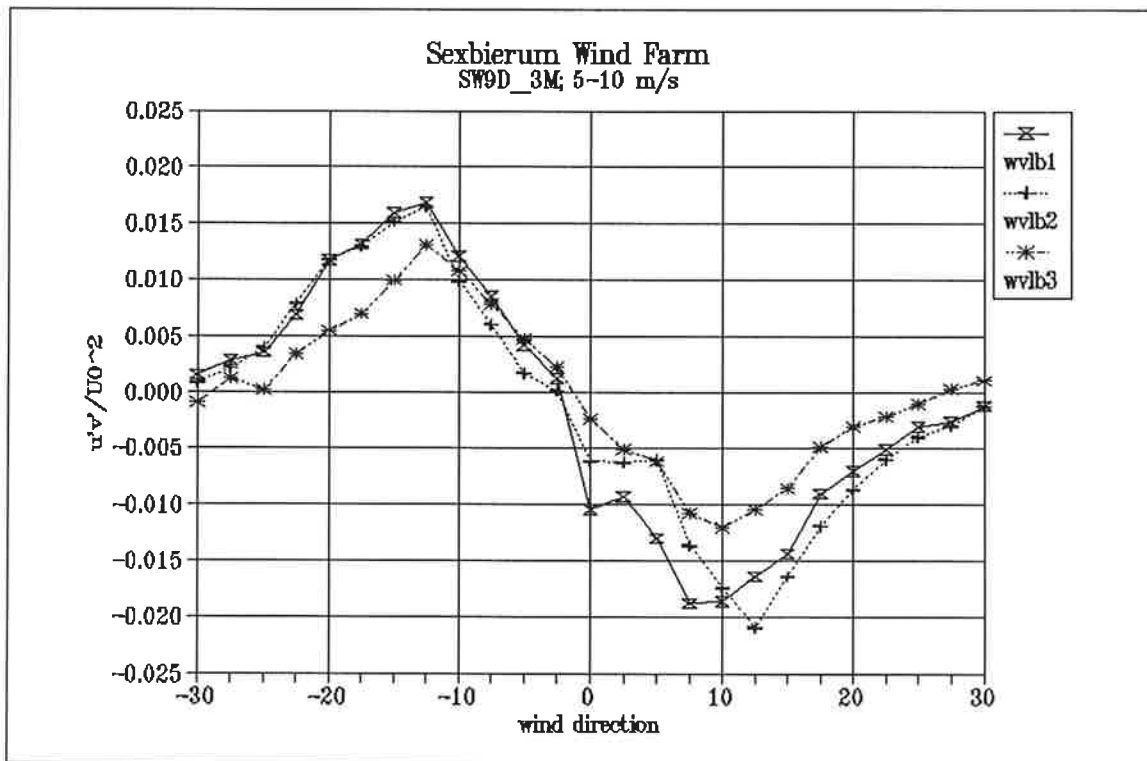


Figure 9 Non-dimensionalized shear stresses  $u'v'/U_0^2$  as a function of wind direction in the wind speed bin 5-10 m/s

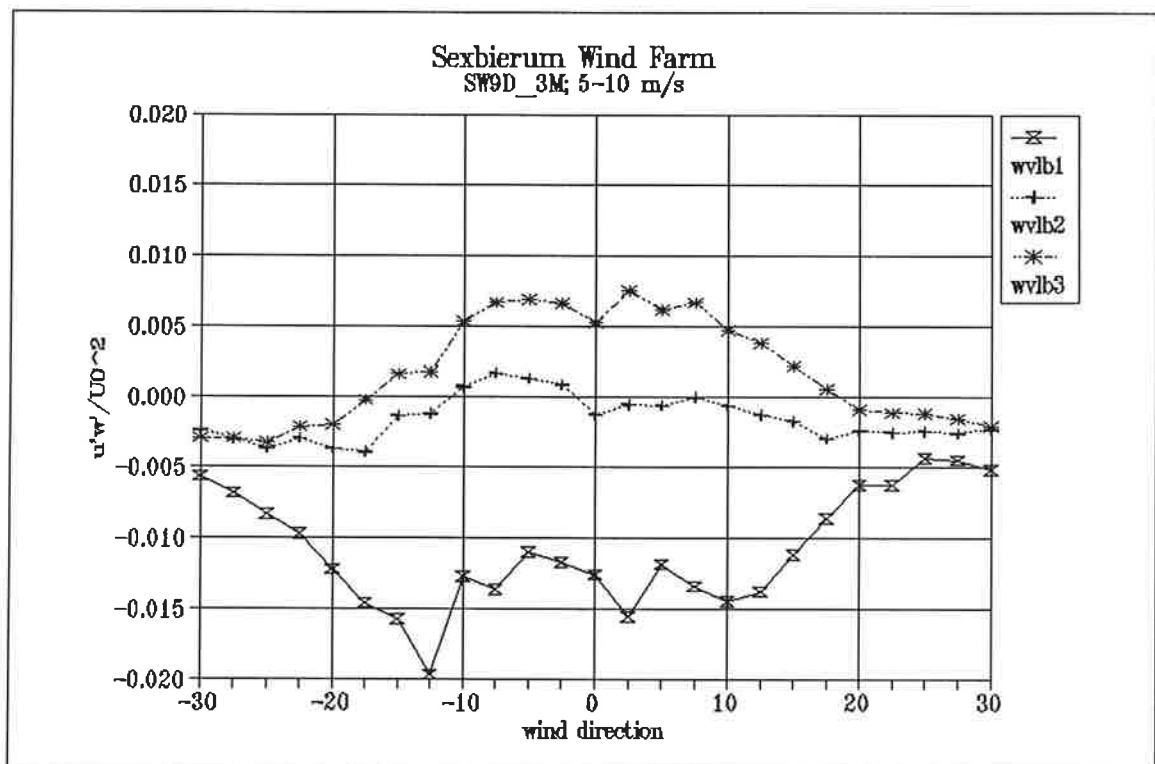


Figure 10 Non-dimensionalized shear stresses  $u'w'/U_0^2$  as a function of wind direction in the wind speed bin 5-10 m/s

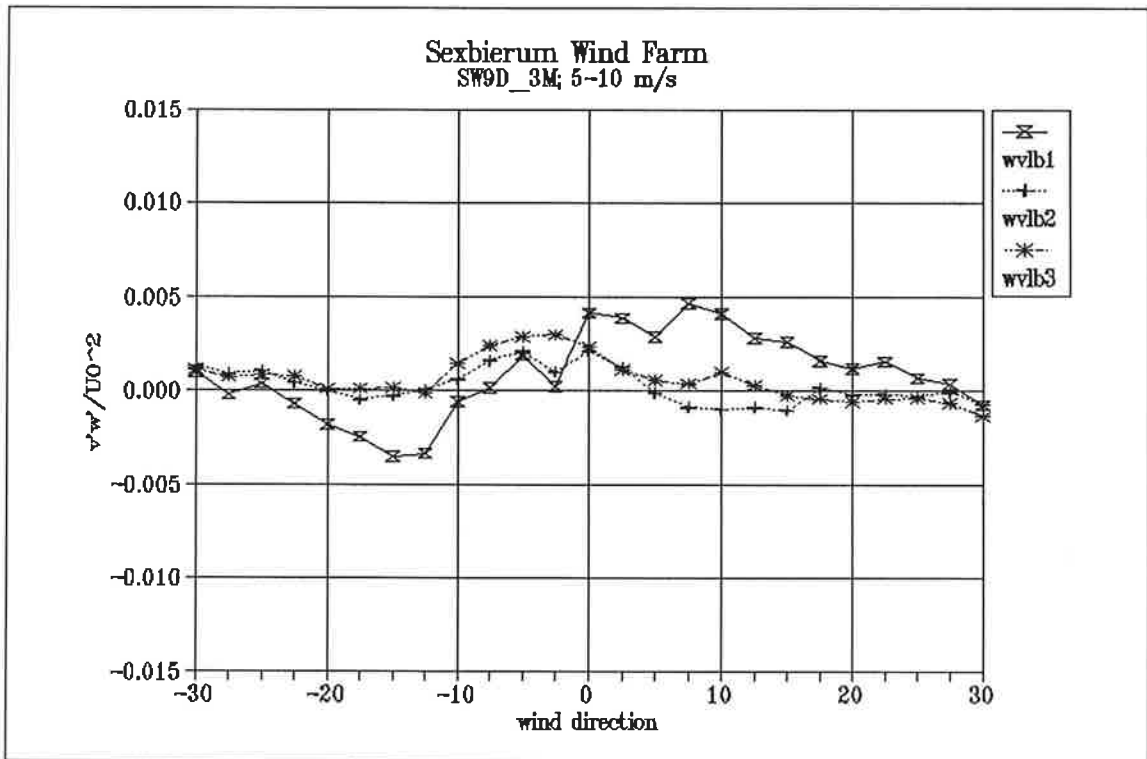


Figure 11 Non-dimensionalized shear stresses  $v'w'/U_0^2$  as a function of wind direction in the wind speed bin 5-10 m/s

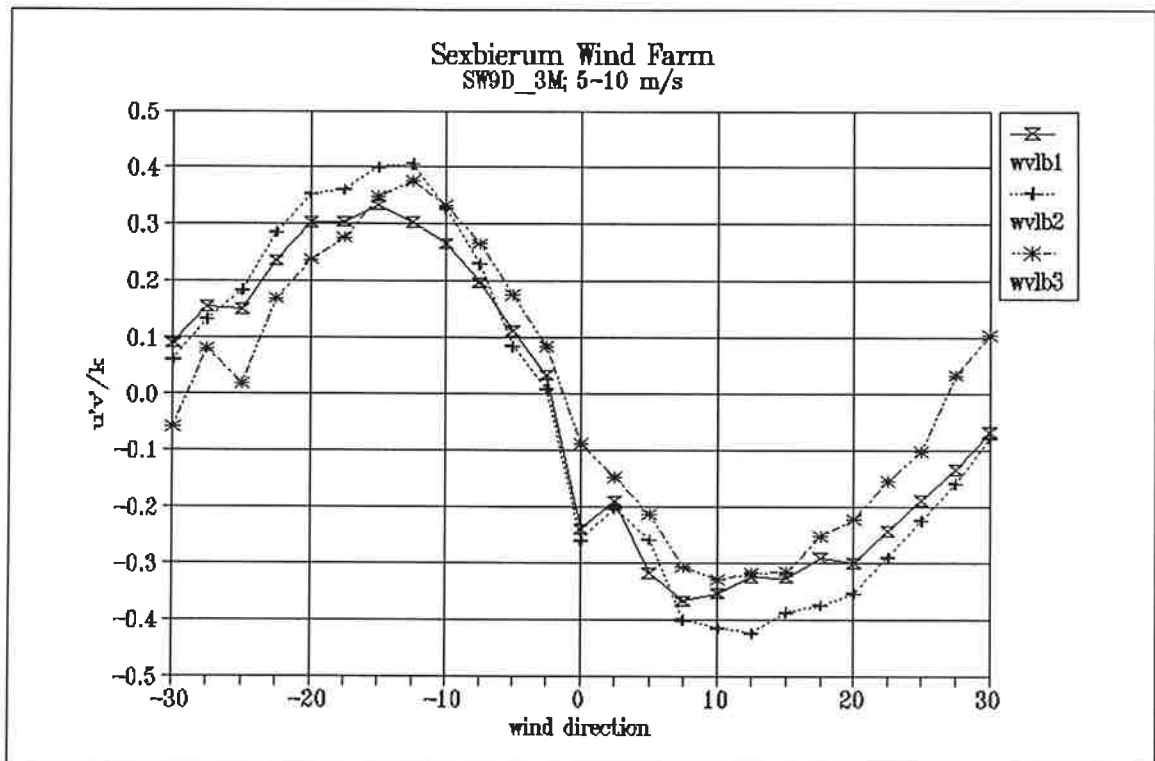


Figure 12 Non-dimensionalized shear stresses  $u'v'/k$  as a function of wind direction in the wind speed bin 5-10 m/s

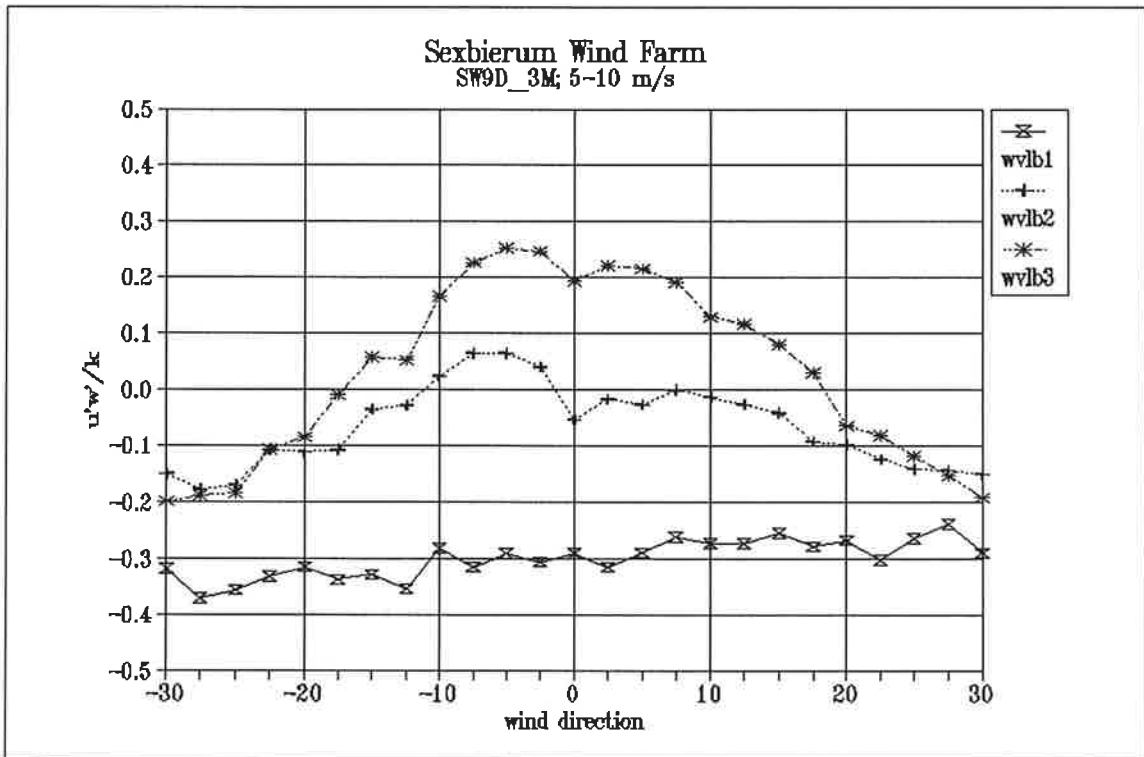


Figure 13 Non-dimensionalized shear stresses  $u'w'/k$  as a function of wind direction in the wind speed bin 5-10 m/s

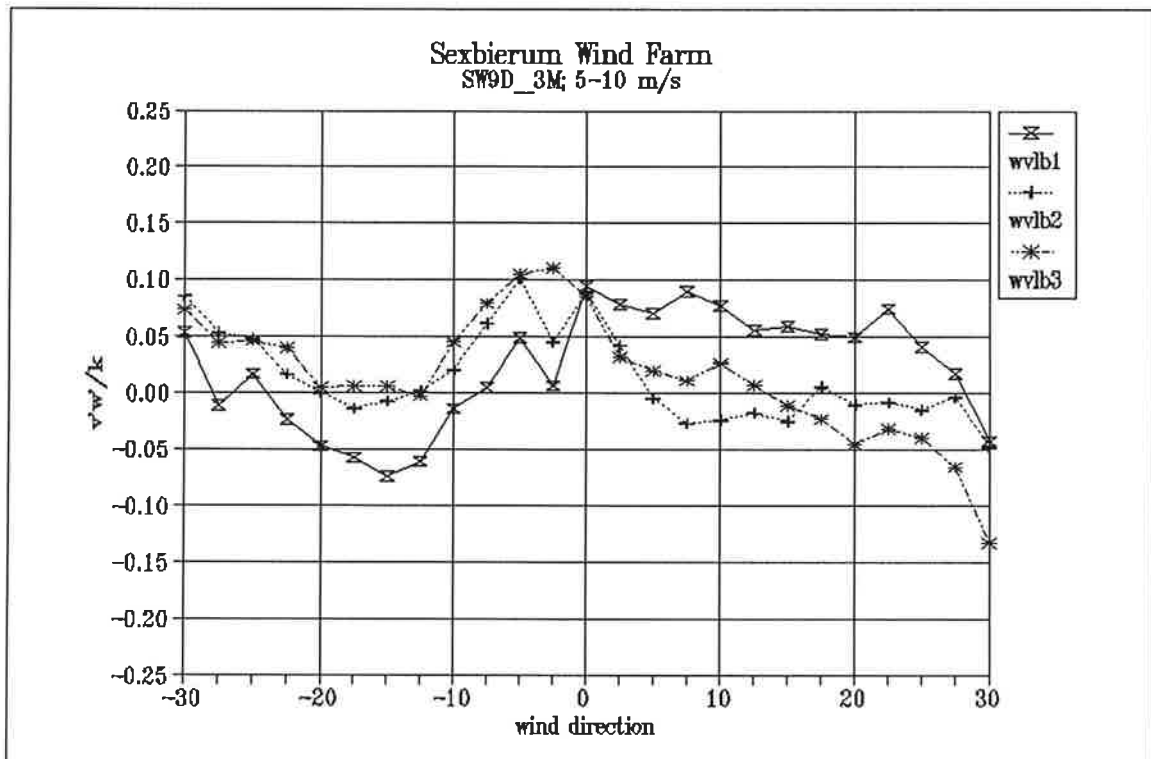


Figure 14 Non-dimensionalized shear stresses  $v'w'/k$  as a function of wind direction in the wind speed bin 5-10 m/s

## **A4.7 Horizontal profiles**

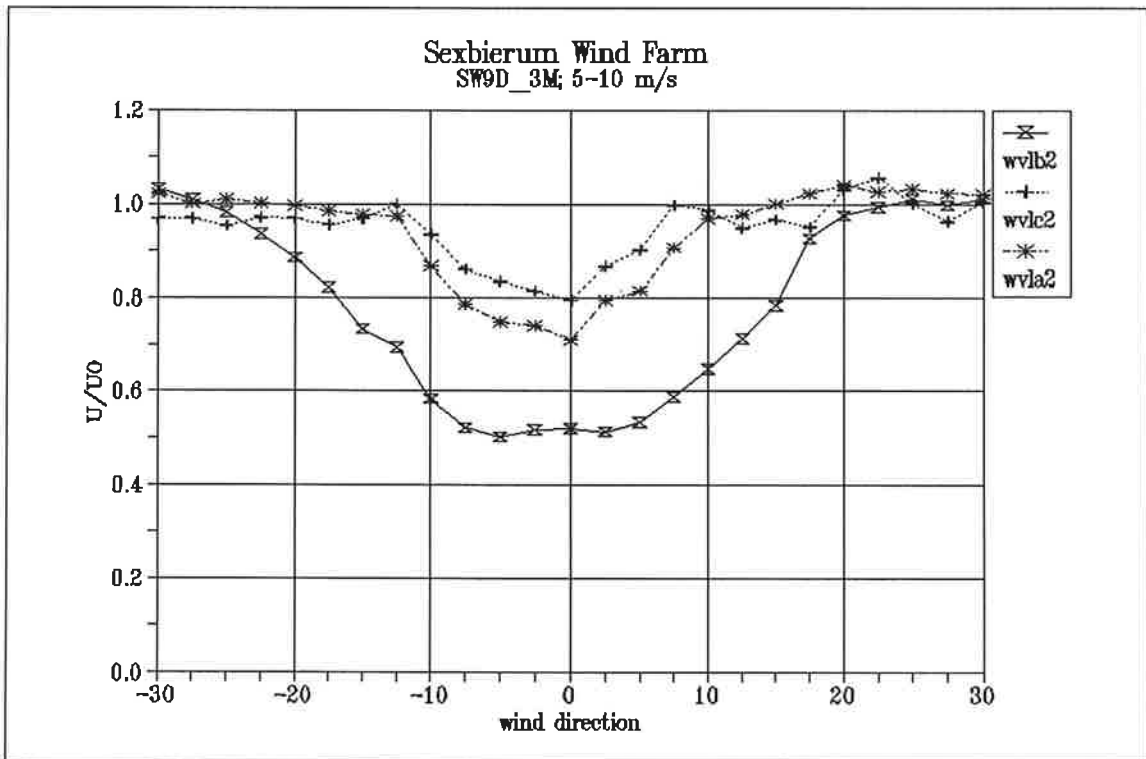


Figure 1 Wake deficit  $U/U_0$  as a function of wind direction in the wind speed bin 5-10 m/s

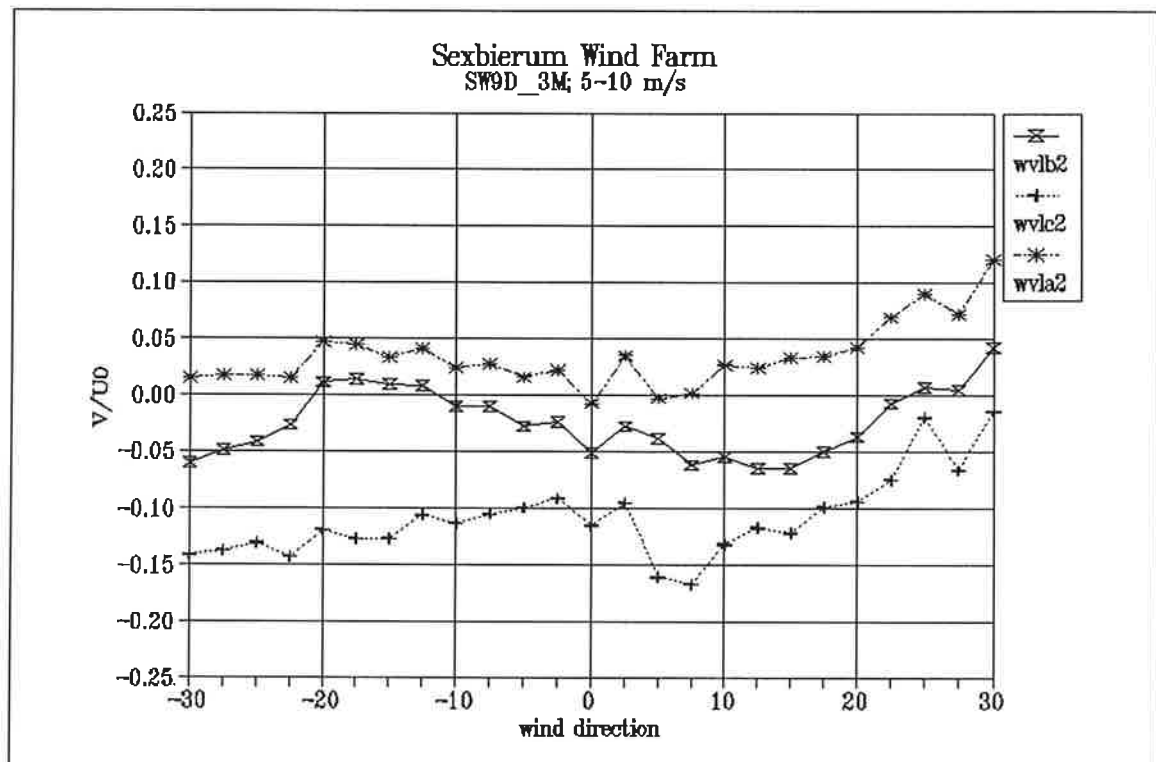


Figure 2 Lateral wind speed  $V/U_0$  as a function of wind direction in the wind speed bin 5-10 m/s

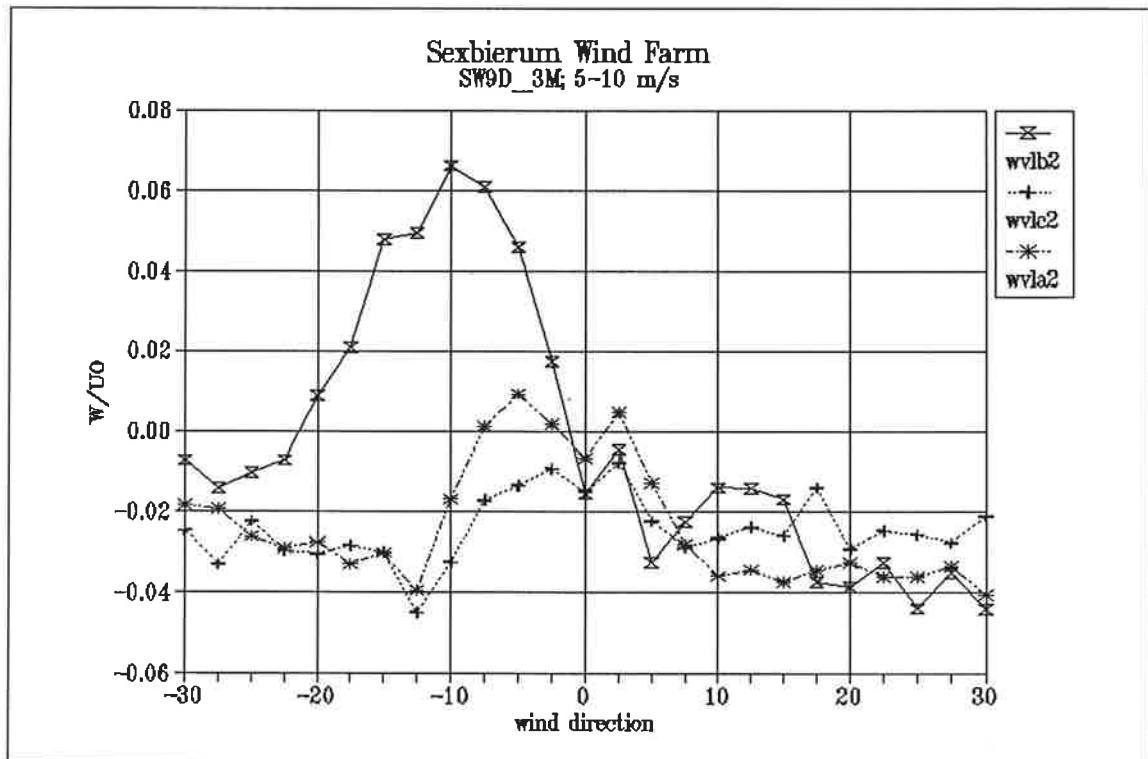


Figure 3 Vertical wind speed  $W/U_0$  as a function of wind direction in the wind speed bin 5-10 m/s

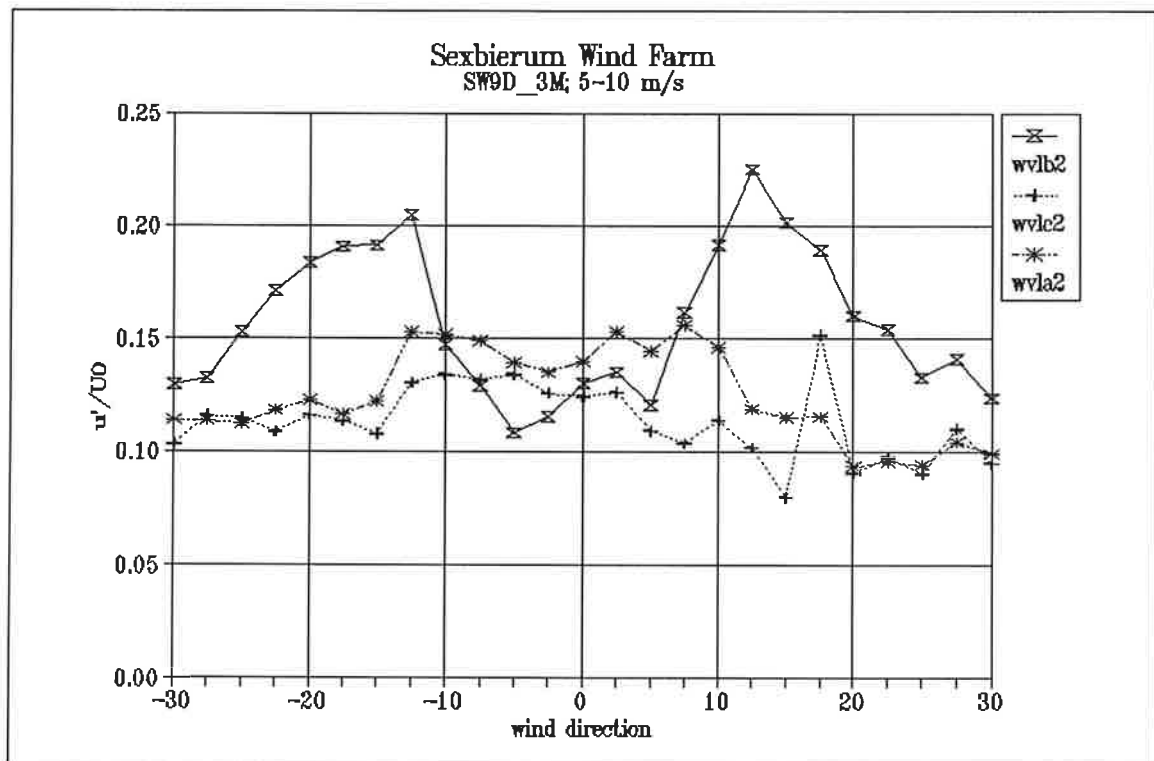


Figure 4 Non-dimensionalized longitudinal turbulent fluctuations  $u'/U_0$  as a function of wind direction in the wind speed bin 5-10 m/s

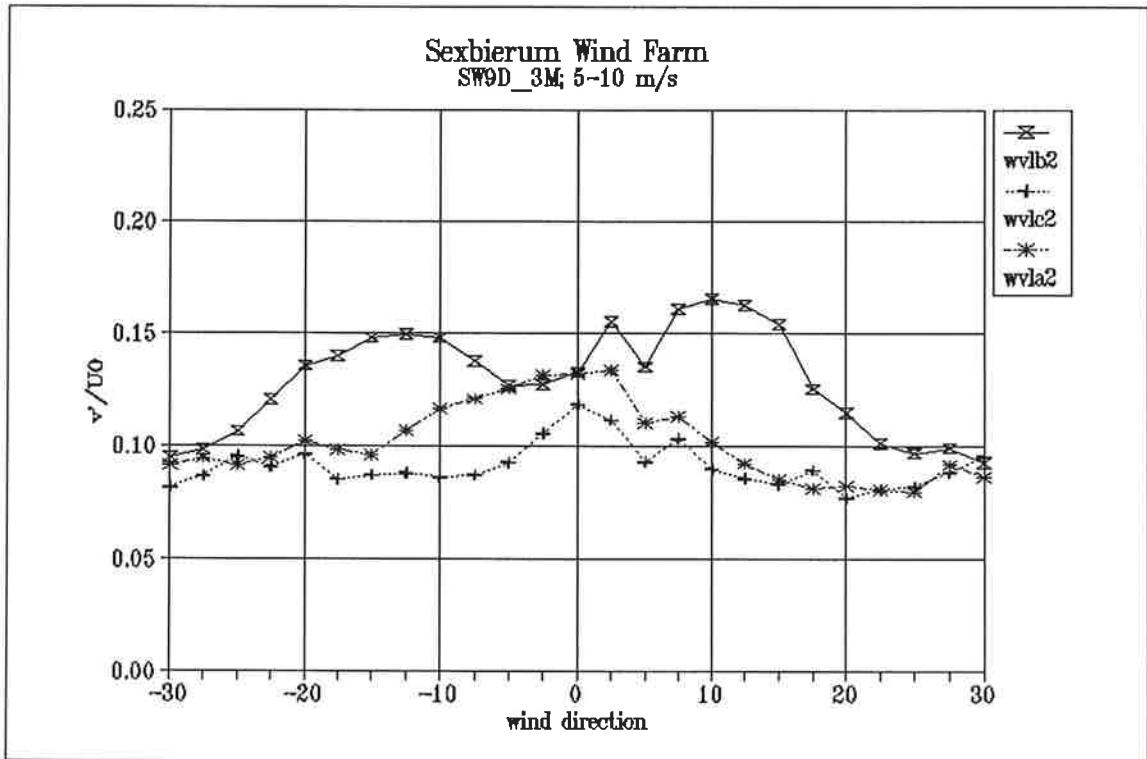


Figure 5 Non-dimensionalized lateral turbulent fluctuations  $v'/U_0$  as a function of wind direction in the wind speed bin 5-10 m/s

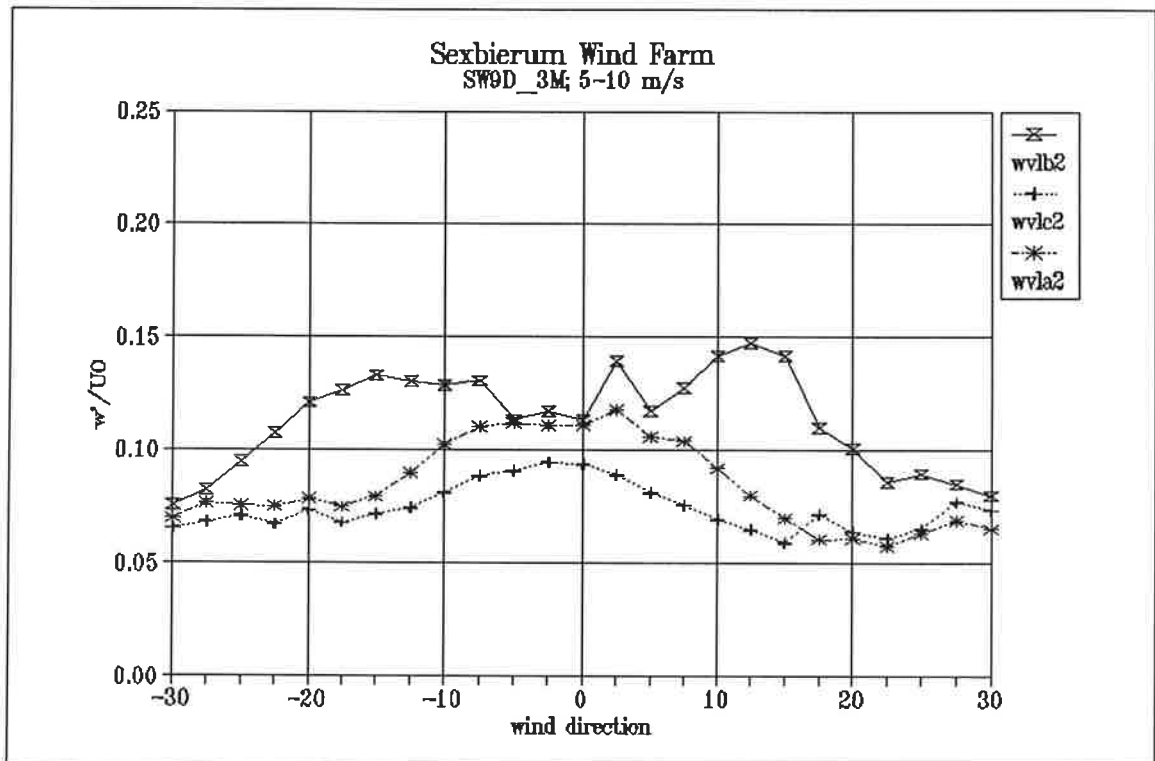


Figure 6 Non-dimensionalized vertical turbulent fluctuations  $w'/U_0$  as a function of wind direction in the wind speed bin 5-10 m/s



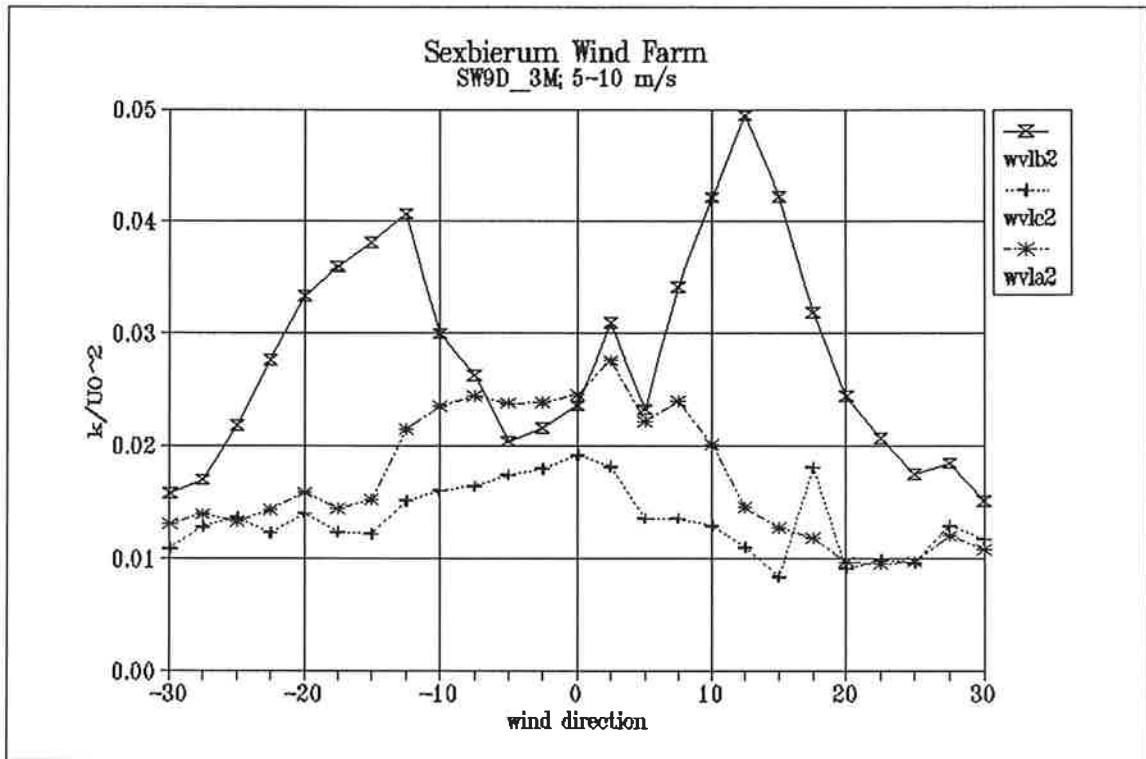


Figure 7 Non-dimensionalized turbulent kinetic energy  $k/U_0^2$  as a function of wind direction in the wind speed bin 5-10 m/s

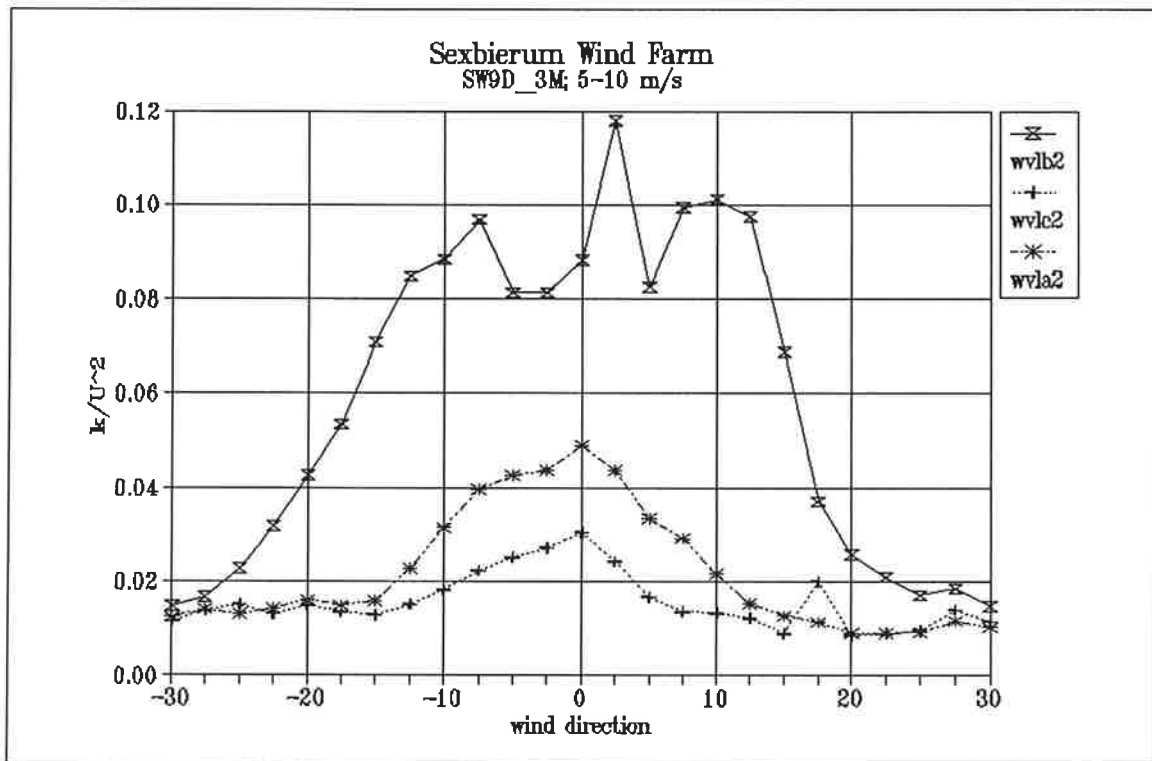


Figure 8 Non-dimensionalized turbulent kinetic energy  $k/U^2$  as a function of wind direction in the wind speed bin 5-10 m/s

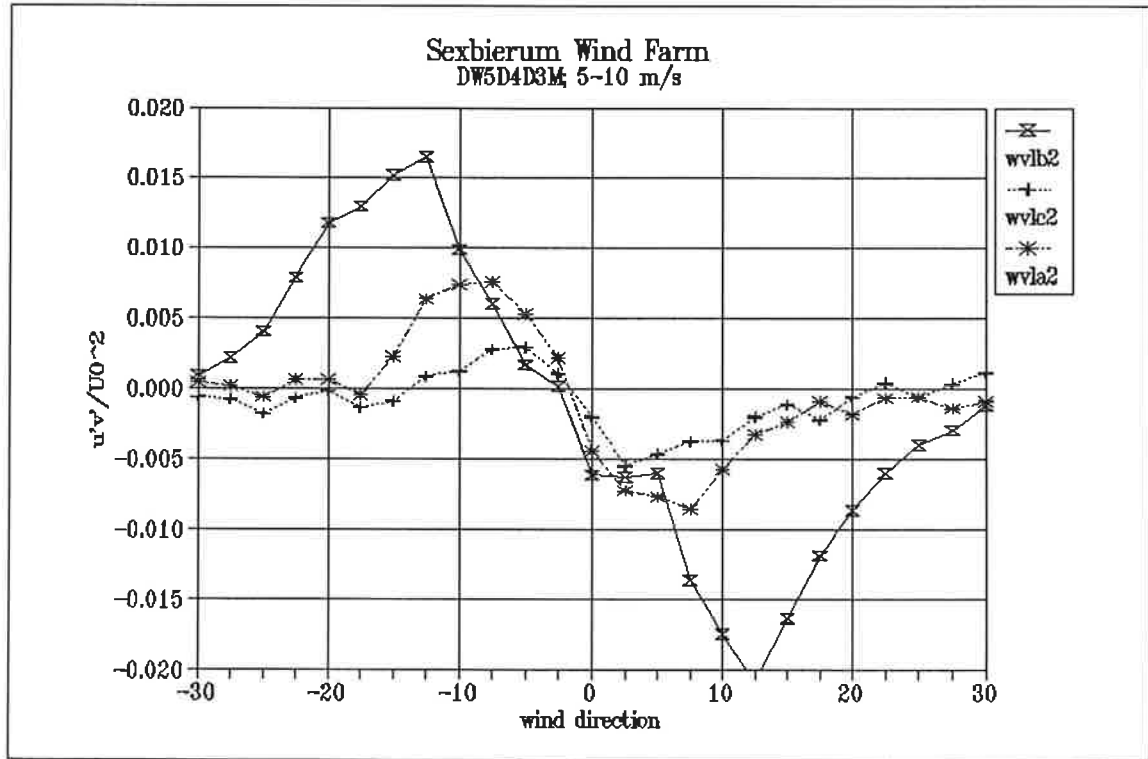


Figure 9 Non-dimensionalized shear stresses  $u'v'/U_0^2$  as a function of wind direction in the wind speed bin 5-10 m/s

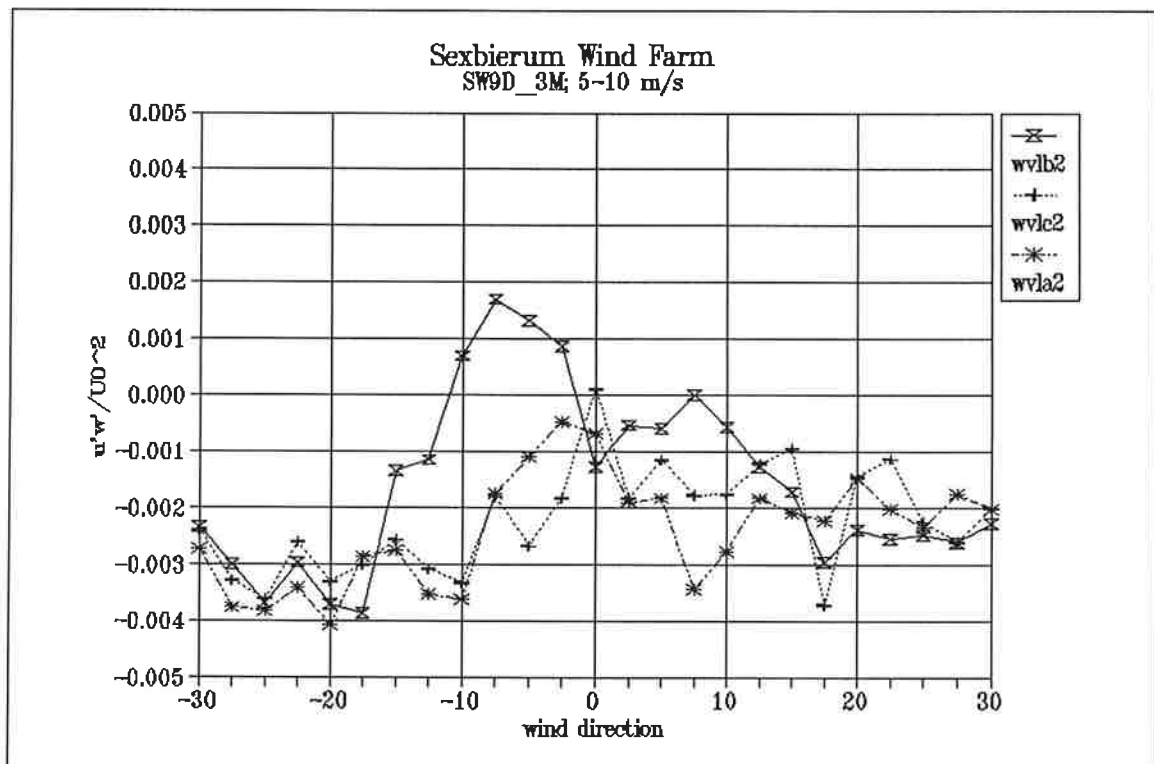


Figure 10 Non-dimensionalized shear stresses  $u'w'/U_0^2$  as a function of wind direction in the wind speed bin 5-10 m/s

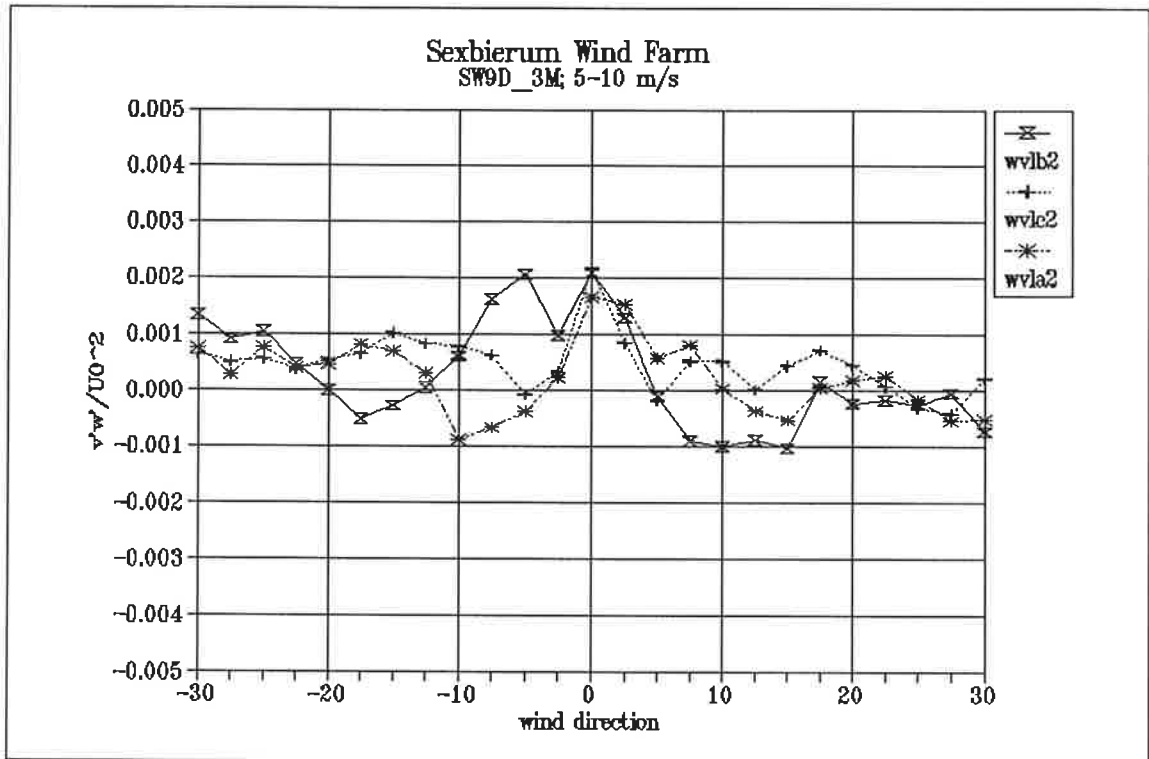


Figure 11 Non-dimensionalized shear stresses  $v'w'/U_0^2$  as a function of wind direction in the wind speed bin 5-10 m/s

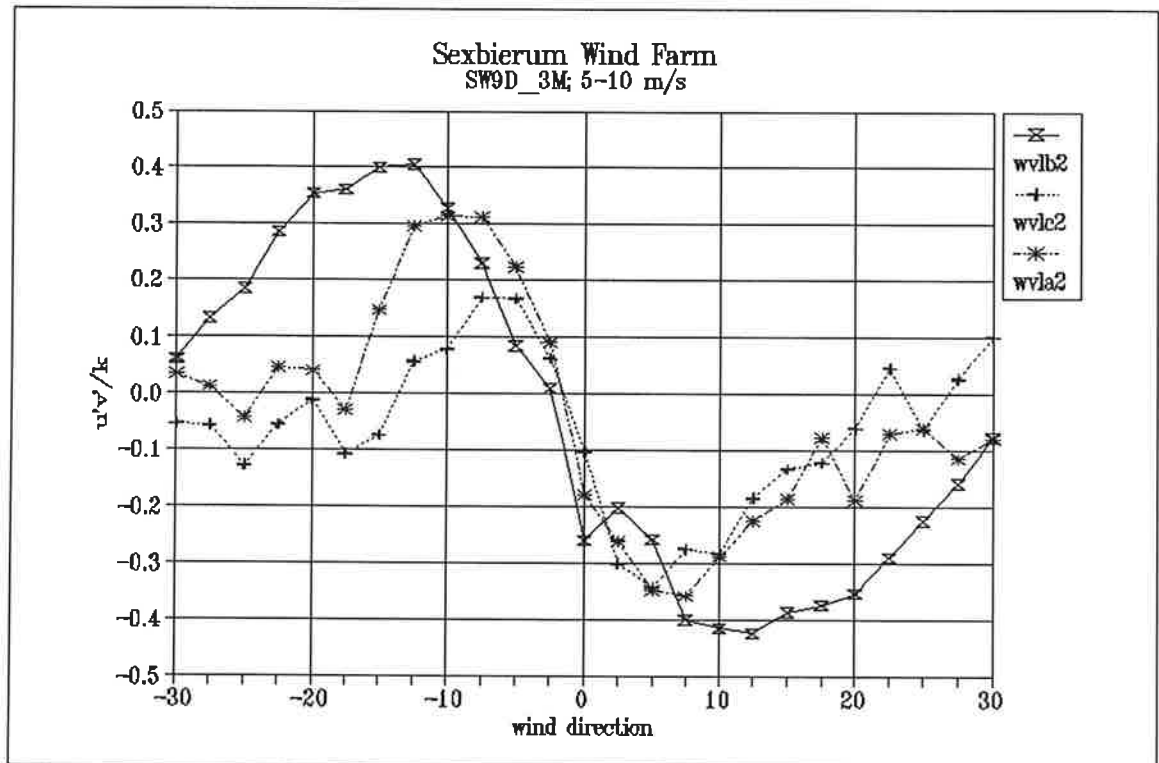


Figure 12 Non-dimensionalized shear stresses  $u'v'/k$  as a function of wind direction in the wind speed bin 5-10 m/s

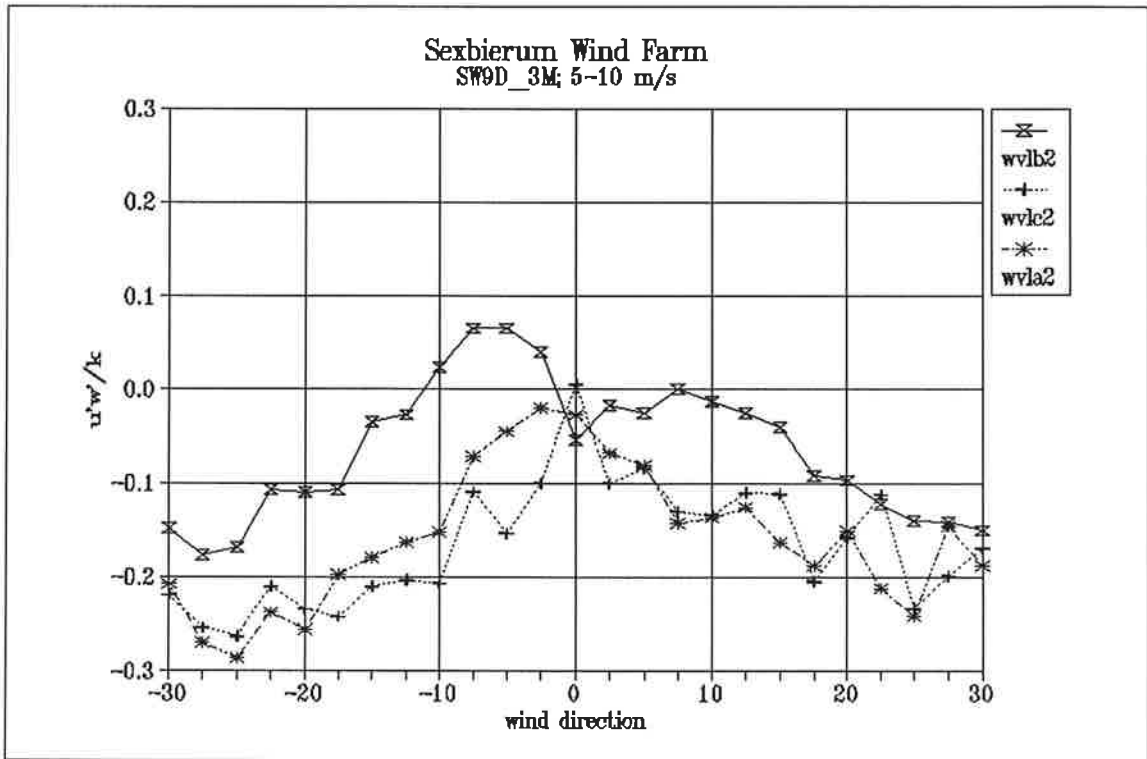


Figure 13 Non-dimensionalized shear stresses  $u'w'/k$  as a function of wind direction in the wind speed bin 5-10 m/s

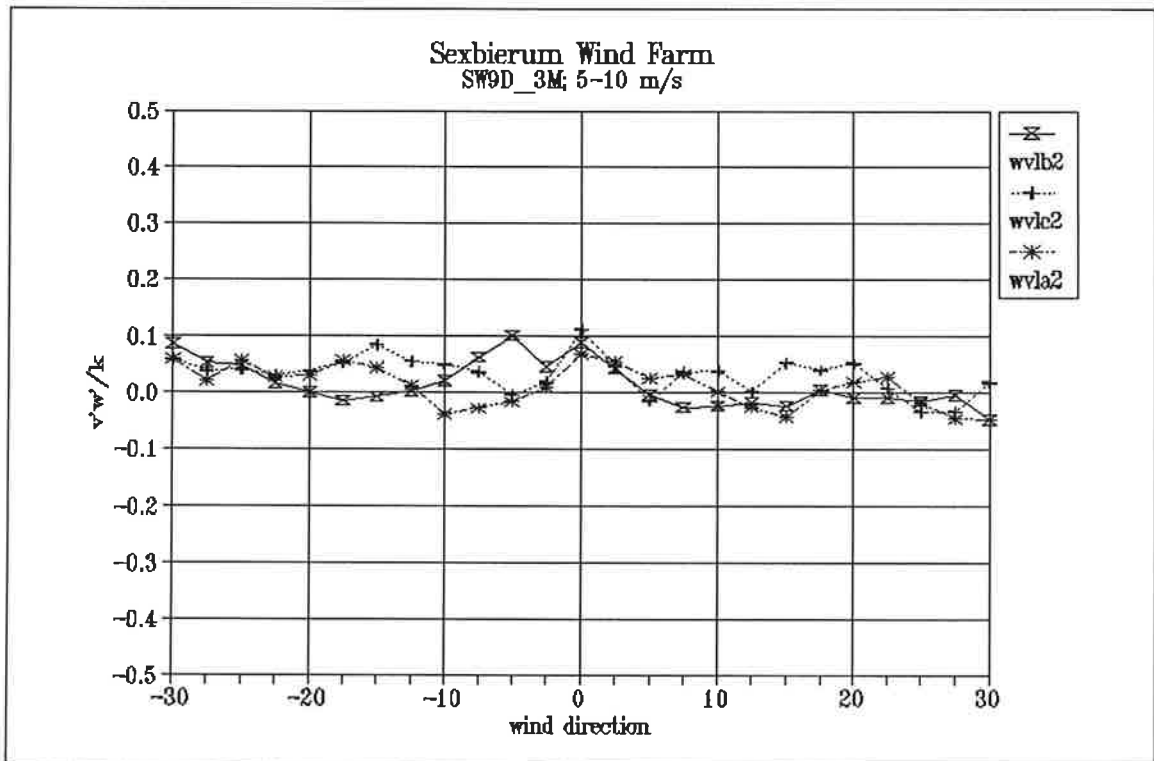


Figure 14 Non-dimensionalized shear stresses  $v'w'/k$  as a function of wind direction in the wind speed bin 5-10 m/s

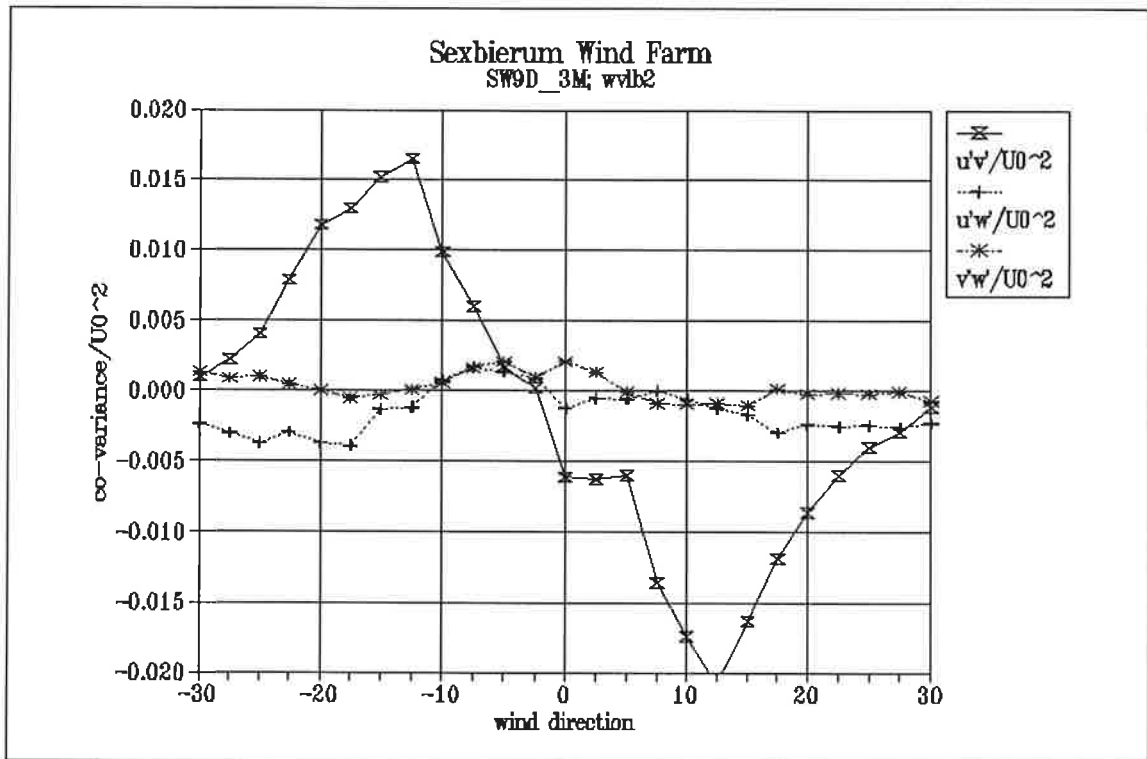


Figure 29 Non-dimensionalized shear stresses  $u'v'/U_0^2$ ;  $u'w'/U_0^2$ ;  $v'w'/U_0^2$  as a function of wind direction in the wind speed bin 5-10 m/s

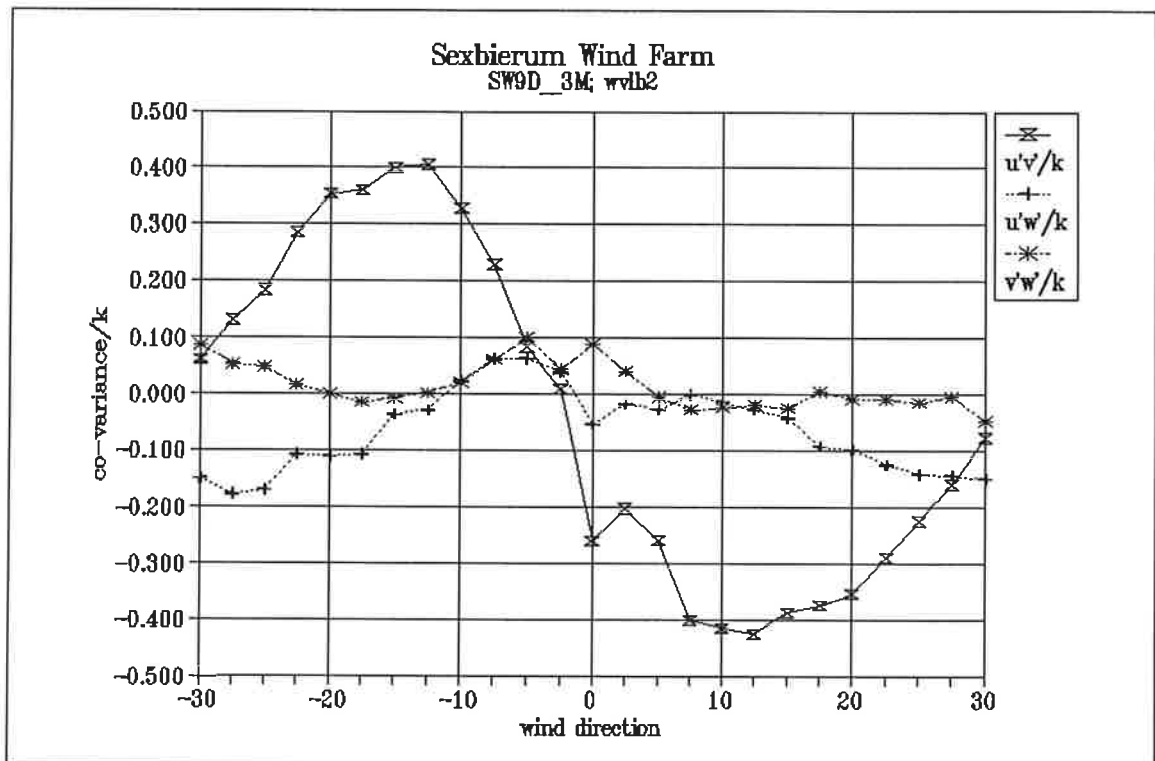


Figure 30 Non-dimensionalized shear stresses  $u'v'/k$ ;  $u'w'/k$ ;  $v'w'/k$  as a function of wind direction in the wind speed bin 5-10 m/s